

NASA CR-

160323

(NASA-CR-160323) POWER EXTENSION PACKAGE  
(PEP) SYSTEM DEFINITION EXTENSION, ORBITAL  
SERVICE MODULE SYSTEMS ANALYSIS STUDY.  
VOLUME 3: PEP ANALYSIS AND TRADEOFFS  
(McDonnell-Douglas Astronautics Co.)

N79-33239

Unclas  
45819

246 p G3/16



**MCDONNELL DOUGLAS ASTRONAUTICS COMPANY**

**MCDONNELL DOUGLAS**

**CORPORATION**



# POWER EXTENSION PACKAGE (PEP) SYSTEM DEFINITION EXTENSION

Orbital Service Module Systems Analysis Study

VOLUME 3  
PEP Analysis and Tradeoffs

AUGUST 1979

MDC G7870

*NAS 9-15532*

**D. C. WENSLEY**  
STUDY MANAGER  
ORBITAL SERVICE MODULE SYSTEMS ANALYSIS STUDY

A handwritten signature in cursive script, reading "D. C. Wensley", written over the printed name and title.

PREPARED FOR: NATIONAL AERONAUTICS AND SPACE ADMINISTRATION  
LYNDON B. JOHNSON SPACE CENTER  
HOUSTON, TEXAS

**MCDONNELL DOUGLAS ASTRONAUTICS COMPANY-HUNTINGTON BEACH**  
5301 Bolsa Avenue Huntington Beach, California 92647 (714) 896-3311

## PREFACE

The extension phase of the Orbital Service Module (OSM) Systems Analysis Study was conducted to further identify Power Extension Package (PEP) system concepts which would increase the electrical power and mission duration capabilities of the Shuttle Orbiter. Use of solar array power to supplement the Orbiter's fuel cell/cryogenic system will double the power available to payloads and more than triple the allowable mission duration, thus greatly improving the Orbiter's capability to support the payload needs of sortie missions (those in which the payload remains in the Orbiter).

To establish the technical and programmatic basis for initiating hardware development, the PEP concept definition has been refined, and the performance capability and the mission utility of a reference design baseline have been examined in depth. Design requirements and support criteria specifications have been documented, and essential implementation plans have been prepared. Supporting trade studies and analyses have been completed.

The study report consists of 12 documents:

- Volume 1 Executive Summary
- Volume 2 PEP Preliminary Design Definition
- Volume 3 PEP Analysis and Tradeoffs
- Volume 4 PEP Functional Specification
- Volume 5 PEP Environmental Specification
- Volume 6 PEP Product Assurance
- Volume 7 PEP Logistics and Training Plan Requirements
- Volume 8 PEP Operations Support
- Volume 9 PEP Design, Development, and Test Plans
- Volume 10 PEP Project Plan
- Volume 11 PL. Post, Schedules, and Work Breakdown Structure Dictionary
- Volume 12 PEP Data Item Descriptions

Questions regarding this study should be directed to:

Jerry Craig/Code EA4  
Manager, Orbital Service Module Systems Analysis Study  
National Aeronautics and Space Administration  
Lyndon B. Johnson Space Center  
Houston, Texas 77058, (713) 483-3751

D.C. Wensley, Study Manager, Orbital Service Module Systems Analysis Study  
McDonnell Douglas Astronautics Company-Huntington Beach  
Huntington Beach, California 92647, (714) 896-1886

## CONTENTS

Section 1	INTRODUCTION	1
1.1	PEP System	1
1.2	PEP Analysis and Tradeoff Tasks	2
Section 2	PEP ANALYSIS AND TRADEOFF TASKS	3
2.1	Clearance Analysis	3
2.2	Bridge Fittings	7
2.3	Sill Latches	11
2.4	RMS Wiring	15
2.5	Wing Deployment Mechanism	23
2.6	Fuel Cell Voltage Control	28
2.7	Regulator Definition	36
2.8	Structural Design Criteria	44
2.9	PEP Gimbal Definition	61
2.10	Mast and Canister Preliminary Design Criteria	64
2.11	Structural Modeling and Dynamic Analysis	67
2.12	Power System Configuration	85
2.13	Solar Array Wing Assembly Requirements	89
2.14	Solar Array Control Avionics Requirements/ Criteria Definitions	91
2.15	Control System Management--General Purpose Computer (GPC) and Array Processor Control Interface	115
2.16	Avionics Thermal Control Requirements	124
2.17	Thermal Control Configuration Definition	128
2.18	Orbiter DAP Utilization/Interface Evaluation	142
2.19	Pointing/Control Avionics Concept and Operations Analysis	149
2.20	EMC Analysis	153
2.21	Alternate Solutions for PEP/RMS Signal and Drive Power Wiring	157
2.22	Collision Hazard Elimination	160
2.23	EVA Operations	166
Appendix A	POWER EXTENSION PACKAGE POWER BUS DESIGN	171
Appendix B	PRELIMINARY SPECIFICATION PEP GIMBAL ASSEMBLY, SOLAR ARRAY DRIVE, TWO-AXIS	217

## Section 1 INTRODUCTION

### 1.1 PEP SYSTEM

The Power Extension Package (PEP) is a solar electrical power generating system to be used on the Shuttle Orbiter to augment its power capability and to conserve fuel cell cryogenic supplies, thereby increasing power available for payloads and allowing increased mission duration. The Orbiter, supplemented by PEP, can provide up to 15 kW continuous power to the payloads for missions of up to 48 days duration.

When required for a sortie mission, PEP is easily installed within the Orbiter cargo bay as a mission-dependent kit. When the operating orbit is reached, the PEP solar array package is deployed from the Orbiter by the remote manipulator system (RMS). The solar array is then extended and oriented toward the sun, which it tracks using an integral sun sensor/gimbal system. The power generated by the array is carried by cables on the RMS back into the cargo bay, where it is processed and distributed by PEP to the Orbiter load buses. After the mission is completed, the array is retracted and restowed within the Orbiter for earth return.

Figure 1-1 shows the PEP system, which consists of two major assemblies -- the Array Deployment Assembly (ADA) and the Power Regulation and Control Assembly (PRCA) -- plus the necessary interface kit. It is nominally installed at the forward end of the Orbiter bay above the Spacelab tunnel, but can be located anywhere within the cargo bay if necessary. The ADA, which is deployed, consists of two lightweight, foldable solar array wings with their containment boxes and deployment masts, two diode assembly interconnect boxes, a sun tracker/control/instrumentation assembly, a two-axis gimbal/slip ring assembly, and the RMS grapple fixture. All these items are mounted to a support structure that interfaces with the Orbiter. The PRCA, which remains in the Orbiter cargo bay, consists of six pulse width modulated voltage regulators mounted to three cold plates, three shunt regulators to protect the Orbiter

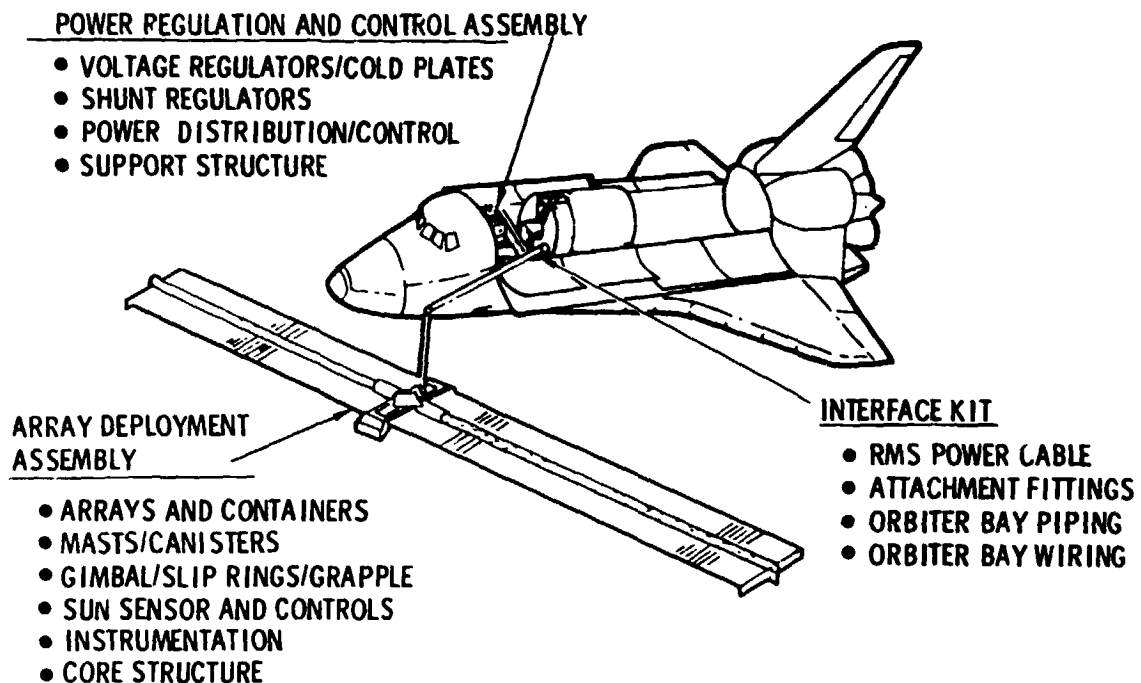


Figure 1-1. PEP System

buses from overvoltage, and a power distribution and control box, all mounted to a support beam that interfaces with the Orbiter.

PEP is compatible with all currently defined missions and payloads and imposes minimal weight and volume penalties on these missions. It can be installed and removed as needed at the launch site within the normal Orbiter turnaround cycle.

## 1.2 PEP ANALYSIS AND TRADEOFF TASKS

This document summarizes the objectives, conclusions and approach to the accomplishment of the 19 specific design and analysis activities which were defined as Task 2.0 of the OSM study extension. In addition, it includes summaries of several additional tasks which were assigned to MDAC as action items during the course of the study.

## Section 2

### PEP ANALYSIS AND TRADEOFF TASKS

#### 2.1 CLEARANCE ANALYSIS

This task consisted of the study of clearances of the PEP, (1) in its stowed form and position inside the Orbiter bay and (2) in its deployed operational orientations as positioned by the RMS.

##### 2.1.1 PEP Stowed Position Clearances

###### Objective

The objective of this analysis was to determine the effects on the original PEP concept geometry from dual RMS envelope constraints, Orbiter dynamic deflections and Spacelab component envelopes. A further objective was to define an allowable dynamic envelope for PEP based on these installation considerations.

###### Conclusions

The analysis showed that the originally selected SEPS geometry array box could not be installed transversely across the Orbiter bay and maintain clearances with both the port and starboard Orbiter RMS envelopes. Also shown was that a further reduction in size would be necessary if it was necessary to restrict the array box to the nominal Orbiter payload 90-inch radius envelope. It was concluded that the array could, from a practical standpoint, violate that 90-inch constraint utilizing a void that results from the RMS installation itself. The Resulting Array box length was reduced from the SEPS 159.04 inch size to 152.8 inch. This length is based on fixing the array box with respect to the starboard sidewall of the Orbiter and being compatible with PEP deflections and the worst case Orbiter sidewall deflections for any position of PEP within the Orbiter bay.

###### Approach

The groundrules require the ADA portion of PEP to be capable of installation at any longitudinal location in the Orbiter payload bay. The most constraining case and its principal forecast use is with Spacelab in its short tunnel

configuration with both elements of PEP installed over the tunnel between the Spacelab module and the external airlock. Examination of the Spacelab module and the airlock showed that the principal clearance requirement was for hand-rails on those elements.

The ADA element of PEP is situated over the tunnel and its principal support point on the Orbiter sidewall lies between those of the tunnel. The PEP structural support concept is strongly influenced by its position over the tunnel. To provide lateral support in the bay, PEP required either a mechanism that would reach around the tunnel to the keel area where payload yaw loads are normally reacted or direct hard mounting to one sidewall of the Orbiter. To reach the keel area for yaw support, a mechanism would be required that would have to be carefully threaded through the tunnel support structure and inserted into the keel fitting under the tunnel or would have to be segmented so as to install part of it prior to tunnel installation and part of it after tunnel installation. Neither approach was considered acceptable. Since the ADA element and the PRCA element are individually of low weight (approximately 1000 lbs. each) their load input into the Orbiter sidewall (for a sidewall fixed concept) would not exceed the trunnion friction load that occurs with a maximum weight payload in a normal installation mode.

A secondary influence on the PEP envelope and clearance requirements is that a Spacelab mission is possible with only pallet elements in which case the ADA would have to be installed above a pallet. The impact of this was the decision to place the ADA trunnion location 6 inches higher than normal payload location and to use custom lightweight support fittings to fit this geometry.

The clearances and the resultant PEP allowable dynamic envelope result from very preliminary deflection data and non-precision analyses. The PEP envelope must be iterated at a future date when firm Orbiter deflections are defined. This study utilized Orbiter sidewall deflection data from a preliminary memorandum on that topic prepared in 1977 and arbitrarily assumed some companion sidewall angular rotations. These deflections were used to estimate the dynamic excursions of the RMS envelope between (port and starboard) which the PEP is installed. The worst case combined sidewall inward deflections from the preliminary data was 4.48 inches. The sidewall (longeron) angular rotation was assumed to be 2 degrees (1 degree from sidewall deflection and 1

degree from local payload loading) which resulted in further RMS excursions of 1.26 inches per side. An add increment of excursion into the PEP envelope region was a 1.0 inch increase in the width of the RMS dynamic envelope due to PEP wire installations on the side of the RMS.

### Results

This study analysis resulted in the PEP allowable dynamic envelope defined in Figure 2.1-1 and the establishment of a maximum length array box of 152.8 inches. The analysis also established the PEP centerline installation offset of 2.24 inches. These dimensions and offsets will require future verification when firm Orbiter deflection data is available.

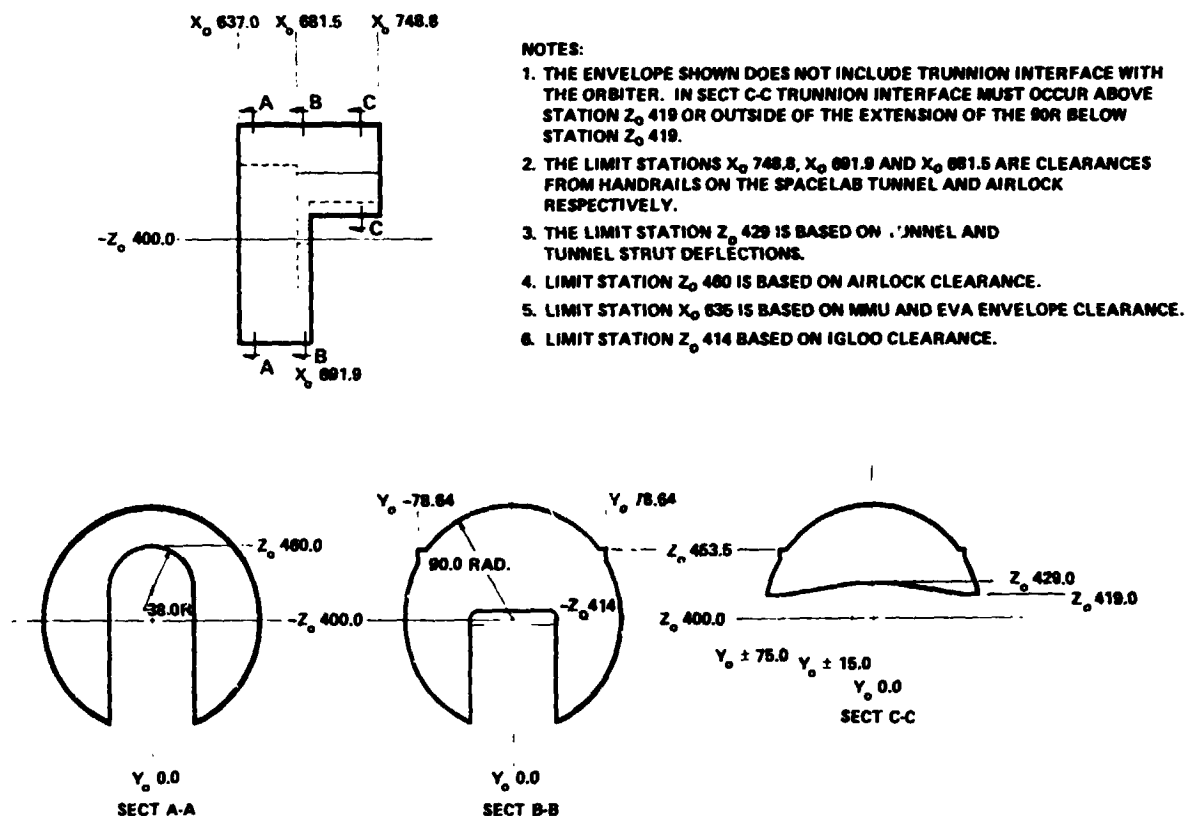


Figure 2.1-1. PEP System Stowed Maximum Dynamic Envelope

### 2.1.2 PEP Deployed/Operational Position Clearances

#### Objective

The purpose of this analysis was to determine clearances between the PEP solar array wings and the Orbiter external surfaces to establish the practicality of holding the PEP array in its operational positions with the Orbiter RMS.

## Conclusions

The analysis of the PEP solar array wings in various deployed positions around the Orbiter using the Orbiter's RMS to position array showed sufficiently large clearances from the Orbiter body to have a high confidence level that safe use in any of these positions is possible.

## Approach

This analysis was accomplished as a combination graphics and calculation task. The basic analysis was done for PEP array positions at the rectilinearly cardinal positions, overhead, off-the-wing, over-the-nose, and under-the-belly. These positions were then inspected for Orbiter skewed attitudes. The geometry of the array, the position of the RMS/PEP interface and the array beta angles were derived from the PEP reference configuration.

## Results

The resulting clearances shown in Figure 2.1-2 are for the PEP reference configuration. Variations of the PEP studied offer only small dimensional changes that would affect this clearance study and would not alter the conclusions.

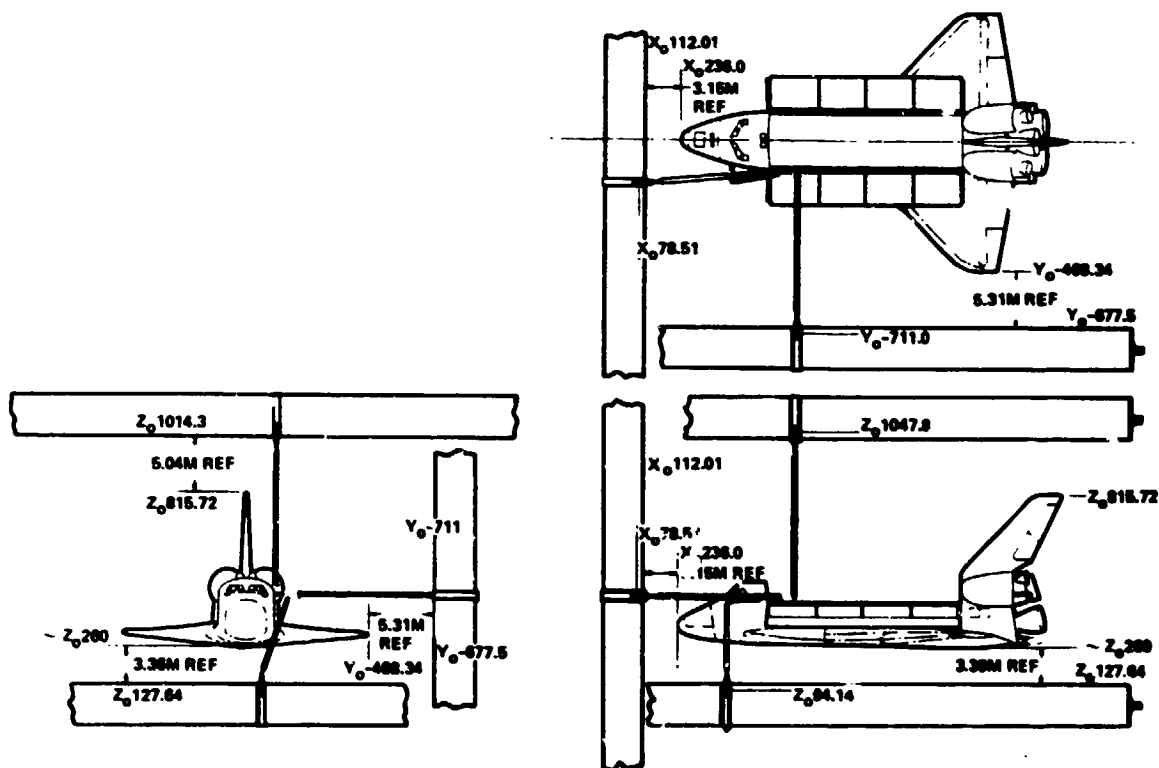


Figure 2.1-2. PEP Clearances - Deployed

There are two basic under-belly positions. Namely, with the RMS upper arm segment oriented forward along the Orbiter nose, as shown in Figure 2.1-2, and with that arm segment oriented laterally toward the wingtip. Due to the RMS shoulder axis being canted outboard by approximately 20 degrees, repositioning the upper arm from the nose position to the off-wing position would increase the under-belly clearance.

Full orbital attitude requirements of the Orbiter for various missions must be examined in depth. For simple POP, solar inertial or earth oriented attitudes, there is adequate clearances, however, further analysis is required if arbitrary attitudes of the Orbiter with large orbital skewed angles are to be desired. The clearances shown in Figure 2.1-2 represent static conditions. Deflections resulting from dynamic deflections of the RMS and the array suspension system must be subtracted from the dimensions shown. The maximum array tip deflection is calculated to be 7.3 ft (2.2M) due to VRCS plume impingement. This tip deflection would reduce the underbelly clearance by 5.47 ft (1.66M), but a clearance of 5.6 ft (1.7M) would remain under worst-case conditions.

## 2.2 BRIDGE FITTINGS

### Objectives

Select and define means of supporting in the payload bay both the Array Deployment Assembly (ADA) and the Power Regulation and Control Assembly (PRCA). Prepare a preliminary design of lightweight custom bridge fittings. Investigate feasibility of common PEP/Spacelab/Tunnel bridge fittings. Verify Orbiter structural load compatibility considering combined loads.

### Conclusions and Recommendations

At the baseline location, the ADA forward support must share a bridge with the two Spacelab tunnel support trunnions. Either the special lightweight bridge design developed for the tunnel must be redesigned to incorporate provisions for ADA support fittings or the tunnel and ADA can share a standard Orbiter Bridge.

Because the only available location for PRCA cross-bay beam is adjacent to the Remote Manipulator System (RMS) base where no payload attach provisions exist, a special lightweight bridge with integral attach fittings is recommended.

Loading magnitude of both the ADA and PRCA are sufficiently low to permit the  $Y_o$  axis loads to be reacted by the longeron bridges, negating the need for keel bridges. The combined loads of the ADA and the Spacelab tunnel are below the allowable loads for a standard Orbiter bridge fitting.

#### Assumptions

Spacelab module configuration and location were taken from ICD 2-05101 and Spacelab tunnel support locations and detail were from MDAC Drawing 1D21326 "Layout, Struts." Load factors were from JSC 07700, Vol. XIV. Bridge loading capabilities were from ICD 2-19001.

#### Approach

Standard Orbiter bridges and custom lightweight bridges were evaluated. Bridge loading for critical flight conditions were determined and combined with all other known payload elements, using the bridges. For the Orbiter bridges, these loadings were then compared with the bridge capabilities.

#### Results

Figure 2.2-1 illustrates the current design of the lightweight bridge fitting to be used to mount the Spacelab short tunnel. This bridge fitting weighs 31 pounds and is a custom design, fabricated from 7075 aluminum, has built-in rails, and used only to support the two tunnel trunnions (2 trunnions each side, total of 4). This bridge fitting can be modified as shown to accept a bolt-on track and the custom retention latch to support the ADA trunnion. With this modification, the weight of the bridge fitting and track will be 34.5 pounds. Figure 2.2-2 illustrates the standard Orbiter bridge fitting that can be used to support both ADA and short tunnel. This bridge is fabricated of titanium and weighs 55 pounds. If standard Orbiter fixed journals were used in combination with the bridge, they would add an additional 40 pounds per side. Therefore, if the tunnel custom bridge fitting with modification is used for the ADA support, the total weight for the two bridge fittings and tunnel journals is 69 pounds. If the standard Orbiter bridge with standard journals is used, the total comparable weight is 190 pounds. The significant items of this total are the four 20 pounds standard journals. Redesign of these journals to reduce weight is possible; however, it appears to be more cost and weight effective to modify and use the existing lightweight bridge fitting design with the integral journals.

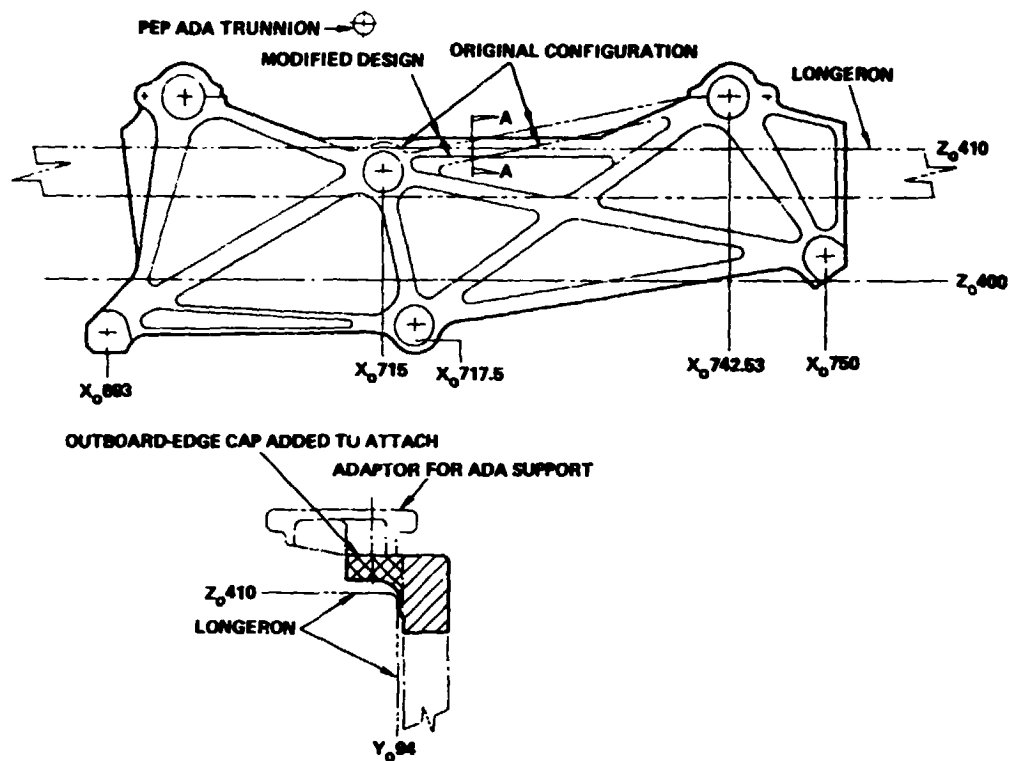


Figure 2.2-1. Custom Lightweight Bridge Fitting for Short Tunnel

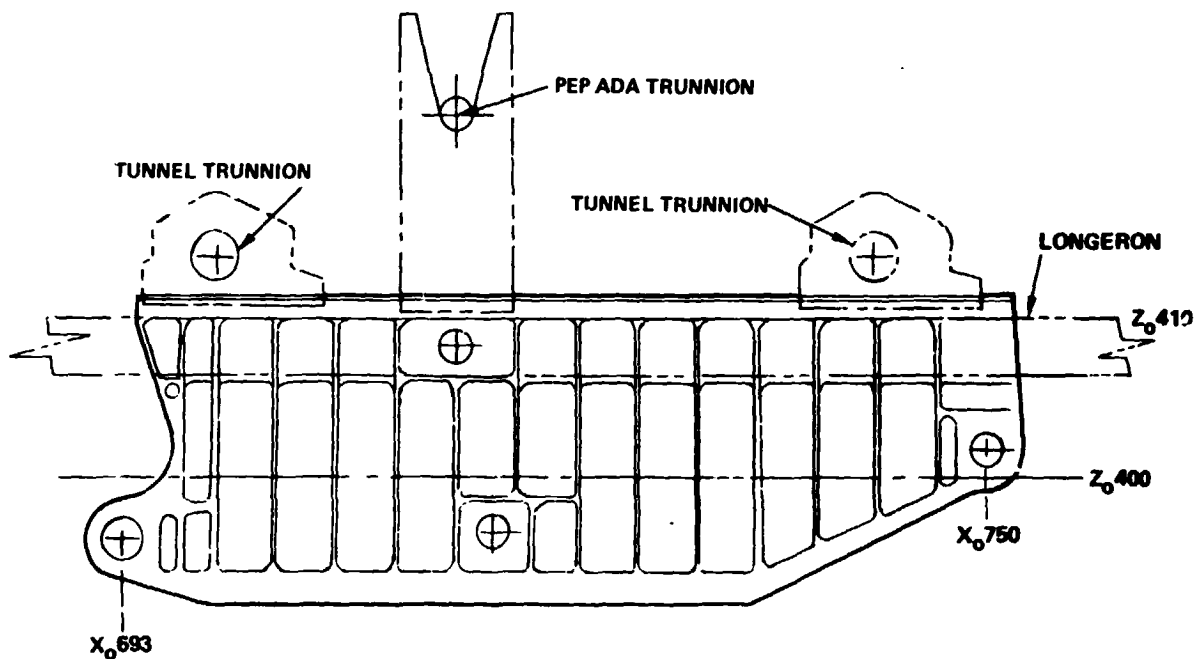


Figure 2.2-2. Standard Bridge Fitting

Figure 2.2-3 illustrates the design of the custom bridge fitting to support the PRCA. The fitting is fabricated of 7075 aluminum, it has integral journals which can withstand both radial and thrust loads and the weight is 15 pounds. Figure 2.2-4 illustrates the standard Orbiter bridge fitting in the area of the PRCA support trunnions. Because of the presence of the RMS mounting base, the structural attachment of the PRCA must be moved down and inboard from the standard trunnion locations. It can be seen that the standard bridge is cut away to clear the RMS mount. It was found that the standard bridge could not be used in combination with the PRCA baseline configurations. In addition, the standard bridge is fabricated of titanium and weighs 45 pounds.

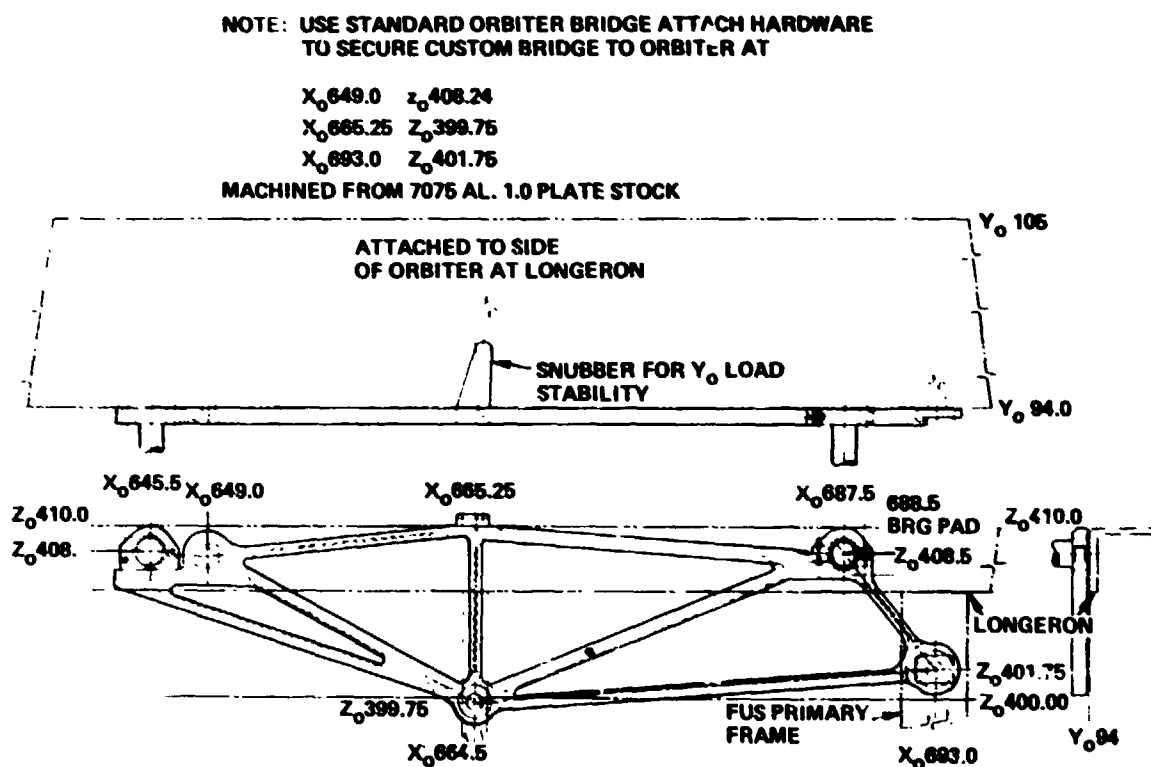


Figure 2.2-3. Custom Lightweight Bridge Fitting

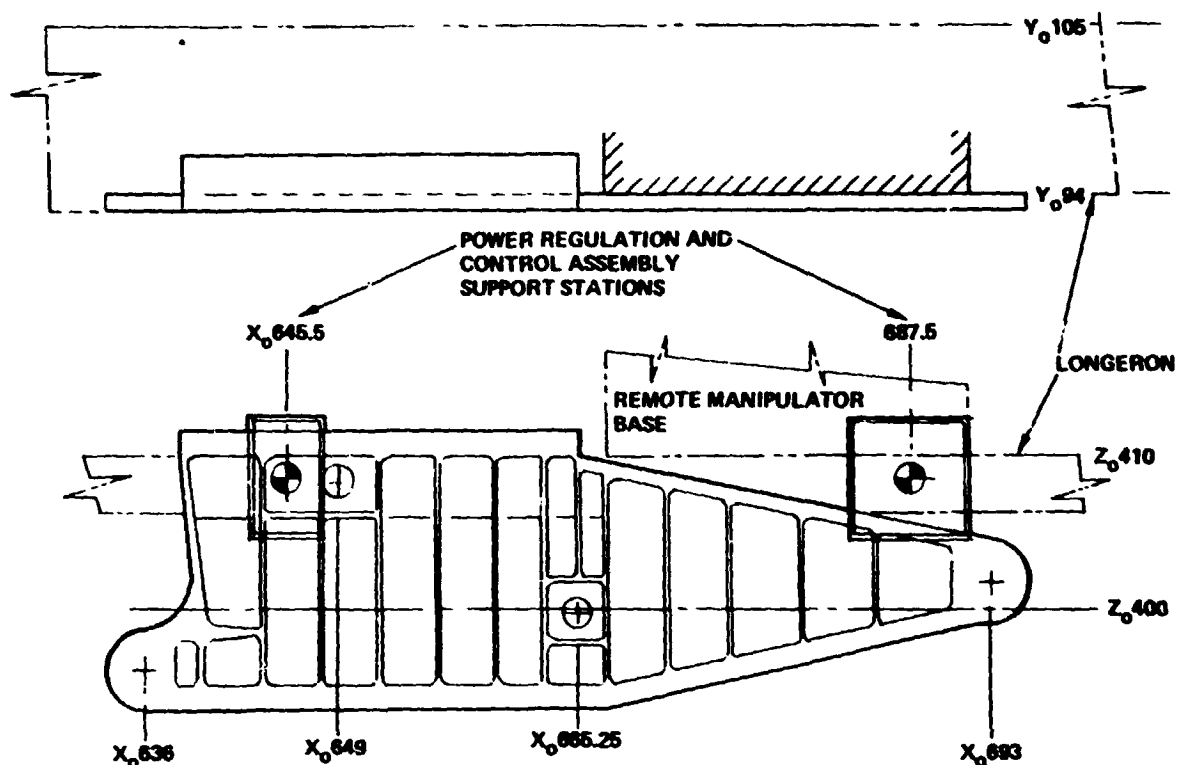


Figure 2.2-4. Standard Bridge Fitting

## 2.3 SILL LATCHES

### Objectives

The objectives of this task are: to verify the definition and availability of remotely operated payload retention latches for PEP Array Deployment Assembly (ADA) and to provide interface definition for payload retention latches.

### Conclusions and Recommendations

The use of standard Orbiter payload retention latches is not an acceptable method of support and retention for the ADA because of size, weight and trunnion elevation. Development of a custom lightweight retention latch, using a standard bridge fitting and electrical interface is recommended.

### Approach

The Phase A study baseline configuration utilized a four trunnion support for the ADA. The concept shared the short tunnel bridge fittings with the ADA retention latches nested between the tunnel trunnion locations. Further investigation has shown that this solution did not provide adequate space for standard retention provisions plus the weight of the standard retention

latches was prohibitive when compared to the weight of the PEP system. A rearrangement of the support provisions for the ADA was undertaken and a new design prepared which provides the features of lightweight, adequate space and flexibility in location of the ADA in the cargo bay.

### Results

The baseline retention provisions for PEP are illustrated by Figure 2.3-1. The ADA support uses three trunnions, two on the right side and one on the left side. Both forward trunnions are at Station  $X_{715}$  and the aft trunnion is at Station  $X_{758.3}$ . The elevation of each trunnion is  $Z_{420}$ . The forward retention latches share the bridge fittings, on both sides, with the short tunnel. The aft retention latch shares the bridge fitting on the right side with the Spacelab. A fitting to react PEP lateral ( $Y_o$ ) loads is also installed on the forward bridge fitting on the right hand side.

It was found that for an all pallet configuration of Spacelab the ADA must be mounted above a standard pallet. In order to accomplish this, the support trunnion elevation must be raised to  $Z_{420}$  to prevent interference with the pallet sills. The current baseline design allows the ADA to be mounted over

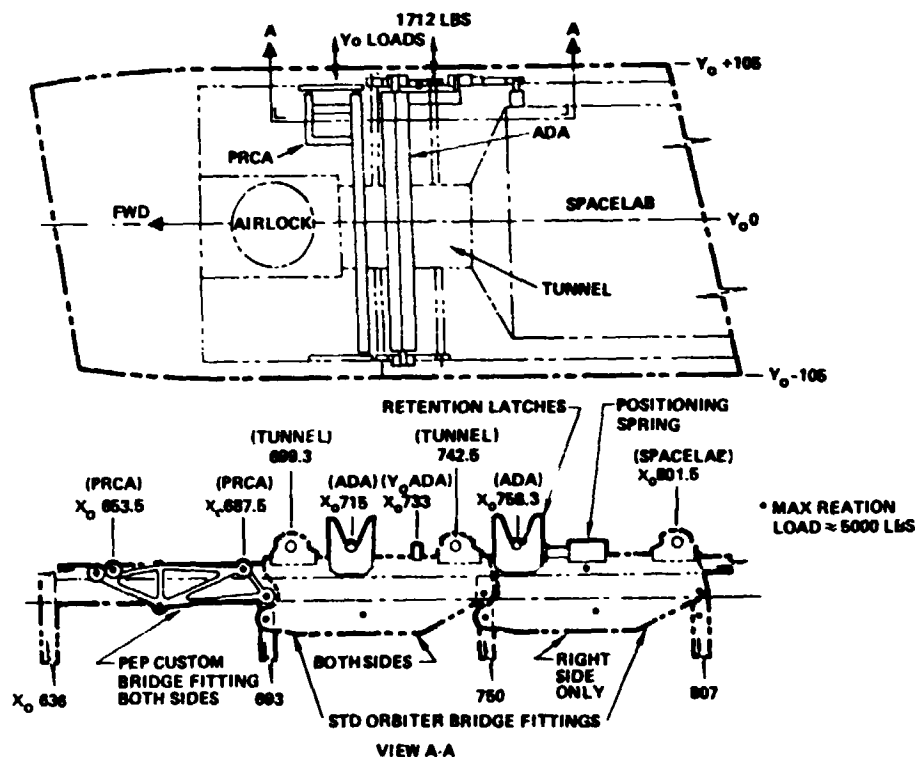


Figure 2.3-1. PEP Retention Provisions

payload pallets at any  $X_0$  location in the bay which is compatible with the payload and RMS reach limit. Figure 2.3-2 illustrates the ADA mounted over the Spacelab pallet. Figure 2.3-3 illustrates PEP mounting flexibility which may be used for Orbiter CG adjustment.

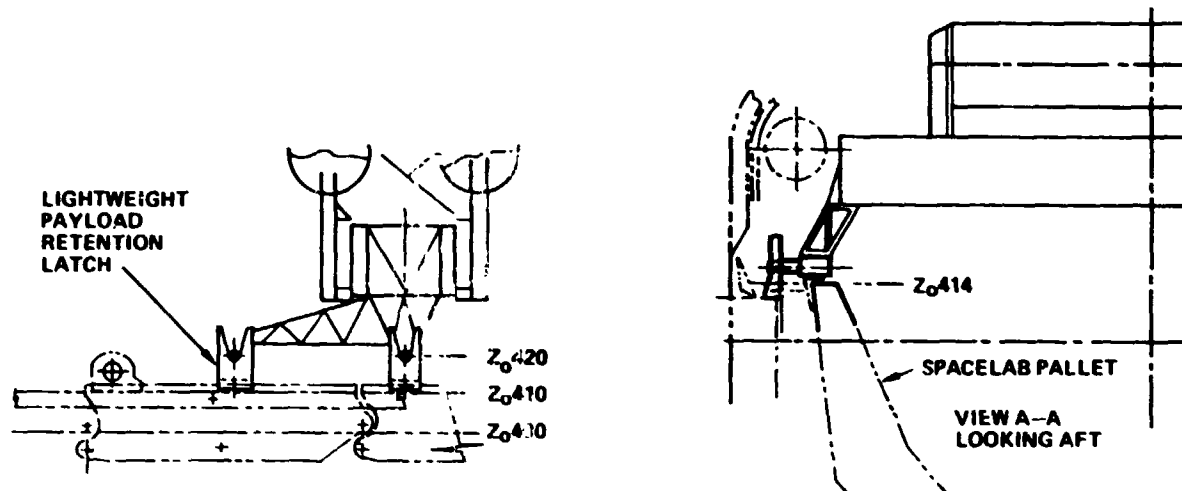


Figure 2.3-2. Array Deployment Assembly - Aft Bay Mounting

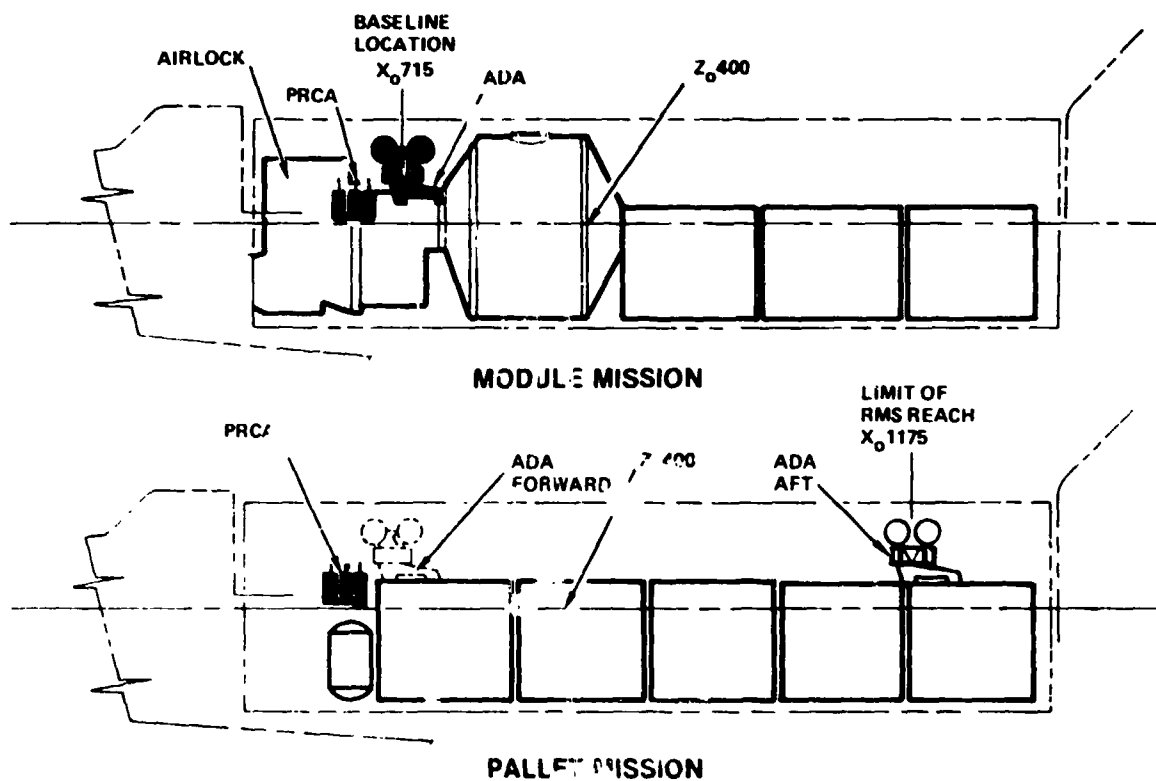


Figure 2.3-3. PEP Integration Flexibility

The standard Orbiter payload retention latch as defined by Rockwell Specification MC287-0025 is designed for a 3.25-inch diameter trunnion at an elevation of  $Z_{O414}$ . The latch is designed for a maximum reaction load of 180,000 pounds and the weight of each unit is approximately 100 pounds.

The maximum reaction load on the PEP-A11 trunnion is approximately 5000 pounds. The trunnion stowed centerline must be at  $Z_{O420}$  and it would be desirable to reduce the ADA trunnion diameter below the standard to reduce weight. The standard retention latch weight would be approximately 15% of the total PEP system weight if they were used. Based on these findings it was concluded that PEP would require a custom lightweight retention latch design. Figure 2.3-4 illustrates a design concept for a retention latch for PEP which is a "scaled down" version of the existing Orbiter standard design. This design could have a dual motor drive system. Figure 2.3-5 illustrates a second latch concept utilizing a single motor drive with a manual override. Both design concepts interface with a standard Orbiter bridge fitting; the journal centerline is located at  $Z_{O420}$ , the journal diameter is two inches, the ultimate load capability is 20,000 pounds, and the electrical interface would mate

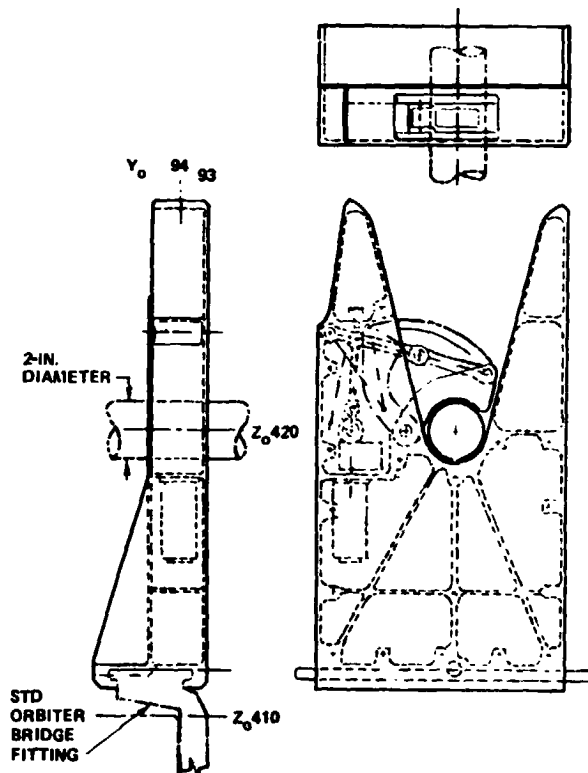


Figure 2.3-4. Lightweight Retention Latch Concept

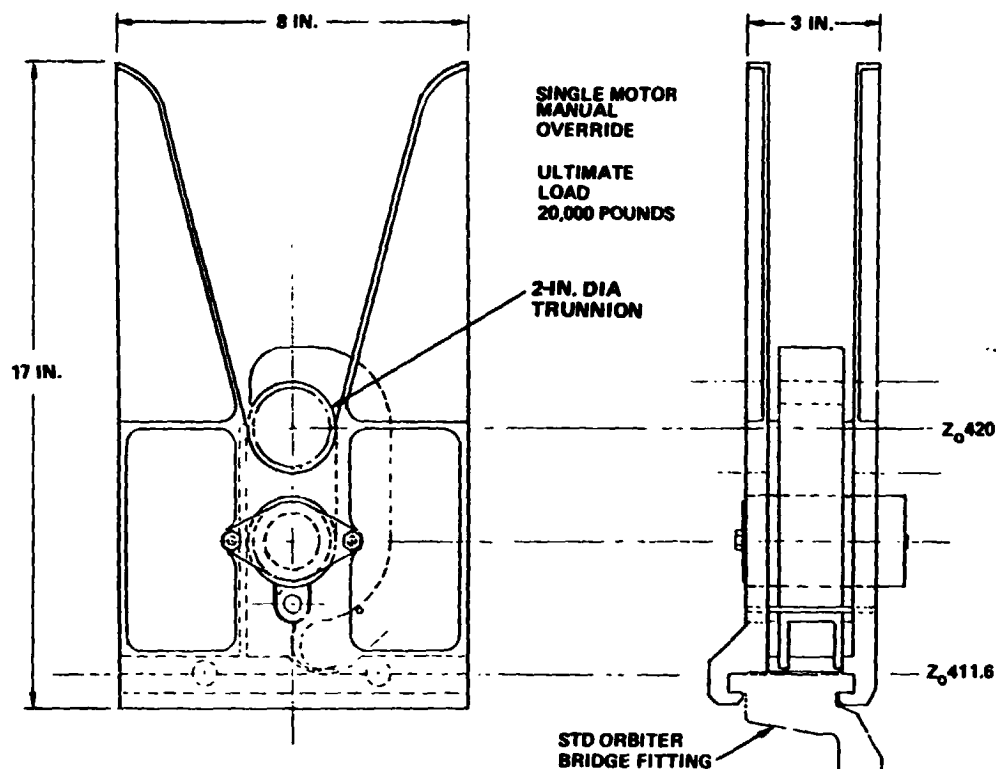


Figure 2.3-5. Lightweight Retention Latch Assembly Concept

with the standard Orbiter connector. The weight of the custom latch is calculated to be less than 15 pounds or approximately 2% of the PEP system weight.

## 2.4 RMS WIRING

### Objectives

The objectives of this task are: verify feasibility of a wiring interface kit concept; provide installation and routing details in support of interface definition activity; quantify impact of RMS power cable on wrist roll performance and acceptability of any limitations; determine compatibility of special purpose end effector (SPEE) wiring with PEP requirements and propose solutions to any incompatibilities; define separation device location.

### Conclusions and Recommendations

The concept of supplying the RMS power cable as a kit for installation on the RMS is feasible, however, the basic RMS must be modified to add attachment provisions for the cable. This modification must be done either during the initial fabrication of the RMS or during a period of major refurbishment. It is recommended that action be initiated to have Spar incorporate the modifications in a deliverable RMS which is compatible with PEP program schedules.

A cable routing has been established which allows unrestricted operation of all RMS joints except for the wrist roll restriction of  $\pm 180^\circ$ . The wrist roll limit has been determined to be adequate for PEP operations and for use with other payloads.

The special purpose end effector wiring is adequate to operate the PEP, however, the electrical power available to operate deployment mechanism gimbal drives and latches is limited.

The power cable umbilical, located at the SPEE and grapple fixture interface, is operated by an electromechanical actuator attached to the grapple fixture. This arrangement requires the SPEE connector be mated prior to mating the power connector.

The power cable, when installed on the RMS and the RMS is stowed in the Orbiter, violates the 93-inch clearance envelope established for the cargo bay. The intrusions are short in length and occur only at the elbow and wrist pitch joints. Investigation has shown that no physical interference will exist with any of the basic Spacelab configurations. It may be possible to eliminate these intrusions, however, the resulting power cable design and installation would be much more complex. It is recommended that the current design be used unless it can be demonstrated that a physical interference exists with a potential payload that will fly with PEP.

#### Approach

The requirements for the RMS wiring (power bus) evolved as a product of the MDAC PEP studies. Spar Aerospace Products, Ltd., of Canada, under contract to MDAC used these requirements to produce a design for the external attachment and handling of PEP power bus on the RMS.

#### Results

Figure 2.4-1 illustrates the PEP power cable installed on the port side RMS. Mounting methods employed in the design of the RMS operational cabling were used for the PEP installation. Split into two bundles of six cables each the wiring is installed on the upper inboard surface of the arm. Loops in the cable accommodate RMS shoulder and wrist roll flexure. A simple "V" Bend

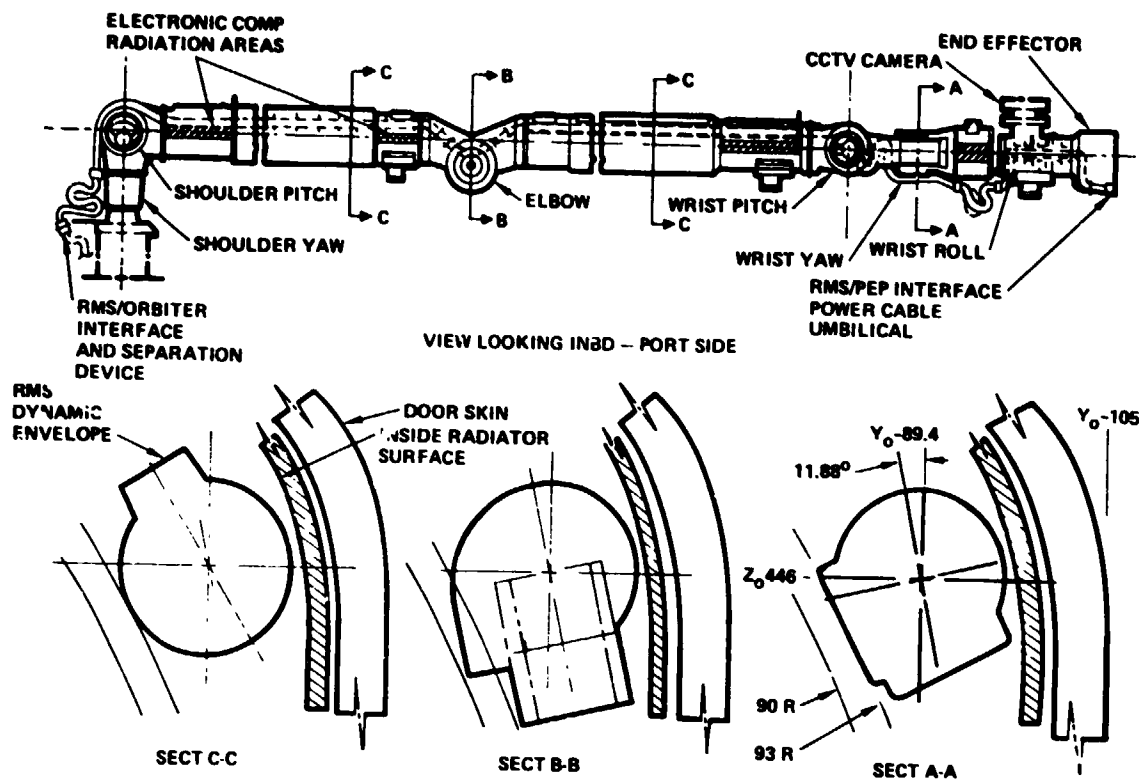


Figure 2.4-1. RMS Power Cable

allows elbow motion and an "S" cable configuration is used for wrist pitch and yaw. Figures 2.4-2 through 2.4-6 contain the mechanical details of cable handling system design. Additional details and analysis are contained in Appendix A, Spar Report SPAR-R 940.

The PEP power cable is attached to the RMS using custom designed cable support assemblies spaced at approximately 8-inch intervals for the entire length of the RMS arm. These supports are attached using screws into bosses which penetrate the Kevlar bumper coating on the exterior surface of the boom and are bonded to the composite structure. At the joints fiberglass guides are attached to contain the cable and allow flexing.

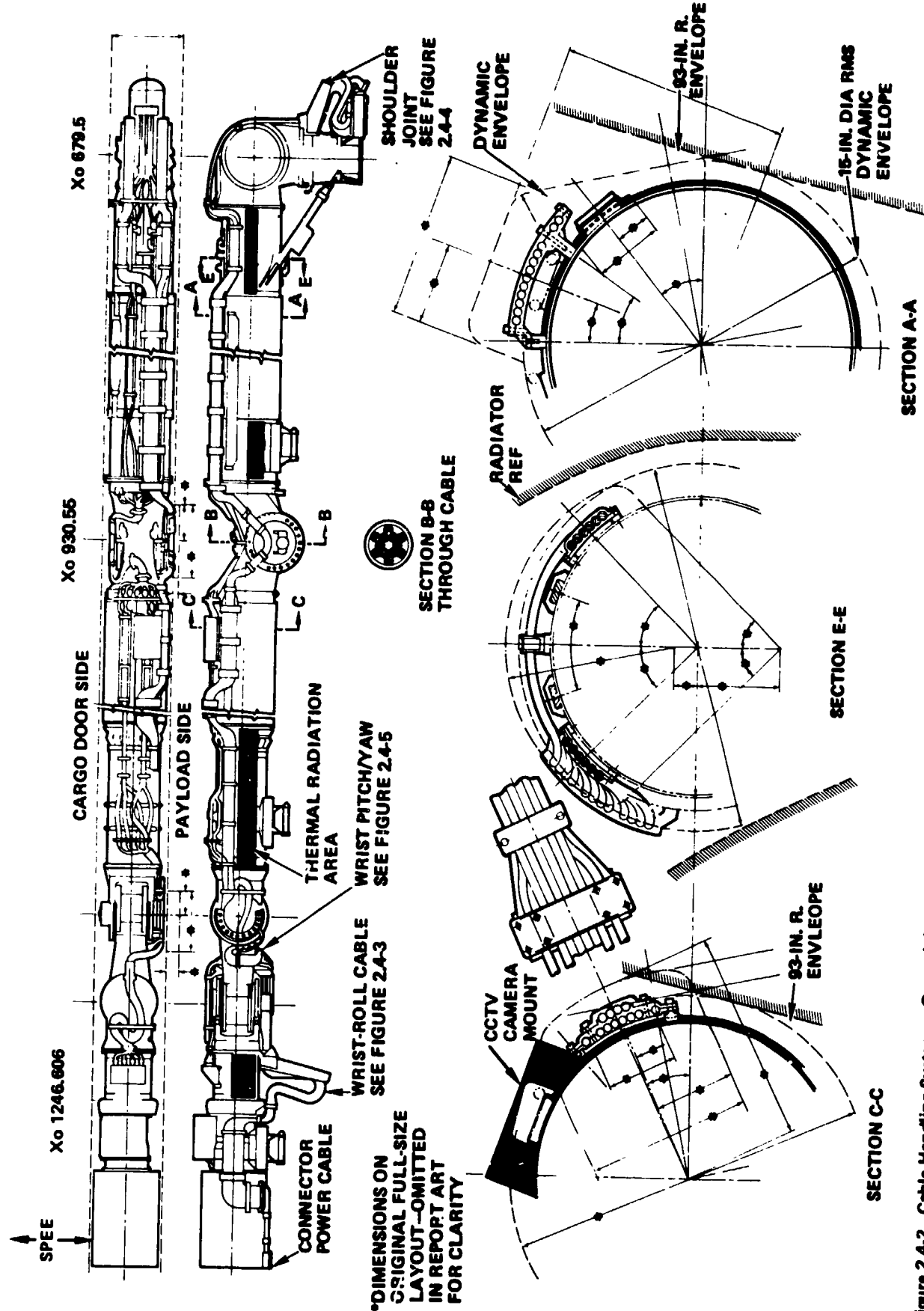


Figure 2.4-2. Cable Handling System - General Arrangement

\*DIMENSIONS ON ORIGINAL  
FULL-SIZE LAYOUT OMITTED  
IN REPORT ART FOR CLARITY

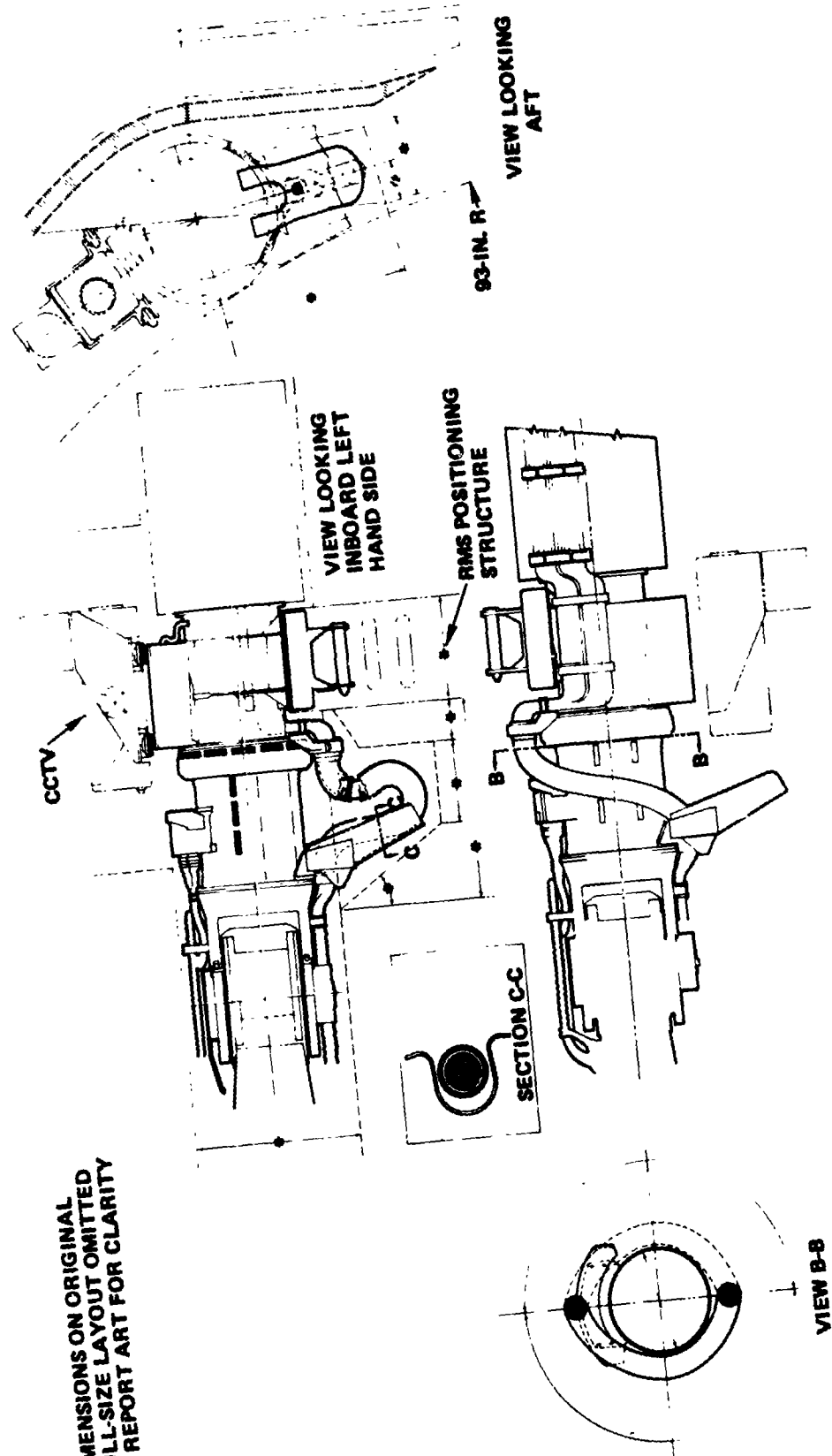


Figure 2.4-3. Cable Handling System - Wrist-Roll Joint

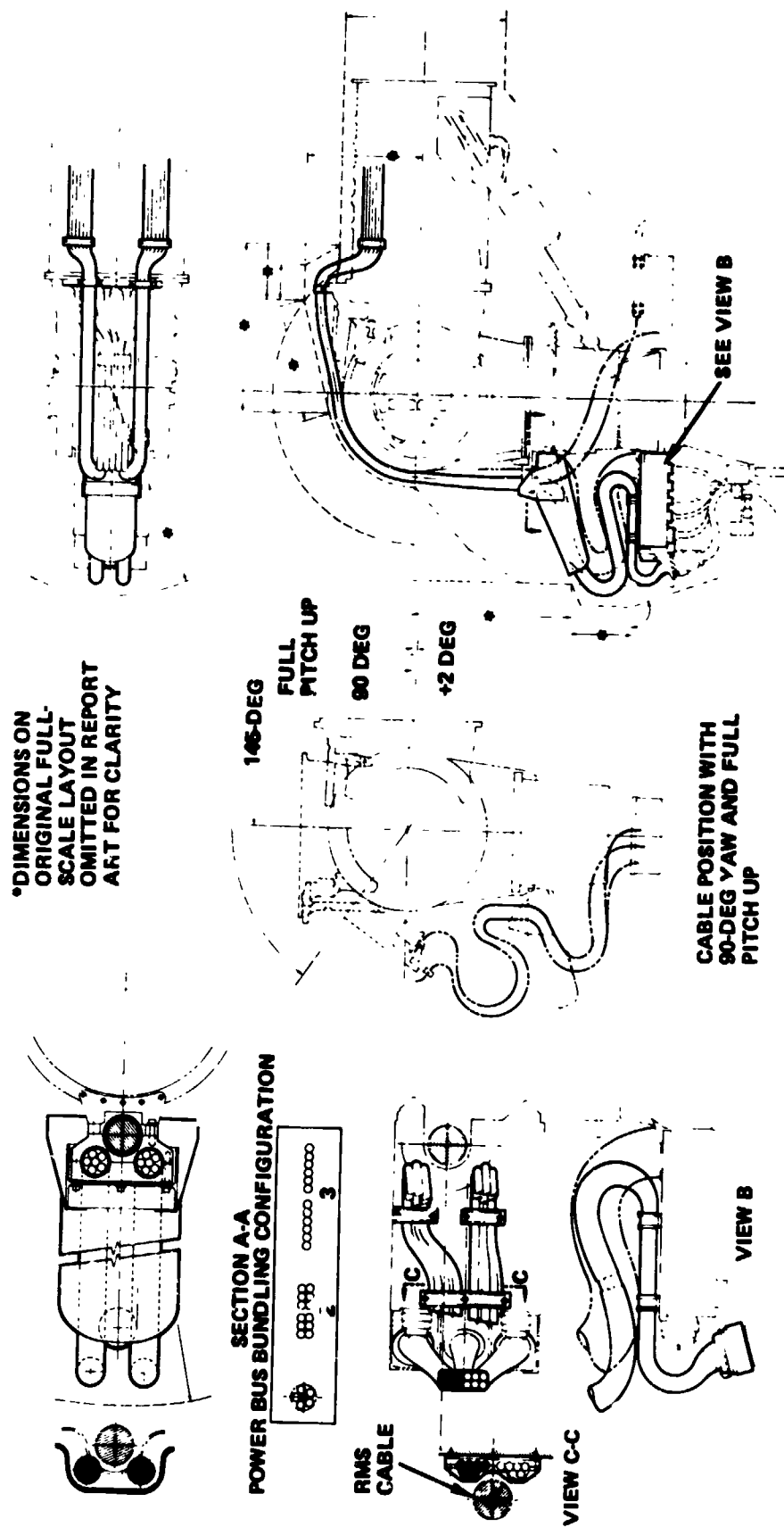


Figure 2.4-4. Cable Handling System - Shoulder Joint

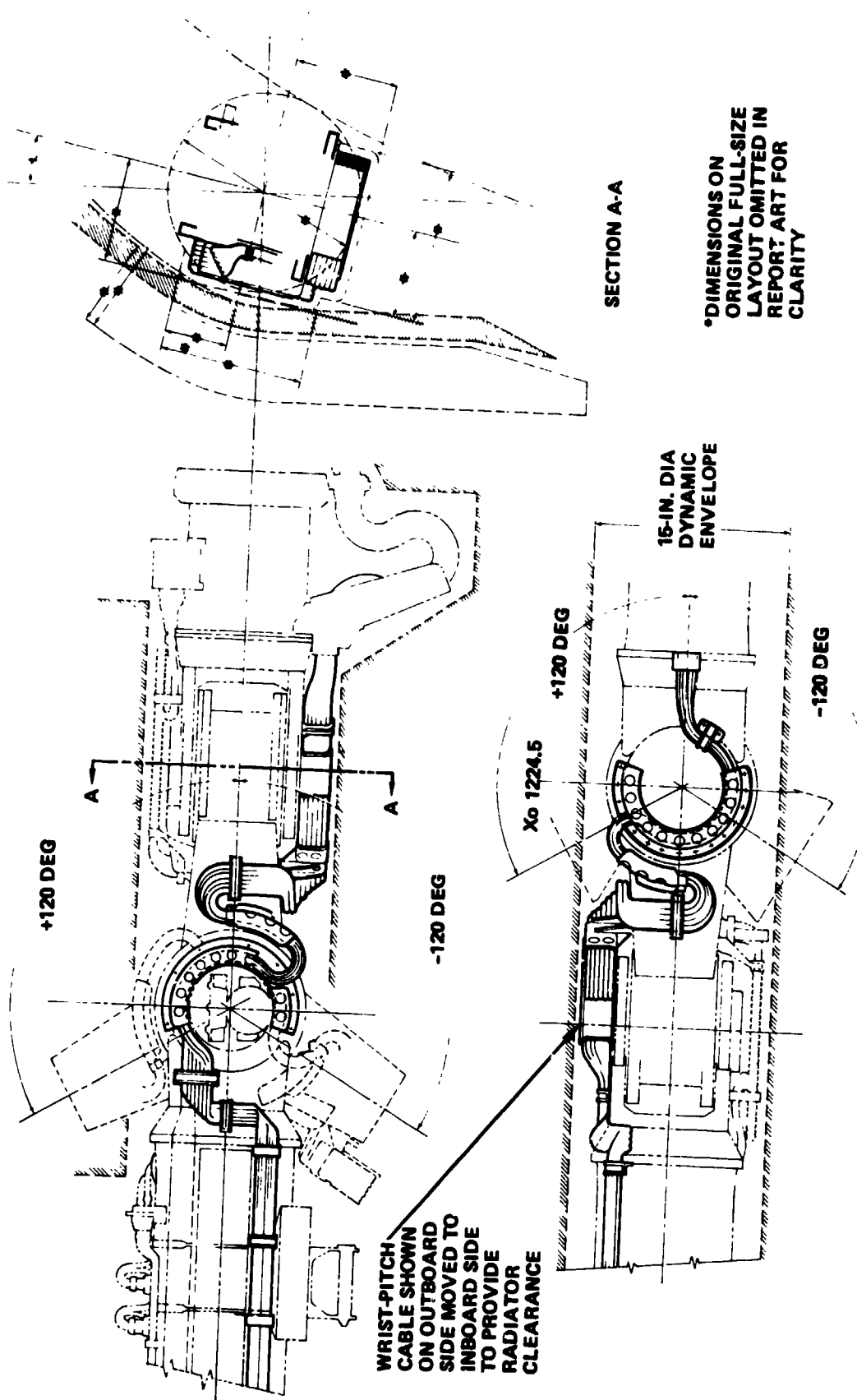


Figure 2.4-5. Cable Handling System -- Wrist Pitch/Yaw Joint

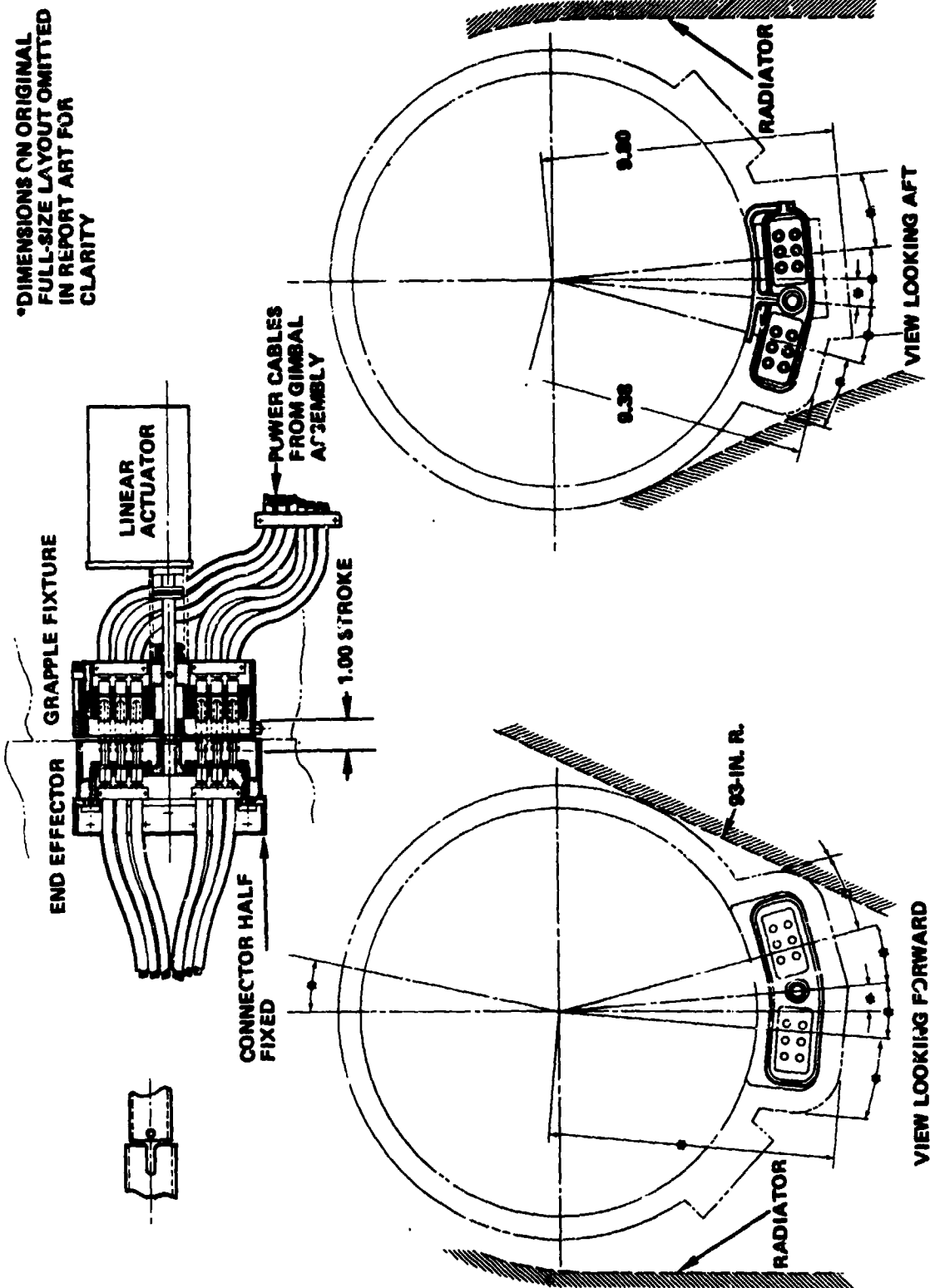


Figure 2.4-6. Cable Handling System Umbilical Interface at SPEE

## 2.5 WJNG DEPLOYMENT MECHANISM

### Objective

The objective of this task was to re-examine the configurational relationship between the array wing box and the mast canisters. The two basic considerations included the packaging subassembly concepts and the issue of rotating versus fixed canisters.

### Conclusions

The analysis concluded that the lowest weight (and probably lowest cost) concepts were either the integral wing box or the strongback versions. The integral wing box concept was recognized early in the study as the concept most likely to meet an early system weight bogie of 2010 pounds and was the primary reference configuration. Late in the study it was determined that wing box flexure from the box cover preloading of the contained array blanket would present an undesirable interface condition between the wing box and the core integration structure. The reference configuration was then altered to reflect the strongback concept features.

The early study selection of the rotating canister concept was related to mast canister sizing criteria of that period which pointed toward very long canister geometry which would not have fit between the airlock and the Spacelab in a fixed canister arrangement. Subsequent canister sizing criteria has resulted in shorter canister geometry and reassessment of canister stowage positions in PEP was done. Canister lengths are now possible which would allow a non-rotating canister PEP configuration. That arrangement is possible by placing the canisters side by side with the mast being eccentric to the array blanket centerline. Reassessment of rotating versus fixed canister issue concluded that either concept will fit the PEP criteria. However, the rotating canister feature was retained for the reference concept because it still allowed a greater degree of tradeoff between canister diameter. In addition, a preliminary examination of the dynamics of the off-center mast indicates satisfactory dynamic behaviour; however, a more rigorous analysis is necessary to verify the preliminary conclusion.

### Approach

PEP was re-examined for the configurational approach to the "where" and "how" to join the wing boxes, the canisters and the integration structure. Four var-

iations on the subassembly concepts were examined and included:

- Integral Wing Box--Wing box as a load-carrying member of the array integration structure.
- Strongback Concept--Wing box as an attachment to the load-carrying integration structure (strongback).
- Modular Wing Concept--Integrated wing box/canister module as an attachment to a strongback.
- Integral ADA-PRCA Concept--A strongback variation in which the ADA has a minimal integration structure and which stows on a strongback which is the PRCA support structure.

The fixed canister variation is applicable to any of the concepts but was examined only in the integral wing box concept (the early reference configuration).

Integral Wing Box Concept--This concept uses lightweight structure to join the two wing boxes into a structural box beam having the largest cross section possible within the envelope constraints of the ADA. This box beam has the mast canisters and the gimbal package installed upon it. This concept results in the most complex mechanical interface between the wing box and the integrating structure. This interface consists of a large number of attachments along the edge of the wing box. This approach rigidizes the two wing boxes to each other and requires a method to decouple the wing masts or canisters from the overall array core structure for a desired low natural frequency. Figure 2.5-1 shows the subassembly concept utilizing the integration core structure to interrelate the mast canisters and the wing boxes. The canisters are supported on the core structure with either single or double trunnions. The masts are decoupled either by providing a method of springing the deployed mast within the canister or by springing the canister on its support structure. This spring system must be so designed as to be locked out during wing box cover locking and canister rotation.

Strongback Concept--This concept, Figure 2.5-2, is very similar to the integral wing box concept except that the wing boxes do not act as load-carrying members of the core structure. They will be attached to the core structure in a manner that will minimize structural coupling. With the clearance necessary for the blanket tensioning and guidewire reels on the bottom of the wing boxes

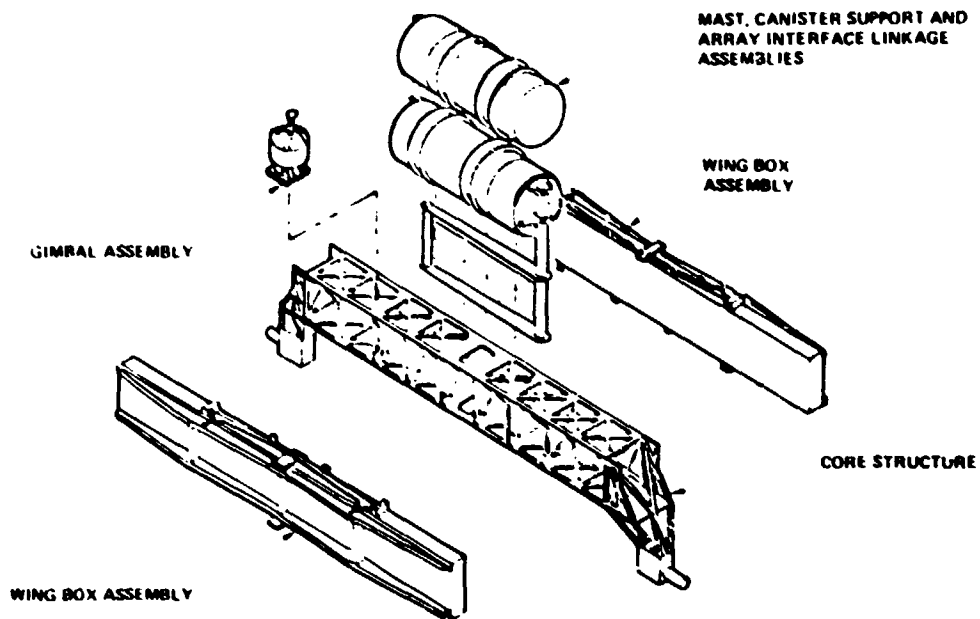


Figure 2.5-1. Subassembly Concept for Integral Box Configuration

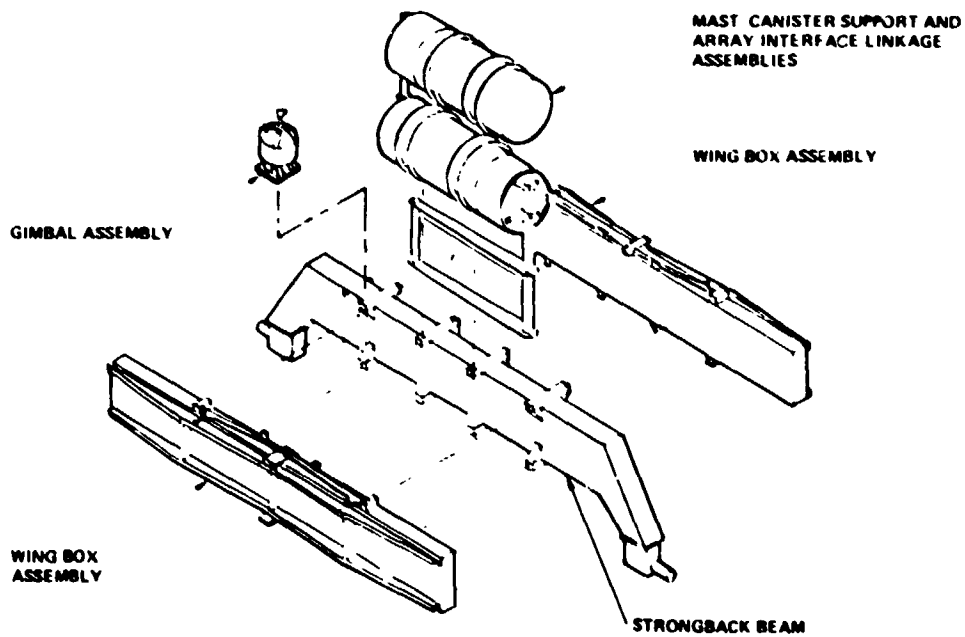


Figure 2.5-2. Subassembly Concept for Strongback Configuration

the width of the core structure is reduced by approximately one-third compared to the integral wing box concept. That, in conjunction with side panels added to replace the wing boxes, will make overall ADA weight larger. In this concept the wing boxes attach to the core structure with only four bolts. The canister mounting and decoupling would be the same as the integral wing box concept.

Modular Wing Concept--This concept is a significant variation in that the wing box and the associated mast canister is joined into a structural assembly which is then mounted on a strongback-like beam. This concept similar to the strongback concept suffers from a narrower and heavier core structure beam. There are two methods of mounting these wing modules. One is decouple the mast from the canister or decouple the canister from its support and then rigidly attach the module to the core structure. The other method is to make the mast-canister-wing box assembly a rigid system and spring mount the module to the strongback as seen in Figure 2.5-3. This concept offers modular assembly and rigging of the mast and wing box assemblies and displays interface and programmatic advantages. This configuration was explored by LMSC during their

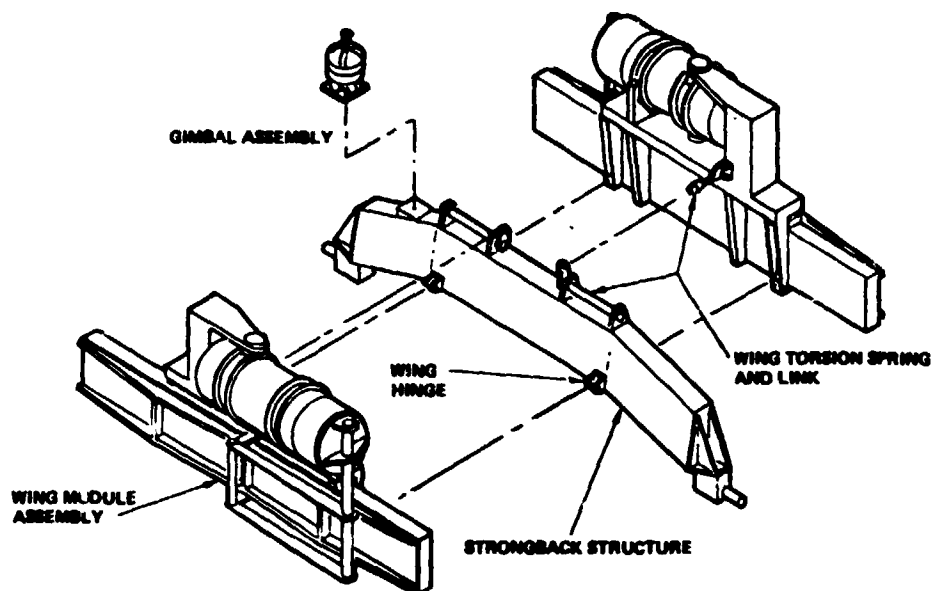


Figure 2.5-3. Subassembly Concept for Modular Wing Configuration

PEP-related studies and selected as their preferred configuration. The modular-wing configuration necessarily suffers the least efficient structural geometries and is the heaviest of the options studied.

Integral ADA-PRCA Concept--This concept is a variation of the strongback concept with significant weight reduction as the primary goal. Examination of the allocation of weight in the various PEP elements shows that a significant amount of non-array weight lies in the bridge and retention fittings necessary to interface PEP with the Orbiter. The concept solution has a strongback structural beam which was configured to support the system electronics from which a small saddle structure is mounted and deployed. The wing boxes and the mast canisters are attached to this saddle structure either as discrete elements as in the strongback concept or as module assemblies as in the modular concept (see Figure 2.5-4).

This concept shows the potential for a very low weight approach if the ADA installation occurs at the forward location where the electrical systems interfaces are. For missions which require the ADA to be located at same aft position for payload viewing or center of gravity control a conflict exists.

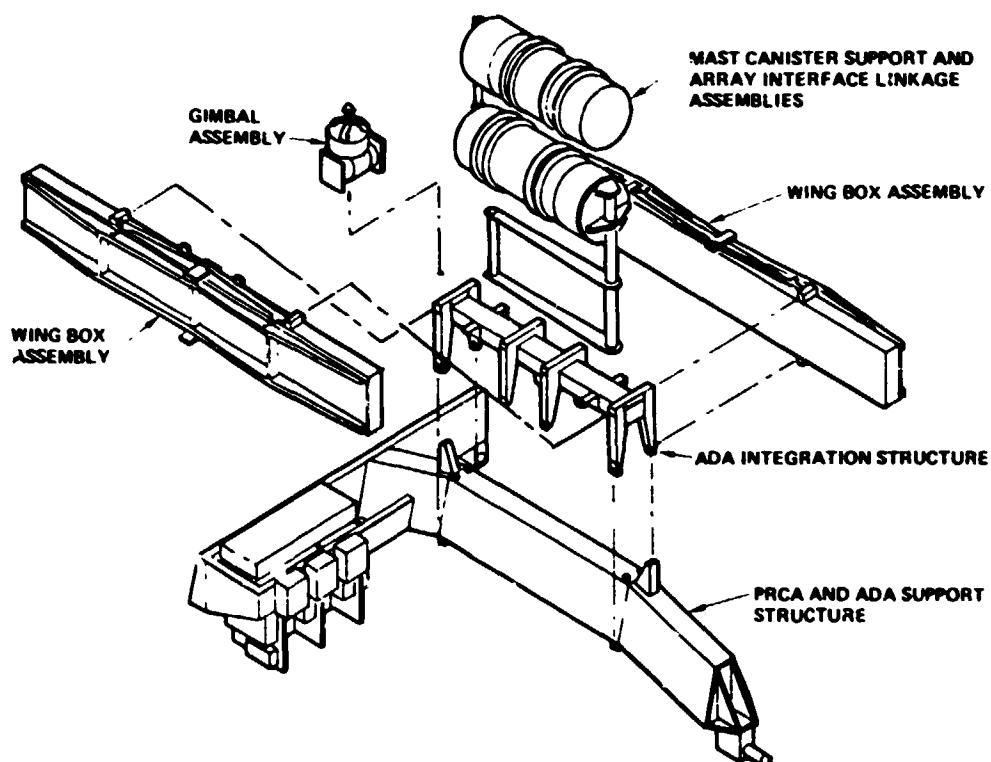


Figure 2.5-4. Subassembly Concept for Integrated ADA and PRCA

If the ADA-PRCA package was moved aft the new electrical interface condition occurs which requires a special kit. If the PRCA/strongback is left in the forward position then a new kit structural beam (possibly a duplicate strongback structure) is required. Also a possibility occurs for the need of additional bridge and retention fittings. Either of these aft location solutions tend to nullify the potential weight improvements of the basic ADA-PRCA integrated concept. Because of the great desirability for aft-bay mounting flexibility of the ADA for Orbiter CG adjustment, the strongback, two-assembly concept was selected as the referenced design.

These concepts were evaluated with the rotating canister approach which PEP was configured for in the original study. More recently mast-canister design criteria and discussions with manufacturers of those systems led to a downsizing of the canister and a reappraisal of the trade between a rotating canister and a fixed canister in the PEP configuration. Some comparison data in the mast-canister sizing for the two approaches is found in Section 2.10. Fundamentally the rotating canister requires a scheme for the rotation and results in a mast-array blanket with symmetrical geometry while the fixed canister requires no scheme or mechanism but results in mast asymmetry of approximately 16 percent of the blanket width and slightly larger and heavier mast-canisters. A PEP configuration for fixed canisters is seen in Figure 2.5-5. All of the first four concepts were evaluated for fixed canister application and were found to be conceptually compatible.

## 2.6 FUEL CELL VOLTAGE CONTROL

### Objective

The objective of this study effort was to assess methods of controlling the fuel cell voltage to assure fuel cell operation at 1.0 kw each while not exceeding allowable Orbiter bus voltages.

### Conclusions and Recommendations

Coordination with JSC on the six Orbiter/PEP interface schemes discussed here led JSC to baseline the use of a 33.0V Orbiter load bus and payload voltage limit. The load bus/regulator sense point must be controlled to a voltage 0.4V below the bus limit. The IDD scheme of tying the PEP into the fuel cell bus feeder provides the best mission duration performance for a given bus voltage limit. PEP system sizing should be updated when Rockwell has a better estimate of Orbiter line lengths/losses and PEP interfaces.

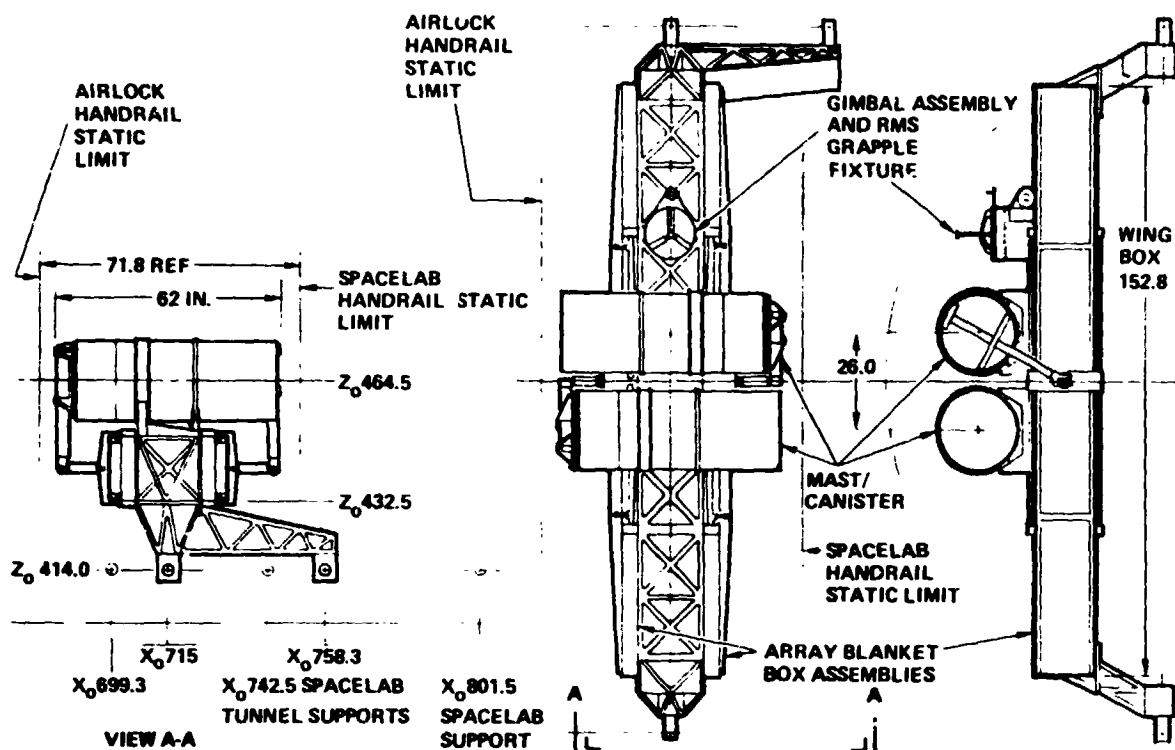


Figure 2.5-5. Fixed Canister Concept

### Assumptions

The PEP/EPS integration must minimize the impact on the Orbiter. The Orbiter bus voltage can be raised to 33.0V, although the present limit of 32.0V is preferred. Fuel cell voltage - current characteristics are as defined in Figure 2.6-1, which will be discussed subsequently. Mission duration performance requirements necessitate fuel cell operation at an average output of 1.0 kw each during the sunlit periods of the orbit.

### Approach

Various power system options were postulated and evaluated for suitability with the Orbiter system and the fuel cell current-voltage characteristics. The fuel cell characteristics used were obtained through the courtesy of United Technologies, Power Systems Division. The data was checked with data from JSC and RI and good agreement was found. Alternate solutions were compared on the basis of FCP idle level, system weight and array size and cost.

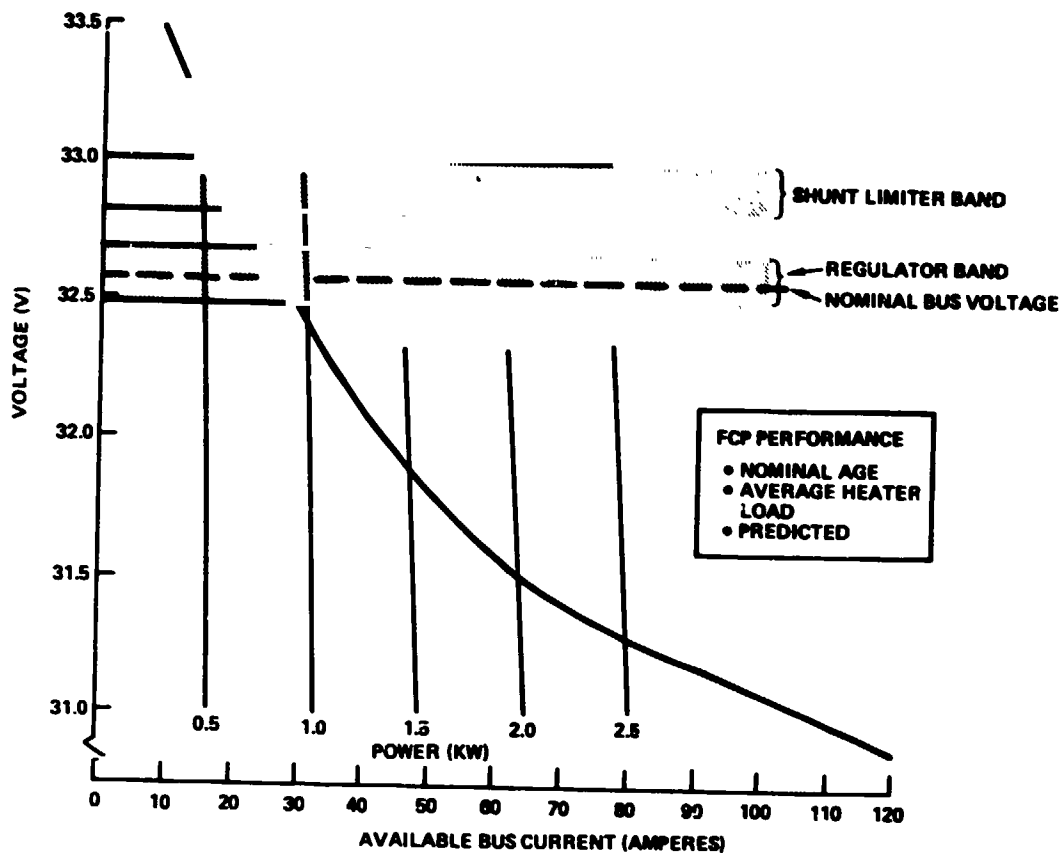


Figure 2.6-1. PEP and Orbiter Fuel Cell Voltage Regulation for 33V Bus Limit

### Results

The Orbiter is currently powered night and day by three fuel cells, nominally one on each of the three load buses. The PEP solar array provides energy only when illuminated, which can vary from 62% to 100% of the orbit period, depending on launch time and inclination; the fuel cell power to the bus must be: (1) reduced to approximately 1.0 kw per fuel cell during the illuminated period, and (2) re-initiated the following night, while maintaining satisfactory steady state and transient voltage regulation.

The relevant fuel cell and voltage regulator voltage characteristics are presented in Figure 2.6-1; the fuel cell curve is for a nominal age fuel cell, midway between the characteristics for new and for old (5000 hour age) fuel cells. The curve is based on analytical predictions by the Power Systems Division and assumes average heater loads. The figure also shows the PEP shunt limiter and voltage regulator operating bands, assuming the maximum allowable Orbiter bus voltage is 33.0V. The shunt limiters, which are discussed in Volume 2, protect the Orbiter buses from overvoltage transients for certain voltage regulator failure modes. The 0.2V wide band allows for all factors

that effect voltage (e.g. adjustment and voltage reference inaccuracies and variations in shunt current). The 0.2V voltage regulator operating band allows for similar inaccuracies and variations. The two bands are separated by 0.1V to assure that the two units do not overlap and interact with each other.

The nominal bus voltage (32.6V for the example), which represents the midpoint of the voltage regulation band, has been used for nominal performance predictions. The nominal bus voltage must always be 0.4V below the maximum allowable bus voltage (e.g., 32.6V for the example, or 31.6 for a 32.0V case). The intersection of the fuel cell curve and the nominal bus voltage represents the fuel cell operating point (~0.9 kw for the 32.6V example of Figure 2.6-1).

The fuel cell power is controlled by adjusting the location of the voltage regulator band. (The setting depicted is the highest allowable for a 33.0V bus limit). The fuel cell power output is ~0.9 kw for a 33.0 volt bus limit and ~1.8 kw for a 32.0V limit.

The location of the voltage regulator sense point and the PEP power feeder ties relative to the fuel cell and the load buses can significantly influence the fuel cell idle power settings just discussed. A parametric evaluation was made of several alternative configurations for each of the 3 fuel cells. This work was completed in the middle of the study and is based on an early set of assumptions regarding PEP and Orbiter line lengths and resistances. These parametric results require a slightly higher PEP power output than is currently required as the result of: (1) the current selection of a less remote interface for payload power delivery and (2) other line loss reductions. An example of the assumptions and results of the parametric analysis is presented in Figure 2.6-2. The example is for fuel cell no. 2 (FCP 2) and the main B bus. The electrical loads assumed for this portion of the system are: (1) 5.0 kw to the payload and (2) an Orbiter load of 4.67 kw on main B (one-third of the Orbiter 14.0 kw load). The example is for the IDD a case wherein the PEP power is fed into the Orbiter near the fuel cell in its feeder to the bus; a wire temperature of 100°C was used, and 32.0V maximum is allowed on Orbiter loads and payloads. The 32.0V limitation necessitates the main B bus to be 31.62V as noted on the figure (the current value would be 31.60 per the above discussion of Figure 2.6-1). Load feeder losses are neglected in setting the 31.62V bus limitation, because the loads on any given bus might be very low at



A summary of the parametric study results is presented in Table 2.6-1. The example just described is the fuel cell power plant (FCP) feeder (IDD) case, column 1; Figure 2.6-2 is for the FCP 2 case where the FCP provides 1.65 kw. The total FCP output is 4.98 kw which yields a 17.0 day mission duration as contrasted to the desired 3.0 kw required to achieve approximately 20 days mission duration (at 21 kw load,  $55^{\circ}$  inclination and solstice launch). The PEP electrical output is relatively low (24.22 kw) for the IDD case, because the fuel cells provide a relatively large amount of power (4.98 kw):  $24.22 + 4.98 \text{ kw} = 29.20 \text{ kw}$ . The long duration options all require larger PEP outputs and solar arrays, as can be noted in the solar array production cost item. Array costs, which are a system driver, are based on  $\$21,850/\text{m}^2$  for production. The blanket weight, which predominates the solar array, is shown in Table 2.6-1.

The following comments apply to the various other options of Table 2.6-1:

A. J-Box Splice (Dec '78 BL), Aft PCA6--This option represents the December 1978 baseline\* wherein the PEP power is fed to the Orbiter relatively remotely from the fuel cells so that line losses and sensor locations have an adverse effect on FCP voltage and, consequently, fuel consumption and mission duration (see Table 2.6-1). The weaknesses of this scheme were recognized late in the previous study phase and the utilization of the MDA's was discussed with JSC personnel at the November 1978 final review. Rockwell International was also queried about the installation feasibility of the IDD approach in telephone discussions in early January 1979.

B. J-Box Splice (Dec '78 BL), Aft PCA4--This scheme is a variant of the previous scheme where in FCP1 operation is improved by feeding PEP power at Aft PCA4 rather than Aft PCA6. This scheme is preferred to the Aft PCA6 approach.

C. FCP Feeder (IDD), 32.68V max--This option assumes that the 32.0V load bus limit can be raised to 32.68V in order to get the fuel cell operation down to 1.0 kw each. The selected reference system is similar to this, except the voltage limit is raised to 33.0V to provide some margin. The PEP power output requirement is higher in this case as discussed earlier, as is the regulator power and, consequently, heat rejection.

\*DaRos, C. J., Orbital Service Module Systems Analysis Study Documentation. MDCG7555, Volume 2 Technical Report, Contract NAS9-15532, December 1978, p. 79.

Table 2.6-1. PEP/Orbiter Power Output Options<sup>1</sup>

	FCP Feeder (IDD)	J-Box/Splice (Dec. '78 BL) Aft PCA 6	J-Box/Splice (Dec. '78 BL) Aft PCA 4
FCP power output, kW			
• Average/total (3 FCPs)	1.66/4.98	2.19/6.56	2.04/6.13
• FCP 1	1.68	2.66	2.23
• FCP 2	1.65	2.00	2.00
• FCP 3	1.65	1.90	1.90
PEP power output, kW (PDB/load bus)	25.99/24.22	23.71/22.64	24.23/23.07
Mission duration days			
• 21kW, Solstice, i = 55°	17.0	15.1	15.6
• 21kW, Equinox, i = 55°	12.2	11.1	11.4
Weight, lb	776	698	714
• Blanket <sup>2</sup>	634	570	583
• Wire and equipment (Δ)	142	128	131
Array blanket cost <sup>2</sup> , \$M	6.61	5.95	6.08
Heat rejection, kW			
• Regulator	2.92	2.66	2.72
• PDB	0.26	0.24	0.24
• Diode	NA	NA	NA
	FCP Feeder (IDD) ~32.68V Max	FCP Feeder (IDD) 1 Diode	FCP Feeder (IDD) 2 Diodes
FCP power output, kW			
• Average/total (3 FCPs)	1.0/3.0	0.91/2.73	0.42/1.26
• FCP 1	1.01	0.91	0.40
• FCP 2	0.99	0.91	0.43
• FCP 3	0.99	0.91	0.43
PEP power output, kW (PDB/load bus)	~28.07/26.20	28.53/26.47	30.14/27.94
Mission duration days			
• 21kW, Solstice, i = 55°	19.8	20.3	22.7
• 21kW, Equinox, i = 55°	13.8	14.0	15.7
Weight, lb	776	878	922
• Blanket <sup>2</sup>	684	684	722
• Wire and equipment (Δ)	142	194	200
Array blanket cost <sup>2</sup> , \$M	7.14	7.14	7.54
Heat rejection, kW			
• Regulator	3.15	3.20	3.38
• PDB	0.28	0.29	0.30
• Diode	NA	0.07	0.06

<sup>1</sup>32.0 V maximum unless noted, Busses A, B, and C at 4.67 kW each and 15 kW to Spacelab

<sup>2</sup>Rated power at end-of-life

E. FCP Feeder (IDD), 2 Diodes--This option is the same as the one described in paragraph D above except 2 diodes are placed in series to get a 1.6V diode drop. The fuel cells operate at an average power level of 0.42 kw and the mission duration is 22.7 days, at the expense of a larger solar array.

The diagram illustrates a power distribution system with the following components and parameters:

- Orbiter Loads:** Represented by a resistor symbol at the top left.
- PL INTERFACE STA 845:** A power load with specifications: 5.00 KW, 159 A @ 31.4 ΔV.
- PEP OUTPUT:** A power load with specifications: 8.97 KW, 278A @ 32.46 ΔV.
- PL LOADS:** Represented by a resistor symbol on the far right.
- FCP2:** A power source with specifications: 1.00 KW (31A).
- Diodes:** A ~0.8 V DIODE and a 307 A diode are shown in the power path.
- Resistors:** Various resistors are labeled with values like 0.17 mΩ, 0.52 mΩ, 0.19 mΩ, 1.70 mΩ, 0.38 mΩ, 0.42 mΩ, 0.525 mΩ, and 180 mΩ.
- Connectors:** STA 838 I/F CONNECTOR is shown in the middle right.
- Voltages:** Labeled voltages include 31.53V, 31.5V, 31.4V, 32.1V, 32.0V, 32.41V, 31.42V, 0.03V, 0.25V, and +32.20V.
- Currents:** Labeled currents include 148 A, 159 A, 169 A, 18 A, 18 FT, 180 mΩ, 0.78 A, 307 A, and 278A.
- Power:** Power ratings include 4.67 KW, 5.00 KW, 8.97 KW, 1.00 KW, and 1.0 KW.

**NOTES:**

1. MAX LOAD VOLTAGE - 32.0V
2. 100°C WIRE TEMP
3. IDD - FC2/MAIN B
4. 1.0 KW/FCP (DIODE EXAMPLE)

**MCDONNELL DOUGLAS**

## 2.7 REGULATOR DEFINITION

Two distinct areas of effort evolved from this task which are separately reported below.

### 2.7.1 Regulator Type and Efficiency

#### Objective

To develop a 5 kw power regulator operating under microprocessor control at efficiencies of 90% or better to demonstrate the technology for application on the Power Extension Package as applied to Shuttle Orbiter.

#### Conclusions and Recommendations

The standard buck type regulator circuit, together with proprietary MDAC low-loss snubbers, can be made to serve the Orbiter Power Extension Package needs. With overall efficiencies approaching 92%, as contrasted to the units developed under separate funding which achieved an overall efficiency of 89% maximum. Adequate over-voltage protection, transient response and failure mode protections were demonstrated.

#### Assumptions

The Orbiter power system specifications, as amended by the MDAC developed PEP specifications were assumed as target goals. The power regulator requirements are listed in Table 2.7-1.

#### Approach

Several regulator configurations were initially studied. These included:

- A. Transformer coupled DC to DC converter.
- B. Resonant regulator.
- C. Buck regulator.

The transformer design approach employs a transistor switch in series with the primary of the transformer and a rectifier and filter in the secondary. Good isolation of input and output can be achieved. The transformer core and winding  $I^2R$  losses produce considerable heating and also represent potentially lower efficiency performance. Since the Orbiter's cooling capacity is limited, this design approach was not pursued.

The resonant design approach is potentially more efficient since switching is done as voltage swings through zero, giving low switching losses. A series

Table 2.7-1. PEP Power Regulator Design Requirements

Rated input voltage, $V_{in}$	111 volts
Maximum input voltage, $V_m$	239 volts
Rated output voltage, $V_o$	33 volts
Voltage regulation (at Orbiter main bus)	32.5 to 32.7 volts nominal
Maximum output voltage ripple	0.1 volts peak to peak
Rated output current, $I_o$	146 amperes
Rated output power, $V_o \times I_o$	4.8 kilowatts
Efficiency at rated $V_{in}$ , $V_o$ and $I_o$	90%
Maximum output current, $I_m$	160 amperes
Maximum output power, $V_o \times I_m$	5.3 kilowatts
Loss of remote voltage sensing	Revert to internal reference and circuit operate at lower output voltage
Peak power tracking	Track solar array peak power point within 2% for output currents less than regulator current limit set point
Electromagnetic interference (EMI)	Meet Orbiter specifications
Heat rejection	To coldplate at TBD °C

resonant tank is employed and circulating currents are higher than in other types.  $I^2R$  losses in the required inductor produce poorer efficiency and additional heating. Resonant regulators present a complex design challenge and did not produce sufficient system advantages to warrant development for use on PEP.

The buck regulator design approach, which was selected, appeared to provide potentially good efficiency, reasonably straightforward design, and good control stability. It employs a transistor switch preceeding an inductor-capacitor filter. When the switch is off, the current is maintained in the inductor by a commutating diode. Large transform ratios are easily accommodated by pulse width modulation. A block diagram of this approach is shown in Figure 2.7-1.

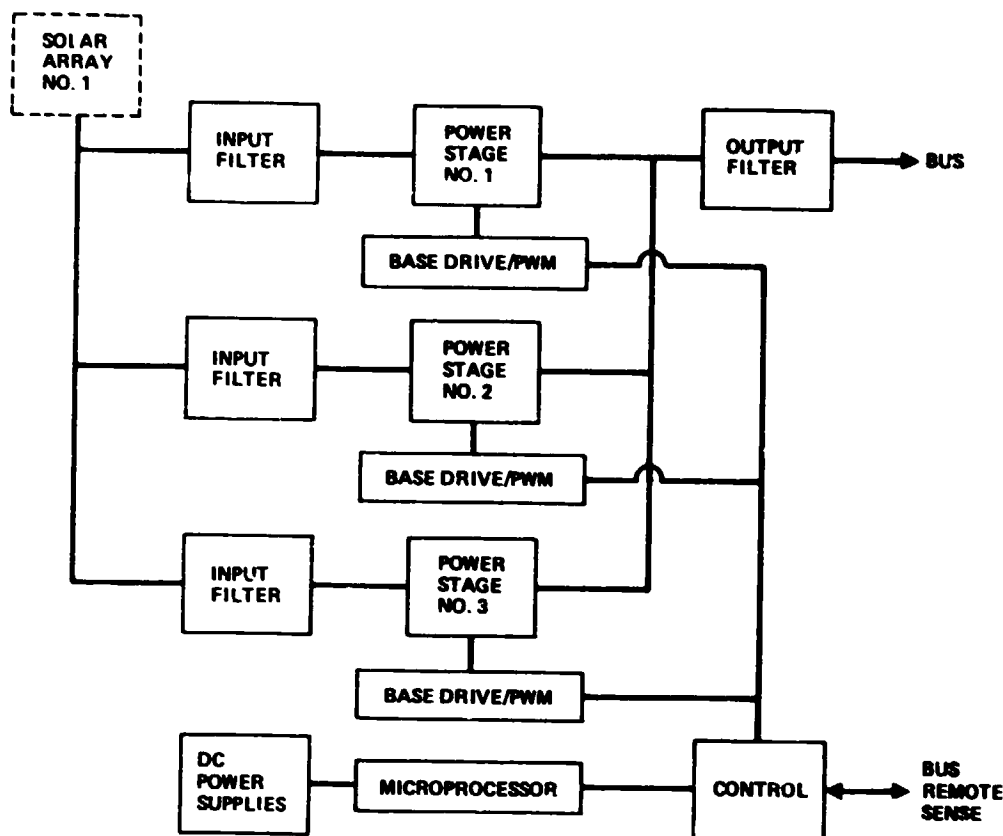


Figure 2.7-1. Buck Regulator Block Diagram (U)

Standard switching transient protection circuits protect the regulator switching transistor from much of the switching transient losses by absorbing the switching energy in storage elements and dissipating this energy in a resistor. A "low-loss" design became available later and will be considered for use in flight units to increase overall system efficiency.

A blocking oscillator drive was selected for low power and maximum pulse width limiting features.

### Results

A pair of 2.5 kw regulators along with microprocessor control were developed and tested under company funds to support this study and the EPDC tests. The efficiency curves with various input voltages are given in Figure 2.7-2. Good transient behavior and regulation were achieved over the load range from 0 to 130%. Overvoltage and fusing protection for internal failures are provided, and any one of the three parallel channels per regulator may fail with no loss of output capability.

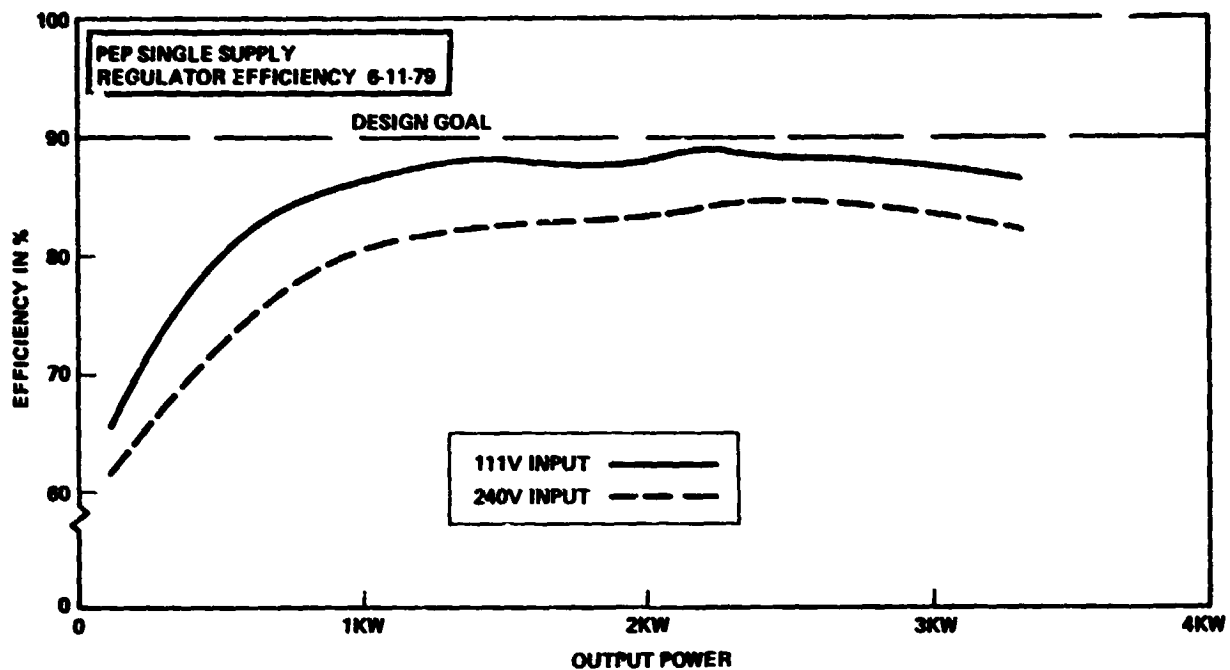


Figure 2.7-2 EPDC Test Regulator Performance

Voltage regulation of 10 millivolts over input variations from 100V to 240V and output load from 2 to 100 Amps for each supply was achieved.

### 2.7.2 Regulator Failure Modes and Effects

#### Objectives

To identify representative failure modes and corrective action and to assess resulting regulator performance and effects on system operation.

#### Conclusions and Recommendations

All identified failure modes result in either fail operational or fail safe conditions, primarily fail operational. Emphasis was placed on analyzing failures leading to bus overvoltage.

Protection against overvoltage is effectively provided by either fuses or compensating circuitry in the regulator, with external shunt regulators providing backup protection. The capability of fuses to limit overvoltage resulting from a shorted power switching transistor was analyzed using the SPICE transient analysis computer program. This analysis shows that fuse blowing occurs fast enough to limit output voltage rise to within the overvoltage envelope allowed by the Orbiter specification (Rockwell document MF0004-002).

Control circuit failures which drive the power switching transistor to maximum duty cycle and produce bus overvoltage are transparent to the fuse system of protection unless a secondary failure (power transistor short) results. Active protection circuits within the regulator provide the required protection for a control failure that does not lead to a transistor short.

A potential problem was identified involving fuses in the output filter capacitor circuits. For a short circuit on the regulator output, the fuses blow and effectively remove the capacitors from the filter circuit. If the regulator remains on line after the short is cleared, output waveform will be poor. Further analysis and testing is required to determine regulator status following the short and to provide an alternate fuse location if needed.

Additional analysis also is recommended to evaluate tradeoffs in flight regulator design. Examples are (a) input capacitor size to meet filter requirements versus capacitor-stored energy required to blow fuses for single part failures (fail operational design), and (b) benefits of fusing for single part failures versus fuse  $I^2R$  losses and resulting lower regulator efficiency.

#### Assumptions

A. Regulator circuit model is based on MDAC breadboard regulator developed for PEP simulation and evaluation tests at JSC.

B. Solar array equivalent circuit is derived from I-V curve for minimum operating temperature (maximum array voltage).

C. Fuel cell equivalent circuit is derived from an I-V curve with 34 volts at no-load. The PEP study groundrules limit the maximum steady state voltage at the load buses to 33 volts.

D. Shunt regulator is not included in equivalent circuits (worst case assumption).

E. Bus loads are not included in simulation (worst case assumption).

F. Regulator remote sensing/control dynamics are not simulated (worst case assumption).

G. Regulator capacitor ESR values are assumed to be 50% of supplier guaranteed maximum ESR.

#### Approach

The study was preliminary in nature, focusing mainly on failure modes which produce overvoltages on the Orbiter buses. Study results are considered conservative as evidenced by the parameter values and input/output conditions

assumed in constructing the analytical model. The model used for evaluation is indicated in Figure 2.7-3. Representative failure modes for the model were identified and resulting failure effects assessed qualitatively. The model was then analyzed quantitatively for selected failure modes using the SPICE transient analysis computer program.

For failures producing excessive or marginal bus overvoltage, the output capacitors of a second regulator in parallel with the first (and required to fully simulate the PEP regulator configuration) were added to the SPICE model. The additional capacitance is effective in reducing bus overvoltage. Fuse melt and clear calculations were coordinated with the fuse supplier (Bussman - FBP fuses). Cold resistance values were used in the analysis.

A split inductor incorporated in the MDAC breadboard (and the SPICE equivalent circuit) eliminates the possibility of fully shorting the inductor. Such a failure would result in prohibitively high instantaneous bus overvoltage.

### Results

The qualitative assessment of failure modes and effects is summarized in Table 2.7-2. In general, failures are only listed for components in the upper stage of Figure 2.7-3. Identical failures in the other two stages have the same failure effects.

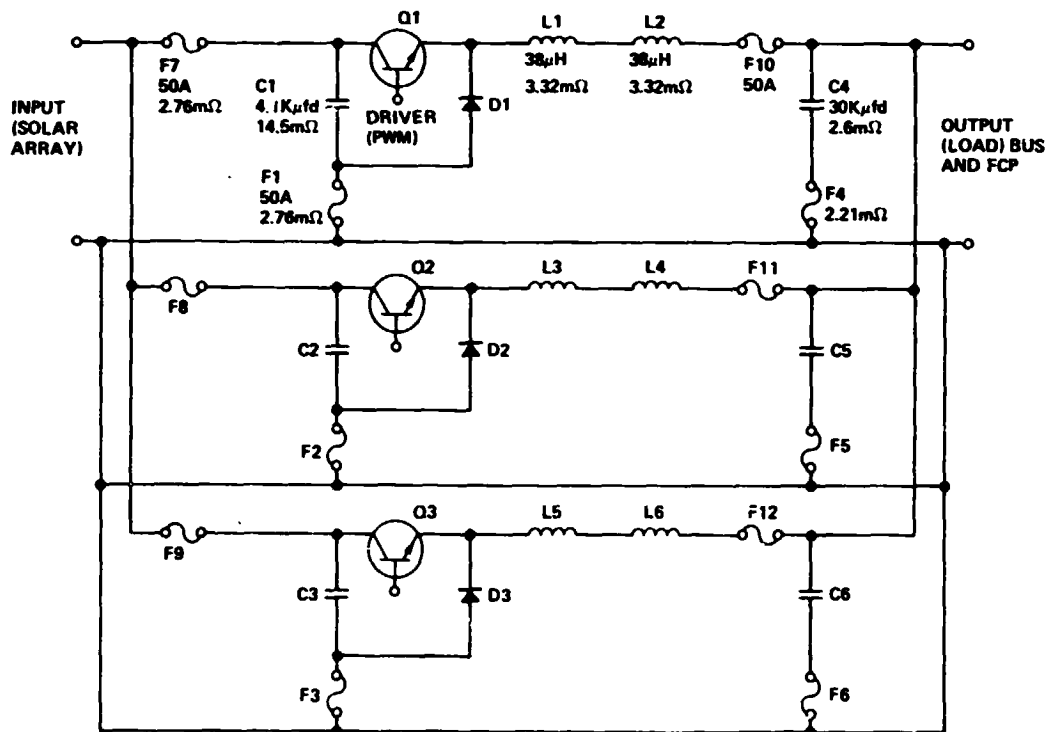


Figure 2.7-3. FMEA Circuit Model

**Table 2.7-2. Failure Modes and Effects Analysis (FMEA) Summary**  
**Two Regulators in Parallel Supplying Load Bus**

Item No.	Component or circuit	Failure mode	Failure effect
1	C1-input capacitor	Open	Loss of 1/3 of input filter--increase in switching noise on array, but within specification limits
2	C1-input capacitor	Short	Fuse F1 blows.
3	C4-output capacitor	Open	Loss of 1/3 of output filter capacitance. Regulator performance remains within specification limits; output ripple increases.
4	C4-output capacitor	Short	Fuse F4 blows. Same effect as Item 3.
5	L1-filter inductor	Open	Loss of one power stage--duty cycle on remaining stages increase--no loss of output power.
6	L1-filter inductor	Short	Faulted stage tends to supply a greater share of bus load--output ripple increases but remains within specification limits.
7	D1-commutating diode	Open	Loss of commutating path for affected stage leads to failure (short) of power transistor. Same effects as Item 10.
8	D1-commutating diode	Short	Fuse F1 should clear fault. Same effects as Items 1 and 7
9	Q1-power transistor	Open (no turn on)	Loss of one power stage--remaining stages capable of supplying regulator rated load.
10	Q1-power transistor	Short	Fuse F10 blows.
11	F7 input fuse	Open	Loss of one complete stage--remaining stages can supply regulator rated load.
12	Driver input to Q1, Q2, Q3	Drives to maximum duty cycle.	Loss of complete regulator.
13	Driver input to Q1, Q2, Q3	Fails off	Loss of complete regulator.
14	External fault	Short on output	Loss of both regulators (fail safe).
15	Remote sensing leads	Open	No interruption in service.
16	Remote sensing leads	Short	No interruption in service.

All items in the table with the exception of 14 result in fail-operational conditions.

A summary of failure modes and operational characteristics is given in Table 2.7-3.

Table 2.7-3. Voltage Regulator Safety Features

Failure mode	Corrective action	Operational status
<b>Overvoltage<sup>1</sup></b>		
Power transistor shorts	Fuse blows	Fail operational
Control drives to maximum duty cycle	Protection circuits isolate faulted regulator from bus	Fail operational <sup>2</sup>
Remote sensing leads short	Fuse blows in sensing circuit. Revert to internal reference and operate at lower output voltage	Fail operational
<b>Overcurrent</b>		
Output short circuited	Fuses blow	Fail safe
Overload	Protection circuits limit output current until overload clears	Fail operational
Control fails off	Output power goes to zero	Fail operational <sup>2</sup>
Remote sensing circuit opens	Revert to internal reference and operate at lower output voltage	Fail operational

<sup>1</sup>Main bus voltage does not exceed 33V limit used as study baseline.

<sup>2</sup>Paralleled fuel cell power output increases to make up for loss of faulted regulator.

## 2.8 STRUCTURAL DESIGN CRITERIA

### Objective

The objective of this analysis is to define a solar array mast design criteria including a compliant structure concept needed to reduce solar array mast and RMS load response to Orbiter PRCS and VRCS firing.

### Conclusions and Recommendations

The following conclusions are based on the dynamics analysis described herein. The major trade in this analysis involves interactions between mast root moment, Orbiter maneuver rate change and wing compliance frequency.

- A preliminary design value of 200 ft/lb ultimate load is recommended for the mast design criteria.
- Compliance structure should be included at the root of the array mast to reduce mast and RMS loads to an acceptable level. The compliance should be about two axes; perpendicular to the array and transverse to the array. A wing first cantilever frequency of 0.02 Hz about both axes is recommended.
- The preliminary baseline solar array blanket tension recommended is 22 pounds and gives adequate margin against mast/blanket collision.
- Since adequate system damping (Sections 2.14 and 2.18), may inherently exist in the PEP structure and RMS (particularly the joints), no damper was included in the baseline design. If additional damping is required, possible approaches are: including a damping mechanism with the compliance structure at the array mast root, utilizing mast and array blanket designs with built-in damping properties, using the PEP gimbal controller for active damping and adding a viscous-mass damper to the PEP wings. This latter approach was analyzed. The damper was mounted on the wing box cover (outer end of the array) and can meet the one percent-of-critical preliminary damping ratio requirement (Sections 2.14 and 2.18) with a 5- to 10-pound total damper weight for both wings.

The following recommendations are made for use in future work:

- The VRCS should be used for nominal limit cycle operations with the deployed PEP when plume impingement occurs.
- Either the PRCS or VRCS may be used for limit cycle operation when no significant plume impingement occurs.
- The VRCS thrusters may be held on indefinitely (except in roll as

described below) when the array is not in the plume. Thus, large maneuver rates are possible with the VRCS. For a full-on VRCS roll maneuver, the PEP c.g. must be less than 40 feet from the Orbiter centerline or the array longitudinal axis must not be close to perpendicular to the Orbiter roll axis.

- When no significant plume impingement occurs, PRCS maneuver rate maximums of 0.15 to 0.35 deg/sec are recommended when the array longitudinal axis parallels the plunge motion (no translation compliance). Rates up to one degree are possible when the plunge motion is perpendicular to the array longitudinal axis.

- When significant plume impingement occurs, maneuver or limit cycle rates should be limited to 0.03 to 0.04 deg/sec. This can only be achieved with the VRCS because of the large PRCS minimum impulse bit.

- The preliminary analysis presented herein should be repeated with a more complex dynamic model. The model should include detailed modeling of RMS mounting flexibility, RMS flexibility and non-linear characteristics and a detailed PEP model. The number of cases considered should be expanded to verify worst case conditions have been identified.

- More detailed plume impingement analysis is required to define optimum RMS/PEP positions and solar array orientations as a function of Orbiter orientation. Further analysis must consider Orbiter orientation and maneuver requirements in detail.

#### Approach/Discussion

Figure 2.8-1 defines three typical RMS/PEP positions. The solar array rotates about the PEP Alpha and Beta gimbal axes from the positions shown. Additional variation is possible by altering the RMS joint angles while maintaining the end effector wrist roll axis constant relative to the Orbiter. The typical Orbiter orientation relative to the orbit plane, used with each RMS/PEP position is noted. Positions 2 and 3 receive significant plume impingement from the aft thrusters and all three positions can be in the plume of the forward thrusters.

The simple model shown in Figure 2.8-2 was used to define the PEP mast root loads and RMS joint loads. The RMS joint loads were calculated by transforming the force ( $F_c$ ) and moment ( $M_c$ ) at the PEP center of gravity to the appropriate RMS joint position. The wing compliance modeled as a clockspring (K) at the

NOTE: SOLAR ARRAY ROTATES ABOUT THE  $\alpha$  AND  $\beta$  AXES FROM THESE POSITIONS

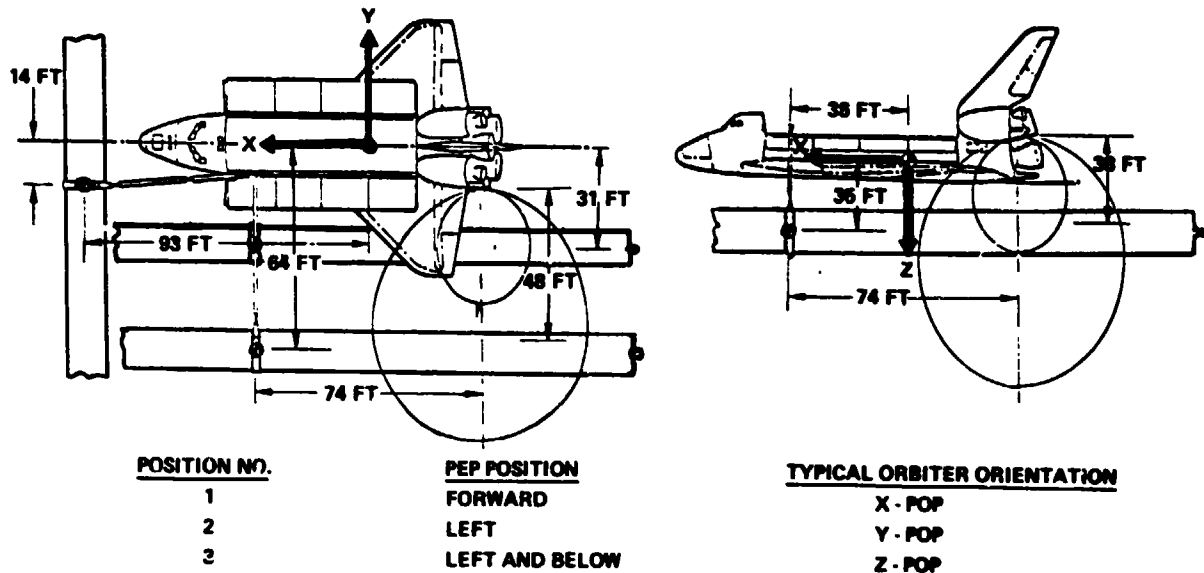
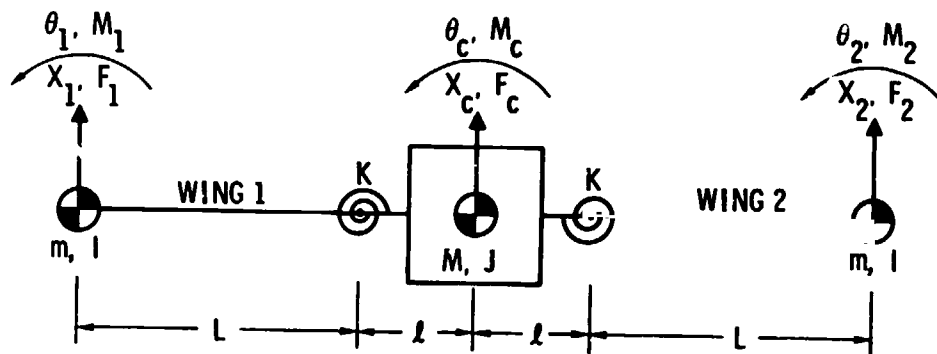


Figure 2.8-1. Typical PEP/RMS Positions



- $M = 10.8 \text{ SLUG (158 Kg)}$
- $m = 15.8 \text{ SLUG (232 Kg)}$
- $J = 18 \text{ SLUG - FT}^2 (24.4 \text{ Kg-M}^2)$
- $I = 25,700 \text{ SLUG-FT}^2 (35,000 \text{ Kg-M}^2)$
- $L = 54.1 \text{ FT (16.5M)}$
- $l = 1.5 \text{ FT (0.46M)}$
- $K = (1 + mL^2)\omega^2$ , WHERE  $\omega$  IS THE COMPLIANCE FREQUENCY (RAD/SEC)

Figure 2.8-2. PEP Dynamic Model

root of each wing represents mast compliance and/or blanket compliance and/or a compliance spring specifically mounted at the mast root. This same model was used for dynamics both in and perpendicular to the solar array plane. The position ( $X_c$ ) and rotation ( $\theta_c$ ) of the PEP center of gravity were calculated as a function of Orbiter rotation for each of the configurations shown in Figure 2.8-1. Mast root moment and RMS joint loads were calculated for a pitch maneuver for RMS/PEP Positions 1 and 3 and a yaw maneuver for Position 2. These maneuvers were analysed since they represent the longest lever arms for PEP plunge motion for each configuration and included a potential for plume impingement loads in addition to inertia loads. Thus, they are expected to be worst case. The compliance of the RMS was calculated based on a 0.3 Hz no-payload cantilever frequency.<sup>1</sup>

The plume impingement forces and moments were calculated for RMS/PEP Positions 2 and 3. They were applied to the model (Figure 2.8-2) as " $F_1$ " and " $M_1$ " and the corresponding mast root moment and RMS joint moments determined. Since Orbiter angular rate increment is proportional to thruster impulse, as is plume impingement impulse, plume impingement impulse is proportional to angular rate increment. It should be noted, also, that since the PRCS and VRCS thrusters are similar, the impingement pressures are proportional to thrust and so impingement impulse per incremental Orbiter rate is the same for the PRCS and VRCS. The PRCS minimum impulse bit is much larger, however.

Since PEP center of gravity linear motion ( $X_c$ ), rotational motion ( $\theta_c$ ) and plume impingement force and moment ( $F_1$  and  $M_1$ ) are assumed to be linear functions of Orbiter rotation, the mast root torques and RMS joint torques can easily be calculated for the single input disturbance, Orbiter rotation.

Loads were calculated based on impulse rather than acceleration since RMS and PEP wing compliance was included. If the disturbance durations are short relative to the compliance oscillation periods of interest, the loads are linear functions of disturbance impulse. This conservative assumption was made and is implicit in the results unless otherwise stated.

---

<sup>1</sup>McDonnell Douglas Report MDC G7555 (Vol. 2), "Orbital Service Module Systems Analysis Study Documentation, Technical Supporting Data," Paragraph 2.1.6, dated December 1978.

Preliminary solar array blanket tension was defined using a detailed dynamic Orbiter/RMS/PEP model<sup>2</sup>. The specific model was of the offset, single blanket with the PEP positioned similar to the Position 3 defined herein in Figure 2.8-1. A compliance spring mounted at each mast root with a rigid wing cantilever frequency of 0.02 Hz was utilized based on preliminary calculations. The blanket tension selection was based on relative blanket/mast deflection resulting from an Orbiter roll maneuver and the plume impingement load associated with a pitch maneuver. Mast root loads and RMS joint loads were also calculated for these cases for various blanket tensions.

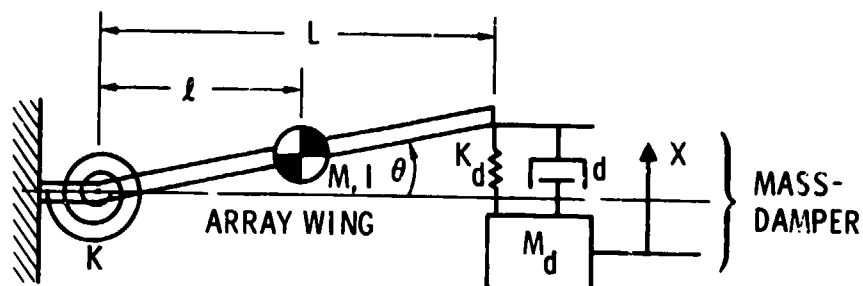
As noted in Sections 2.14 and 2.18, some system damping is desirable to dissipate disturbance-induced energy in the PEP. The structural damping will be hard to define and is expected to be quite low so damping may have to be designed in. If a high compliance structure at the mast root is used, a damper may be mounted along with the compliance structure to act against the compliance motion. An alternate approach would be to place a viscous-spring-mass damper somewhere on the solar array wing. The damping potential for this concept was analyzed with the model shown in Figure 2.8-3.

### Results

The rigid body linear displacements of the PEP center of gravity (c.g.) are shown in Figure 2.8-4 for small roll, pitch, and yaw Orbiter rotations for the three RMS/PEP positions in Figure 2.8-1. Using the model defined in Figure 2.8-2, the 12 transfer functions in which apply to the array compliance axes were derived (Table 2.8-1). The maximum value of the impulse response for each transfer function was calculated (excluding the initial value if non-zero) and is also shown in Table 2.8-1. The magnitudes are shown as a function of the wing cantilever frequency ( $f$ ). These transfer functions apply to both in and out of the solar array plane motions. They do not apply to motions along the PEP longitudinal axis or to rotations about that axis. The transfer functions used for these longitudinal axis motions were based on an RMS cantilever frequency of 0.15 Hz and are also shown in Table 2.8-1. The 0.15 Hz RMS frequency was derived by mounting a 42 slug (614 Kg) point mass (mass of PEP) on an extended RMS with an unloaded cantilever frequency of 0.3 Hz.<sup>3</sup> A point

---

<sup>2,3</sup>Ibid.



$$\begin{aligned}
 M &= 15.8 \text{ SLUG (232 Kg)} \\
 I &= 25,700 \text{ SLUG-FT}^2 \text{ (35,000 KgM}^2\text{)} \\
 l &= 54.1 \text{ FT (16.5M)} \\
 L &= 115 \text{ FT (35.1M)} \\
 K_c &= 1,136 \text{ FT-LB/RAD (0.02 Hz CANTILEVER FREQUENCY)} \\
 \left. \begin{aligned}
 M_d &\cong \alpha M \\
 K_d &\cong M_d (2\pi f_d)^2 \\
 d &\cong M_d \zeta_d (2\pi f_d)
 \end{aligned} \right\} \text{PARAMETERIZED} \\
 &\quad \text{ON } \alpha, f_d \text{ and } \zeta_d
 \end{aligned}$$

Figure 2.8-3. Mass-Damper Model

#### RMS/PEP POSITION 1

$$\begin{pmatrix} \Delta X \\ \Delta Y \\ \Delta Z \end{pmatrix} = \begin{pmatrix} 0.23 \Delta \psi \\ 1.6 \Delta \psi \\ -0.23 \Delta \phi - 1.6 \Delta \theta \end{pmatrix}$$

#### RMS/PEP POSITION 2

$$\begin{pmatrix} \Delta X \\ \Delta Y \\ \Delta Z \end{pmatrix} = \begin{pmatrix} 1.1 \Delta \psi \\ 0.63 \Delta \psi \\ -1.1 \Delta \phi - 0.63 \Delta \theta \end{pmatrix}$$

#### RMS/PEP POSITION 3

$$\begin{pmatrix} \Delta X \\ \Delta Y \\ \Delta Z \end{pmatrix} = \begin{pmatrix} 0.59 \Delta \theta + 0.51 \Delta \psi \\ -0.59 \Delta \phi + 0.63 \Delta \psi \\ -0.51 \Delta \phi - 0.63 \Delta \theta \end{pmatrix}$$

#### NOTES

- $\Delta \phi, \Delta \theta, \Delta \psi$  = ORBITER ROLL, PITCH, YAW
- ANGLES IN DEGREES
- PEP TRANSLATIONS IN FEET ( $\Delta X, \Delta Y, \Delta Z$ )
- RATES AND ACCELERATIONS USE THE SAME PROPORTIONALITY CONSTANTS

Figure 2.8-4. PEP Translation to Orbiter Rotation Relations

Table 2.8-1. PEP Load Transfer Functions

Load	Input disturbance				
	$\Delta \dot{X}_C$ (ft/sec)	$\Delta \dot{\theta}_C$ (deg/sec)	$F_1 \Delta t$ (lb/sec)	$M_1 \Delta t$ (ft-lb/sec)	
$F_C$ (lb)	-125f	0	4f	0.075f	PEP wing compliance frequency f (Hz)
$M_C$ (ft-lb)	0	-16,400f	-340f	6.5f	
$T_1$ (ft-lb)	5,350f	-8,000f	-335f	6.3f	
$F_C$ (lb)	40	-	{ RMS compliance (0.15 Hz) for PEP longitudinal translation		
$M_C$ (ft-lb)	-	367	{ RMS compliance (0.15 Hz) for rotation about PEP longitudinal axis		

## Nomenclature

- $\Delta \dot{X}_C$  - Translation rate change at PEP center of gravity (cg)  
 $\Delta \dot{\theta}_C$  - Rotational rate change at PEP cg  
 $F_1$  - Plume force impulse at wing 1 cg  
 $M_1$  - Plume moment impulse about wing 1 cg  
 $F_C$  - Force at PEP cg  
 $M_C$  - Moment about cg  
 $T_1$  - Mast root moment (wing 1)

mass was used because it was assumed that the PEP rotational compliance was much higher than the RMS rotational compliance (about the two large moment of inertia axes) and that the small PEP longitudinal axis moment of inertia had little effect on the RMS/PEP cantilever frequency. By using the translation data in Figure 2.8-4 with the transfer functions in Table 2.8-1, the applied force and moment at the PEP c.g. and the mast root moment were calculated for an arbitrary Orbiter rate change.

The force and moment at the wing c.g. are used for calculating the response to plume impingement. Figure 2.8-5 defines the steady-state VRCS plume force on the solar array as a function of distance from the thruster for the conditions noted. Figure 2.8-6 defines steady state mast root moment for variations on RMS/PEP Position 2 for the array perpendicular to the thruster centerline ( $\theta = 90$  degrees) and canted 45 degrees ( $\theta = 45$  degrees). Since the impact pressure on the array goes as the square of the sine of the angle of incidence, a 45-degree cant reduces the load in half. This dynamic load is attenuated relative to the steady-state load by the short thruster firing time in conjunction with the wing compliance.

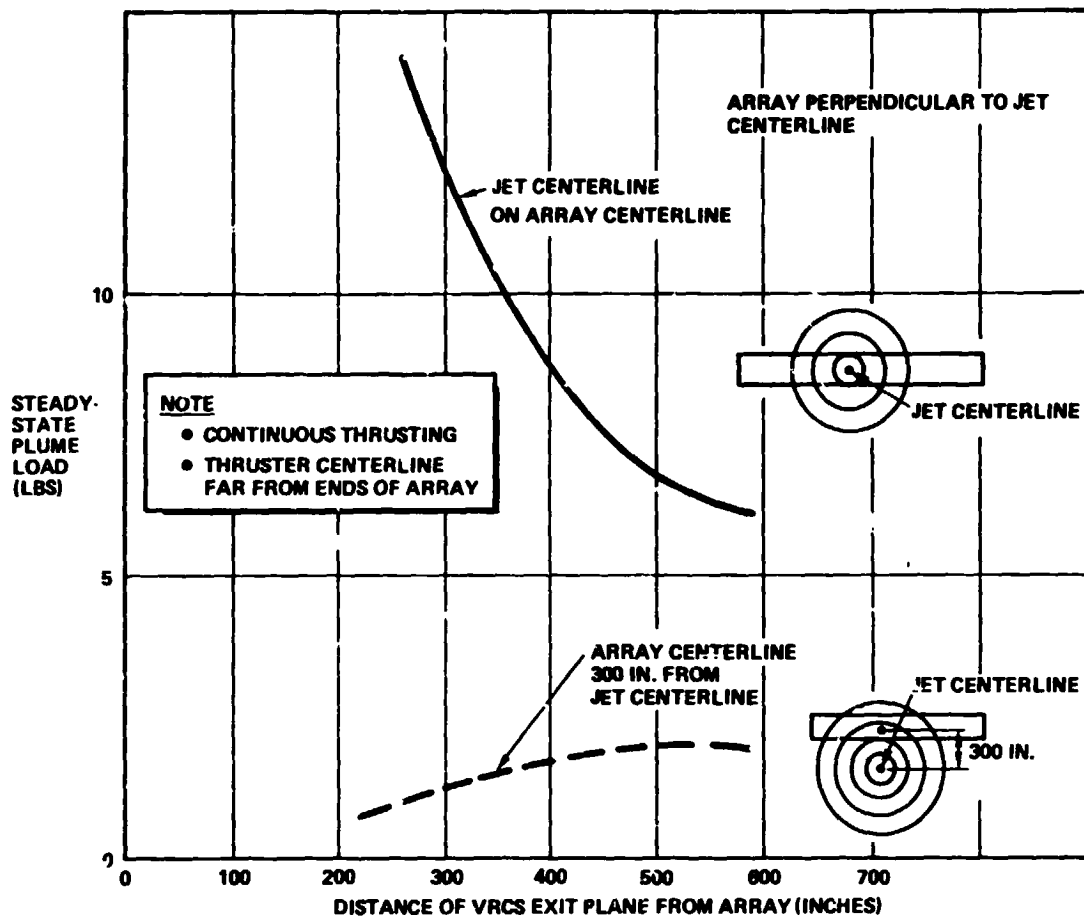


Figure 2.8-5. VRCS Plume Load

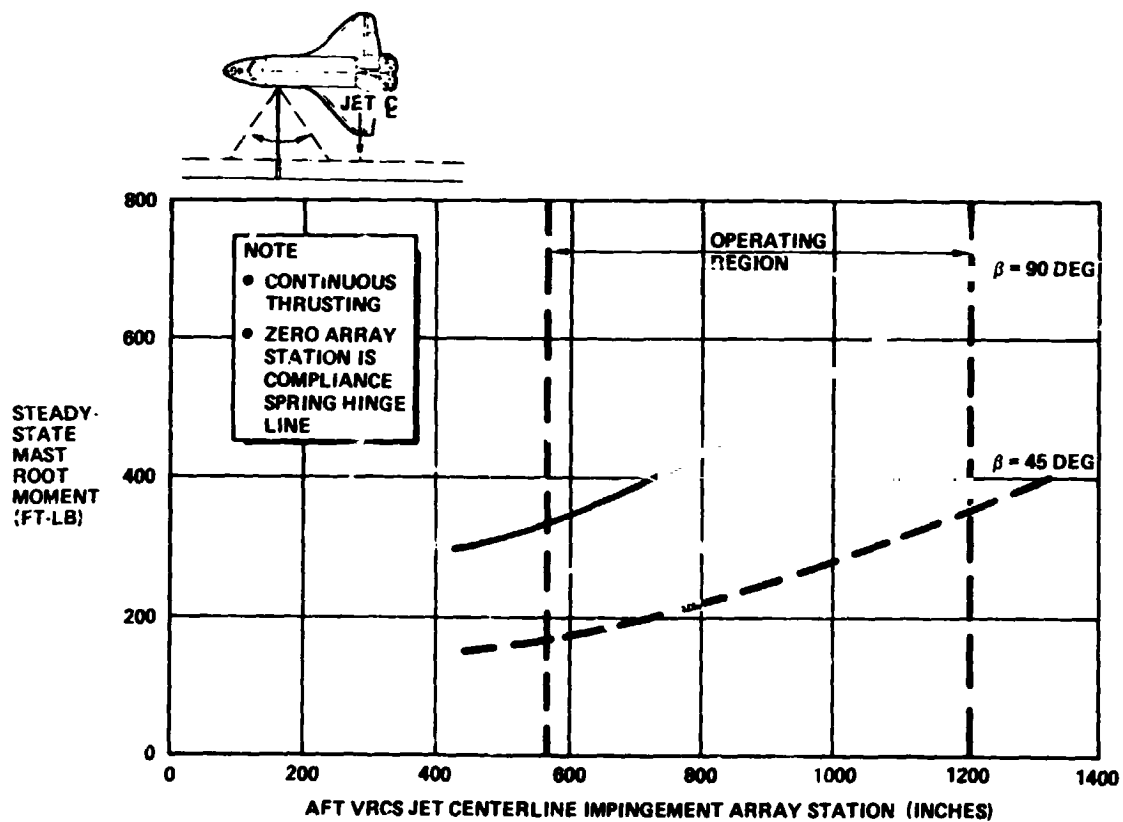


Figure 2.8-6. VRCS Plume Load, RMS Position 2 (Y-POP-ZLV)

Figure 2.8-7 corresponds to RMS/PEP Position 3 (Figure 2.8-1). The effects of tilting the array about a transverse and Beta axes are shown. The 10-degree transverse axis tilt increases the distance between the aft jet and the array by 10 to 17 feet (nominal of 38 feet) depending on the RMS shoulder yaw position. As noted above, the load is attenuated by short thruster firing time in conjunction with the wing compliance.

Based on the above impingement data, the maximum steady state aft VRCS plume impingement forces and moments at the wing c.g. are:

<u>RMS/PEP position</u>	<u>Force (<math>F_{12}</math>)</u>	<u>Moment (<math>M_{12}</math>)</u>
2	-6.4 lb (-Y)	90 ft-lb (-Z)
3	-7.4 lb (+Z)	300 ft-lb (+Y)

The PRCS forces and moments are about 36 times larger since the impact pressure scales with the thrust. Plume loads were not calculated for the forward thrusters since it was assumed that the effects are similar or less severe than for the aft thrusters. The aft VRCS maximum plume loading for RMS/PEP

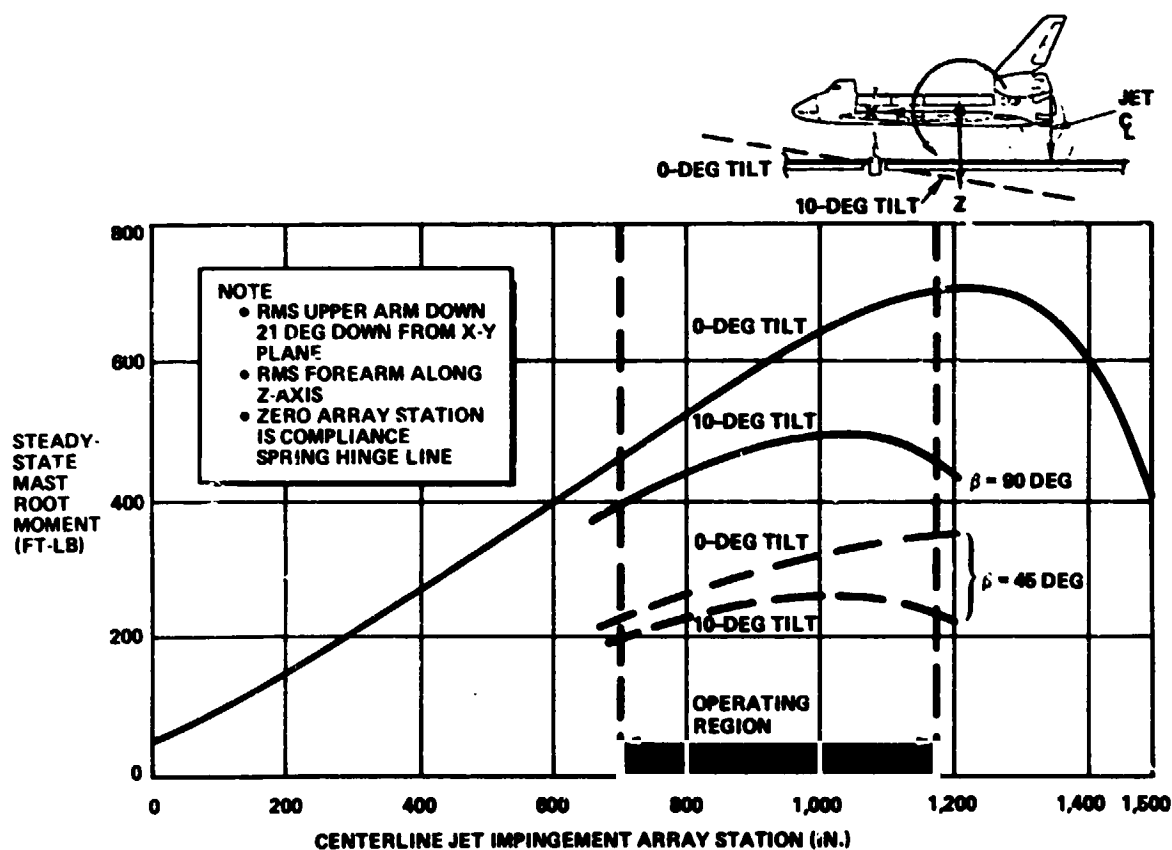


Figure 2.8-7. VRCS Plume Load, RMS Position 3 (Z-POP, YLV)

Position 1 is small. The aft PRCS plume loads result in a maximum steady state force and moment at the wing c.g. of about 3.2 lb and 62 ft-lb, respectively.

Since the aft VRCS and PRCS thrusters have about the same lever arms from the Orbiter c.g., the thruster impulse for a given rate change is the same for the PRCS and VRCS. Likewise with the plume impingement impulse. Therefore, the plume impingement impulse is proportional to Orbiter rate change and independent of the thrust level. The impingement impulse per Orbiter rate change can be summarized as follows:

<u>RMS/PEP position</u>	<u>Force impulse (<math>F_1 \Delta t</math>)</u> <u>(lb-sec/deg/sec)</u>	<u>Moment impulse (<math>M_1 \Delta t</math>)</u> <u>(ft-lb-sec/deg/sec)</u>
2	-490	6900
3	-460	19,000

Using the data described above, the force and moment at the PEP c.g. and the mast root moment can be defined for a given Orbiter rate change including plume impingement effects. One conservatism should be kept in mind, however. The impulse response calculation assumes that the Orbiter rate change takes place over a short time relative to the period of the compliance resonances being considered. If the acceleration occurs over a quarter of the compliance period, the short duration pulse assumption is conservative by about 11 percent. This corresponds to 1.7 seconds firing time for the RMS compliance frequency of 0.15 Hz and  $1/(4f)$  seconds for an "f" Hz wing compliance frequency. Corresponding rate changes are shown in Table 2.8-2.

The data described above defines the maximum force and moment at PEP c.g. and the maximum mast root moment for a given Orbiter rate change. The RMS joint torques are calculated from the PEP c.g. force and moment and the appropriate lever arms.

The loads are proportional to Orbiter rate change and a function of the wing compliance frequency. Assuming a maximum allowable load defines a region of allowable Orbiter rate changes and wing compliance frequencies. Figures 2.8-8, -9 and -10 define these regions for the three RMS/PEP positions and the conditions noted. The maximum loads assumed are ultimate loads. The RMS joint load limits are minimum brake-slip loads and the 200 ft-lb mast root load limit is

Table 2.8-2. Rate Changes for One-Quarter Compliance-Period Firing

Thrusters	Compliance frequency (Hz)		
	0.01	0.1	0.15
PRCS (two aft thrusters)			
Roll	30	3	2
Pitch	15	1.5	1
Yaw	15	1.5	1
VRCS			
Roll (two thrusters)*	0.50	0.050	0.033
Pitch (two aft thrusters)	0.43	0.043	0.029
Yaw (one aft thruster)	0.22	0.022	0.015

\*One forward, one aft

Note: rates are in deg/sec

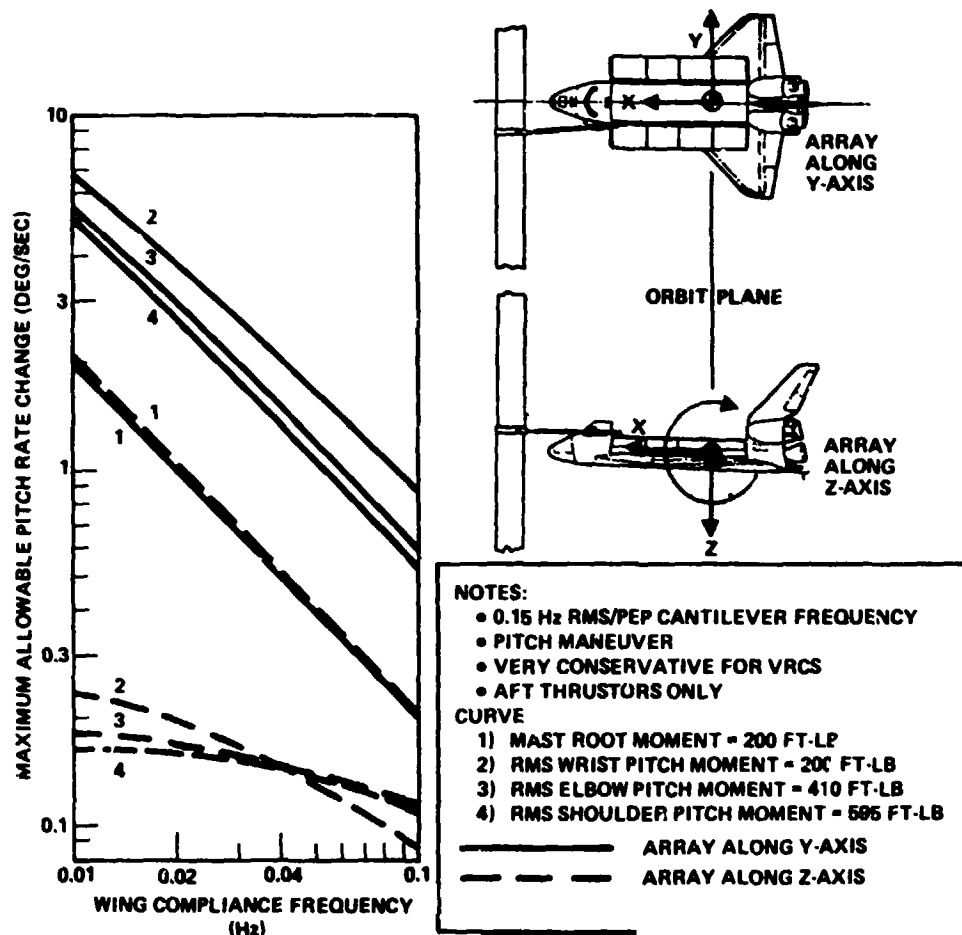


Figure 2.8-8. PEP Compliance Frequency Versus Pitch Rate Change, PEP/RMS Position 1

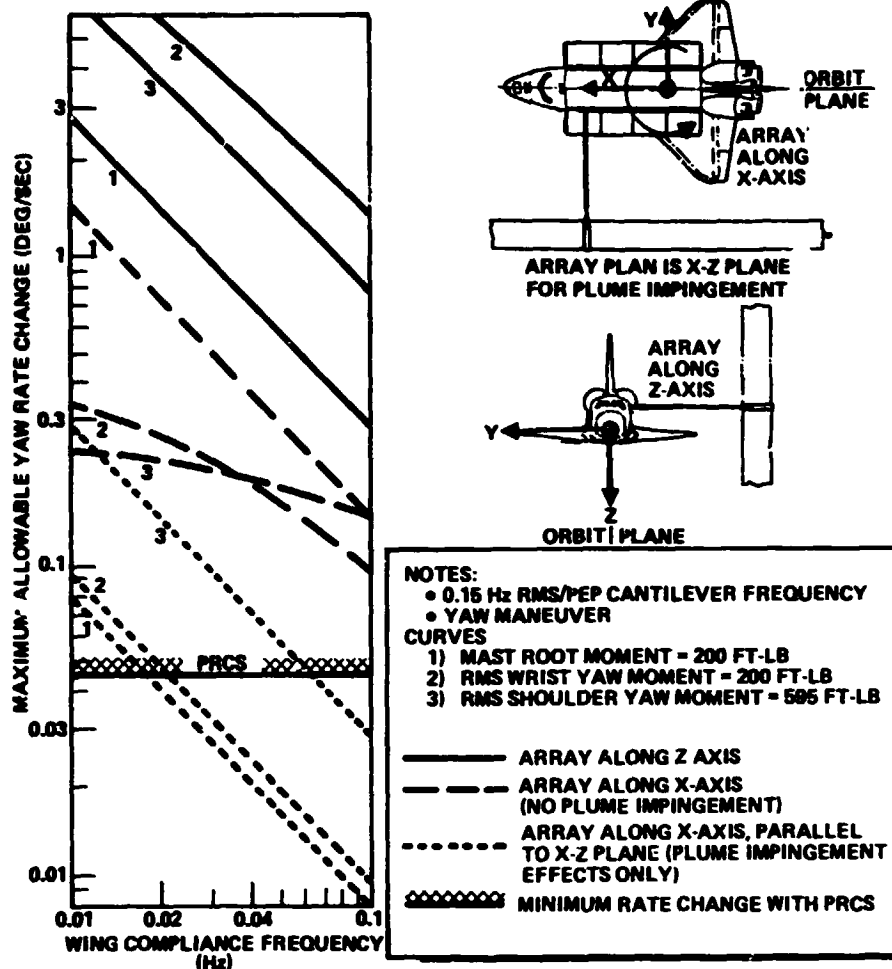


Figure 2.8-9. PEP Compliance Frequency Versus Yaw Rate Change, RMS/PEP Position 2

the preliminary design load and includes a blanket tension bias load of 33 ft-lb (22-lb blanket tension). Selecting a mast ultimate load capability of 200 ft-lb results in rate change constraints imposed by the mast being similar to those imposed by the RMS wrist joints which are 200 ft-lb. The rate changes on Figures 2.8-8 through -10 scale proportionally to the allowable loads assumed except for mast root moment which has a bias of 33 ft-lb due to the blanket tension of 22 lb. Thus, the mast-root-moment rate changes scale proportionally with the assumed load minus 33 ft-lb rather than with the assumed load.

Note that the data on Figures 2.8-8 through 2.8-10 become more conservative as the firing time required to achieve the rate increases. These curves are very conservative for the VRCS except for the plume impingement data where the rate changes are small. Table 2.8-2 defines the rate changes that result in about 11 percent conservatism (firing time of 1/4 of a compliance oscillation period).

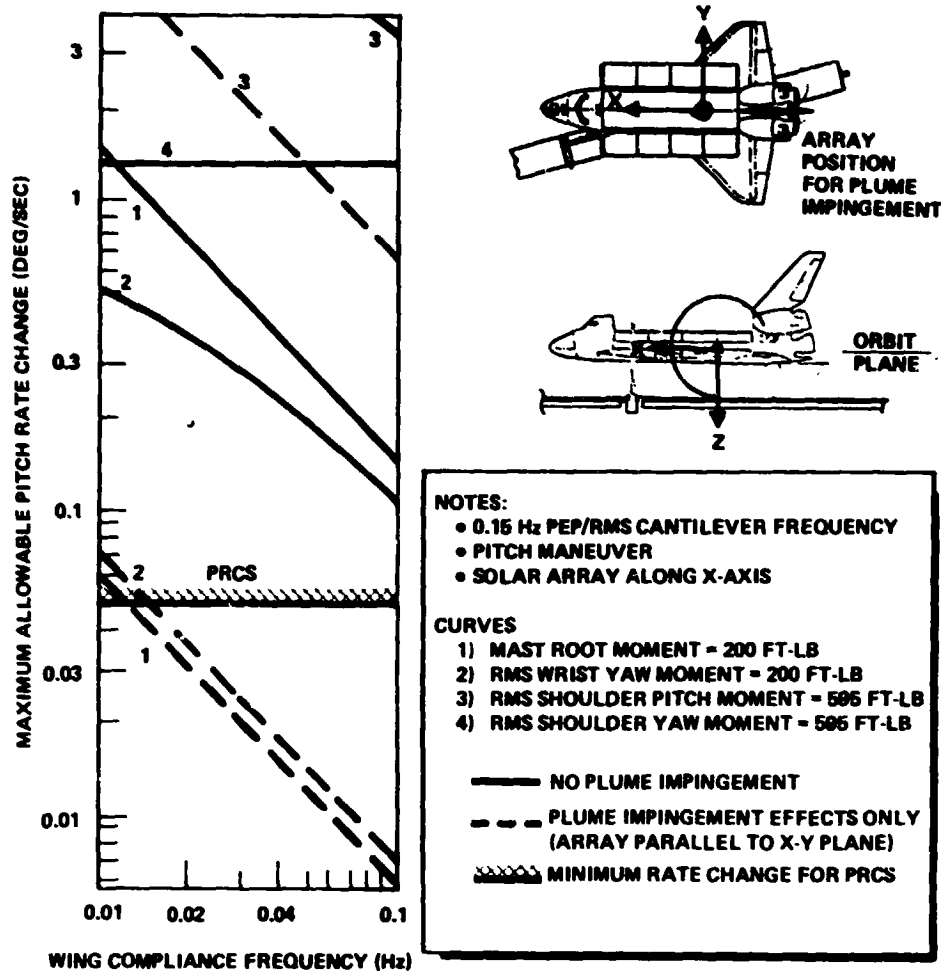


Figure 2.8-10. PEP Compliance Frequency Versus Pitch Rate Change, RMS/PEP Position 3

The constraints which apply to the VRCS are primarily due to plume impingement effects (Figures 2.8-9 and -10). The mast root and RMS joint inertia loads associated with the VRCS are acceptable when continuously firing except for roll maneuvers with the PEP c.g. over 40 feet from the Orbiter X-axis and the solar array oriented perpendicular to the Orbiter X-axis. As discussed in Paragraph 2.18, the VRCS pitch and yaw limit cycle rates expected are  $\pm 0.006$  deg/sec or rate changes of 0.012 deg/sec. With the array in the plume, some wing compliance is required to maintain the mast root moment under 200 ft-lb during VRCS limit cycle (Figures 2.8-9 and -10). For RMS/PEP Position 3, the wing compliance frequency must be less than 0.05 Hz. Since large uncertainties are likely regarding plume impingement effects, at least a factor of two margin is desirable. Based on this thinking, a preliminary design wing compliance frequency of 0.02 Hz was chosen. This compliance applies to motion perpendicular to the array plane.

The PRCS maximum pitch and yaw limit cycle rates described in Paragraph 2.18 were  $\pm 0.06$  deg/sec or rate changes of 0.12 deg/sec. Figures 2.8-9 and -10 show that wing compliance frequencies below 0.01 Hz would be required to reduce loads to acceptable values for these PRCS limit cycle conditions when plume impingement occurs. Thus, PRCS limit cycle with plume impingement is not allowed by the baseline wing compliance frequency of 0.02 Hz.

Maneuver rate limitations can also be determined from Figures 2.8-8 through -10. When plume impingement is significant, maneuver rate changes must be less than 0.03-0.04 deg/sec for the baseline wing compliance. Feathering the array to the plume using the Beta gimbal could be used to reduce plume loads significantly for maneuvers. Also, tilting the array as shown in Figure 2.8-7 can reduce load somewhat. When plume loads are not significant, allowable maneuver rate changes are much greater (typically over 0.25 deg/sec).

The maneuver rate limitations are a strong function of array orientation relative to the maneuver axis. When the array longitudinal axis is along the maneuver axis, the wing compliance concept allows for load reduction to both plunge and rotational motions. The wing compliance concept does not include compliance for plunge motion along the array longitudinal axis. The RMS 0.15 Hz cantilever frequency assumption provides the only compliance for the baseline configuration for longitudinal plunge. The allowable maneuver rate is a function of wing compliance, however, because most bending moments do contain a component due to rotation which is a function of the wing compliance (Curve 4, Figure 2.8-10 is an exception).

As discussed above, plume effects require significant wing compliance for motion out of the array plane. Figures 2.8-8 through -10 show that significant wing compliance is also necessary to allow maneuver rates using the PRCS above 0.08 to 0.1 deg/sec. This requirement applies to wing deflections in the array plane as well as out of the array plane as required by plume considerations. Thus, wing compliance both along the array transverse axis and perpendicular to the array were included in the baseline. The perpendicular axis compliance frequency was preliminarily chosen the same as the transverse axis (0.02 Hz) so that out of plume maneuver capability would be independent of orbit Beta angle (Beta gimbal angle position). Also, it can be noted that the allowable rate change begins to decrease rapidly for wing compliance frequencies above 0.02 Hz.

Since the allowable maneuver rates with the array perpendicular to the maneuver axis may be lower than required (Spacelab II requires a 0.25 deg/sec pitch maneuver), RMS/PEP position and array orientation constraints may be required for certain maneuvers. This is quite feasible since many RMS degrees of freedom allow wide variations on the three RMS/PEP positions discussed here. Mission specific analysis will be required to define operating procedures for each mission.

Adding an additional compliance along the array longitudinal axis would reduce the load sensitivities to the array orientation/maneuver axis relationship. Mechanizing this type of compliance appears more complex than the wing compliances modeled for this analysis. Therefore, since no clear requirement was seen for this general maneuver capability, longitudinal compliance was not included in the baseline.

The wing compliance discussed above can result from many places including array mast flexibility, array blanket flexibility on a specifically included compliance structure at the root of the mast. The strength requirement for the mast (200 ft-lb) forced the mast stiffness up to a value which precluded wing cantilever frequencies near the 0.02 Hz requirement.

The baseline array is a single blanket per wing, clearing the mast by 13 inches. Dynamic clearance between the blanket and the mast was analyzed and the results shown as a function of blanket tension on Figure 2.8-11. This data was generated with the detailed finite element model defined in the Reference.<sup>4</sup> The RMS/PEP position analyzed was similar to Position 3 defined herein. The plume load clearances were determined with the array rotated under an aft VRCS thruster and the inertia loading with the array along the Orbiter Y-axis. A preliminary blanket tension of 22 pounds was chosen to provide a factor of two clearance margin. A blanket frequency of 0.088 Hz resulted which is higher than the desired 0.02 Hz wing compliance previously discussed. Since neither the mast or the blanket could provide the needed wing compliance, it was decided to baseline the compliance at the root of the mast.

A comparison of the loads generated by the model shown in Figure 2.8-2 used in this analysis and the more detailed model described in the Reference<sup>5</sup> showed the simpler model used here to be conservative. The case compared was 0.25 deg/sec roll maneuver with RMS/PEP Position 3 and the array along the Orbiter

---

<sup>4,5</sup>  
Ibid

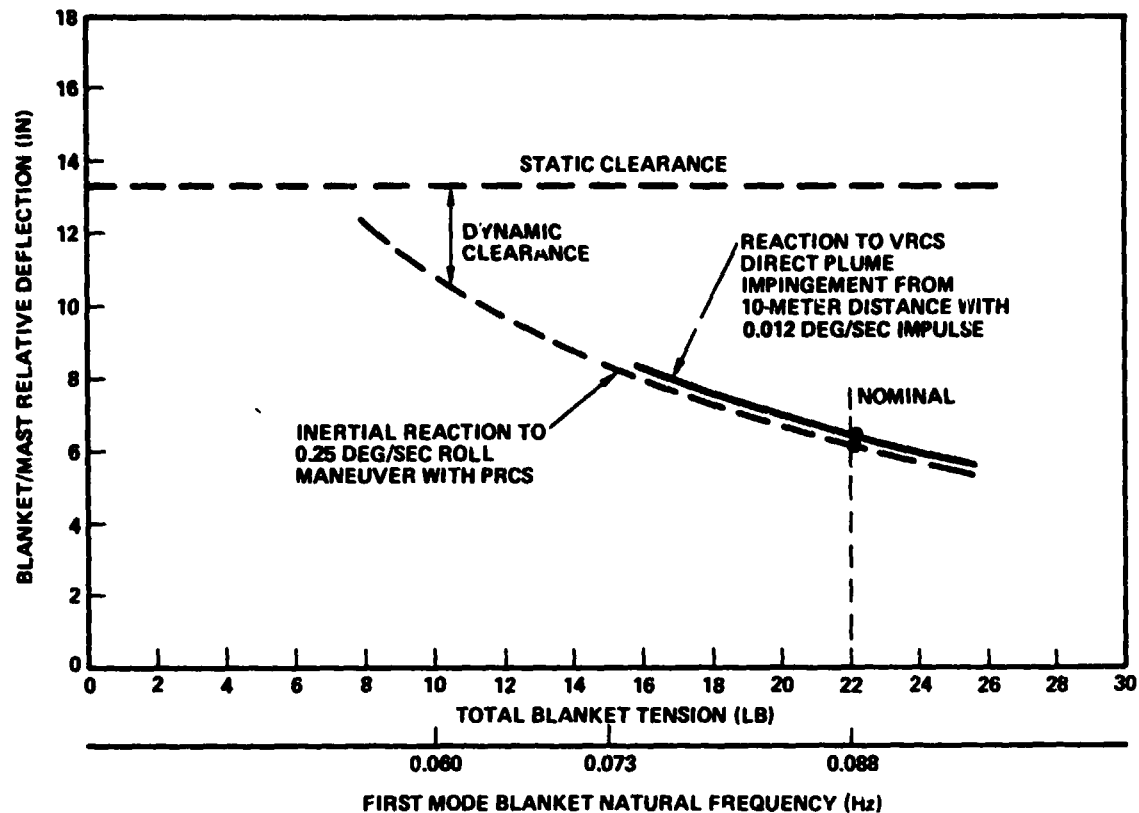


Figure 2.8-11 Higher Blanket Tension Increases Blanket/Mast Dynamic Clearance

Y-axis. Two blanket tensions were analyzed with the finite element model of the Reference.<sup>6</sup> The results are:

Load	Model from Figure 2.8-2	Reference <sup>7</sup> model blanket tension	
		22 lb	10 lb
Mast root moment (ft-lb)	87	70	48
RMS wrist pitch moment (ft-lb)	145	100	83

The additional flexibility in the detail model relative to the simple rigid-wing model results in the lower loads.

Sections 2.14 and 2.18 identify a requirement for mechanical damping of the compliance structure modes. Since the damping requirement may be as low as one percent of critical, a viscous-spring-mass damper module mounted at the outer

<sup>6,7</sup> Ibid

end of the mast was considered. Figure 2.8-3 shows the analysis model. The system damping was evaluated for various damper system parameter values. The main consideration was weight since the damping system represents added mass to the system. Table 2.8-3 contains the results. The optimum damping system (maximum system damping for a given damper weight) was not defined, but it is clear that system damping well in excess of one percent of critical is possible with small damper mass values relative to the total wing weight of 509 pounds.

Table 2.8-3. System Damping With Mass Damper

$\frac{m_d}{m} \times 100^*$	Damper damping ratio	System damping (percent of critical)			
		Damper frequency (Hz)			
		0.01	0.015	0.02	0.04
0.5	0.2	0.23	0.75	1.9+	0.06
	0.7	0.47	0.57	0.50	1.1
	1.5	0.37	0.30	0.23	0.09
1	0.2	0.47	1.5	4.0+	1.0
	0.7	0.95	1.1	0.98	0.22
	1.5	0.74	0.59	0.45	0.18
2	0.2	0.93	2.8	6.3+	0.19
	0.7	1.9	2.3	1.9	0.40
	1.5	1.5	1.1	0.87	0.34
5	0.2	2.3	6.3+	6.2	0.35
	0.7	4.8	5.6	4.2	0.80
	1.5	3.5	2.6	1.9	0.73
10	0.2	4.3	10	5.4	0.46
	0.7	9.9	11+	6.6	1.2
	1.5	6.2	4.1	3.2	1.1
20	0.2	8.0	8.9	4.3	0.05
	0.7	21+	16	8.0	1.4
	1.5	10	6.6	4.6	1.5

\*Ratio of damper mass to wing mass in percent

+Maximum values

Notes: 0.02 Hz wing compliance frequency

Based on model on Figure 2.8-3

## 2.9 PEP GIMBAL DEFINITION

### Objective

The objective of this task is to define the gimbal mechanism required for PEP to a level suitable for concept validation and specification preparation.

### Conclusions and Recommendations

Based on the PEP reference design for the ADA, the available envelope for the two-axis gimbal assembly is adequate to provide the required functions.

The critical design development element within the gimbal assembly is the mechanism used to transfer the high current power circuits together with the sensitive low power instrumentation and control circuits across the continuously rotating Alpha axis joint. Although the technology exists to solve this design problem it will require development testing of specific designs to demonstrate function and reliability of this element. The first phase of this development is underway as part of RTOP 906-51. It is recommended that this effort be continued as a pre-ATP development item.

### Approach

Using the reference configuration for PEP the gimbal assembly requirements were derived. These requirements established envelope, axis relative location, torque, rate, number of power and signal conductors, current levels, voltage levels, voltage drop across the slip rings, drive power limits, travel, etc. From these requirements a preliminary specification has been prepared which can easily be converted into the final procurement specification. In addition, a conceptual layout was done primarily to evaluate mechanism sizes, gear ratios and envelope restrictions.

### Results

Figure 2.9-1 illustrates the relationship between the RMS, power cable, gimbal assembly, and ADA structure. The gimbal assembly Alpha axis rotor is equipped with a standard design grapple fixture which interfaces with the SPEE. The power cable connector is fixed to the external surface of the SPEE and after the mechanical hookup between the grapple fixture and the SPEE is made, the electromechanical actuator which is attached to the gimbal assembly engages the power cable electrical connectors.

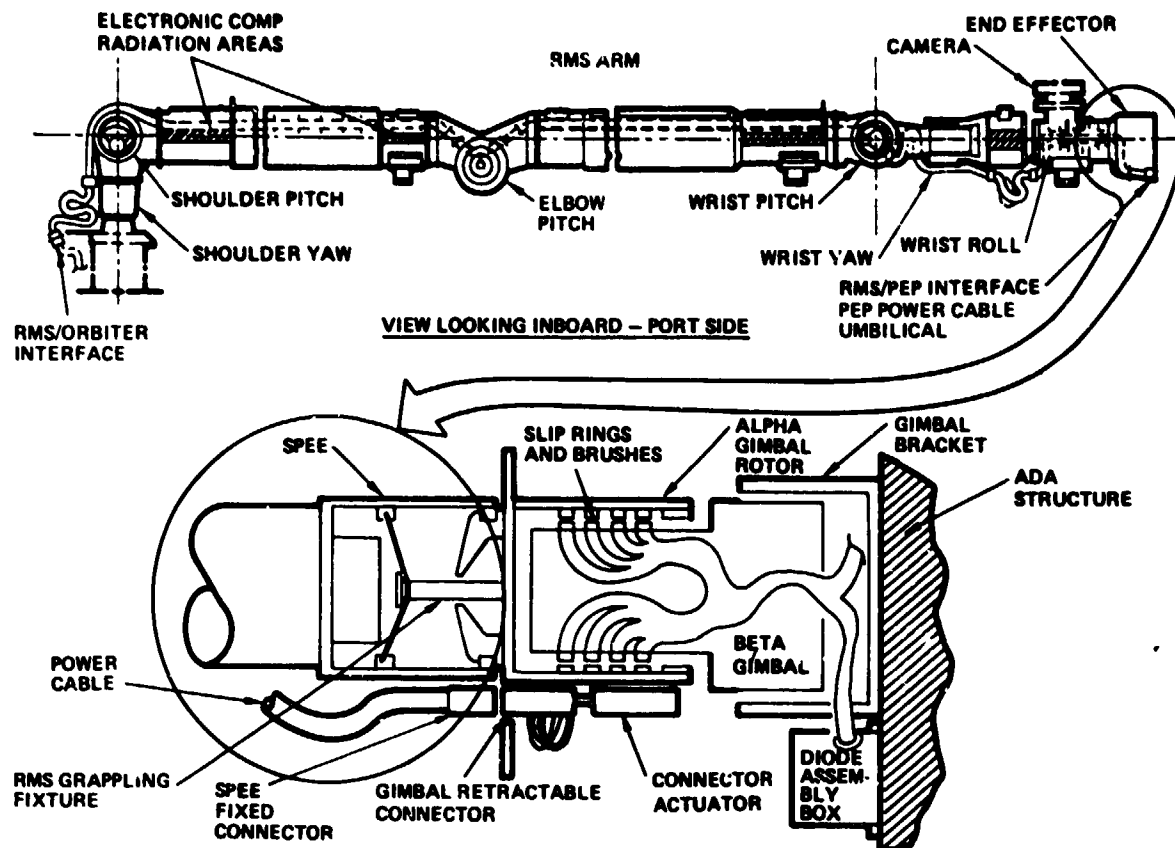


Figure 2.9-1. RMS Power Cable and Gimbal Schematic

Figure 2.9-2 illustrates the conceptual layout which was produced to explore the drive concept and envelope restriction. The design uses a unique planetary friction drive system incorporating dual motors. Conventional slip rings and brushes are shown for the electrical power transfer mechanism. Since this layout was produced additional study has indicated that redundant drive motors are probably not necessary. The ADA can be stowed in the Orbiter bay by the RMS with the gimbal in any position within its limits of travel. Therefore, a motor failure would not constitute a safety hazard or loss of the array. Additional work under RTOP-906-51 is exploring the use of an invention by Sperry Flight Systems called Roll-Rings to replace conventional slip ring-brush assemblies.

The preliminary specification for the PEP gimbal is contained in Appendix B. The requirements for the performance of the Alpha and Beta drive systems are identical except for travel. This will allow a common drive system to be used on both axes. The stall torque minimum limit was based on retaining the ability of the gimbal to track during plume loads on the array combined with

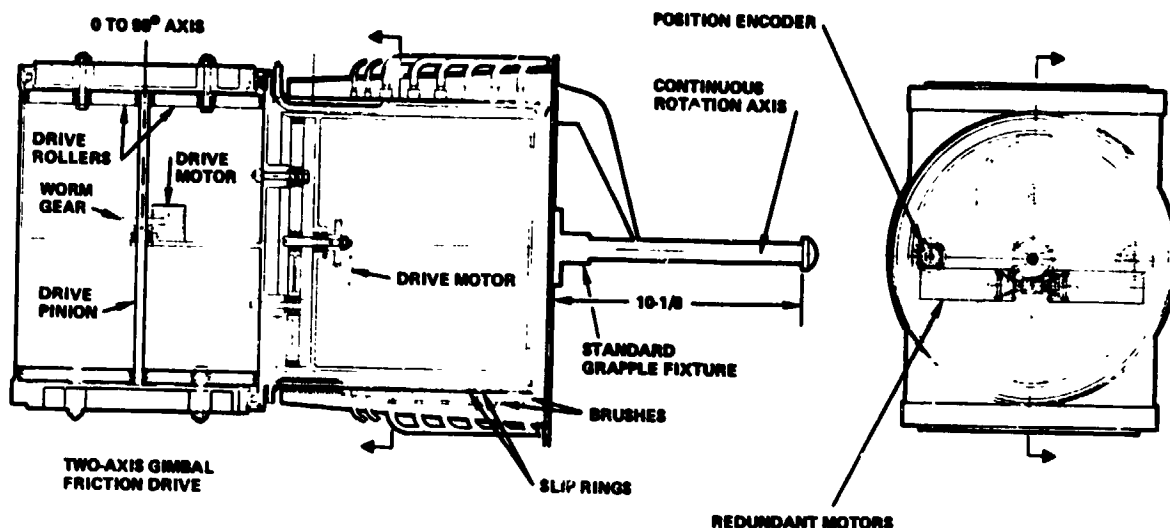


Figure 2.9-2. PEP Gimbal Concept

dynamic loads. The maximum stall torque is specified to a level below the bending strength of the mast. The rate is based on dynamic considerations of tracking during an Orbiter maneuver and the potential of using gimbal motion to impart damping to array oscillations.

The weight of the gimbal assembly is specified as 40 pounds. This is based on a target weight of the complete assembly including umbilical actuator and grapple fixture of 73 pounds.

The slip ring assembly carries 12 wires (six circuits) for the solar array power. These circuits are specified to carry 60 amps at a voltage from 90 to 240. The current level was derived from the power system analysis for the maximum current level expected. There are 24 wires for low power, instrumentation and control. These wires match the circuits of the RMS and SPEE.

The maximum voltage drop requirements were based on Sperry Flight Systems data on Roll-Ring performance.

The envelope and electrical schematic show three connectors with four pins each for the power hookup. Further study into connector availability and harness fabrication indicates that four smaller connectors with three pins each would be more compatible with the power system diode assemblies.

## 2.10 MAST AND CANISTER PRELIMINARY DESIGN CRITERIA

### Objective

The objective of this task was to assess array/mast deployment kinematics, operational and maneuver loads and PEP configuration concepts to develop design criteria for preliminary sizing and concept selection for the array wing mast and its related stowage canister.

### Conclusions

The analysis concluded that the mast and canister sizing used in the PEP configurations is realistically representative for the deployment, maneuver and Orbiter VRCS plume loads derived as a result of the dynamic analysis reported in Section 2.8. Agreement has been obtained from two commercial sources of stowable masts as to that opinion. One commercial source presented later advance material indicating that new concepts evolving for coilable masts may yield substantially smaller canister diameters for the same strength if lower bending stiffness is acceptable. Such concepts should be pursued in the future, since lower mast stiffness results in lower natural frequency, and the compliance requirement necessary within the wing canister central support would be less and may be more easily implemented. The mast for the reference configuration requires a bending strength of 143 ft-lb limit, 200 ft-lb ultimate, has a deployed length of 1450 inches, and is contained in a canister 21 inches in diameter and 55.7 inches long.

### Approach

The overall sizing of the mast is derived from the deployed geometry of the solar array blanket and the blanket tensioning loads, maneuver loads and ACS plume impingement loads on the blanket.

Blanket tensioning provides a continuous compression load, and due to its eccentric location, a continuous bending moment on the mast. These load conditions are selected in conjunction with the mast stiffness to establish the nominal steady state clearance between the blanket and the mast longerons (due to mast bowing). This clearance is necessary to minimize impact of the blanket with its solar cells against the mast as the result of dynamic flexure of the blanket and the mast. The principal determination of mast bending strength stems from the ACS plume loads on the blanket, in fact, for the worst case conditioning plume loading was approximately 70 percent of the design loading.

Variations in configurations such as the geometry resulting from the rotating canister concept (the reference configuration) and from the fixed canister configuration show approximately 10 percent variation in design bending moment. Figure 2.10-1 compares the reference configuration with the fixed canister concept first with the canister located with the same mast centroid to blanket distance and second with the same mast longeron to blanket clearance.

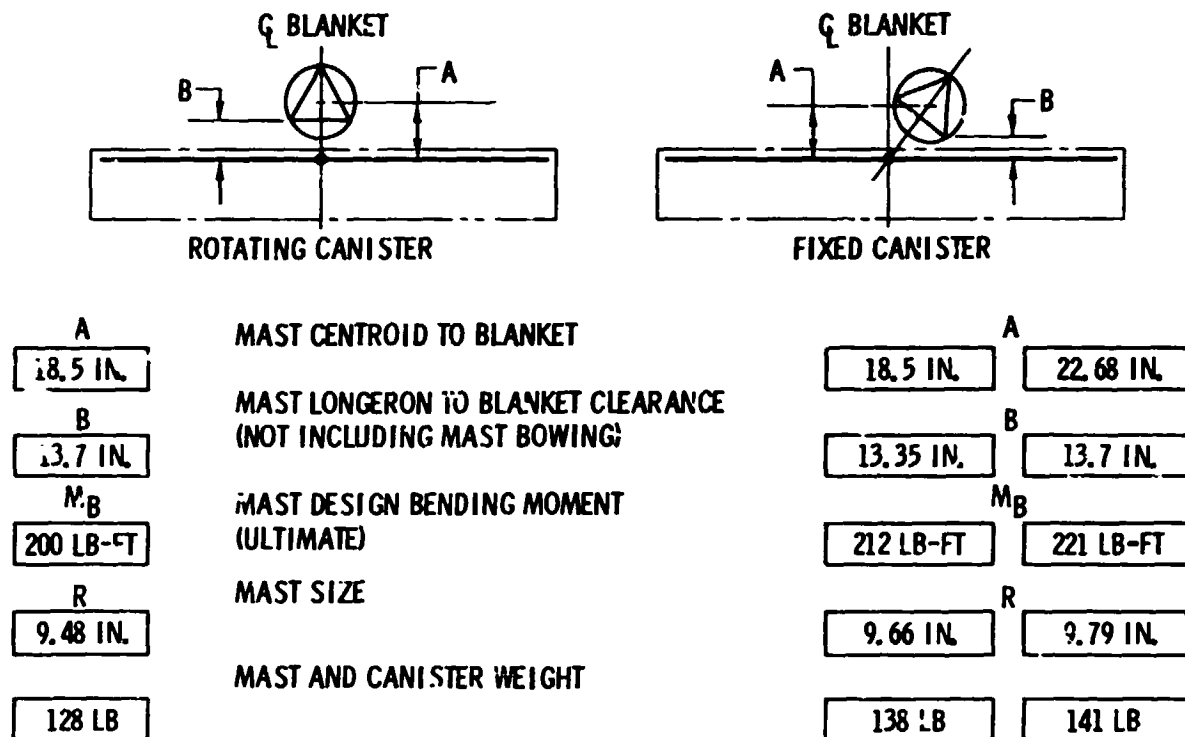


Figure 2.10-1. Fixed and Rotating Canister Sizing

The general mast column loading which is due to blanket tensioning is relatively low, approximately 22 pounds. The column load during the last few inches of mast retraction or extension from the canister stems from the solar array box cover locking (or unlocking) loads is approximately 140 pounds. There is an associated bending moment which requires special treatment of that terminal portion of the mast to accommodate.

The deployment rate for the mast and blanket is keyed to accomplishing full deployment in a 6-15 minute time range. In order to achieve this kind of deployment time, the mast rates are too high to satisfactorily lock the box

Table 2.10-1. PEP Mast Requirements

1. Type--Automatically deployed and retractable mast using open lattice structure. The mast may be either a continuous longeron or an articulated longeron.
2. Deployed length--1450 inches
3. Bending moment--143 ft lbs limit, 200 ft lbs ultimate
4. Compressive load--20 lb @ full extension, 140 lb @ 0 to 10 in. extension
5. Tension load--140 lb @ 0 to 10 in. extension
6. Extension/retraction rate--Normal rate will be 4 inches/second. The rate from 0 to 10 inches extension shall be 0.4 inch per second.
7. Canister nut drive--The canister drive shall be equipped with redundant 28 volt DC motors. Extension and retraction shall be possible with either motor inoperative. A two speed drive system shall be incorporated which will allow shifting from the 0.4 to 4.0 inches per second by applying a TBD volt/TBD amps signal to the gear box control. The maximum power to be consumed by the drive system when operating at maximum rate or maximum load shall be 100 watts.
8. Weight--The canister, drive sysetem and mast shall not exceed 132 pounds.
9. Life--The mast and associated mechanism shall have a useful life without maintenance of 100 minimum extension/retraction cycles.
10. Altitude--The operation of the mast will be at sea level for test and checkout and at an altitude of 400 nautical miles maximum.

Mast preliminary design

Canisters: Diameter--21 inches, Length--55.7 inches

Mast: Diameter--18.96 inches, EI-- $64.23 \times 10^6$  lb in<sup>2</sup>

cover and provide acceptable canister rotation rates in the reference configuration concept of self rotating canisters. Therefore, a two speed rate technique is necessary and with approximately a 10:1 ratio of rates.

Redundant motors for the mast deployment/retraction are considered necessary. Other implementations are acceptable; however, this study has conceived a concept wherein the dual motors are used to provide the dual deployment rate (one motor for low rate, both motors for high rate) as well as redundancy (either motor provides low rate).

## Results

The results of this analysis are presented as dimensional characteristics of PEP shown in configuration figures in Volume II and in Table 2.10-1, PEP Mast Preliminary Design Requirements.

### 2.11 STRUCTURAL MODELING AND DYNAMIC ANALYSIS

#### Objective

The objective of this task was the analytical simulation of the PEP array deployment assembly and the use of this simulation in a dynamic analysis to obtain load factors. These were used to demonstrate that the design would maintain its structural integrity when subjected to the transient environments at liftoff and landing.

#### Conclusions and Recommendations

Comparisons of specification load factors from Table 4.2-2 of Volume 4, PEP Environmental Specifications, and computed load factors indicate positive margins of safety, since computed load factors are generally well below specification values. For the case of liftoff in the X and Z directions, the computed load factors are nearly equal to the specification values. However, because of the very conservative nature of the analysis which neglects phasing, the actual load factors would be below the specification levels.

This load factor approach and the conclusions reached from this method are applicable to primary structure in the preliminary design phase. When the array deployment assembly design becomes more definitive, a dynamic analysis will be performed in which an expanded mathematical model of the array deployment assembly will be coupled to the Space Transportation System and structural member loads will be obtained as a function of time.

#### Approach

The PEP array deployment assembly was dynamically modeled using the Nastran Computer Program. NASTRAN (Version 48), which was used, is a finite element computer program which is designed to analyze large complex structures for a variety of structural problems. Mathematical models of structures may be constructed from the different finite elements of the program and either static or dynamic analysis performed on the model. Some analytical procedures in the

program include: static response to applied loads, thermal expansion, and imposed deformations; dynamic response to time dependent loads, steady-state sinusoidal loads, and random loads; computation of the natural modes of vibration. The PEP was idealized as an assemblage of quadrilateral plates, triangular plates, and beam elements. A total of 180 gridpoints were used to define the PEP geometry, and the final system totaled 334 degrees of freedom. Figures 2.11-1, -2 and -3 present schematics of the mathematical model. Also, definitions of the gridpoints, coordinate system, elements, material properties and constraints are given in Tables 2.11-1 through -6.

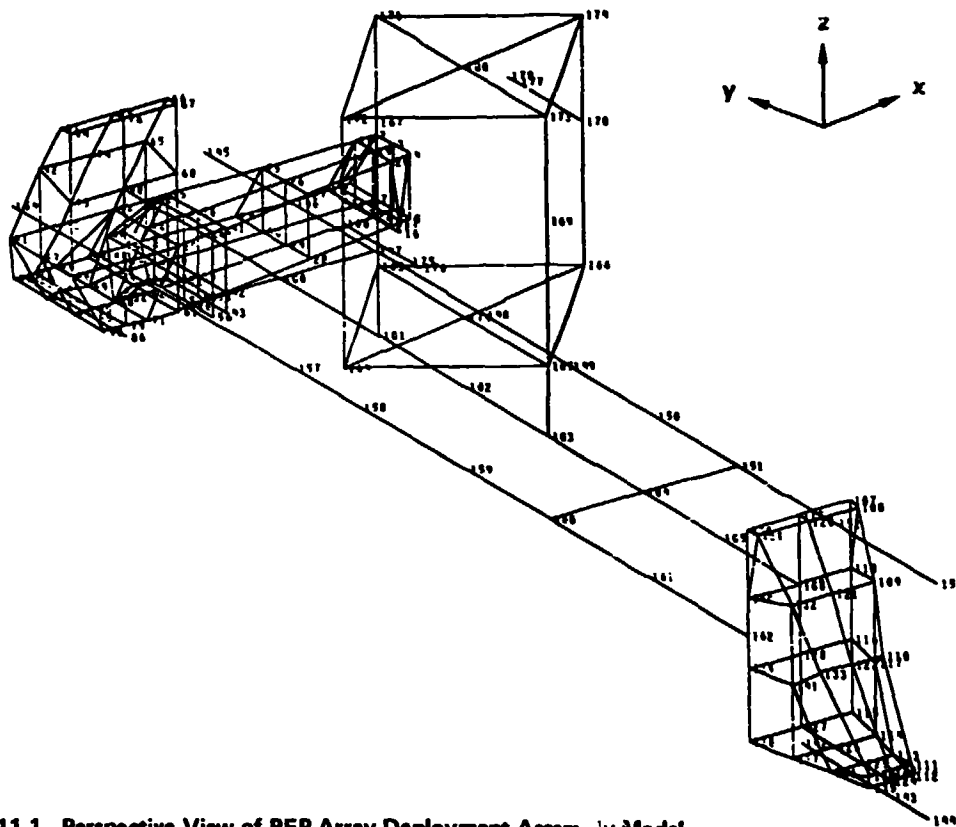


Figure 2.11-1. Perspective View of PEP Array Deployment Assembly Model

From the dynamic model, the first 17 constrained modes of vibration were computed. These modes ranged in frequency of 5.65 to 49.54 Hz and are listed in Table 2.11-7.

Shock spectra from a previous analysis of the Shuttle transport/cradle system with a 2320-lb baseline spacecraft were then used to define the individual modal responses. These spectra which are shown on Figures 2.11-4 through -9 are envelopes of 10 liftoff and five 6 ft per sec landing conditions.

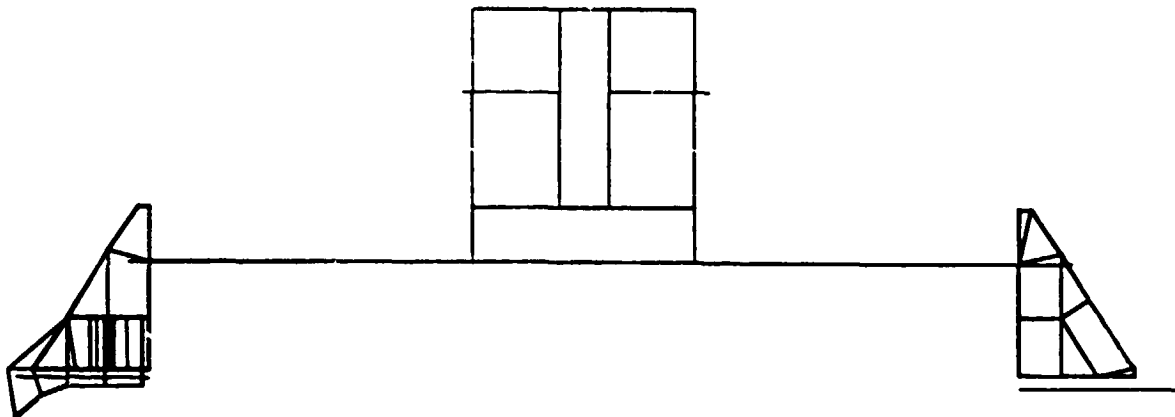


Figure 2.11-2. Front View (+x) of Array Deployment Assembly Model

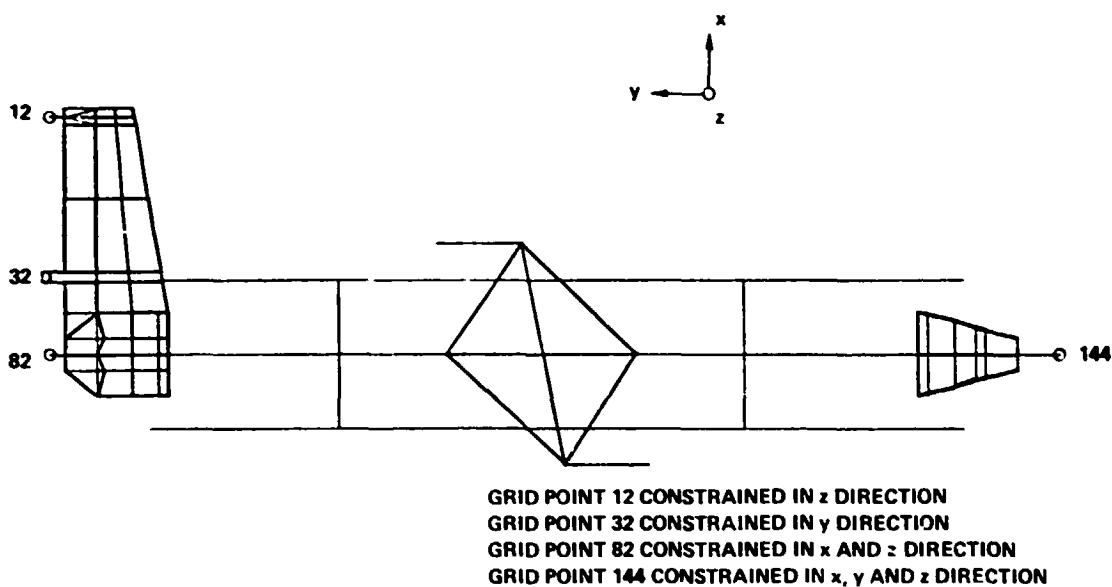


Figure 2.11-3. Top View (z) of PEP Array Deployment Assembly Model

Maximum spectrum values were used to compute the modal responses, which were squared and summed. The square root of the sum for any direction was then computed for the load factors.

### Results

The results of analysis are presented on Table 2.11-8. The computed load factors are well below the specification values except for the case of liftoff in the X and Z directions. However, as noted, the analytical approach is conservative and the refined load factors will be below the specification levels.

Table 2.11-1. Array Deployment Assembly Math Model  
Gridpoint Definition (Page 1 of 4)

GRIDSET	1	X	Y	Z	1
GRID 1		-5.7	44.5	-8.0	
GRID 2		0.0	44.5	0.0	
GRID 3		3.9	44.5	0.0	
GRID 4		6.9	44.5	0.0	
GRID 5		6.9	44.5	-8.0	
GRID 6		3.9	44.5	-8.0	
GRID 7		0.0	44.5	-8.0	
GRID 8		-5.7	43.0	-8.0	
GRID 9		0.0	43.0	-8.0	
GRID 10		3.6	43.0	-8.0	
GRID 11		7.1	43.0	-8.0	
GRID 12		-8.2	43.0	-9.3	
GRID 13		-5.7	43.0	-9.3	
GRID 14		0.0	43.0	-9.3	
GRID 15		3.6	43.0	-9.3	
GRID 16		7.1	43.0	-9.3	
GRID 17		-5.7	41.5	-8.0	
GRID 18		0.0	41.5	0.0	
GRID 19		3.7	41.5	0.0	
GRID 20		7.4	41.5	0.0	
GRID 21		7.4	41.5	-8.0	
GRID 22		3.7	41.5	-8.0	
GRID 23		0.0	41.5	-8.0	
GRID 24		-5.7	28.3	-8.0	
GRID 25		0.0	28.3	0.0	
GRID 26		4.7	28.3	0.0	
GRID 27		9.5	28.3	0.0	
GRID 28		9.5	28.3	-8.0	
GRID 29		4.7	28.3	-8.0	
GRID 30		0.0	28.3	-8.0	
GRID 31		-9.7	15.0	-8.0	
GRID 32		-8.4	15.0	-15.5	
GRID 33		-5.7	15.0	-8.0	
GRID 34		-4.2	15.0	-12.0	
GRID 35		0.0	15.0	0.0	
GRID 36		0.0	15.0	-8.0	
GRID 37		0.0	15.0	-10.5	
GRID 38		5.9	15.0	0.0	
GRID 39		5.9	15.0	-8.0	
GRID 40		5.9	15.0	-10.5	
GRID 41		11.8	15.0	0.0	
GRID 42		11.8	15.0	-8.0	
GRID 43		11.8	15.0	-10.5	
GRID 44		-9.7	13.0	-8.0	
GRID 45		-8.4	13.0	-15.5	
GRID 46		-5.7	13.0	-8.0	
GRID 47		-4.2	13.0	-12.0	

Table 2.11-1. Arra Deployment Assembly Math Model  
Gridpoint Definition (Page 2 of 4)

GRID	48			
GRID	49	0.0	13.0	0.0
GRID	50	0.0	13.0	-8.0
GRID	51	0.0	13.0	-10.5
GRID	52	6.0	13.0	0.0
GRID	53	6.0	13.0	-8.0
GRID	54	6.0	13.0	-10.5
GRID	55	12.0	13.0	0.0
GRID	56	12.0	13.0	-8.0
GRID	57	12.0	13.0	-10.5
GRID	58	-8.7	7.5	-8.0
GRID	59	0.0	7.5	0.0
GRID	60	6.5	7.5	0.0
GRID	61	13.0	7.5	0.0
GRID	62	13.0	7.5	-8.0
GRID	63	6.5	7.5	-8.0
GRID	64	0.0	7.5	-8.0
GRID	65	-8.7	3.0	-8.0
GRID	66	6.5	7.5	10.8
GRID	67	11.2	7.5	17.6
GRID	68	13.0	7.5	17.6
GRID	69	13.0	7.5	0.0
GRID	70	11.2	3.0	-8.0
GRID	71	6.5	3.0	-8.0
GRID	72	13.0	3.0	-8.0
GRID	73	-8.7	0.0	-8.0
GRID	74	0.0	0.0	0.0
GRID	75	6.5	0.0	10.8
GRID	76	11.2	0.0	17.6
GRID	77	13.0	0.0	17.6
GRID	78	13.0	0.0	0.0
GRID	79	13.0	0.0	0.0
GRID	80	13.0	0.0	-8.0
GRID	81	6.5	0.0	-8.0
GRID	82	0.0	0.0	-8.0
GRID	83	-8.4	0.0	-9.3
GRID	84	-8.7	0.0	-9.3
GRID	85	0.0	0.0	-9.3
GRID	86	6.5	0.0	-9.3
GRID	87	13.0	0.0	-9.3
GRID	88	-8.7	-3.0	-8.0
GRID	89	1.2	-3.0	-8.0
GRID	90	6.5	-3.0	-8.0
GRID	91	13.0	-3.0	-8.0
GRID	92	0.0	-7.5	0.0
GRID	93	6.5	-7.5	10.8
GRID	94	11.2	-7.5	17.6
GRID	95	13.0	-7.5	17.6
GRID	96	13.0	-7.5	0.0
GRID	97	6.5	-7.5	0.0

Table 2.11-1. Array Deployment Assembly Math Model  
Gridpoint Definition (Page 3 of 4)

GRID	98			
GRID	99	13.0	0.0	9.0
GRID	100	30.0	0.0	9.0
GRID	101	45.0	0.0	9.0
GRID	102	60.0	0.0	9.0
GRID	103	83.5	0.0	9.0
GRID	104	101.0	0.0	9.0
GRID	105	121.0	0.0	9.0
GRID	106	137.0	0.0	9.0
GRID	107	153.7	0.0	9.0
GRID	108	153.7	7.5	17.6
GRID	109	153.7	7.5	17.6
GRID	110	160.7	6.0	10.5
GRID	111	164.6	4.5	3.0
GRID	112	172.4	3.0	-7.2
GRID	113	172.4	3.0	-8.5
GRID	114	166.4	4.5	-8.5
GRID	115	160.7	6.0	-8.5
GRID	116	153.7	7.5	-8.5
GRID	117	153.7	7.5	.5
GRID	118	160.7	6.0	.5
GRID	119	153.7	7.5	9.2
GRID	120	153.7	0.0	17.6
GRID	121	153.7	0.0	17.6
GRID	122	160.7	0.0	10.5
GRID	123	164.6	0.0	3.0
GRID	124	172.4	0.0	-7.2
GRID	125	172.4	0.0	-8.5
GRID	126	166.4	0.0	-8.5
GRID	127	160.7	0.0	-8.5
GRID	128	153.7	0.0	-8.5
GRID	129	153.7	0.0	.5
GRID	130	153.7	0.0	9.2
GRID	131	153.7	-7.5	17.6
GRID	132	153.7	-7.2	17.6
GRID	133	160.7	-6.0	10.5
GRID	134	164.6	-4.5	3.0
GRID	135	172.4	-3.0	-7.2
GRID	136	172.4	-3.0	-8.5
GRID	137	166.4	-4.5	-8.5
GRID	138	160.7	-6.0	-8.5
GRID	139	153.7	-7.5	-8.5
GRID	140	153.7	-7.5	.5
GRID	141	153.7	-7.5	9.2
GRID	142	160.7	-6.0	.5
GRID	143	153.7	0.0	-10.5
GRID	144	172.4	0.0	-10.5
GRID	145	180.2	0.0	-10.5
GRID	146	9.5	13.5	9.0
GRID	147	28.0	13.5	9.0
GRID		45.0	13.5	9.0

Table 2.11-1. Arra Deployment Assembly Math Model  
Gridpoint Definition (Page 4 of 4)

GRID	148	67.5	13.5	9.0
GRID	149	83.7	13.5	9.0
GRID	150	103.5	13.5	9.0
GRID	151	121.	13.5	9.0
GRID	152	141.5	13.5	9.0
GRID	153	162.5	13.5	9.0
GRID	154	9.5	=13.5	9.0
GRID	155	28.0	=13.5	9.0
GRID	156	45.0	=13.5	9.0
GRID	157	67.5	=13.5	9.0
GRID	158	81.3	=13.5	9.0
GRID	159	103.5	=13.5	9.0
GRID	160	121.	=13.5	9.0
GRID	161	141.5	=13.5	9.0
GRID	162	162.5	=13.5	9.0
GRID	163	65.5	0.0	17.6
GRID	164	87.5	=20.	17.6
GRID	165	101.	0.0	17.6
GRID	166	79.5	20.	17.6
GRID	167	63.5	0.0	35.6
GRID	168	87.5	=20.	35.6
GRID	169	101.	0.0	35.6
GRID	170	79.5	20.	35.6
GRID	171	63.5	0.0	48.6
GRID	172	87.5	=20.	48.6
GRID	173	101.	0.0	48.6
GRID	174	79.5	20.	48.6
GRID	175	101.	=20.	35.6
GRID	176	103.5	=20.	35.6
GRID	177	65.5	20.	35.6
GRID	178	63.5	20.	35.6
GRID	179	83.5	0.0	17.6
GRID	180	83.5	0.0	48.6

1  
2  
3  
4  
5  
6  
7  
8  
9  
10  
11  
12  
13  
14  
15  
16  
17  
18  
19  
20  
21  
22  
23  
24  
25  
26  
27  
28  
29  
30  
31  
32  
33  
34  
35  
36  
37  
38  
39  
40  
41  
42  
43  
44  
45  
46  
47  
48  
49  
50  
51  
52  
53  
54  
55  
56  
57  
58  
59  
60  
61  
62  
63  
64  
65  
66  
67  
68  
69  
70  
71  
72  
73  
74  
75  
76  
77  
78  
79  
80  
81  
82  
83  
84  
85  
86  
87  
88  
89  
90  
91  
92  
93  
94  
95  
96  
97  
98  
99  
100  
101  
102  
103  
104  
105  
106  
107  
108  
109  
110  
111  
112  
113  
114  
115  
116  
117  
118  
119  
120  
121  
122  
123  
124  
125  
126  
127  
128  
129  
130  
131  
132  
133  
134  
135  
136  
137  
138  
139  
140  
141  
142  
143  
144  
145  
146  
147  
148  
149  
150  
151  
152  
153  
154  
155  
156  
157  
158  
159  
160  
161  
162  
163  
164  
165  
166  
167  
168  
169  
170  
171  
172  
173  
174  
175  
176  
177  
178  
179  
180  
181  
182  
183  
184  
185  
186  
187  
188  
189  
190  
191  
192  
193  
194  
195  
196  
197  
198  
199  
200  
201  
202  
203  
204  
205  
206  
207  
208  
209  
210  
211  
212  
213  
214  
215  
216  
217  
218  
219  
220  
221  
222  
223  
224  
225  
226  
227  
228  
229  
230  
231  
232  
233  
234  
235  
236  
237  
238  
239  
240  
241  
242  
243  
244  
245  
246  
247  
248  
249  
250  
251  
252  
253  
254  
255  
256  
257  
258  
259  
260  
261  
262  
263  
264  
265  
266  
267  
268  
269  
270  
271  
272  
273  
274  
275  
276  
277  
278  
279  
280  
281  
282  
283  
284  
285  
286  
287  
288  
289  
290  
291  
292  
293  
294  
295  
296  
297  
298  
299  
300  
301  
302  
303  
304  
305  
306  
307  
308  
309  
310  
311  
312  
313  
314  
315  
316  
317  
318  
319  
320  
321  
322  
323  
324  
325  
326  
327  
328  
329  
330  
331  
332  
333  
334  
335  
336  
337  
338  
339  
340  
341  
342  
343  
344  
345  
346  
347  
348  
349  
350  
351  
352  
353  
354  
355  
356  
357  
358  
359  
360  
361  
362  
363  
364  
365  
366  
367  
368  
369  
370  
371  
372  
373  
374  
375  
376  
377  
378  
379  
380  
381  
382  
383  
384  
385  
386  
387  
388  
389  
390  
391  
392  
393  
394  
395  
396  
397  
398  
399  
400  
401  
402  
403  
404  
405  
406  
407  
408  
409  
410  
411  
412  
413  
414  
415  
416  
417  
418  
419  
420  
421  
422  
423  
424  
425  
426  
427  
428  
429  
430  
431  
432  
433  
434  
435  
436  
437  
438  
439  
440  
441  
442  
443  
444  
445  
446  
447  
448  
449  
450  
451  
452  
453  
454  
455  
456  
457  
458  
459  
460  
461  
462  
463  
464  
465  
466  
467  
468  
469  
470  
471  
472  
473  
474  
475  
476  
477  
478  
479  
480  
481  
482  
483  
484  
485  
486  
487  
488  
489  
490  
491  
492  
493  
494  
495  
496  
497  
498  
499  
500  
501  
502  
503  
504  
505  
506  
507  
508  
509  
510  
511  
512  
513  
514  
515  
516  
517  
518  
519  
520  
521  
522  
523  
524  
525  
526  
527  
528  
529  
530  
531  
532  
533  
534  
535  
536  
537  
538  
539  
540  
541  
542  
543  
544  
545  
546  
547  
548  
549  
550  
551  
552  
553  
554  
555  
556  
557  
558  
559  
560  
561  
562  
563  
564  
565  
566  
567  
568  
569  
570  
571  
572  
573  
574  
575  
576  
577  
578  
579  
580  
581  
582  
583  
584  
585  
586  
587  
588  
589  
590  
591  
592  
593  
594  
595  
596  
597  
598  
599  
600  
601  
602  
603  
604  
605  
606  
607  
608  
609  
610  
611  
612  
613  
614  
615  
616  
617  
618  
619  
620  
621  
622  
623  
624  
625  
626  
627  
628  
629  
630  
631  
632  
633  
634  
635  
636  
637  
638  
639  
640  
641  
642  
643  
644  
645  
646  
647  
648  
649  
650  
651  
652  
653  
654  
655  
656  
657  
658  
659  
660  
661  
662  
663  
664  
665  
666  
667  
668  
669  
670  
671  
672  
673  
674  
675  
676  
677  
678  
679  
680  
681  
682  
683  
684  
685  
686  
687  
688  
689  
690  
691  
692  
693  
694  
695  
696  
697  
698  
699  
700  
701  
702  
703  
704  
705  
706  
707  
708  
709  
710  
711  
712  
713  
714  
715  
716  
717  
718  
719  
720  
721  
722  
723  
724  
725  
726  
727  
728  
729  
730  
731  
732  
733  
734  
735  
736  
737  
738  
739  
740  
741  
742  
743  
744  
745  
746  
747  
748  
749  
750  
751  
752  
753  
754  
755  
756  
757  
758  
759  
760  
761  
762  
763  
764  
765  
766  
767  
768  
769  
770  
771  
772  
773  
774  
775  
776  
777  
778  
779  
780  
781  
782  
783  
784  
785  
786  
787  
788  
789  
790  
791  
792  
793  
794  
795  
796  
797  
798  
799  
800  
801  
802  
803  
804  
805  
806  
807  
808  
809  
810  
811  
812  
813  
814  
815  
816  
817  
818  
819  
820  
821  
822  
823  
824  
825  
826  
827  
828  
829  
830  
831  
832  
833  
834  
835  
836  
837  
838  
839  
840  
84

**MCDONNELL DOUGLAS** 

Table 2.11-3. Bay Deployment Assembly Math Model  
 Near Elements (Page 1 of 2)

CBAR	1		12	13	8	2
CBAR	2		13	14	8	2
CBAR	3		14	15	8	2
CBAR	4		15	16	8	2
CBAR	5		82	83	72	2
CBAR	6		83	84	72	2
CBAR	7		84	85	72	2
CBAR	8		85	86	72	2
CBAR	9		98	99	76	2
CBAR	10		99	100	76	2
CBAR	11		100	101	76	2
CBAR	12		101	102	76	2
CBAR	13		102	103	76	2
CBAR	14		103	104	76	2
CBAR	15		104	105	76	2
CBAR	16		105	106	76	2
CBAR	17		142	143	123	2
CBAR	18		143	144	123	2
CBAR	19		144	145	102	2
CBAR	20		100	156	102	2
CBAR	21		104	151	102	2
CBAR	22		104	160	102	2
CBAR	23		145	146	102	2
CBAR	24		146	147	102	2
CBAR	25		147	148	102	2
CBAR	26		148	149	102	2
CBAR	27		149	150	102	2
CBAR	28		150	151	102	2
CBAR	29		151	152	102	2
CBAR	30		152	153	102	2
CBAR	31		153	154	102	2
CBAR	32		154	155	102	2
CBAR	33		155	156	102	2
CBAR	34		156	157	102	2
CBAR	35		157	158	102	2
CBAR	36		158	159	102	2
CBAR	37		159	160	102	2
CBAR	38		160	161	102	2
CBAR	39		161	162	102	2
CBAR	40		162	163	166	2
CBAR	41		163	164	164	2
CBAR	42		164	165	165	2
CBAR	43		165	166	163	2
CBAR	44		166	167	163	2
CBAR	45		167	168	173	2
CBAR	46		168	169	173	2
CBAR	47		169	170	173	2
CBAR	48		170	171	173	2
CBAR	49		171	172	173	2
CBAR	50		172	173	173	2

Table 2.11-3. Array Deployment Assembly Math Model  
Beam Elements (Page 2 of 2)

CBAR	51	1	165	169	171	
CBAR	52	1	169	173	171	2
CBAR	53	1	171	172	173	2
CBAR	54	1	171	174	173	2
CBAR	55	1	172	173	171	2
CBAR	56	1	173	174	171	2
CBAR	57	1	168	173	167	2
CBAR	58	1	173	176	167	2
CBAR	59	1	170	177	167	2
CBAR	60	1	177	178	167	2
CBAR	61	1	171	180	172	2
CBAR	62	1	172	180	171	2
CBAR	63	1	173	180	172	2
CBAR	64	1	174	180	171	2
CBAR	65	1	163	179	164	2
CBAR	66	1	164	179	163	2
CBAR	67	1	165	179	164	2
CBAR	68	1	166	179	163	2

Table 2.11-4. Array Deployment Assembly Math Model  
 Quadrilateral Plate Elements (Page 1 of 3)

CQUAD4	100	1	2	3	6	7
CQUAD4	101	1	3	4	5	6
CQUAD4	102	2	2	3	19	18
CQUAD4	103	2	3	4	20	19
CQUAD4	104	1	18	19	22	23
CQUAD4	105	1	19	20	21	22
CQUAD4	106	3	5	6	10	11
CQUAD4	107	3	10	11	21	22
CQUAD4	108	3	6	7	9	10
CQUAD4	109	3	9	10	22	23
CQUAD4	110	3	1	7	9	8
CQUAD4	111	3	8	9	23	17
CQUAD4	112	1	17	18	25	24
CQUAD4	113	1	18	19	26	25
CQUAD4	114	1	19	20	27	26
CQUAD4	115	1	20	21	28	27
CQUAD4	116	1	21	22	29	28
CQUAD4	117	1	22	23	30	29
CQUAD4	118	1	17	25	30	24
CQUAD4	119	1	25	26	29	30
CQUAD4	120	1	26	27	28	29
CQUAD4	121	1	24	25	35	33
CQUAD4	122	1	25	26	38	35
CQUAD4	123	1	26	27	41	38
CQUAD4	124	1	27	28	42	41
CQUAD4	125	1	28	29	39	42
CQUAD4	126	1	29	30	36	39
CQUAD4	127	1	24	30	36	33
CQUAD4	128	2	31	32	34	35
CQUAD4	129	2	33	34	37	36
CQUAD4	130	2	38	36	39	38
CQUAD4	131	2	36	37	40	39
CQUAD4	132	2	38	39	42	41
CQUAD4	133	2	39	40	43	42
CQUAD4	134	1	31	32	45	44
CQUAD4	135	1	31	44	48	35
CQUAD4	136	1	33	35	48	46
CQUAD4	137	1	38	38	51	48
CQUAD4	138	1	38	41	54	51
CQUAD4	139	1	41	42	55	54
CQUAD4	140	1	31	33	46	44
CQUAD4	141	1	33	36	49	46
CQUAD4	142	1	34	39	52	49
CQUAD4	143	1	39	42	55	52
CQUAD4	144	2	44	45	47	46
CQUAD4	145	2	46	47	50	49
CQUAD4	146	2	48	49	52	51
CQUAD4	147	2	49	50	53	52
CQUAD4	148	2	51	52	55	54
CQUAD4	149	2	52	53	56	55

Table 2.11-4. Array Deployment Assembly Math Model  
 Quadrilateral Plate Elements (Page 2 of 3)

CQUAD4	150	1	46	48	58	57
CQUAD4	151	1	48	51	59	58
CQUAD4	152	1	51	54	60	59
CQUAD4	153	1	54	55	61	60
CQUAD4	154	1	55	55	61	62
CQUAD4	155	1	49	52	62	63
CQUAD4	156	1	46	49	65	57
CQUAD4	157	1	58	59	70	69
CQUAD4	158	1	39	60	71	70
CQUAD4	159	1	57	63	69	64
CQUAD4	160	1	62	63	69	70
CQUAD4	161	1	61	62	70	71
CQUAD4	162	3	64	69	81	72
CQUAD4	163	3	69	70	80	81
CQUAD4	164	3	70	71	79	80
CQUAD4	165	3	72	81	80	87
CQUAD4	166	3	80	81	88	89
CQUAD4	167	3	79	80	89	90
CQUAD4	168	1	63	66	87	88
CQUAD4	169	1	59	60	68	65
CQUAD4	170	1	58	59	70	69
CQUAD4	171	1	59	60	71	70
CQUAD4	172	1	88	89	97	91
CQUAD4	173	1	89	90	96	97
CQUAD4	174	1	92	95	96	97
CQUAD4	175	1	92	93	94	95
CQUAD4	176	1	67	69	77	76
CQUAD4	177	1	76	77	95	94
CQUAD4	178	1	60	68	77	78
CQUAD4	179	1	77	78	96	95
CQUAD4	180	1	66	71	79	78
CQUAD4	181	1	78	79	90	96
CQUAD4	182	1	58	64	72	73
CQUAD4	183	1	58	65	74	73
CQUAD4	184	1	65	66	75	74
CQUAD4	185	1	66	67	76	75
CQUAD4	186	1	72	73	81	87
CQUAD4	187	1	73	74	92	91
CQUAD4	188	1	74	75	93	92
CQUAD4	189	1	75	76	94	93
CQUAD4	190	1	107	108	120	119
CQUAD4	191	1	108	109	121	120
CQUAD4	192	1	109	110	122	121
CQUAD4	193	1	110	111	123	122
CQUAD4	194	1	111	112	124	123
CQUAD4	195	1	119	120	131	130
CQUAD4	196	1	120	121	132	131
CQUAD4	197	1	121	122	133	132
CQUAD4	198	1	122	123	134	133
CQUAD4	199	1	123	124	135	134

Table 3.11-- Array Deployment Assembly Matrix Model  
 Quadrilateral Plate Elements (Page 3 of 3)

CQUAD4	200	1	110	111	113	117
CQUAD4	201	1	114	115	116	117
CQUAD4	202	1	109	117	116	118
CQUAD4	203	1	133	134	136	141
CQUAD4	204	1	132	140	139	141
CQUAD4	205	1	137	138	139	141
CQUAD4	206	1	107	118	129	119
CQUAD4	207	1	119	129	140	130
CQUAD4	208	1	116	118	129	128
CQUAD4	209	1	128	127	140	139
CQUAD4	210	1	115	11	128	127
CQUAD4	211	1	127	126	139	134
CQUAD4	212	2	114	115	117	121
CQUAD4	213	2	113	114	126	125
CQUAD4	214	2	112	113	125	124
CQUAD4	215	2	124	127	136	137
CQUAD4	216	2	123	126	137	134
CQUAD4	217	2	124	125	136	135

Table 2.11-5. Array Deployment Assembly Math Model  
Triangular Plate Elements and Added Masses

CTRIAS	1000	1	1	2	7
CTRIAS	1001	2	1	2	8
CTRIAS	1002	2	2	8	18
CTRIAS	1003	2	8	17	18
CTRIAS	1004	1	17	18	23
CTRIAS	1005	2	11	20	21
CTRIAS	1006	2	4	11	20
CTRIAS	1007	2	4	5	21
CTRIAS	1008	1	24	25	30
CTRIAS	1009	2	31	33	35
CTRIAS	1010	2	33	35	36
CTRIAS	1011	2	44	46	48
CTRIAS	1012	2	46	48	49
CTRIAS	1013	1	57	58	64
CTRIAS	1014	1	40	61	71
CTRIAS	1015	1	58	59	65
CTRIAS	1016	1	58	64	69
CTRIAS	1017	1	91	92	97
CTRIAS	1018	1	87	88	91
CTRIAS	1019	1	107	108	113
CTRIAS	1020	1	108	109	118
CTRIAS	1021	1	109	110	117
CTRIAS	1022	1	111	112	113
CTRIAS	1023	1	113	114	117
CTRIAS	1024	1	130	131	140
CTRIAS	1025	1	131	132	140
CTRIAS	1026	1	132	133	141
CTRIAS	1027	1	134	135	136
CTRIAS	1028	1	136	137	141
:					
:					
CONM2	1	99	0	22.0	
CONM2	2	105	0	37.5	
CONM2	3	100	0	63.0	
CONM2	4	106	0	15.5	
CONM2	5	176	0	140.0	
CONM2	6	170	0	140.0	

81

Table 2.11-7. PEP Array Deployment Assembly

Mode number	Frequency (Hz)
1	5.65
2	7.91
3	12.60
4	14.12
5	15.12
6	17.03
7	18.01
8	18.90
9	19.40
10	22.20
11	27.52
12	34.86
13	37.51
14	44.49
15	45.77
16	48.22
17	49.54

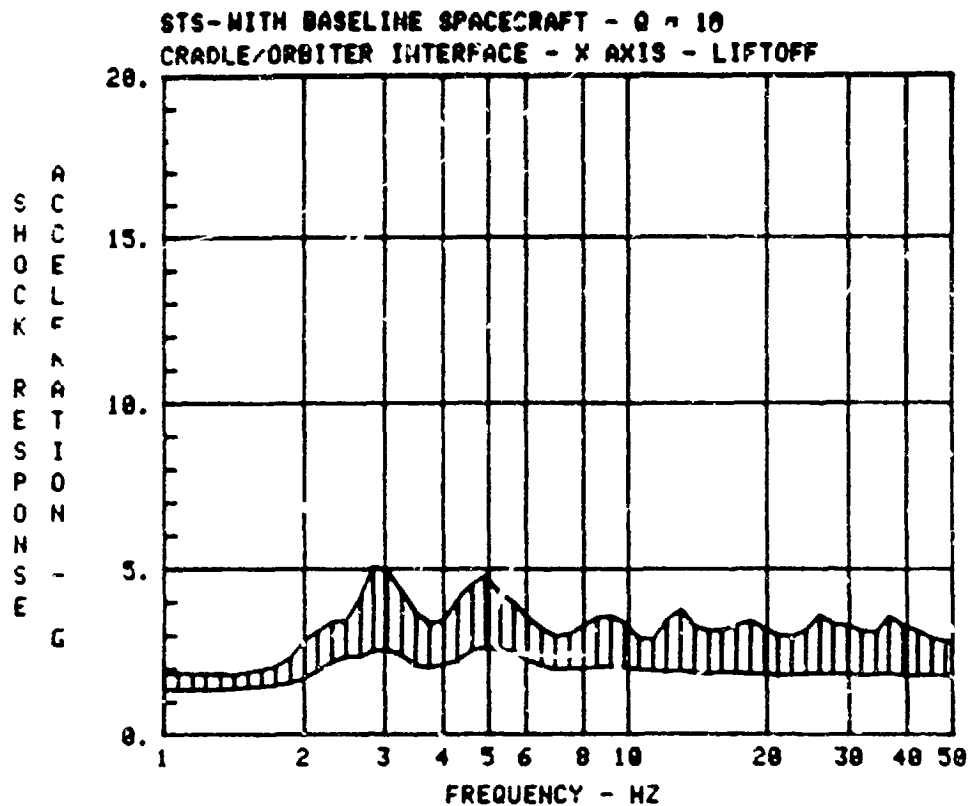


Figure 2.11-4. STS/Baseline Spacecraft Cradle/Orbiter interface X-Axis Shock Spectrum - Liftoff

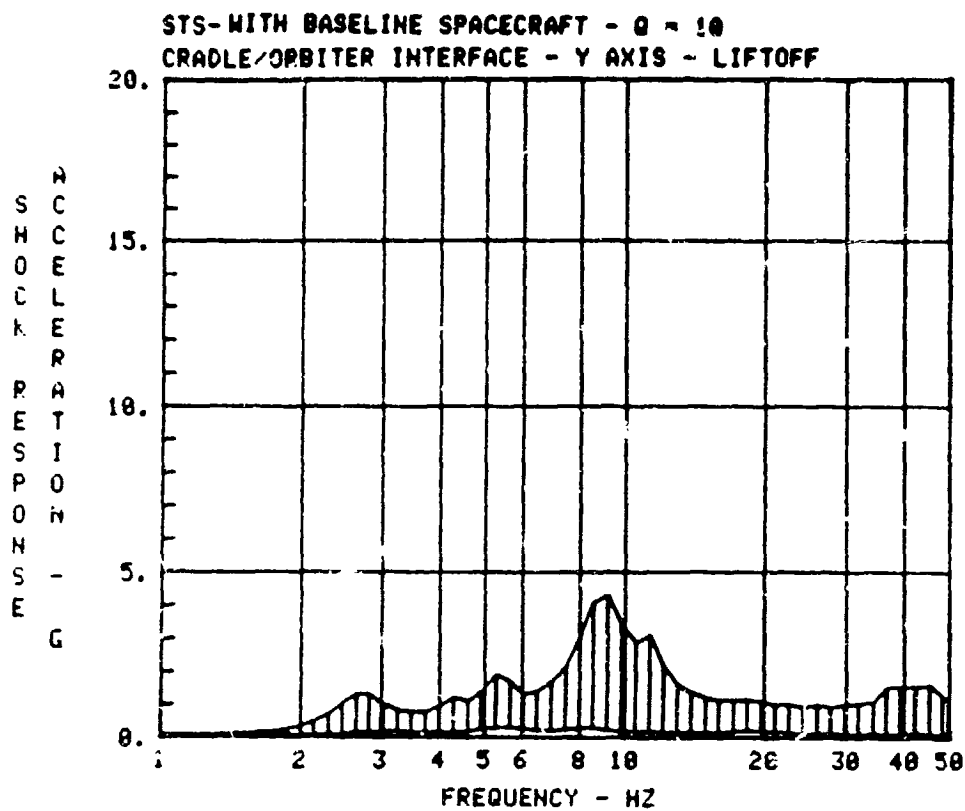


Figure 2.11-5. STS/Baseline Spacecraft Cradle/Orbiter Interface Y-Axis Shock Spectrum - Liftoff

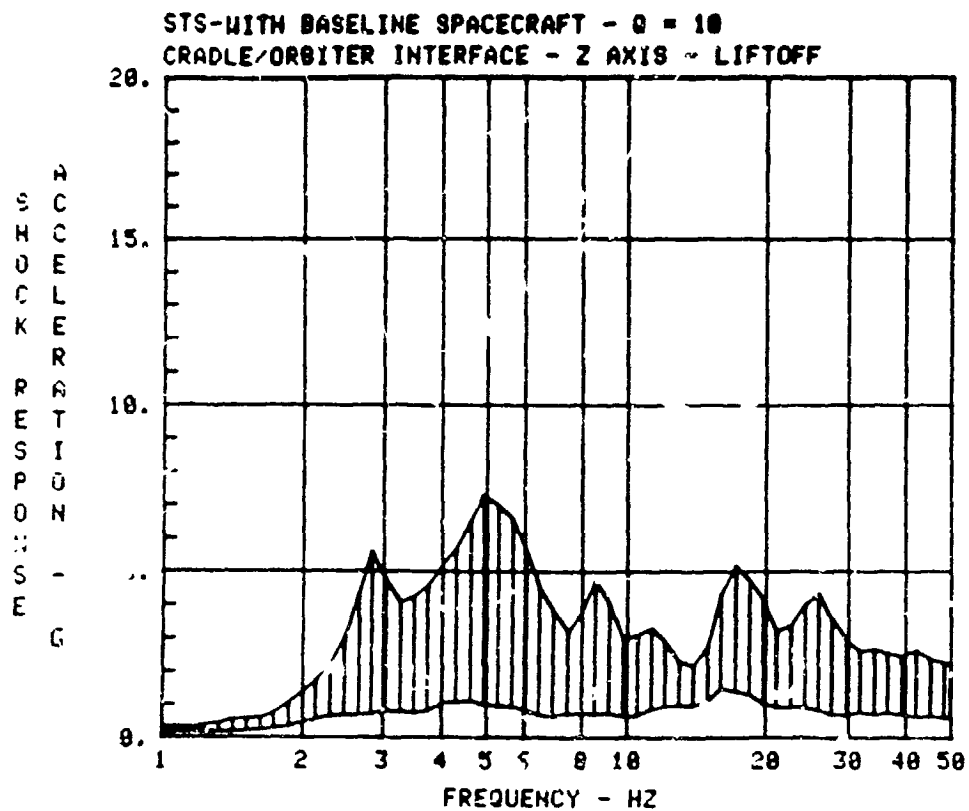


Figure 2.11-6. STS/Baseline Spacecraft Cradle/Orbiter Interface Z-Axis Shock Spectrum - Liftoff

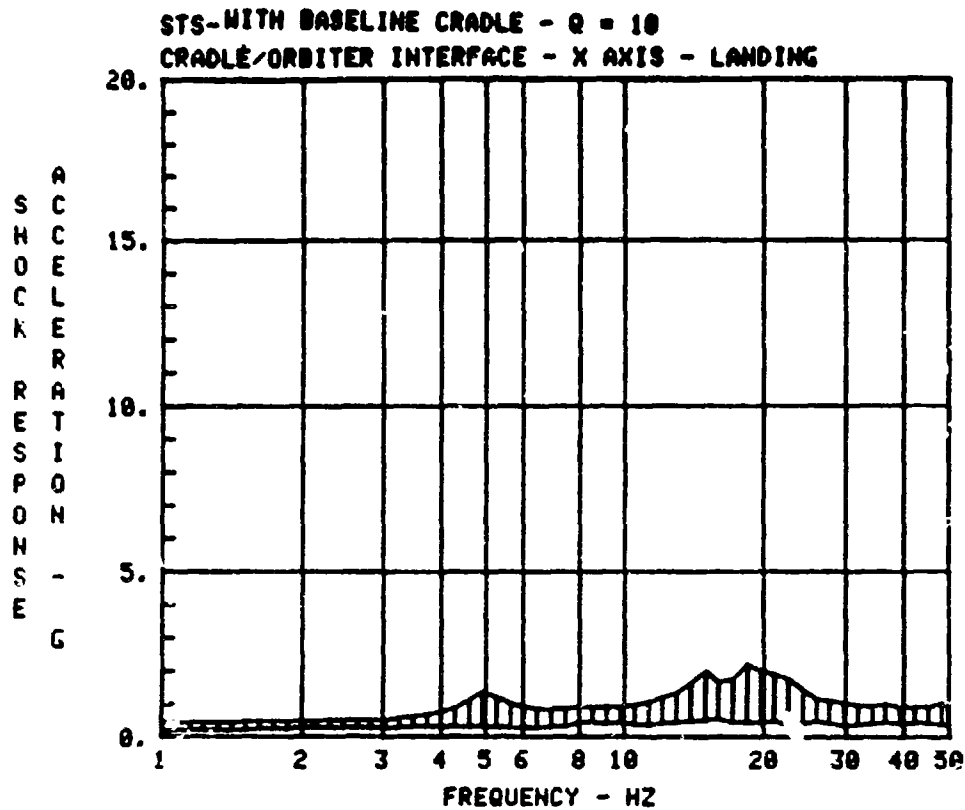


Figure 2.11-7. STS/Baseline Spacecraft Cradle, Cradle/Orbiter Interface X-Axis Shock Spectrum — Landing

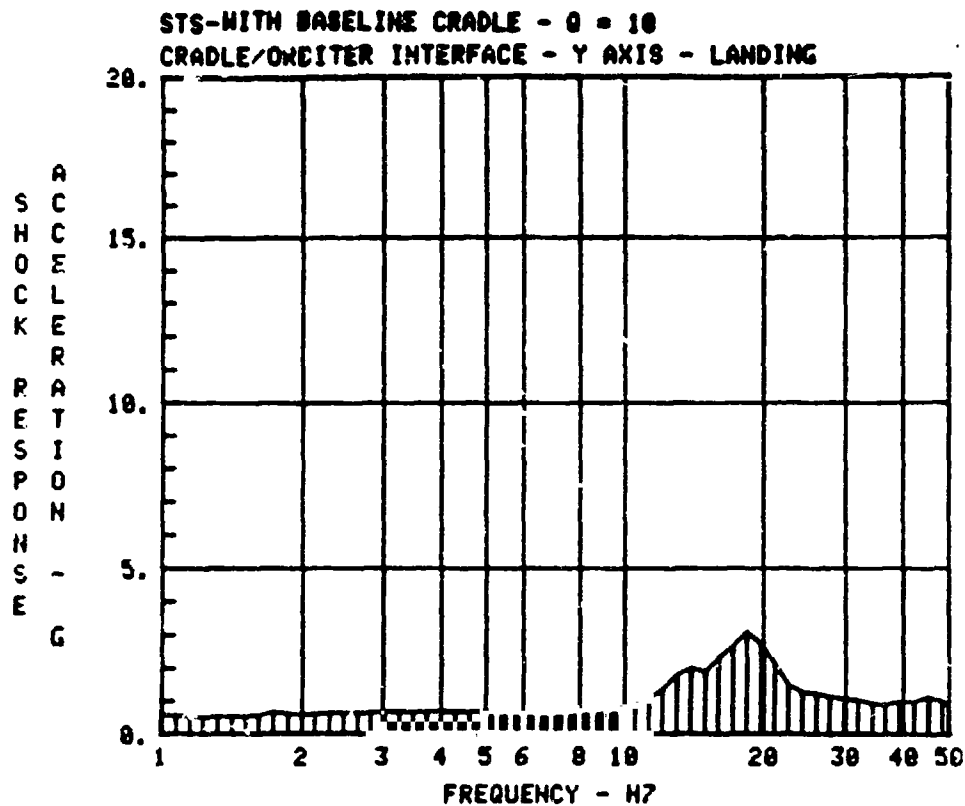


Figure 2.11-8. STS/Baseline Spacecraft Cradle, Cradle/Orbiter Interface Y-Axis Shock Spectrum — Landing

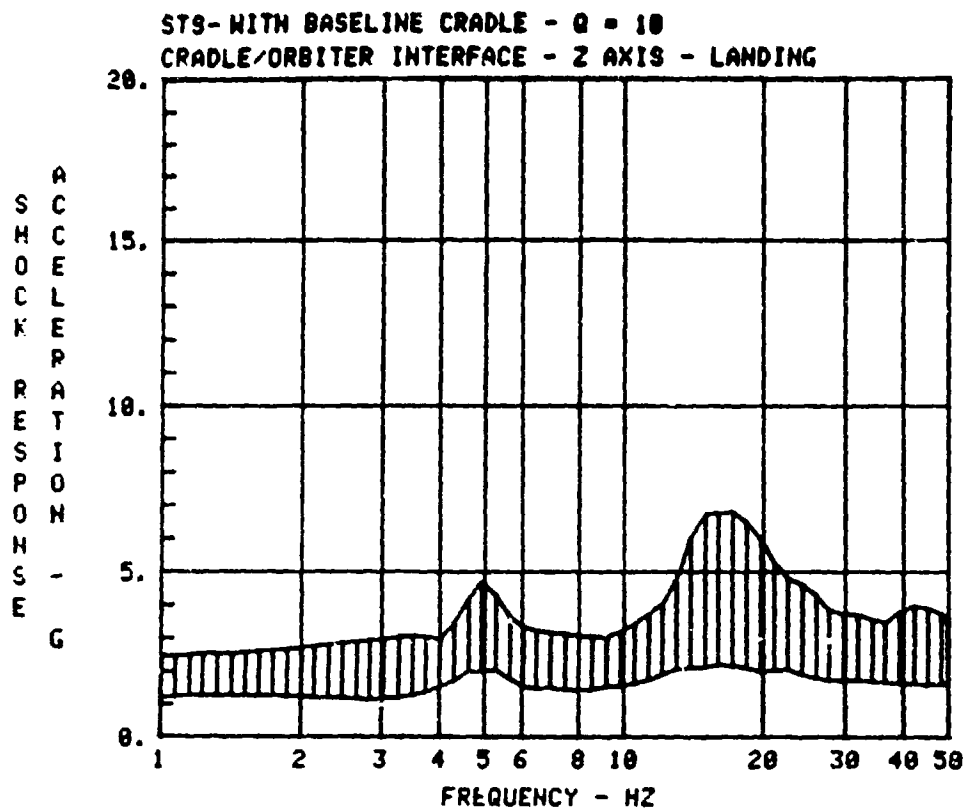


Figure 2.11-9. STS/Baseline Cradle, Cradle/Orbiter Interface Z-Axis Shock Spectrum - Landing

Table 2.11-8. Specification and Computed Load Factors

Flight event		Load factor (Gs)		
		Nx	Ny	Nz
Lift-off	Spec value	3.2	1.0	2.5
	Computed value	3.3	0.3	2.3
Landing	Spec value	2.0	1.0	4.2
	Computed value	0.8	0.1	2.5

## 2.12 POWER SYSTEM CONFIGURATION

### Objective

The objective of this study effort was to determine the overall electrical power system (EPS) sizing and electrical configuration, including sizing of the major components: (1) solar array, (2) voltage regulators, (3) distribution and control, and (4) system wiring and cabling.

### Conclusions and Recommendations

The PEP solar array output power requirement is 32.9 kW (16.4 kW for each of the 2 wings). Each of the 2 array wing blankets is  $3.84 \times 37.8 \text{ m} = 145 \text{ m}^2$  in area. Each of the 6 power regulators must be sized for approximately 5.27 kW at the regulator terminals. The PEP power output is 26.9 kW at the PEP interfaces (stations 693 and 636).

### Assumptions

The system is assumed to require a net electrical output of 29.0 kW for sizing purposes; it is further assumed that the fuel cells will contribute all of this power at night and 3.0 kW nominal (3 FCP's at 1.0 kW each) during the daylight periods as required by mission duration objectives. The 29.0 kW is assumed to be rated/delivered as follows: (1) 4.67 kW for Orbiter at main C; (2) 4.67 kW for Orbiter at main A; (3) 4.67 kW for Orbiter at main B and 5.0 kW for payloads at station 603 (both positive and return wires); (4) 10 kW for payloads at station 645 (both positive and return wires). The PEP to Orbiter interface is assumed to occur in connectors at station 693 (port side for main A) and station 636 (starboard side for mains B and C). PEP and Orbiter cable losses down to the above assumed load interfaces are per the discussion and examples of section 2.6 above.

### Approach

Cable and component losses and mismatches were evaluated and applied to the system/component sizing analysis.

### Results

The PEP EPS electrical configuration and sizing is summarized in Figure 2.12-1. The system consists of a 2 wing solar array, 2 diode assembly boxes, a 6 circuit cable system down the RMS to 6 pulse width modulated power regulators, a power distribution box, shunt limiters and PEP cabling; in addition, the PEP power traverses some Orbiter cables and equipment before it reaches the Orbiter and payload loads. The load requirement is 29.0 kW net; in addition, an allowance of 0.20 kW has been made for operation of the PEP system. Hence, PEP must supply more than 26.2 kW gross at the load interface (26.8 kW at the PEP interface), considering that the fuel cells deliver an average of 3.0 kW during the daytime.

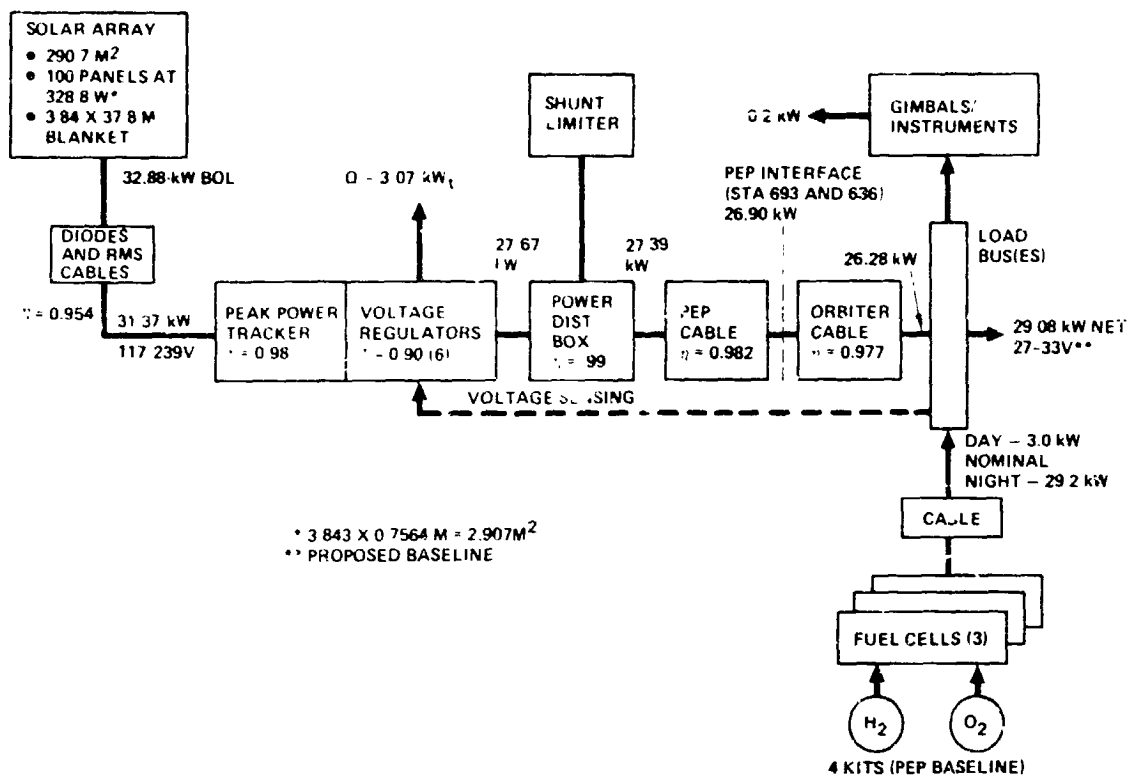


Figure 2.12-1. PEP Electrical Power System

The system has been sized to deliver a net of 29.1 kW to the loads based on an integral number of panels in each solar array wing; the resulting power is 26.9 kW at the PEP interface at stations 693 and 636. The Orbiter cable efficiency (0.977) and the PEP cable efficiency (0.982) are based on the analysis discussed in section 2.6. The power distribution box (PDB) power efficiency is 0.99; since part of the losses are not series resistance losses, the voltage efficiency is 0.994. Power distribution box losses total approximately 279 watts which includes 172 watts for series elements such as fuses, contacts and wiring, and 107 watts operating power for components such as current sensors and relay drivers.

The voltage regulator block of Figure 2.12-1 represents 6 regulators that are paralleled in pairs, one pair associated with each of the 3 fuel cells. The output power requirements for these regulators are presented in Table 2.12-1, based on the analysis discussed in section 2.6.

Table 2.12-1. Voltage Regulator Power Output Requirements  
Output

Associated FCP	Nominal power <sup>1</sup> , kW	Design power <sup>1</sup> , kW (Nominal x 1.1)	Design current <sup>1</sup> , A (at 33 V)	Unit design current <sup>2</sup> , A
FCP 1	8.95	9.85	298.5	149.3
FCP 2	9.14	10.05	304.5	152.3
FCP 3	<u>9.58</u>	<u>10.54</u>	<u>319.4</u>	159.7
Total	27.67	30.44	922.4	

<sup>1</sup>Two regulators in parallel.

<sup>2</sup>Each of two regulators.

It should be noted that the regulator design precludes the voltage output from exceeding 33 volts in event of loss of remote sensing; when the remote sensing leads are connected the voltage will increase by an amount equal to the system voltage drop between the sense point and the regulator terminals and may exceed 33 volts.

The nominal power requirement for each of the 3 pairs of regulators is shown in the first column of the table; the design power (second column) is 10% higher to provide flexibility to accommodate: (1) a different split of loads among the 3 buses than the nominals assumed in the analysis of section 2.6 and (2) permit the utilization of the extra capability available from the solar array much of the time when the array is colder than the design case (e.g., during continuous sunlight orbits). The current ratings of the table are based on a regulator output voltage of 33V.

The regulator efficiency of 90% used in Figure 2.12-1 is conservative, based on MDAC breadboard test results and extrapolations thereof (see section 2.7). The peak power tracker efficiency allows for a mismatch between the regulator and solar array operating points; this results in an array sizing penalty, but does not result in regulator heat rejection.

Transmission losses for the number-6 gage conductors are calculated to be 1147 watts for a conductor operating temperature of 95°C. Slip ring losses are 108 watts assuming a contact drop of 0.2 volt. Connector losses total 44 watts using a 20 milliwatt contact drop at 95°C. Diode box assembly losses are 215 watts total for both boxes based on 0.8 volt diode drop. Total transmission losses are 1,514 watts. These losses result in the 95.4% efficiency for the diode and RMS cable block of the figure.

The solar array output power requirement is about 32.9 kW to deliver 29.0 kW net to the loads. The array is rated at beginning-of-life power; the resulting array end-of-life power is approximately 30 kW. The array voltage at the peak power point is approximately 122V as determined in the previous phase of the PEP study.

## 2.13 SOLAR ARRAY WING ASSEMBLY REQUIREMENTS

### Objective

The objectives of this effort were to define: (1) the major requirements for the solar array wing assembly (the PEP array consists of two wing assemblies) and (2) the performance/characteristics of the solar array wing assembly.

### Conclusions and Recommendations

The nominal PEP solar array wing electrical power output requirement is 16.4 kW, BOL. The output voltage requirement is 122<sup>V</sup> (max power at 60°C) and 239<sup>V</sup> (open circuit at -70°C). A 145<sup>m</sup><sup>2</sup> blanket on each of the two wings, which are 3.84 x 37.8m, will provide the required power.

### Assumptions

The requirements and designs discussed in this section are based on the following assumptions: (1) power output and sizes are based on the nominal conditions specified herein and is considered to be nominal beginning of life (BOL) performance, as contrasted to maximum or minimum performance, (2) 29.0 kW net (29.2 kW gross) power (BOL, constant continuous), (3) the Orbiter fuel cells typically operate at an average of 1.0 kW each, which is obtained by allowing the Orbiter loads to operate at up to 33<sup>V</sup> at the load interface, and (4) the solar array wing/solar cell characteristics are as indicated in Figure 2.13-1.

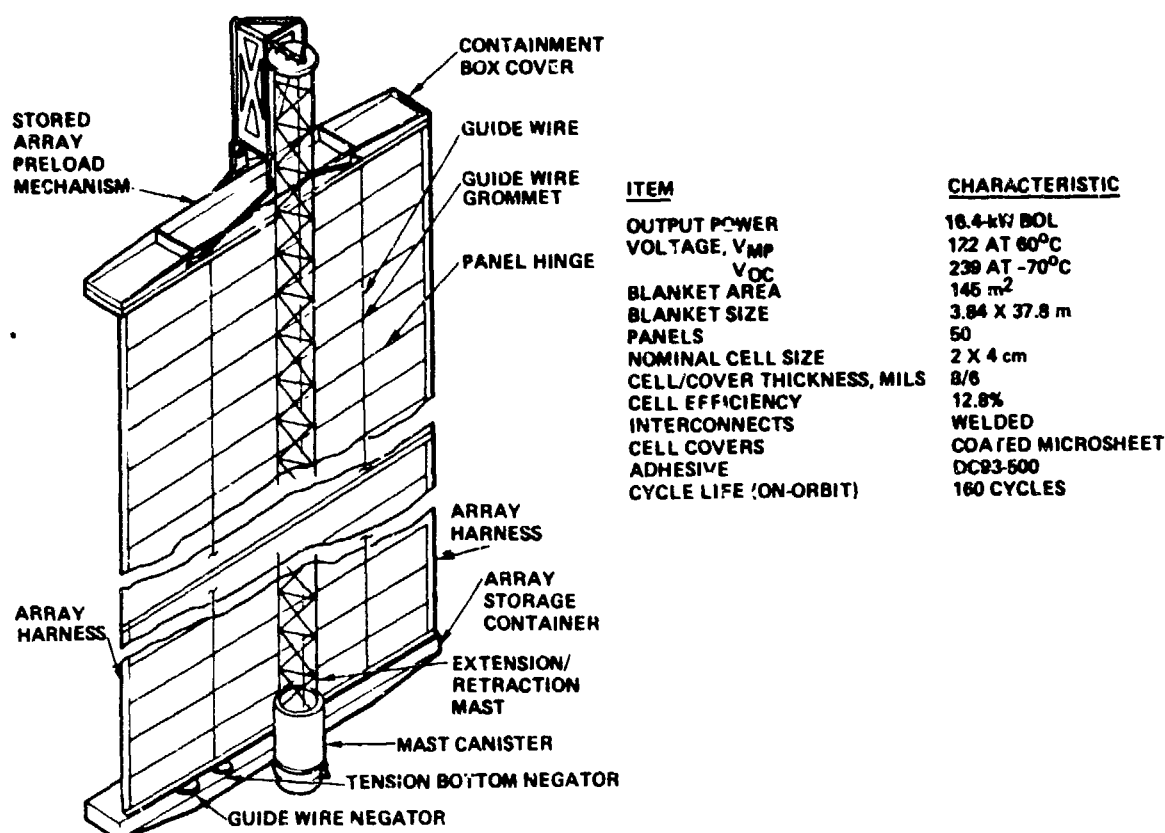


Figure 2.13-1. Solar Array Wing Characteristics (LMSC Example)

### Approach

The solar array assembly requirements were derived as the result of analysis of the PEP mission, the Orbiter interfaces and the PEP electrical power system (EPS). The reference system example described herein is based on the LMSC SEP/PEP work.

### Results

The mission-related PEP solar array assembly requirements are presented in Table 2.13-1 and the array performance and design requirements are presented in Table 2.13-2. The PEP dedicated to ETR operates 78% of its time in a  $28.5^{\circ}$  orbit and 22% of the time in a  $55^{\circ}$  orbit. The PEP dedicated to WTR operates 100% of the time in  $90-104^{\circ}$  orbits.

The array wing power requirement of 16.4 kW is based on the assumptions noted above. The requirement for a large number of independent modules results from the need to retain flexibility to allocate varying percentages of the solar array to the Orbiter load buses and the payloads. The mast deployment and retraction power limits are based on RMS SPEE wiring limitations.

Table 2.13-1. PEP Solar Array Mission Requirements  
(Each of Two Wing Assemblies)

Item	Range	Nominal
1. Orbit altitude, km (n. mi)	185-1,110 (100-600)	407 (220)
2. Orbit inclination, deg/% time		
a. ETR PEP	NA	28.5°/78%; 55°/22%
b. WTR PEP	NA	104°/100%
3. Solar vector/orbit plane angle ( $\beta$ ), deg	±127.5	50
4. Array orientation	All attitudes	Normal to solar vector
5. Array shadowing	0-100%; orbit rate	none
6. Launch vehicle	Shuttle Orbiter - payload bay within RMS reach	Shuttle Orbiter; Payload Bay - Station 715

A summary of a representative design (LMSC example) that meets the above requirements is presented in Figure 2.13-1. The life is 160 complete on-orbit deployment and retraction cycles.

## 2.14 SOLAR ARRAY CONTROL AVIONICS REQUIREMENTS/CRITERIA DEFINITIONS

### Objectives

The objective of this study is to define the functional and operational requirements for the PEP Solar Array Pointing Subsystem (SAPS). The study should include applicable array dynamics considerations. Software and hardware specifications shall be defined.

### Conclusions and Recommendations

#### Conclusions:

- Either a proportional or an on-off PEP gimbal controller concept will satisfy the pointing requirements for the PEP solar array.
- The Alpha and Beta gimbal rotations do not result in effective damping of all compliance spring flexible modes for all Beta gimbal positions. Effective compliance spring modal damping is available for some modes at some PEP Beta gimbal positions.

Table 2.13-2. PEP Solar Array Performance and Design Requirements  
(Each of Two Wing Assemblies)

Item	Range	Nominal
1. Output power*, kW		
a. BOL (design to)	TBD	16.4
b. EOL (reference)	TBD	~15.2
2. BOL output voltage*, V		
a. Vmp	NA	125 > V > 100
b. Voc	NA	< 250
3. BOL output current*, A		
a. Isc	TBD	Isc > 1.1 X Imp
4. Electrical modularity/interface		
a. Electrical modules, independent circuits	> 50	> 50
b. Instrumentation circuits	> 5	> 5
5. Operational usage		
a. Time Period		Late 1982-Late 1990
b. Mission frequency, mission/year	TBD	8
c. Mission duration, days	7-48	14
6. Deploy/retract cycles per mission		
a. On-orbit	TBD	2
b. On-ground	0 -	TBD
7. Deployment and retraction		
a. Time, min	TBD	6
b. Power		
(1) Current (retraction, lockup),	TBD	40
(2) Voltage	18-33	18
8. Magnetic forces	TBD	Minimize
9. Storage		
a. On-orbit	TBD	3.07 yr
b. Orbiter payload bay		
(1) Launch/reentry	TBD	50 hr
(2) VAB	TBD	960 hr
(3) Hangar S and OCF	TBD	~7 yr
Storage - Hangar		
c. Reliability		
Orbiter/crew safety	0.9999-1.0	0.9999
b. Return from orbit	TBD	TBD
c. Mission completion	TBD	TBD

\*At array base to diode assembly, at 1,353 W/m<sup>2</sup> illumination and nominal conditions herein.

- The on-off PEP gimbal controller concept meets all requirements when the augmented system damping requirement is dropped.

- The PEP gimbal control system will function autonomously in all flight modes except for occasional keyboard or ground link inputs and updates.

- The on-off PEP gimbal controller concept can easily be mechanized in most available microprocessors.

#### Recommendations:

- The on-off PEP gimbal controller concept should be considered the baseline concept.

- The baseline PEP gimbal controller should not be used to damp the PEP structure dynamic motion.

- Further analysis with the proportional controller with induced damping is worthwhile. A dynamic model including both linear and rotational motions induced by the gimbals and a compliance spring model giving two spring degrees of freedom to each half of the array should be used.

#### Assumptions

It was assumed that the major components of the Solar Array Pointing System (SAPS) are the Alpha and Beta gimbals, the gimbal drives, the sensor(s) for closed loop feedback and the control law. The Alpha gimbal axis will normally be oriented perpendicular to the orbit plane and gimbal at orbit rate for Orbiter local vertical orientations. The Alpha gimbal will have continuous bidirectional rotation capability (i.e., no stops). The Alpha gimbal axis is oriented via the Beta gimbal from roughly parallel to the solar array plane, to perpendicular to the solar array plane. (Figure 2.14-1). The Beta gimbal provides orbit Beta angle compensation when the Alpha axis is perpendicular to the orbit plane.

The basic solar array pointing accuracy requirements are quite loose from a maintenance of electrical power viewpoint. Assuming power is proportional to cosine of the angle between the array normal and the sun line and an allowable power drop of 1 percent, results in an acceptable pointing error of 8 degrees. Another consideration is "feathering" the array for low altitude, high aerodynamic force missions. An 8-degree misalignment would project 14 percent of the array face to the wind which may be undesirable. Thus, a  $\pm 2$  degree accuracy requirement was assumed. Though sun track will not require  $\pm 2$  degree accuracy, that capability should be reasonable.

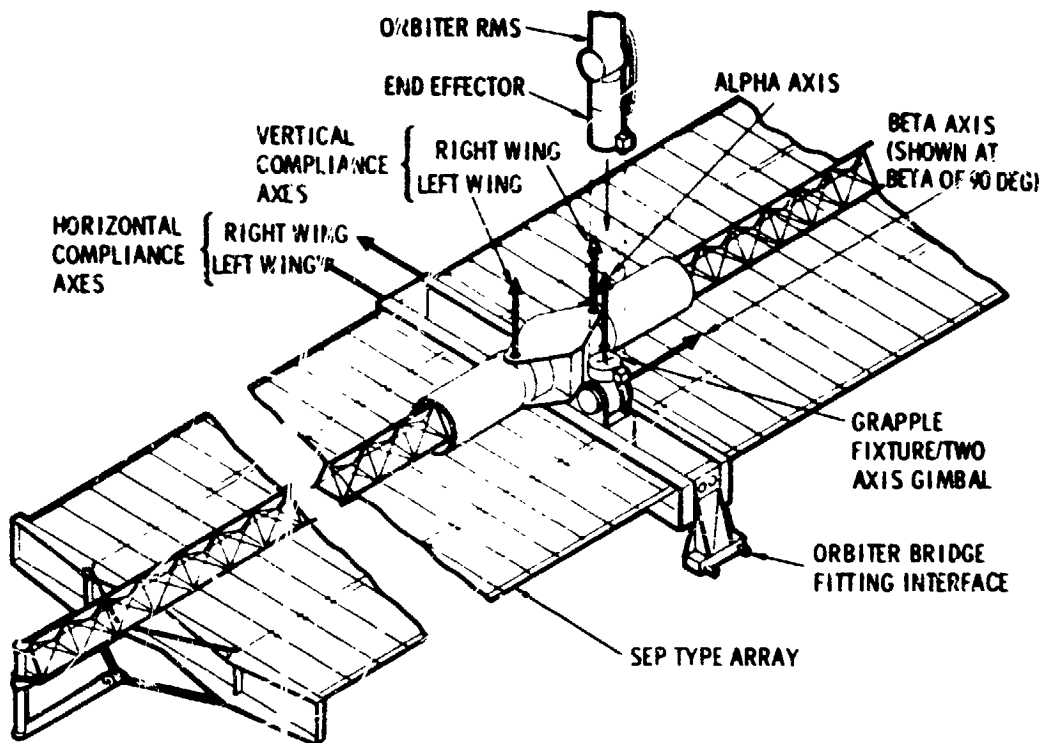


Figure 2.14-1. PEP Gimbal and Compliance Geometry

It was assumed that array separation from the Orbiter was not a SAPS requirement because the RMS will be positioned and the end effector oriented so that any motion of the Alpha or Beta gimbals will not result in a collision from a rigid array viewpoint. A dynamic envelope must be considered, however, and Orbiter/SAPS/PEP dynamics interactions must be evaluated.

It was assumed that the SAPS should not aggravate, and reduce if possible, the PEP flexible body dynamic motions which are important because of the structural loads which could be developed. The pointing control system/flexible dynamics interactions must not result in an unstable SAPS. The SAPS should not generate forces and moments which could slip the RMS joint brakes.

The basic operational requirements assumed for the SAPS are:

1. tracks the sun within 2 degrees,
2. slew to defined Alpha and Beta gimbal positions (usually used for initialization),
3. slew at defined angular rates for an indefinite time,

4. gimbal position and slew rate commands will be defined via the keyboard, ground links or a preprogrammed table used as part of an autonomous procedure,

5. any slewing can be stopped at any time by keyboard or ground link command, and

6. operate with sun sensor feedback in either gimbal axis and gimbal encoder feedback in the other axis.

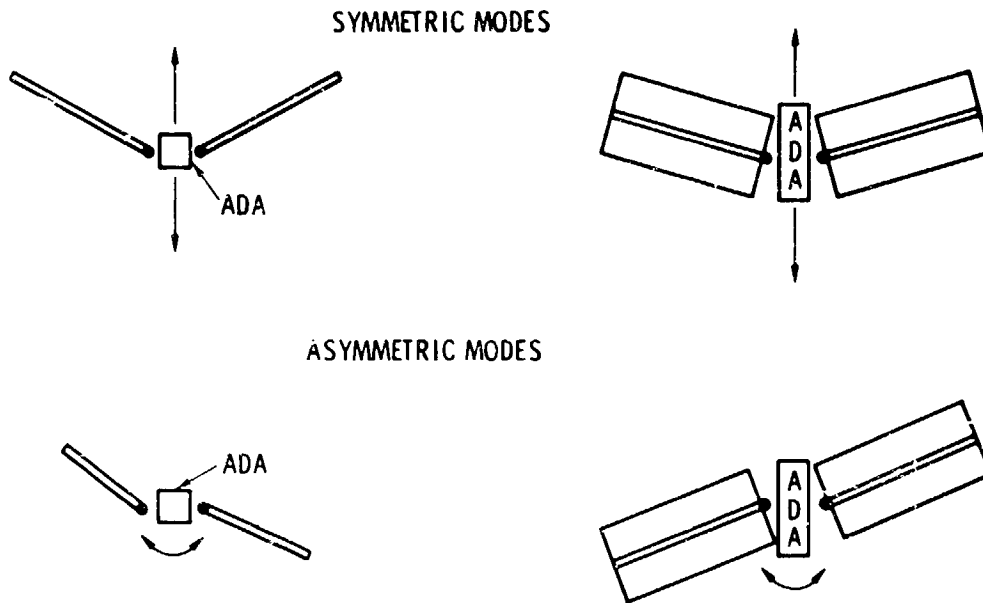
The last requirement facilitates feathering the array with one gimbal while tracking the sun as close as possible with the other which is desirable for a low altitude orbit. A wide angle sun sensor (at least about one array axis) is required to make this concept useful.

#### Approach/Discussion

Two Solar Array Pointing System (SAPS) concepts were considered. The two were proportional control (with nonlinear friction) and on-off control. The first was analyzed as a continuous system using sun sensor or gimbal encoder feedback and tachometer feedback. It was assumed the gimbal was back driveable and its ability to damp compliance spring motion was evaluated for a simple case. Since the Alpha and Beta gimbals cannot damp all the compliance spring modes, the on-off controller concept was defined. The on-off controller can provide some damping if gimbal backdrive occurs. The on-off controller meets the other SAPS requirements when system damping augmentation is not required. The on-off controller has been defined as the Baseline SAPS.

Proportional Controller - The "compliance spring" concept discussed in Paragraph 2.8 requires damping to minimize the solar array response to Orbiter limit cycle disturbances, Orbiter orientation maneuvers, and PEP gimbal rotations. This prompted an analysis to determine the effectiveness of using a gimbal servo concept to induce system damping.

In the reference configuration the two solar arrays on either side of the ADA are each independently sprung about two axes (Figure 2.14-1). These four degrees of freedom result in both symmetric and asymmetric compliance spring modes. The asymmetric modes can be damped by rotational motion of the ADA while the symmetric modes require linear motion of the ADA for damping (Figure 2.14-2). In the reference configuration, Alpha and Beta gimbal rotations do



NOTE: ARROWS SHOW ARRAY DEPLOYMENT ASSEMBLY (ADA) MOTION  
NEEDED TO DAMP THE MODES

**Figure 2.14-2. PEP Compliance Spring Modes**

not generally provide linear and rotational ADA motions along and about the required axes, which means that servo damping is not sufficient to damp the four compliance degrees of freedom for general disturbances.

The primary solar array disturbances are Orbiter limit cycle motions including any thrust impingement effects, Orbiter maneuvering and Alpha and Beta gimbal motions. Maneuvers are not expected to be cyclic and by limiting maneuver magnitudes, the compliance reduces structural loads to an acceptable level. Orbiter limit cycling has the potential to continuously (on the average) input energy into the compliance modes (because of its cyclic characteristics) which may ultimately result in large deflections and unacceptable mast or RMS loads. Evaluation of Orbiter limit cycle effects was accomplished by reviewing the Orbiter limit cycle characteristics defined by 25 simulation cases. The Orbiter simulation was the JSC/LEC Space Shuttle Functional Simulation (SSFS) high fidelity rigid body simulation. These limit cycle characteristics were simplified and input to a simple one-axis simulation to assess the effectiveness of gimbal induced damping and the resulting solar array limit cycle amplitudes and loads. Further analysis is required with more detailed simulations.

The model (Figure 2.14-3) used for gimbal induced damping analysis was a single axis model of a torque motor driving through a transmission (gimbal) to an angular compliance spring connected to a moment of inertia representing a rigid solar array. The feedback sensors were an inertial position sensor (sun sensor), a relative position sensor (gimbal encoder), and a relative rate sensor (tachometer). The sensors were mounted on the gimbal side of the compliance spring so actual array position could be sensed only indirectly via the servo backdrive effects. Linear analysis and simulation analysis including nonlinear friction effects were used to evaluate servo induced damping. The Orbiter limit cycle motion was input as a disturbance.

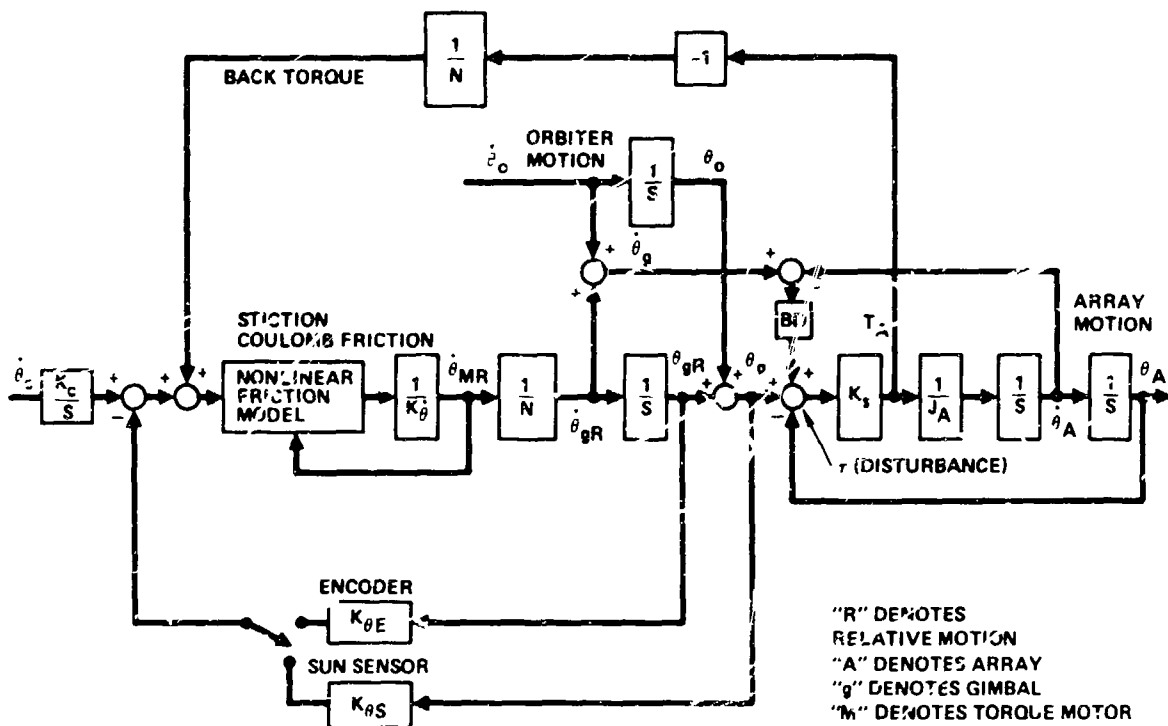


Figure 2.14-3. PEP Proportional Control Simulation Block Diagram

The JSC/LEC SSFS Orbiter flight control simulation, used for reference Orbiter limit cycle disturbances, includes a full on-orbit functional flight control system software simulation and includes aerodynamic and gravity gradient disturbances. The 25 simulations included both primary and vernier thruster limit cycles with several attitude dead bands and various local vertical, inertial hold and passive thermal control (barbecue roll) orientations.

On-Off Controller - This is the Baseline SAPS and assumes adequate structural damping will be supplied mechanically. Allowing the gimbal to backdrive will

add further damping. The extent of the added damping was not evaluated in this analysis.

The on-off and proportional controller concepts are similar except for the control law. Figure 2.14-4 is a functional block diagram of the on-off controller. Also shown are the primary controller operational requirements and capabilities. No tachometer is included in the baseline. The parts included in the dashed lines are mechanized in the PEP digital processor. If highly accurate gimbal slew rates are not required, no angular rate feedback will be required. Figure 2.14-5 is a flow chart defining a derived rate concept for a low resolution sun sensor or gimbal encoder which could be mechanized in the processor if needed.

The drive logic is a two rate drive. The achieved rate generated by the output  $V_b$ , could be much higher than the required rate (e.g. orbit rate) and the servo will be "turned on" intermittently to realign the array with the reference. The hysteresis provides over shoot so that the average array position will be near nominal. An alternate procedure is to set the achieved rate

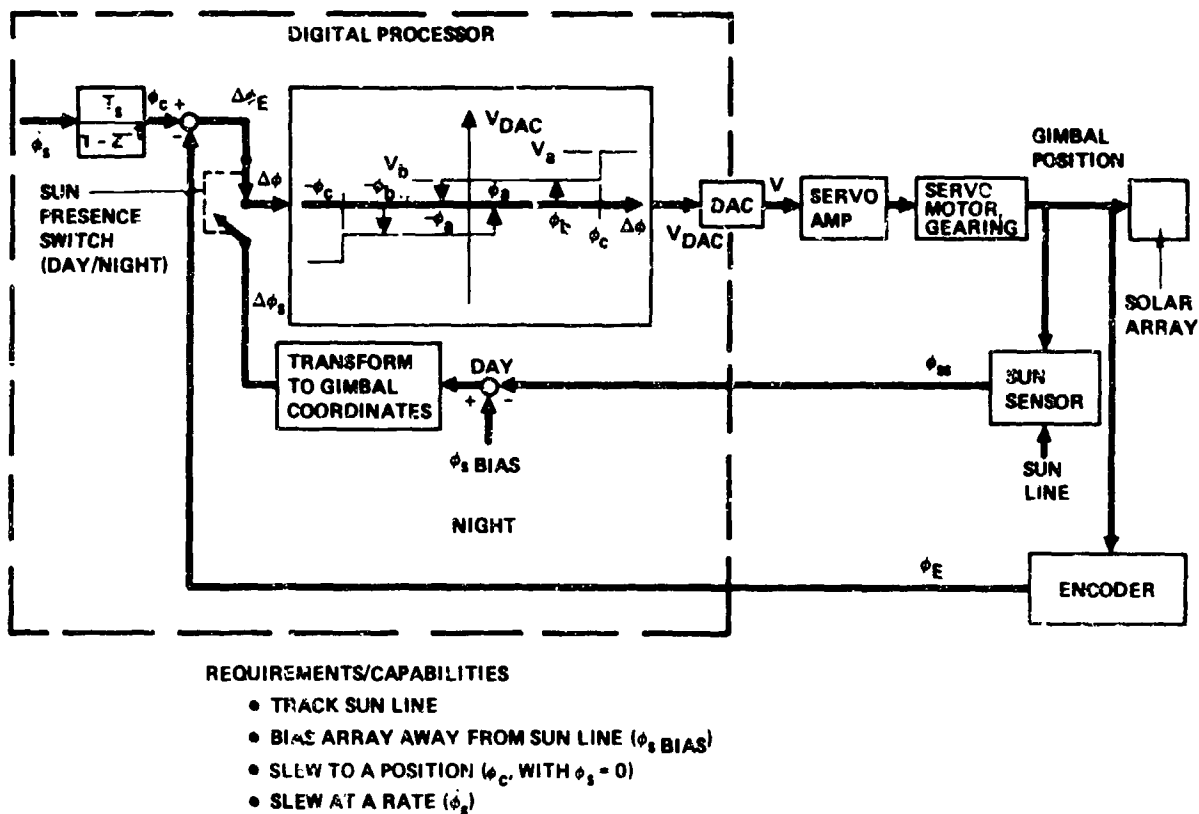


Figure 2.14-4. Baseline PEP Solar Array Pointing System

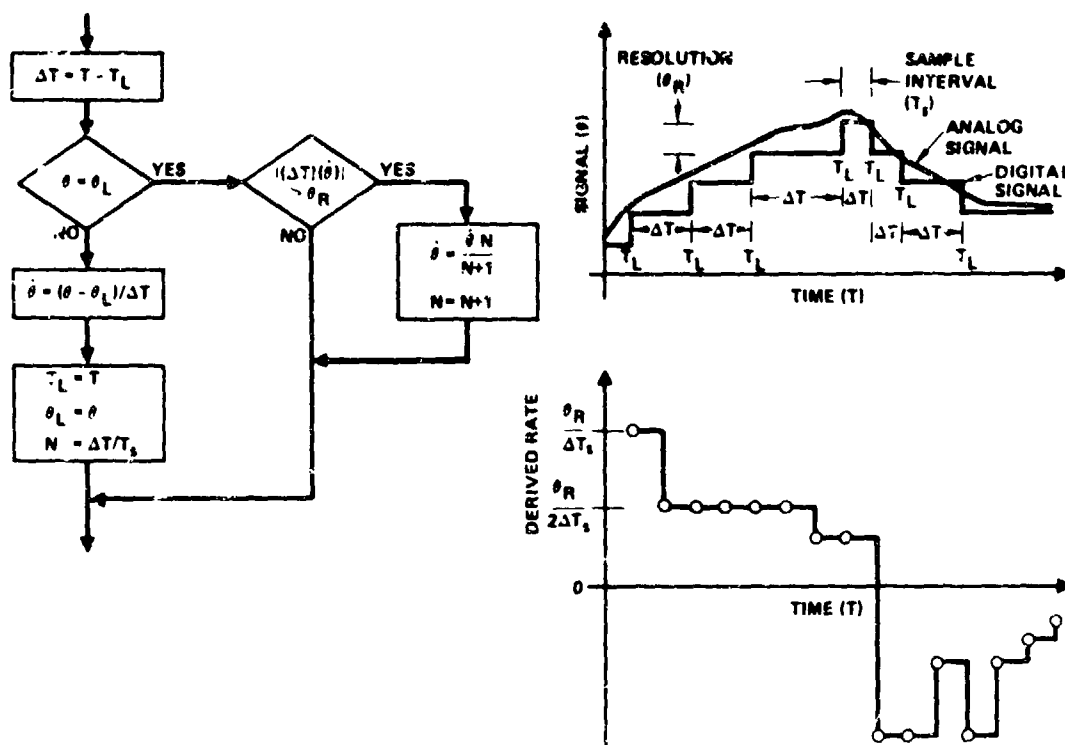


Figure 2.14-5. Derived Rate Concept for a Low-Resolution Signal

near the commanded rate, and the array smoothly tracks the reference with occasional high or zero achieved rate periods occurring to adjust the average achieved rate to the required rate. The constant rate is desirable since structural resonance excitation is minimized. The controller is effectively an open loop controller for long periods of time which can eliminate stability problems associated with structural resonances.

Most of the control law parameters can be updated via the keyboard or ground links so that on-orbit experience can be used. Since there is no direct gimbal rate feedback, the open-loop servo characteristics (including friction) will have a significant effect on the closed loop characteristics and on-orbit updates will be valuable.

The "Transformation to Gimbal Coordinates" block (Figure 2.14-4) on the sun sensor output may not be required even though the Alpha gimbal axis doesn't generally line up with a sun sensor axis. The closed-loop nature of the Alpha and Beta servos will drive the Alpha and Beta sensor within the dead zones even for large initial errors. Solving directly for the gimbal angles required to zero the sun sensor error involves solving trigonometric functions for

large Beta angles in the processor. No requirement has been identified for this direct computation, but it has been included for generality.

The inputs shown on the block diagram (Figure 2.14-4)  $\dot{\phi}_s$ ,  $\phi_c$  and  $\phi_{sbias}$  define the slew rate, position and sun sensor bias commands respectively. The sun sensor bias was included so that the array could operate at less than max power by biasing it away from the sun. The bias angle must be small enough to keep the sun within the sun sensor FOV so the sun sensor FOV would have to be relatively large for a significant power reduction.

The day/night switch will be activated by the sun presence signal. Smooth transition between sun sensor and encoder control will be facilitated by insertion of a slew rate ( $\dot{\phi}_s$ ) command of the appropriate magnitude (normally orbit rate for local vertical orientations) at the loss-of-sun event. Also, the  $\dot{\phi}_s$  integration (digital) will be initialized to the sun sensor error (i.e.,  $\Delta\phi_E = \Delta\phi_s$ ). At dawn the command rate will be removed and  $\Delta\phi_s$  used. The dark side rate command can be preprogrammed and updateable or calculated based on the rates required by the sun sensor feedback during orbit daylight.

Initialization upon deployment will be accomplished by keyboard input of the appropriate Alpha and Beta gimbal angles ( $\phi_s$  in Figure 2.14-4). An automatic sun finding mode can be accomplished with a preprogrammed sequence of Alpha and Beta slew rate and position commands. A solar array power indication may be useful if the approximate location of the sun is not known (unlikely). The sun presence signal defines when the sun has been acquired.

Hardware Specification - The functional SAPS hardware blocks are shown in Figure 2.14-6. The Alpha and Beta SAPS are assumed identical except for gimbal travel and some software. The computational requirements for SAPS are well within the speed and complexity ranges of most available microprocessors. An 8-bit digital-to-analog converter (DAC) will have a servo rate command resolution of 0.004 deg/sec (6 percent of typical orbit rate) with a  $\pm 0.5$  deg/sec gimbal rate range. This command resolution is adequate since the closed-loop characteristics of the servo will result in an average achieved gimbal rate as accurate as required to meet the sun sensor or encoder position commands. The accuracy of the closed-loop achieved rate will be proportional to the processor clock accuracy also, and is a consideration.

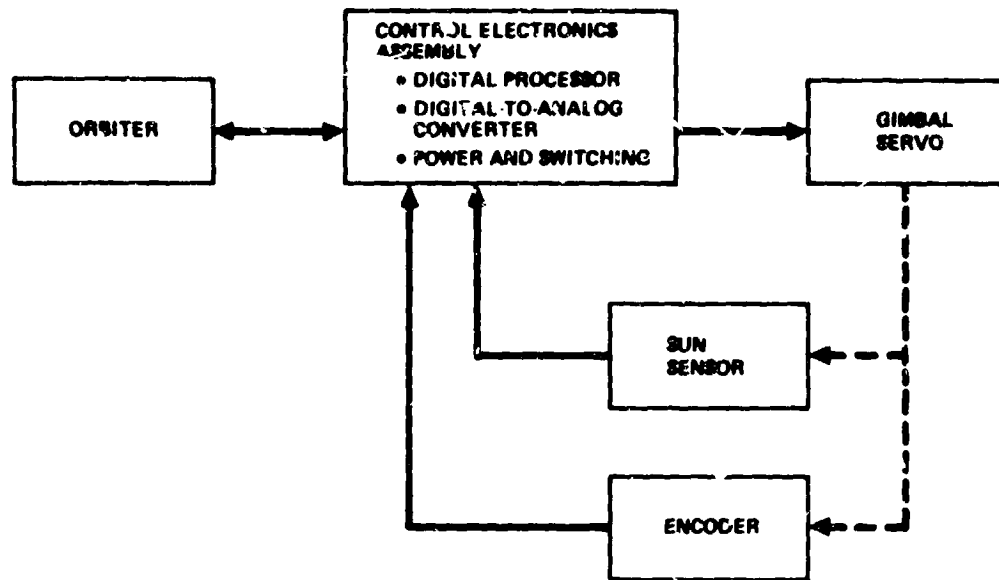


Figure 2.14-6. PEP Solar Array Pointing System Hardware Functional Blocks

The gimbal/servo stall torque requirement was defined to preclude over stressing the solar array mast. The mast design ultimate load capability is 200 ft-lb per mast and a maximum Alpha gimbal torque of 100 to 150 ft-lb is recommended with the Beta gimbal being defined the same for symmetry. The gimbal travel is defined as continuous bidirectional for the Alpha axis and 0 to 90 degrees for the Beta axis. The maximum gimbal rate capability is  $\pm 0.5$  deg/sec. The Alpha gimbal travels 180 degrees in 6 minutes and the Beta gimbal travels stop-to-stop in 3 minutes.

Further analysis is required to define the limits of acceptable open-loop servo response. Based on the simulation model, an open-loop servo bandwidth of greater than 0.25-0.5 hz is acceptable for the proportional controller. A response time (time constant) of 1 to 10 sec is acceptable for the on-off controller. Quicker response is not required because the servo is controlling the array through the compliance spring with a resonant frequency of 0.02 hz.

The gimbal friction characteristics are of particular interest for a proportional controller design. The position feedback gain used in the simulation of the proportional system was sized by the stiction value. The position loop gain was made large enough to limit the position hang-off due to 22 ft-lb of stiction to  $\pm 1$  degrees. This resulted in a higher closed-loop servo bandwidth than would be necessary based on a linear analysis.

Gimbal backdrive is essential to the proportional controller if induced system damping about some axes is a goal. Energy is removed from the solar array by backdriving the gimbal against the friction and back EMF of the servo motor. The on-off controller does not require backdrive but will provide some system damping if backdrive is present. No backdrive results effectively in a brake.

The sun sensor and gimbal encoder resolution were sized based on the  $\pm 2$  degrees solar array pointing accuracy requirements. A 1 degree resolution encoder is adequate and reasonable and 0.5 degree sun sensor is reasonable.

A sun sensor field of view (FOV) of 20 degrees is adequate for most sun acquisitions but a wide FOV is desirable if an autonomous acquisition from an arbitrary initial condition or tracking biased away from the sun is desired. PEP software needs will include ground computers and Orbiter computers as well as the PEP processor. Ground and Orbiter software are expected to be minimal.

Software Specifications - The SAPS software will be executed in the processor on the PEP. Modes of control will be defined via preprogrammed sequences and real time updating. Figure 2.14-7 shows a flowchart for the basic SAPS module. The nomenclature is derived from Figure 2.14-4. Table 2.14-1 defines the data and parameters the SAPS module requires for execution. This information will be defined by other software modules such as mode control and data acquisition. An execution rate of once per second is adequate, and the sensor data must be sampled at the same rate.

The logic allows the Alpha and Beta gimbals to each work in independent modes (i.e., sun track, slew to a position, etc.). In the sun track mode, a smooth transition from day to night is facilitated by initializing the appropriate slew rate ( $\dot{\phi}_c$ ) and initializing  $\phi_c$  such that  $\Delta\phi$  is continuous. The various non-sun-track modes are facilitated by setting  $\phi_c$  and  $\dot{\phi}_s$  to the appropriate time histories.

On Figure 2.14-7, two software modules are shown to process the sun sensor data. The output of the solid lined option are gimbal angle errors. This calculation could be as simple as transmitting the sun sensor errors directly as gimbal errors. This simplification is acceptable since the sign of the sun sensor errors and gimbal angles are the same for Beta angles under 90 degrees.

Table 2.14-1. PEP SAPS Interrupt Routine Inputs Required

- Mode in each axis ( $\alpha, \beta$ )
  - Sun track
  - Other
- Position commands ( $\phi_{Ca}, \phi_{Cb}, SBIAS_x, SBIAS_y$ )
- Slew rate commands ( $\phi_{Sa}, \phi_{Sb}$ )
- Switch logic parameters for each axis ( $\phi_a, \phi_b, \phi_c, V_a, V_b$ )
- Gimbal limit logic parameters ( $\beta_0, \beta_{90}, \beta_{min}, \Delta\phi_0$ )
- Sensor inputs ( $\phi_{SSX}, \phi_{SSY}, \alpha, \beta, \text{sun presence}$ )

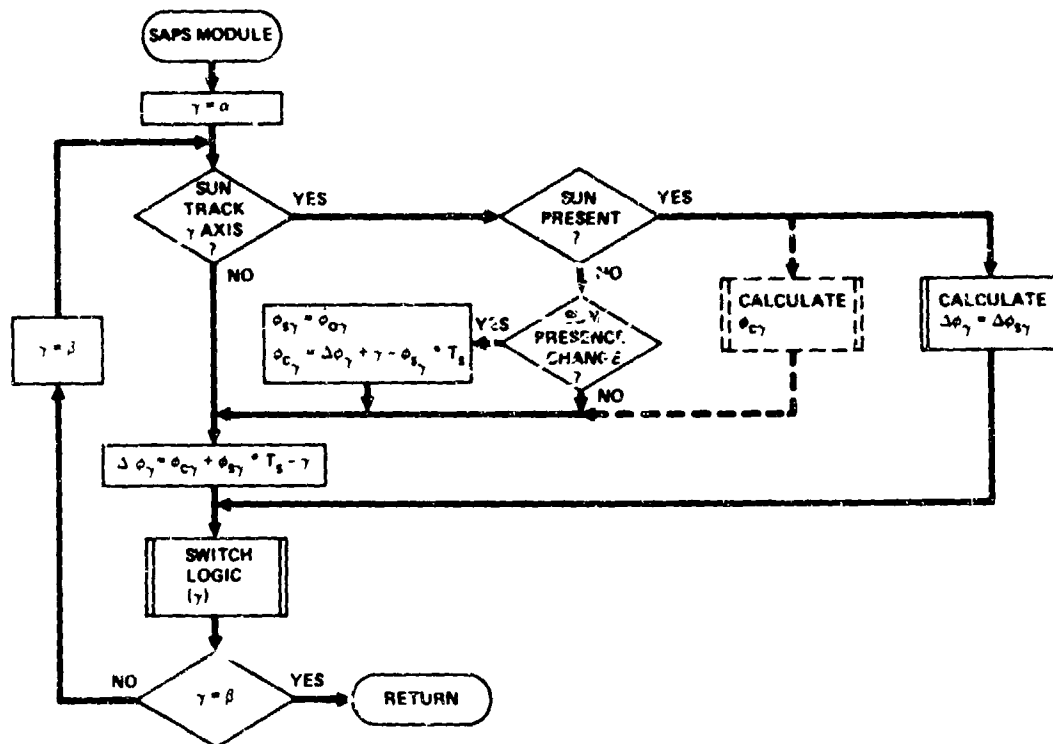


Figure 2.14-7. PEP Solar Array Pointing System Software Module Flow Chart

The magnitudes are actually related trigonometrically rather than linearly but the same sign means the closed-loop servo will converge toward zero error. Using the full trigonometric equations will result in defining the exact change in gimbal angle required or the exact gimbal position (dashed lines)

required to zero the sun sensor attitude error signal. No requirement has been identified for the full trigonometric versions even for large angle cases if the Beta gimbal angle is limited to 0 to 90 degrees.

The switch logic module is detailed in Figure 2.14-8. This module mechanizes the switch lines shown in Figure 2.14-4. The capability to make the Alpha and Beta gimbal switch lines different is provided. The gimbal limit logic is detailed on Figure 2.14-9 and provides software gimbal stops for the Beta gimbal by setting  $V_{DAC\beta}$  to zero when the switch logic is commanding into the stop.  $\beta_0$  and  $\beta_{90}$  represent the typical 0 and 90 degree stop values respectively, but can be updated during flight for special operations.

The Alpha gimbal limit logic is required for Beta angles near 90 degrees when the plane of the solar array is nearly perpendicular to the Alpha rotation axis. When these Beta gimbal angles occur, small changes in sun sensor error theoretically require 90 to 180 degrees of Alpha gimbal angle change. The Alpha gimbal limit logic inhibits the Alpha gimbal command for Beta gimbal angles greater than  $\beta_{min}$  unless the Alpha axis attitude error ( $\Delta\phi_\alpha$ ) is greater than  $\Delta\phi_0$ .

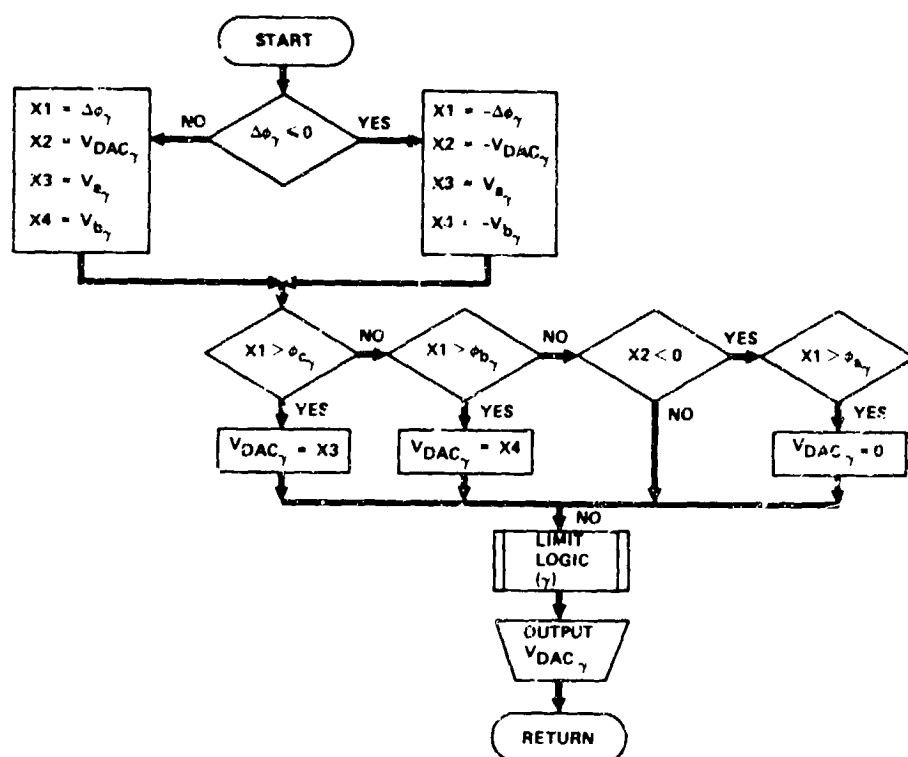


Figure 2.14-8. PEP SAPS Servo Switch Logic Software Module



Word length requirements may exceed 8-bits for the gimbal encoder and attitude error calculation, slew rate command and the sun sensor data processing. For example, assuming a slew command range of  $\pm 0.5$  deg/sec, the 8-bit rate resolution is 14 deg/hr which may be excessive for some operations where the sun sensor is not used for extended periods of time. Double-precision in 8-bit processors is no problem and gives more than adequate precision.

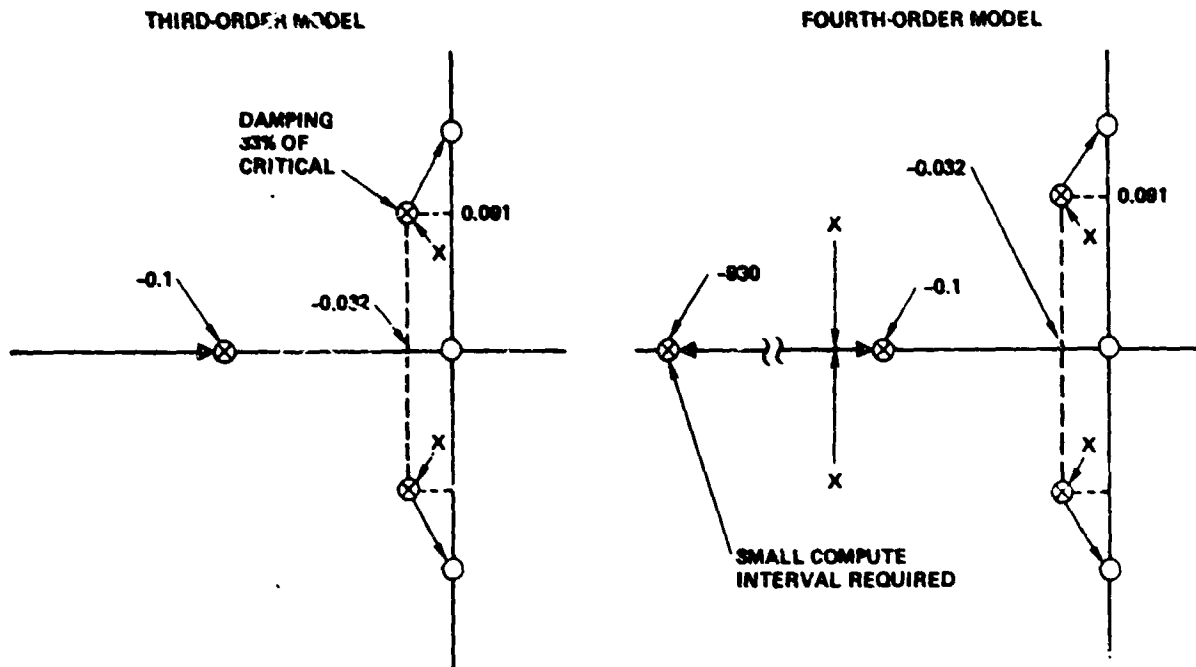
The following is a summary of the simulation effort to evaluate the potential for damping the PFF compliance spring modes with the proportional controls with backdrive. The simple 1-axis model (Figure 2.11-3) simulated only an asymmetric compliance mode. The system parameters used in the simulation are

defined in Table 2.14-2. Figure 2.14-10 shows the closed-loop root locations for a fourth order model and the reduced order (third order) model used for the simulation results shown herein. The high frequency real root obviously was not significant for the frequencies of interest and resulted in large computer run times so it was eliminated (Figure 2.14-3).

Table 2.14-2. PEP SAPS Simulation Parameter Values

Parameter	Value	Units
Total array inertia	133,000	slug-ft <sup>2</sup>
Compliance spring rate	2,100	ft-lb/rad
Compliance spring damping ratio	0.001	N.D.
Gimbal		
Inertia	0	slug-ft <sup>2</sup>
Coulomb friction	7.26	ft-lb
Stiction	10.89	ft-lb
Gear ratio	250	N.D.
Torque motor (Inland Model T-3910; data referred to gimbal)		
Rotor inertia	21	slug-ft <sup>2</sup>
Back EMF constant	2,060	ft-lb/rad/sec
Coulomb friction	10.5	ft/lb
Stiction	10.5	ft/lb
Gains (referred to gimbal)		
Sun sensor and gimbal encoder	1,000	ft-lb/rad
Tachometer	15,600	ft-lb/rad/sec

Many simulation runs were made simulating Orbiter rate maneuvers, commands and limit cycles. Both sun sensor and gimbal encoder feedback were used. The runs showed that the PEP solar array mast loads are acceptable for Orbiter angular rate steps of greater than a 0.25 deg/sec. Figures 2.14-11 and -12 show the torque at each mast root for a 0.25 deg/sec Orbiter step rate for gimbal encoder and sun sensor feedback cases, respectively. In the encoder feedback case, the pointing system damps the motion well until the gimbal locks due to stiction at about 10 ft-lb torque per mast. With the gimbal locked, the only damping is in the compliance spring itself which is essentially zero in the



$K_0 = 1230 \text{ FT-LB/RAD}$   
 $\otimes K_0 = 2,000 + 15,600 = 17,700 \text{ FT-LB/RAD/SEC}$

Figure 2.14-10. MDAC PEP Solar Array Pointing System Simulation Motor Damping ( $K_0$ ) Root Locus

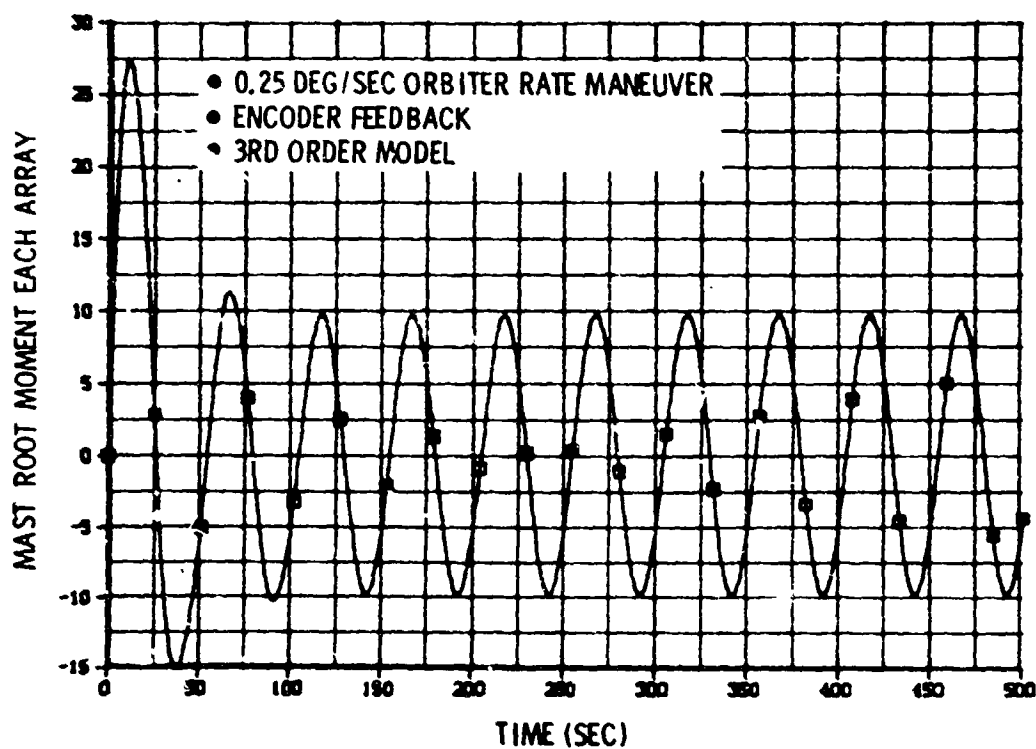


Figure 2.14-11. MDAC PEP Pointing Control System Simulation - Rate Maneuver with Encoder Feedback

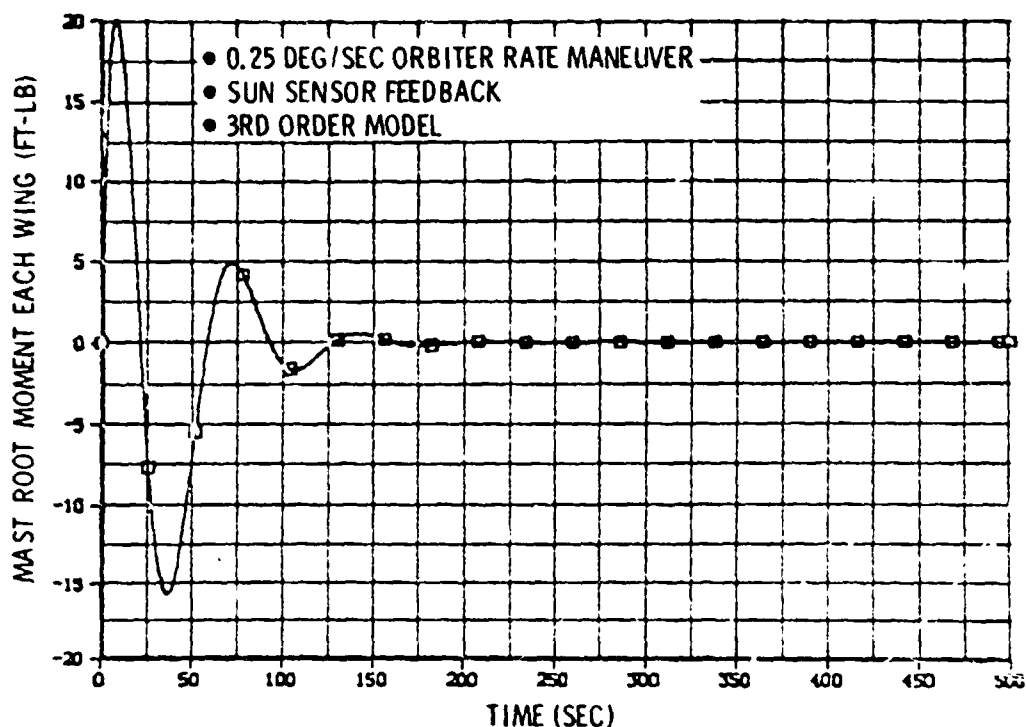


Figure 2.14-12. MDAC PEP Pointing Control System Simulation — Rate Maneuver with Sun Sensor Feedback

simulation. The sun sensor feedback case shows a different characteristic because the solar array is controlled to remain inertially constant by commanding a 0.25 deg/sec average gimbal rate and the gimbal never locks. The 33% system damping indicated in Figure 2.14-10 applies and the response is well damped.

A preliminary evaluation of the response to Orbiter limit cycle motion was evaluated by inputting approximations of Orbiter limit cycle attitudes and rates. Limit cycles with frequency content near multiples of the compliance frequency (0.02 Hz in the simulation) are of concern. Twenty-five high fidelity Orbiter on-orbit flight control system simulations (JSC/LEC SSFS) were reviewed. A VRCS case was chosen as a potentially severe case and the Orbiter motion approximated and input to the simulation. Figures 2.14-13 and -14 show the high fidelity simulation output and the approximation, respectively. Figure 2.14-15 shows the mast root torque on each wing for the input shown on Figure 2.14-14. The stiction was reduced to 6 ft-lb in order to break the gimbal loose early in the run. Note that the torque on each wing is effectively limited to one-half the stiction torque indicating that induced system damping is feasible.

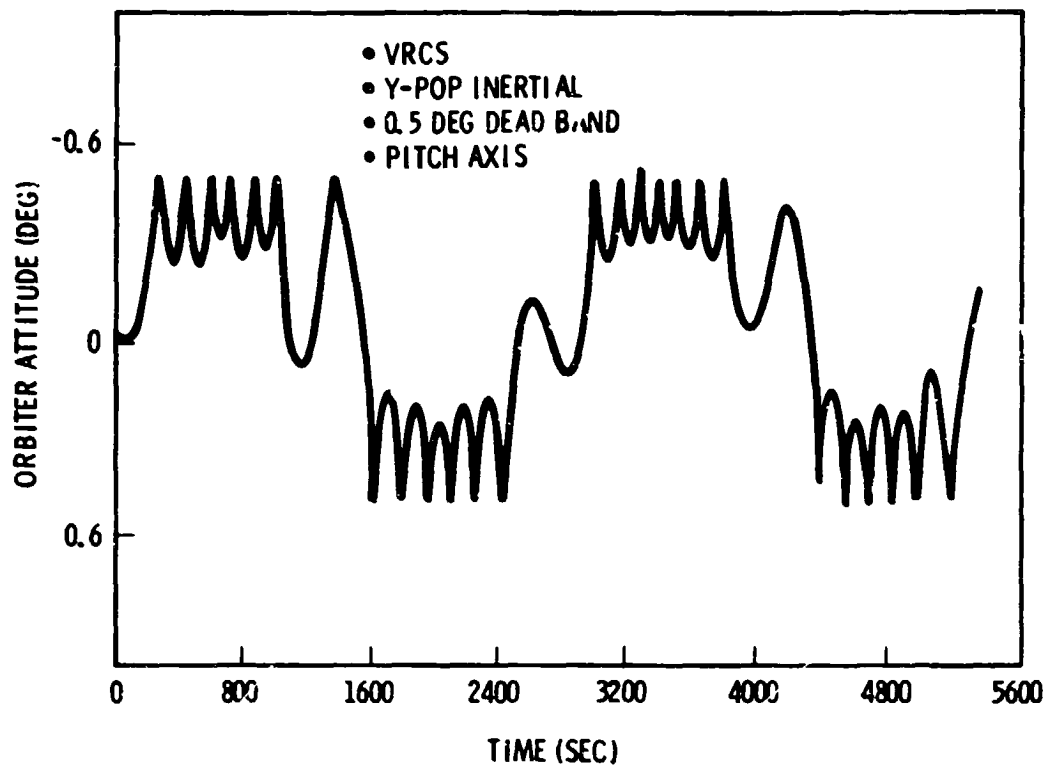


Figure 2.14-13. JSC/LEC Orbiter Flight Control Simulation

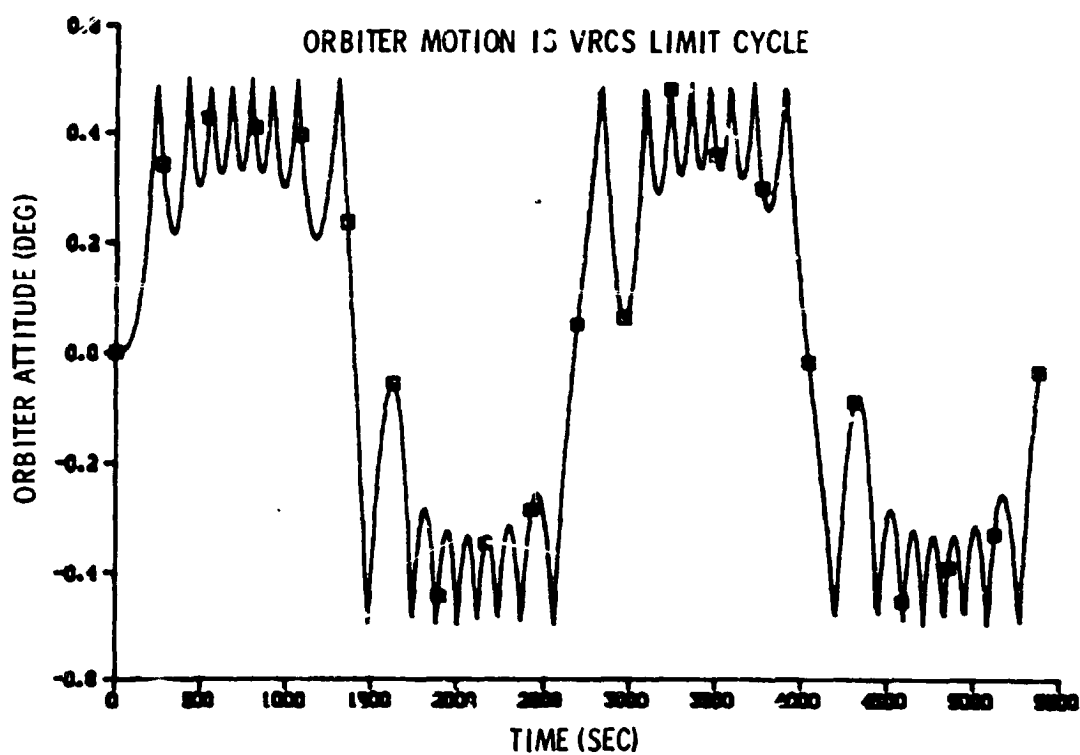


Figure 2.14-14. MDAC PEP Solar Array Pointing System Simulation - VRCS Limit Cycle

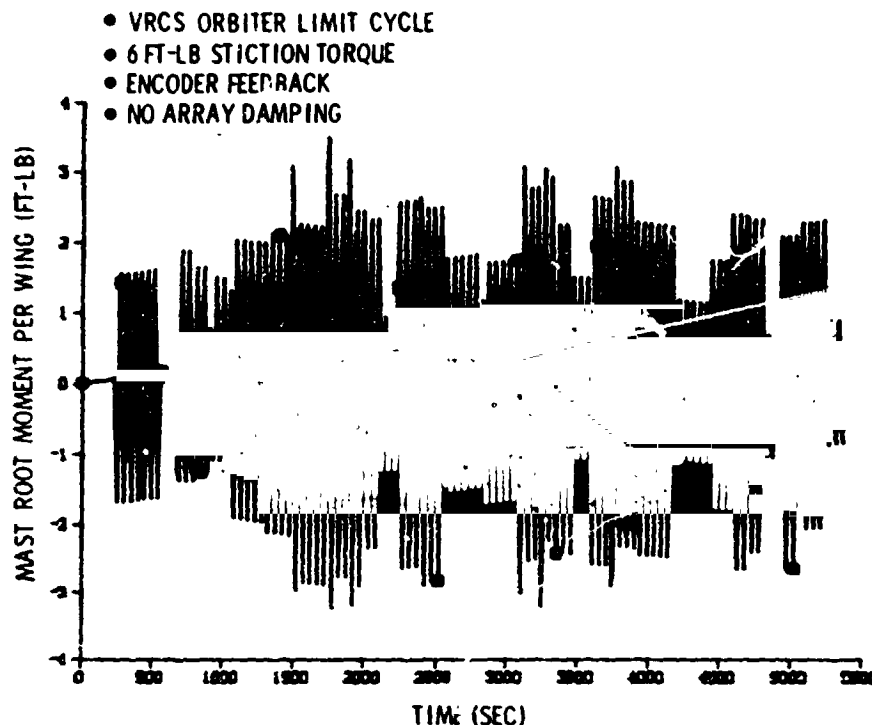


Figure 2.14-15. MDAC PEP Solar Array Pointing System Simulation - Mast Moment for VRCS Limit Cycle

A simple approximation of a PRCS limit cycle proved elusive. Therefore, a reasonable worst case was "manufactured" based on PRCS limit cycle rates and attitudes observed in the high fidelity JSC/LEC SSFS simulations. An attitude dead zone of  $\pm 3$  degrees with a rate of  $\pm 0.034$  deg/sec was chosen (Figures 2.14-16 and -17). This represents the largest Orbiter limit cycle motion expected. The two-sided limit cycle period was about 350 seconds which is an odd multiple of the 50 second compliance spring period, so energy is input to the array very efficiently.

This is obvious on Figure 2.14-18 which is the mast root torque on each wing for a case where the gimbal has been locked and no damping is available. The mast root torque reaches 200 ft-lb after about 1 orbit.

Figure 2.14-19 shows the effect of compliance spring damping. The conditions are the same as that in Figure 2.14-18 but a compliance spring damping of 1% of critical has been included. The mast root torque is limited to an acceptable 4 ft-lb.

Figures 2.14-20 and -21 show similar cases where the gimbal friction has been reduced to the nominal values (Table 2.14-2) and the compliance spring damping ratio has been set to 0.001. Figure 2.14-20 is a gimbal encoder feedback case and Figure 2.14-21 is a sun sensor feedback case. Note that the root torque

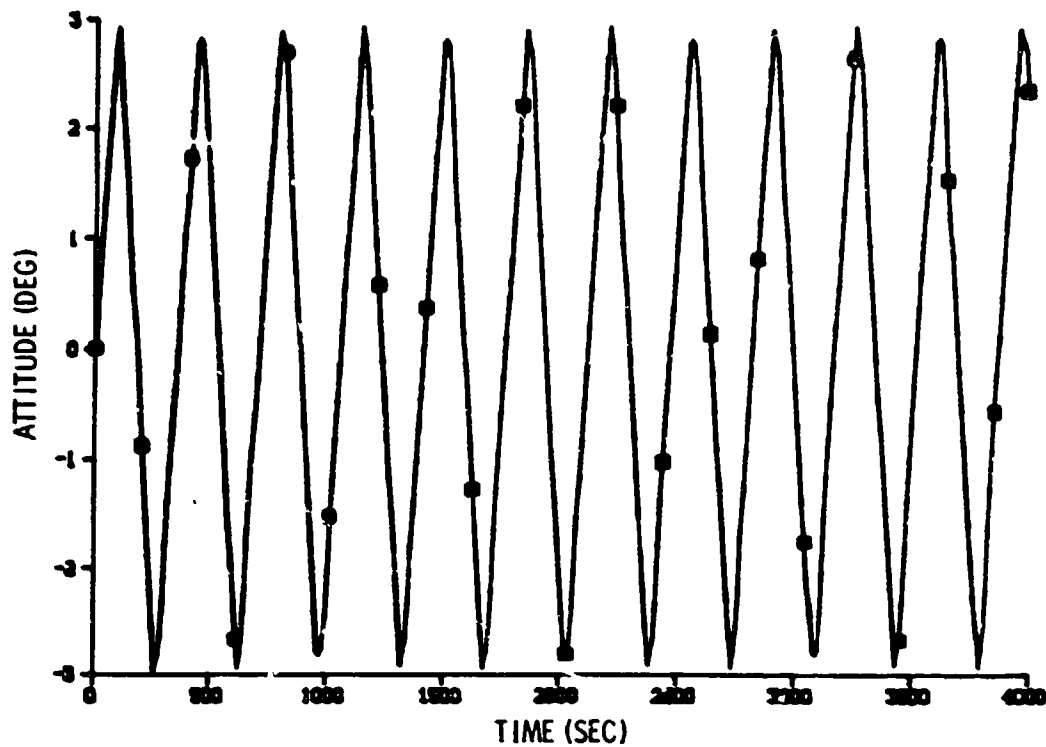


Figure 2.14-16. Orbiter PRCS Limit-Cycle Attitude History - MDAC Simulation

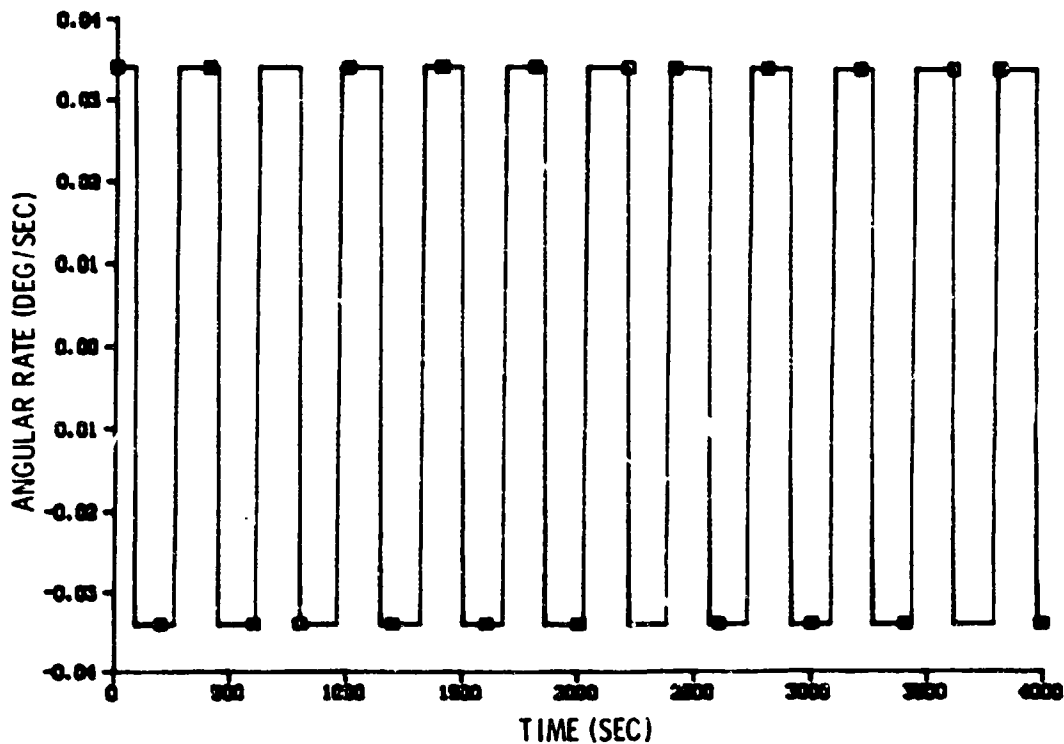


Figure 2.14-17. Orbiter PRCS Limit-Cycle Rate History - MDAC Simulation

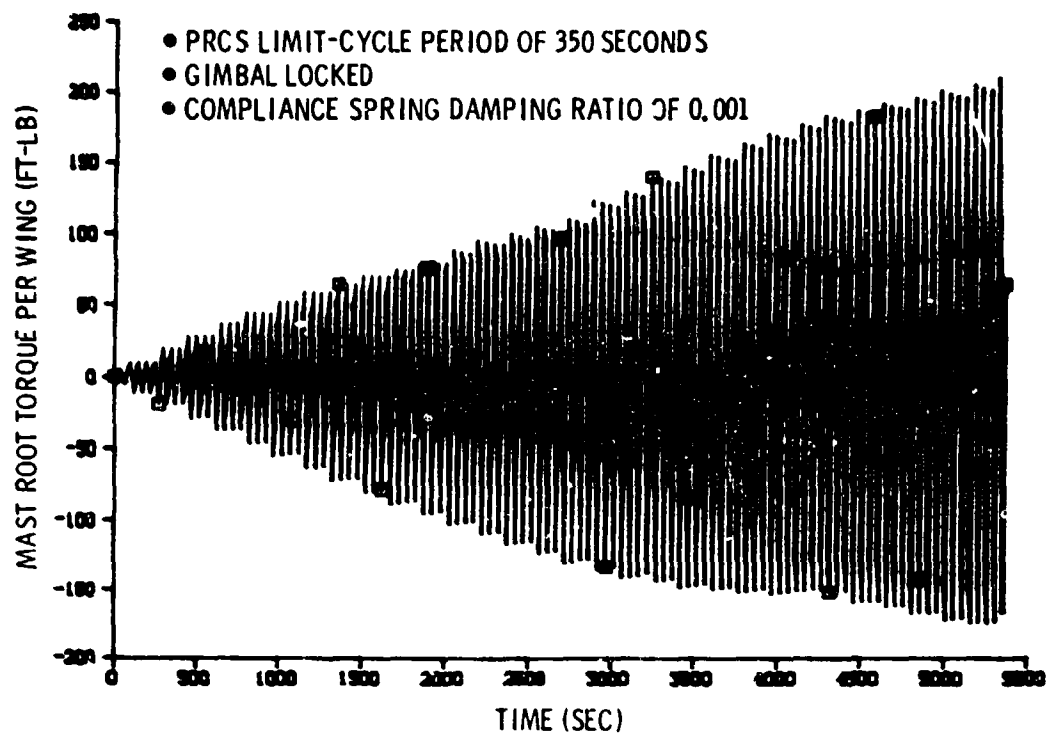


Figure 2.14-18. MDAC SAPS Simulation - 0.1-Percent Compliance Damping

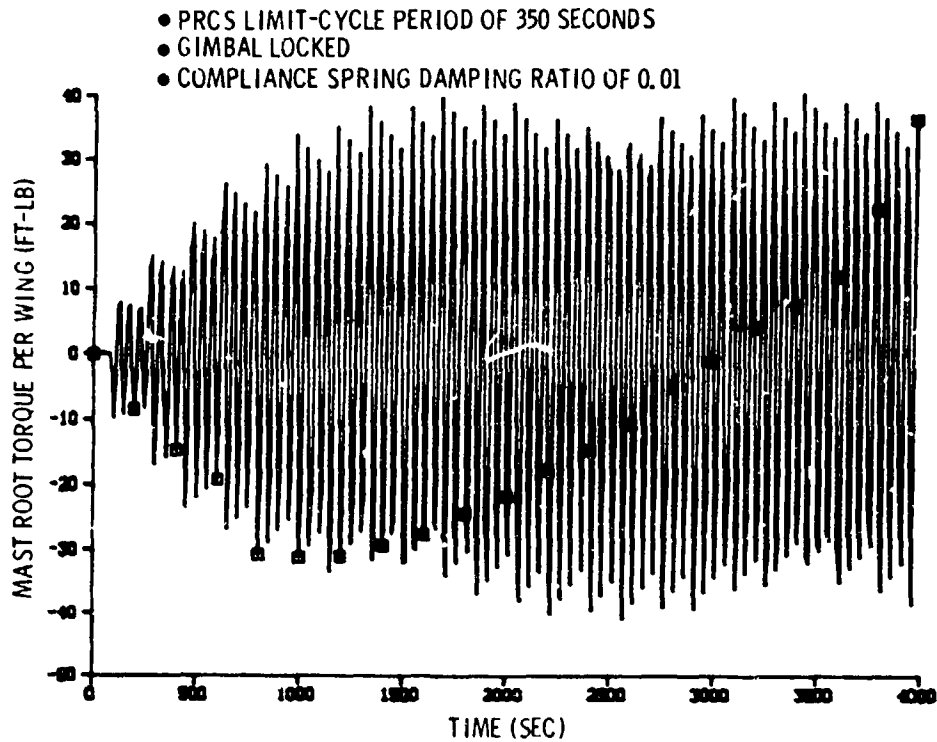


Figure 2.14-19. MDAC SAPS Simulation - 1-Percent Compliance Damping

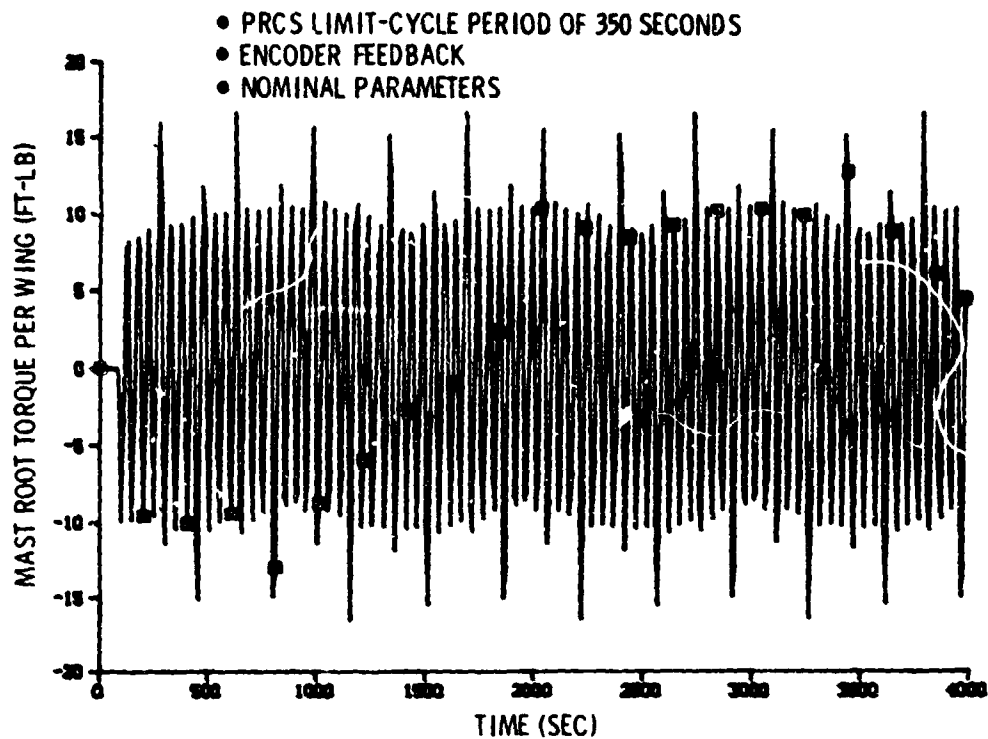


Figure 2.14-20. MDAC SAPS Simulation - PRCS Limit Cycle With Gimbal Encoder

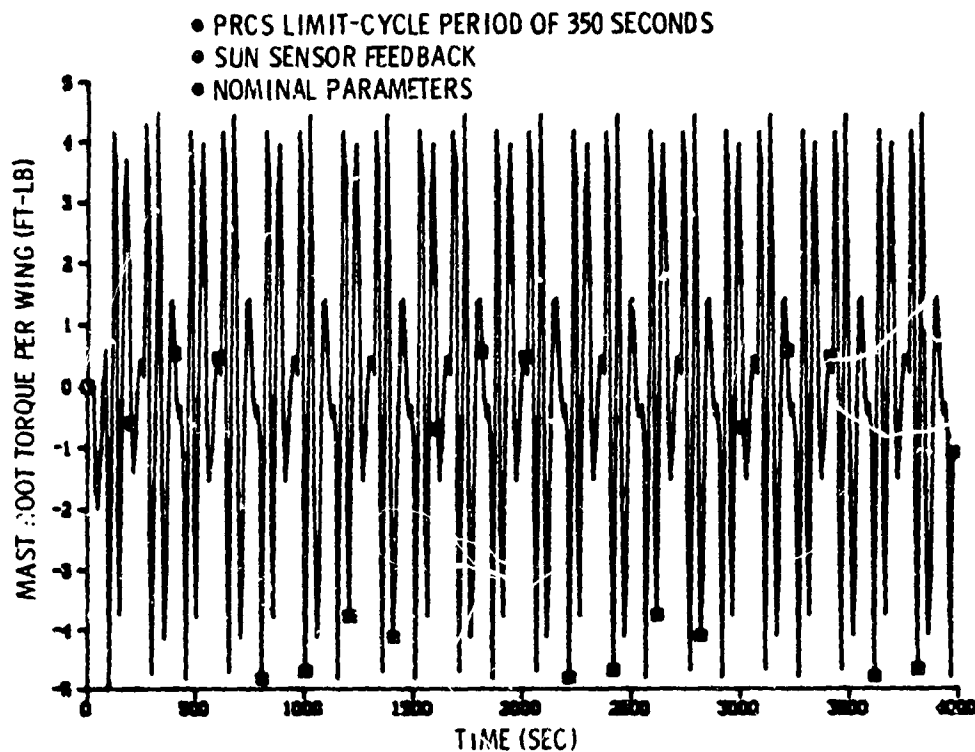


Figure 2.14-21. MDAC SAPS Simulation - PRCS Limit Cycle With Sun Sensor

amplitude is limited in the encoder feedback case (Figure 2.14-20) to near one-half (per wing) the total gimbal stiction value of 22 ft-lb, indicating that the friction and back EMF torques effectively absorb the energy input by the limit cycle motion. The sun sensor feedback case (Figure 2.14-21) exhibits much the same characteristics as the sun sensor case mentioned previously in that the gimbal rate is non-zero most of the time and the linear system damping ratio of 0.33 applies. Note the very small mast root torque which results.

The effects of gimbal encoder resolution were cursorily evaluated with the SAPS simulation. Figure 2.14-22 shows angular rate histories for the gimbal and the array for a case corresponding typically to dark side operation. The array is commanded at orbit rate relative to the Orbiter.

The gimbal encoder resolution was set at 0.5 degrees (half the present baseline) and the resolution effects are visible in the limit-cycling gimbal rate shown in Figure 2.14-22. The gimbal rate never reaches zero and the gimbal never sticks. Thus, the 33 percent linear damping applies as can be seen in the well damped array rate response. Decreasing the gimbal encoder resolutions to the baseline one degree, would approximately double the gimbal rate limit cycle amplitude. The gimbal would not stick, and good array damping would be available for orbit rate command rates.

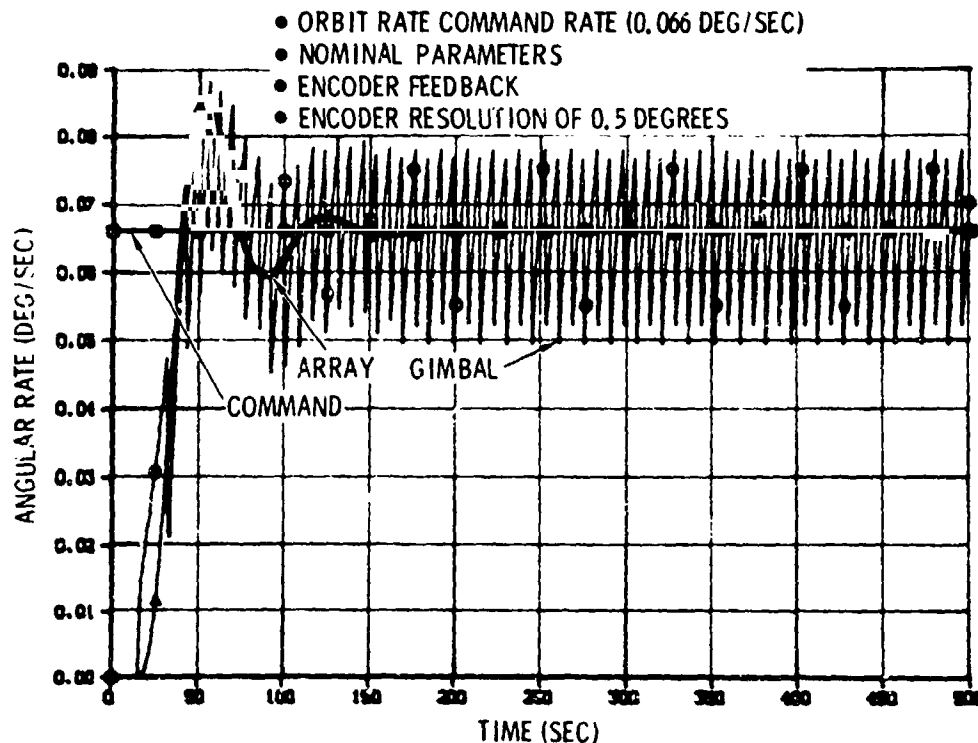


Figure 2.14-22. MDAC SAPS Simulation - Encoder Resolution Effects

## 2.15 CONTROL SYSTEM MANAGEMENT--GENERAL PURPOSE COMPUTER (GPC) AND ARRAY PROCESSOR CONTROL INTERFACE

### Objective

To define software functions for PEP activation, checkout, and operation performed by the Systems Management GPC and the Array Pointing and Control Electronics Assembly (CEA).

### Conclusions and Recommendations

The software functions to be performed in the Systems Management GPC will be minimal. Its use can generally be confined to status monitoring and checkout (comparison of actual to desired parameter values), the transfer of commands and data between the MCDS and PEP equipment and configuration of power regulation and control equipment.

### Approach

The various operations required by PEP were analyzed to determine what software functions were required and decisions were made in regard to their location. Brief descriptions of the functions were then prepared and input requirements were defined.

### Results

The results of the analysis are contained in the following paragraphs.

PEP Software Functions--The PEP function is operative during SM OPS 2, as specialist Function No. TBD and interfaces with the following:

- Multiplexer/Demultiplexer Assembly (MDA)
- Control Electronics Assembly (CEA)
- Table Maintenance Specialist Function (TM SPEC)
- PEP Control Display (PEP CNTL)
- Systems Software (SYS SW)

PEP software is organized into four principal functions within the SM computer. The following paragraphs briefly describe the principal functions. Figure 2.15-1 contains a block diagram of the functions performed within the SM GPC and their external and internal interfaces.

In addition to the four principal functions, there are three processing functions which are germane to the PEP detailed requirements:

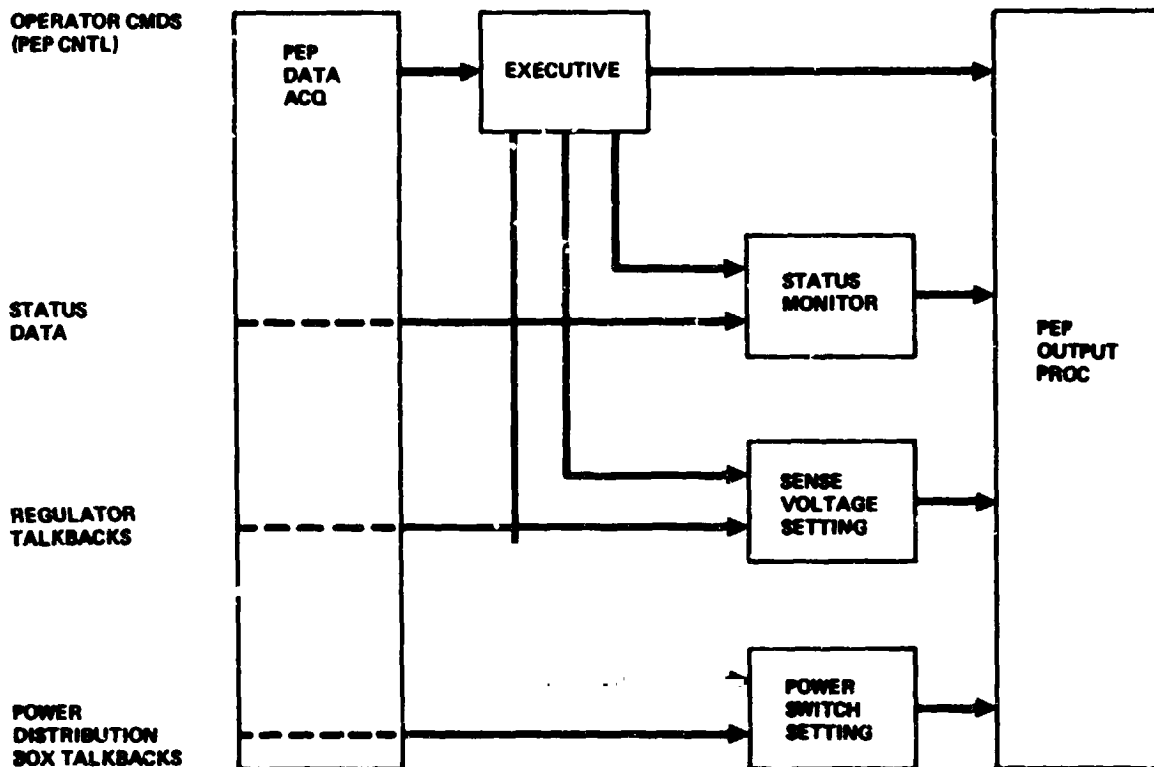


Figure 2.15-1. PEP Software (Systems Management GPC)

A. PEP Data Acquisition (PDA)--The PDA monitors the status of the Multiplexer/Demultiplexer Assembly (MDA) and CEA-to-GPC communication to determine if the MDA response data block is valid.

B. PEP Output Processing (POP)--The POP outputs the results of the principal functions to the MDA and CEA via the command data block.

C. PEP Specialist Processing (PSPEC)--The PSPEC organizes the sequence of processing RDA, EXEC, and POP.

#### PEP SM Principal Functions

A. Executive Function (EXEC)--The EXEC function performs function initialization and calls the required principal functions in the proper sequence to execute the selected software mode.

B. Power Switch Setting (PSS)-- The PSS function prevents more than one regulator per bus having control authority, removes shunt regulators operating improperly from the buses, and provides the power cable disconnect function in the event of an emergency.

C. Status Monitor (SM)-- The SM monitors critical measurements obtained from PEP units in order to determine if anomalies exist in equipment operation. Information is provided to System Software for CRT display of equipment status.

D. Sense Voltage Setting (SVS)-- The SVS compares the regulator voltage settings to commanded values and commands changes to setting levels until agreement is reached.

#### PEP Processor General Requirements

A. Initialize and self check the Electronics Assembly, Control (CEA) and all interfaces with ADA components when power is turned on.

B. Accept control commands and provide digital data and internal status to the Orbiter's Systems Management GPC.

C. Provide sequencing for cannister rotation and mast extension retraction.

D. Provide rotation drive levels for alpha and beta gimbals.

#### Functional Requirements

A. The CEA software should execute in a microprocessor. A minimum of two channels should be available for data transfers between the CEA and GPC; one channel for data transfer from/to a redundant micro-processor.

B. The CEA software program should perform ADA sequencing and array gimbal control upon receipt of commands input to the keyboard of the MCDS. It would examine a location in memory to determine its mode of operation.

C. Gimbal Control Modes are classified as manual or automatic and should consist of the following:

1. Manual Mode, Slew to Position - causes the CEA to slew to given alpha and/or beta angles.

2. Manual Mode, Track at Constant Rate - causes the CEA to slew alpha and/or beta gimbals at commanded angular rates.

3. Automatic Mode, Track Sun - causes the CEA to maintain PEP array faces perpendicular to the sunline based upon data provided by a two axis sun sensor.

4. Automatic Mode, Trail Position - causes the CEA to track the sun in one axis while maintaining the other axis in a given angular position in respect to the velocity vector.

D. A stop mode should be provided which terminates the current ADA activity and causes the ADA to revert to a safe condition.

E. A test mode (disabled during flight) would allow the loading and execution of special test software.

F. The software should monitor external events via digital or discrete inputs and or analog signal. These should include latch position, shaft encoder and sun sensor inputs. Provision should also be made for monitoring solar array and other ADA component status and formatting and buffering this data for transfer to the GPC.

Control Inputs--Control of PEP requires three general types of inputs: (1) those required to define the configuration of the Power Regulation and Control Assembly (PRCA); (2) those which insure the proper functioning of the equipment; and (3), those effecting the Array Deployment Assembly (ADA) in manual and automatic modes. Table 2.15-1 lists the inputs for PRCA control while Table 2.15-2 lists those for the ADA.

Control Display--Figure 2.15-2 illustrates the PEP Control Display Format. Numbers on the figure are described below.

1. After engagement of the SPEE connector the power switch is activated. The status of the power switch (On/Off) is shown.

2. A command is entered via the keyboard to engage the power connector. The status of the command (Engage/Release) is displayed.

3. A command is entered to rotate the canisters and extend the masts after the Array Deployment Assembly has been placed in the desired position by the RMS. The command is automatically sequenced by the Array Pointing Control Electronics Assembly (CEA). The reverse operation is performed for retraction of the arrays and canister stowage. Item 3 illustrates the command status of canister rotation (CS, CCW) and mast extension and retraction (ETD, RTC).

4. The selected CEA mode is indicated by two discrete bits (0, 1). The bits indicate whether the manual mode (slew to position, constant rate) or automatic mode (sun track, trail) are to be performed.

5. The position of the Alpha ( $0^{\circ}$ - $360^{\circ}$ ) and Beta ( $0^{\circ}$ - $90^{\circ}$ ) gimbals is displayed by Item 5.

6. Gimbal rate commands ( $0.5^{\circ}$ /sec maximum) input via the keyboard are displayed by Item 6.

Table 2.15-1. Power Control Inputs (SM Computers)

MDA power on/off	Power distribution box
Voltage regulator no. 1 - enable/inhibit	Voltage regulator 1
Voltage regulator no. 2 - enable/inhibit	Voltage regulator 1
Voltage regulator no. 3 - enable/inhibit	Voltage regulator 1
Voltage regulator no. 4 - enable/inhibit	Voltage regulator 1
Voltage regulator no. 5 - enable/inhibit	Voltage regulator 1
Voltage regulator no. 6 - enable/inhibit	Voltage regulator 6
Voltage regulator no. 1 - control authority on/off	Voltage regulator 1
Voltage regulator no. 2 - control authority on/off	Voltage regulator 1
Voltage regulator no. 3 - control authority on/off	Voltage regulator 1
Voltage regulator no. 4 - control authority on/off	Voltage regulator 1
Voltage regulator no. 5 - control authority on/off	Voltage regulator 1
Voltage regulator no. 6 - control authority on/off	Voltage regulator 6
Voltage regulator no. 1 - voltage adjust level	Voltage regulator 1
Voltage regulator no. 2 - voltage adjust level	Voltage regulator 2
Voltage regulator no. 3 - voltage adjust level	Voltage regulator 3
Voltage regulator no. 4 - voltage adjust level	Voltage regulator 4
Voltage regulator no. 5 - voltage adjust level	Voltage regulator 5
Voltage regulator no. 6 - voltage adjust level	Voltage regulator 6

'On' command  
restricted to  
one regulator  
on each bus  
(exclusive OR)

Table 2.15-1. Power Control Inputs (SM Computers) (Continued)

MDA power on/off	Power distribution box	} Open if I <sup>x</sup> is negative (reverse current)
Voltage regulator no. 1 - switch - open/close	Power distribution box	
Voltage regulator no. 2 - switch - open/close	Power distribution box	
Voltage regulator no. 3 - switch - open/close	Power distribution box	
Voltage regulator no. 4 - switch - open/close	Power distribution box	
Voltage regulator no. 5 - switch - open/close	Power distribution box	
Voltage regulator no. 6 - switch - open/close	Power distribution box	} 2 follows 1 in 10 sec. if no disconnect
In-flight disconnect - no. 1 arm	Power distribution box	
In-flight disconnect - no. 1 fire	Power disconnect box	
In-flight disconnect - no. 2 arm	Power distribution box	
In-flight disconnect - no. 2 fire	Power distribution box	

7. Regulator sense voltage matching regulator output levels to the bus are controlled to within 0.02 volts. Setting levels are displayed in Item 7 adjacent to their reference number designation.

8. The position of the power distribution contactors are set via the keyboard. Their commanded positions to open or close are indicated by a discrete bit (0, 1) adjacent to their number designation.

It should be noted that parameters associated with the ADA latches are displayed on the RMS display format type SPEC/094 as follows:

A. A numeric value (1-5) will be displayed adjacent to PL SELECT to indicate the payload selected to activate the circuitry associated with the retention latches. This reflects the position of the PL SELECT switch on Panel A6.

B. PL LAT RDY are discrete outputs providing an indication that A, B and C micro switches selected by the PL SELECT switch are in the proper position for latching. Text outputs are 1 or 0.

Table 2.15-2. PEP ADA Control Inputs (SM Computer)

Input	Destination	Notes
Power connector engage/release	Power connector actuator	Requires MDA "ON"
Restraint release	Elec. assembly control/solenoids	
Cannister rotate, mast extend	Elec. assembly control/motors	
Manual/automatic mode	Elec. assembly control/motors	
Suntrack/trail submode	Elec. assembly control/motors	
Slew to position/constant rate submode	Elec. assembly control/motors	
Gimbal rate (alpha)	Elec. assembly control/motors	
Gimbal rate (beta)	Elec. assembly control/motors	
Gimbal position (alpha)	Elec. assembly control	

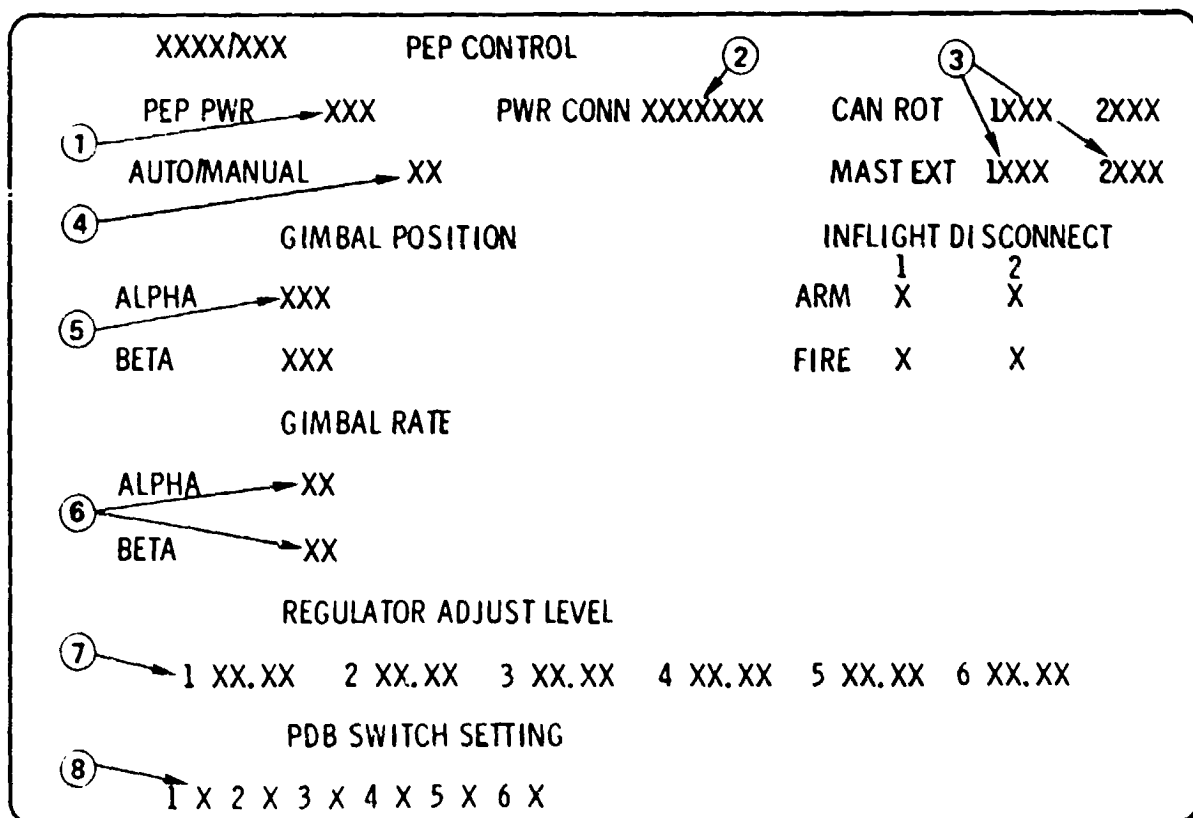


Figure 2.15-2. PEP Control Display Format

C. PL LATCHED are discretes indicating A, B and C micro switches have been latched. Text outputs are 1 or 0.

Status Display—This display provides the crew with the capability for on-orbit monitoring of Array Deployment and Power Regulation and Control Assembly component failures.

Figure 2.15-3 is the PEP Status Display Format. It is formatted with data processed by the Systems Management GPC with raw and semi-processed data obtained from the PEP system. The data will be continuously displayed when the PEP is in operation.

1. The gimbal rate portion of this display shows the actual rates commanded by the rate algorithm within the CEA and the actual rate derived from changes of the shaft encoder position data with respect to time. The rates are given in degrees per second. The status column after the actual rates will display an "M" to indicate when data is missing.

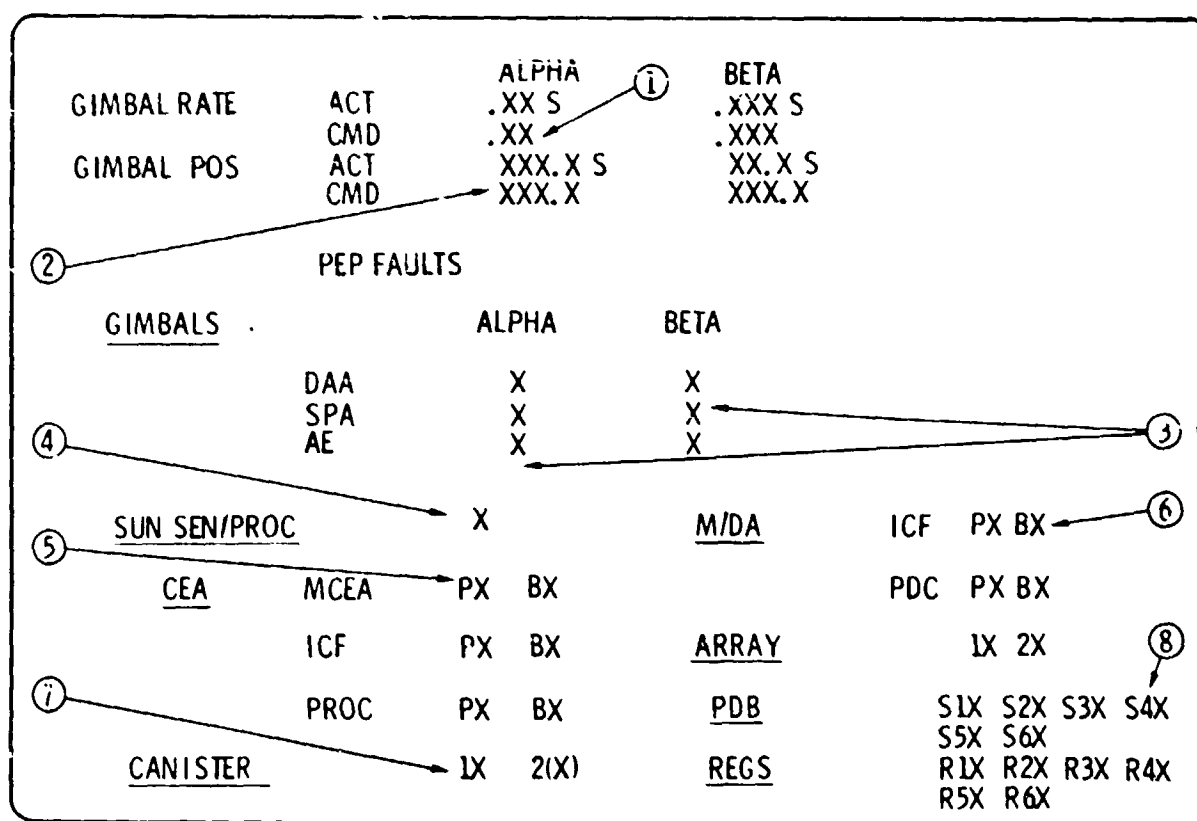


Figure 2.15-3. PEP Status Display Format

2. Gimbal position is also provided in terms of actual and commanded values. Commanded values will vary with mode; for manual modes the data will be that input by the crew while that provided when in automatic mode will be that provided by the sun sensor and output by the CEA. The position is given in degrees. The status column after the actual position will display an "M" to indicate when data is missing.

3. PEP faults attributable to the gimbal system are shown to ensure that operations will be modified or halted should a failure occur. The offending units comprising the Drive Actuator Assy (DAA), Servo Power Amplifier (SPA) or Angle Encoder (AE) will be indicated by a down pointing arrow (+).

4. Loss of the sun sensor or processor, indicated by a down pointing arrow (+), is provided to indicate that the crew should revert to fixed rate operation.

5. Loss of functions in the Control Electronics Assembly (CEA) are indicated by a down pointing arrow (+) for primary and backup systems. They include faults within the multiplexing and encoding assemblies (MCEA), interface control function (ICF) and microprocessors (PROC). Since the systems are dual redundant their loss does not require mission cancellation; alternate units may be selected by addressing. However, the readouts allow the crew and/or ground to assess reasons for the failure(s) and perhaps alter procedures or improve environmental conditions.

6. Item 6 provides a similar assessment of a fault in the multiplexer/demultiplexer assembly (M/DA). They include the interface control function with the CEA and the power distribution control (PDC) module. A fault is indicated by (+).

7. Failure of array or canister motors to operate is a critical failure indicated by an (+). EVA action to free or jettison the faulty unit is required. Alternatively the ADA may be jettisoned.

8. Item 8 indicates a loss of either a switch or regulator and is indicated by an (+). The option in either case is to reconfigure the switch settings.

## 2.16 AVIONICS THERMAL CONTROL REQUIREMENTS

### Objectives

The objective of this study task was to determine the suitability of the thermal control design for ADA located avionics and electrical power components.

### Conclusions and Recommendations

Key Orbiter orientations and orbits were examined to define worst hot and transient conditions. This analysis included effects of Orbiter bottom infrared (IR) energy impinging on the array deployment assembly; solar and re-reflection effects were not included. The hottest case identified consists of an astronomy mission at 90° beta angle which locates the array under the Orbiter bottom (~2 solar inertia).

The worst case transient occurs at low earth orbit where the avionics see high levels of earth albedo and IR on sun side and then cold space on the shade side of the orbit.

A compilation of avionics thermal requirements shows that non-operating limits range as great as -22 to 149°F (-30 to 65°C). The smallest range is 5 to 122°F (-15 to 50°C). Some operating limits are more stringent, 32 to 149°F (0 to 40°C) for sun sensor processor. Sustained power levels are small, the maximum being 150 watts for the array diode assembly.

The thermal analysis showed that non-operating temperatures were low, down to -79.6°F (-62°C). Electrical heaters or other means of obtaining heat input will be necessary for non-operating cold cases.

The highest operating temperature occurs for control electronics, which reached 98.6°F (37°C) at 90° beta condition when operating at 40 watts normal power level. This is below the maximum allowable of 122°F (50°C). The control electronics would exceed the 122°F (50°C) limit if the 80 watt peak power level was sustained.

The cursory analysis results reported herein indicate the feasibility of the current PEP design to maintain avionics temperatures within limits. A more detailed analysis is recommended for Phase C/D to precisely size heaters and determine detailed design for the avionics components.

### Assumptions

The following assumptions were made.

- Heat is lost from the top surface of the components except for array diode assembly which assumes top and two side surfaces.
- Insulation sized for  $10^{\circ}\text{F}$  ( $-12^{\circ}\text{C}$ ) temperature drop between equipment and surface at sustained power levels.
- Orbiter bottom surface characteristics, solar absorptivity/emmissivity = 1.0.
- Orbiter orientations
  - Space Processing and Life Sciences - nose gravity gradient, -X LV, Z POP (low beta)
  - Earth Observation - bay to earth, Z LV, Y POP (all beta)
  - Solar Observation - bay to sun, Z SI (high beta)
  - Astronomy - bay perpendicular to orbit plane, Z inertial, X IOP (all beta)
- Avionics surface emissivity = 0.9

### Approach

The approach to assessing the suitability of the avionics thermal control design was to calculate expected component temperature histories for severe environment conditions and then compare the results with allowable temperatures. Allowable temperatures for the components were obtained from supplier data and is given in Table 2.16-1.

Table 2.16-1. PEP Deployed Avionics Cooling Requirements

Item	Temperatures ( $^{\circ}\text{C}$ )		Power (watts), nominal/max
	Operating	Nonoperating	
Sun sensor processor	0 to 40	-25 to 50	2.5/2.6
Control electronics	0 to 50	-15 to 50	40/80
Actuator and power connectors	--	-30 to 65	--
Drive motor	-29 to 66	--	11.5/TBD
Array diode assy	-65 to 115	--	150/150

Worst case conditions for the analysis were determined by comparing the individual contributions of earth infrared (IR) and albedo and Orbiter IR. Maximum hot case and maximum orbital fluxuation cases were selected for analysis.

A two-node transient model was used to calculate temperatures at 10 points around the orbit. Several orbits were run until the equipment temperature change at the start of successive orbits was less than  $0.05^{\circ}\text{F}$  ( $0.028^{\circ}\text{C}$ ).

### Results

Table 2.16-2 shows the approximate levels of expected heat fluxes which would impinge on the shade side of the array deployment assembly. The hottest environment is expected to occur during an astronomy mission at high beta angle where the bottom of the Orbiter produces the maximum infrared influx to the avionics. Substantial earth IR also strikes the avionics for this condition. The  $90^{\circ}$  beta condition is severe since the Orbiter/PEP is in the sun continuously; the cooler earth shade environment is not encountered.

The greatest environment extreme occurs with the astronomy mission a low beta angle. Full earth albedo and IR are experienced during sun side operation and cold space is encountered during shade side operation.

Table 2.16-2. PEP Avionics Incident Heat Fluxes for Typical Missions

Mission type	Orientation	Beta angle	Heat influxes		
			Earth IR and albedo	Orbiter	Total
Space processing and life sciences	-X LV Z POP	Low	Med to high	Low	Med
Earth observation	Z LV Y POP	All	Med to high	Low	Med
Solar observation	Z SI	High	Med	Low	Low
Astronomy	Z inertial X IOP	Low	Med to high	Low	Med
		Low	Med	High	Med to high

\*Worst case bottom to sun - PEP located under bottom.

Calculated avionics temperatures are given in Table 2.16-3 for expected levels of power output and for the two worst case environment cases. The allowable temperature ranges are also given for reference. Power-on cases for the actuator and power connectors and drive motor are not given since operation of this equipment is of short duration, occurring only during deployment and retrieval where worst case orientations are not expected.

The results show that low temperatures occur when equipment is not operating, ranging as low as  $-79.6^{\circ}\text{F}$  ( $-62^{\circ}\text{C}$ ). Heaters or warm mounting locations may be necessary for these conditions. Normal operating power levels result in acceptable temperatures, however, the maximum power level of 80 watts for the control electronics results in an over-temperature of up to  $73.4^{\circ}\text{F}$  ( $23^{\circ}\text{C}$ ) for the hottest environment. The high power level is expected to be short duration, however, and not a design condition.

Table 2.16-3. PEP Avionics Cooling - Equipment Temperature Predictions

Item	Power (watts)	Allowable range ( $^{\circ}\text{C}$ )	Temperature ( $^{\circ}\text{C}$ )		
			0 $^{\circ}$ beta		90 $^{\circ}$ beta
			Maximum	Minimum	
Sun sensor processor	0	-25 to 50	-57 <sup>(1)</sup>	-62 <sup>(1)</sup>	-14
	2.5	0 to 40	-30 <sup>(1)</sup>	-35 <sup>(1)</sup>	6
Control electronics	0	-15 to 50	-57 <sup>(1)</sup>	-62 <sup>(1)</sup>	-14
	40	0 to 50	13	10	37
	80	0 to 50	56 <sup>(2)</sup>	53 <sup>(2)</sup>	73 <sup>(2)</sup>
Actuator and power connectors	0	-30 to 65	-57 <sup>(1)</sup>	-62 <sup>(1)</sup>	-14
Drive motor	0	-29 to 66	-57 <sup>(1)</sup>	-62 <sup>(1)</sup>	-14
Array diode assy	0 to 150 <sup>(3)</sup>	-65 to 115	55	-3	82

(1) Heaters may be required.

(2) Not a sustained power level.

(3) No power on shade side of orbit, 150 watts on sun side.

## 2.17 THERMAL CONTROL CONFIGURATION DEFINITION

### Objectives

This task compared active versus passive thermal control configurations for cooling PEP voltage regulators. Since the thermal control configuration has a major impact on overall PEP structural configuration, the trade addressed the major affected program parameters of cost, weight, bay volume considerations and ground operations.

### Conclusions and Recommendations

The passive concept improves heat rejection, eliminates fluid interfaces between the PEP and Orbiter and simplifies ground operations. These advantages are offset somewhat by a 1/2 million dollar cost increase and a 38 lb (17.3 kg) weight increase. Some planned EVA routes may require minor modification due to the assumed passive configuration location.

Use of the passive concept reduces the Orbiter heat rejection load by an amount equal to PEP regulator parasitic loss, approximately 3 kw. This enables the PEP/Orbiter to operate at higher power levels, up to 3.4 kw.

Freon 21 fluid interfaces between the Orbiter and PEP are eliminated with the passive concept. This results in reduced complexity, Orbiter scar weight and costs to modify Orbiter for PEP installation. Safety is improved because fluid lines, disconnects and cold plates are eliminated. The passive concept is judged to be more reliable than the fluid concept. Ground operations are simplified and schedules shortened by the elimination of fluid interfaces. Orbiter serial impact time for initial installation is reduced from 34.5 hours to zero by the passive concept. This corresponds to costs of up to 0.7 million dollars in 1980 dollars. A significant time saving results for operational PEP installation and removal of about 1.5 hours per operation.

Based on the results of this trade study, it is recommended that the passive concept be studied in greater depth with particular attention given to the following issues:

1. EVA route intrusion
2. Orbiter bay thermal impact
3. Use of honeycomb structure
4. Design optimization

Satisfactory resolution of these issues is expected to provide sufficient data for a final decision on passive versus active thermal control.

### Assumptions

The following assumptions were made for the passive concept:

- Sun side regulator heat load = 2.92 kw (29 kw total power)
- Coating performance, absorptivity solar/emmissivity thermal = 0.105; emissivity thermal = 0.76
- 270 nm attitude
- Adiabatic surface on passive panel undersides
- 3 kw fuel cell power level in sun
- Regulator temperature limit at base = 150°F (65°C)
- 4 man/orbiter crew
- Flash evaporator performance limit = 30 lb/hr (13.6 kg/hr) of water throughput
- Heat pipe temperature drop = 10°F (5.6°C)
- 6 regulators with baseplate of 16 x 20 inches (40.6 x 50.8 cm) for each regulator
- Orbiter orientations
  1. Earth viewing, XPOP, ZLV and YPOP, ZLV with 45° roll (low beta)
  2. Solar observation; ZSI (high beta)
  3. Space processing and life sciences, -XLV, ZPOP (low beta)

### Approach

The approach to this trade is shown in block diagram form in Figure 2.17-1. The trade compares the passive versus reference design active configurations by examining the change in key program parameters when incorporating the passive concept.

Referring to Figure 2.17-1, initial trade tasks included identification of key trade criteria and definition of requirements to be used in the passive concept preliminary design. These requirements are derived primarily from the reference design effort but supplemented in areas unique to the passive approach.

A preliminary design was generated on the passive concept to a depth consistent with the reference design with particular attention given to characteristic definition corresponding to the trade criteria. Supporting analyses were

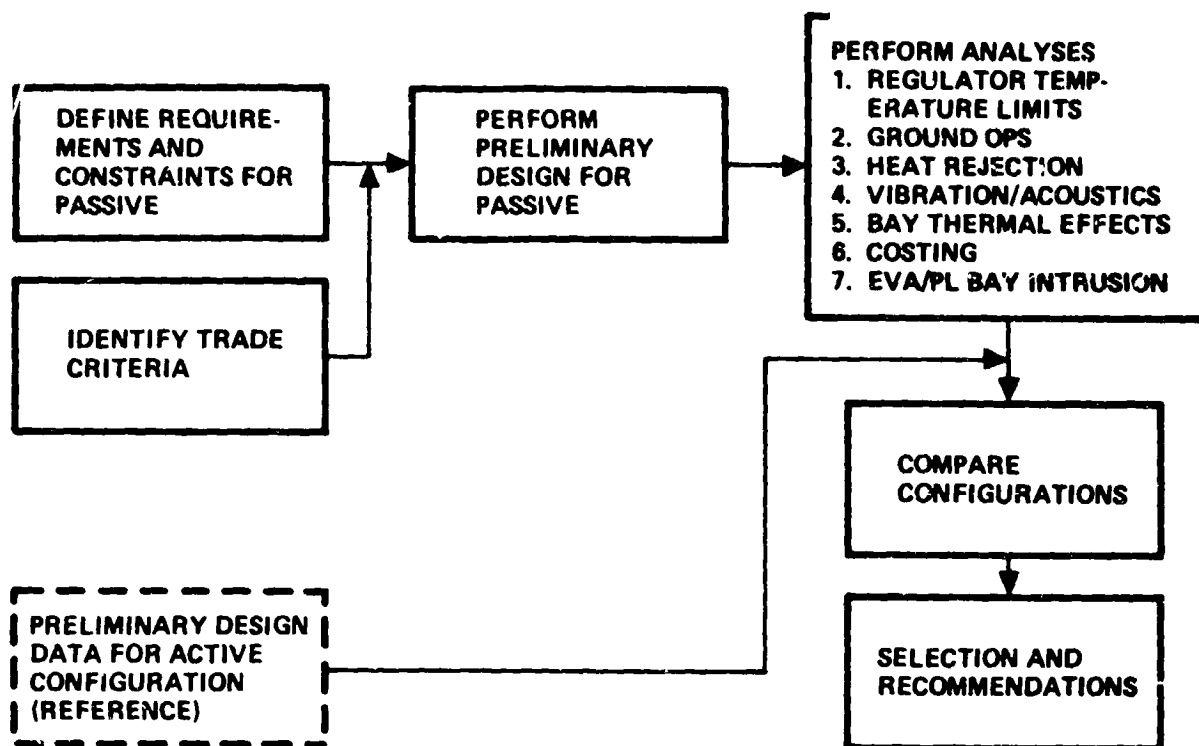


Figure 2.17-1. Approach to Task 2.17 - Thermal Control Configurations Definition

performed to 1) determine adequacy of the design, 2) develop detailed data corresponding to trade criteria and 3) determine performance characteristics.

The configurations were then compared in a systematic manner based on the trade criteria. The preferred configuration was selected and recommendations made for program action.

### Results

The passive thermal control requirement is to provide up to 2.92 kw of cooling for the PEP voltage regulators and limit the temperature to 150°F (65°C). Location of the PEP equipment is constrained based on EVA path and payload reserved volumes. EVA reserved envelopes summarized in Figure 2.17-2 were obtained from "Space Shuttle System Payload Accommodation," JSC 07700, Volume XIV.

Figure 2.17-3 presents the passive thermal control configuration in isometric form. The configuration consists of two flat panels, each is positioned between the Orbiter sill and a point just above the airlock. The two panels

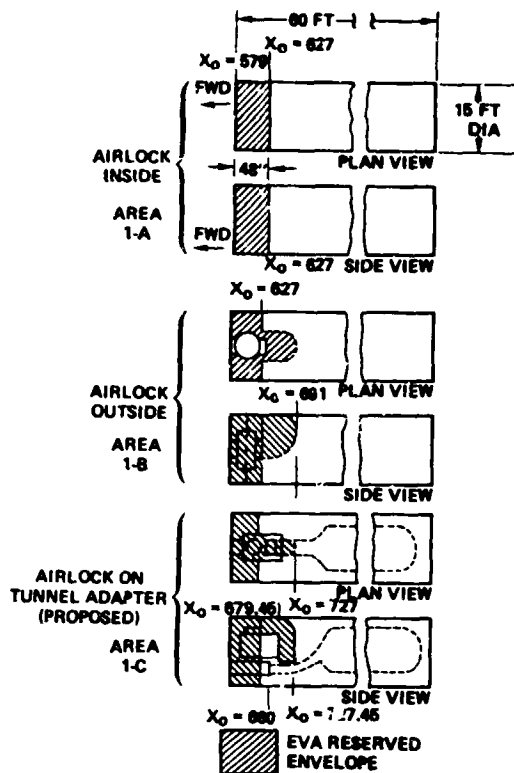


Figure 2.17-2. EVA Reserved Envelopes for Forward Cargo Bay Area

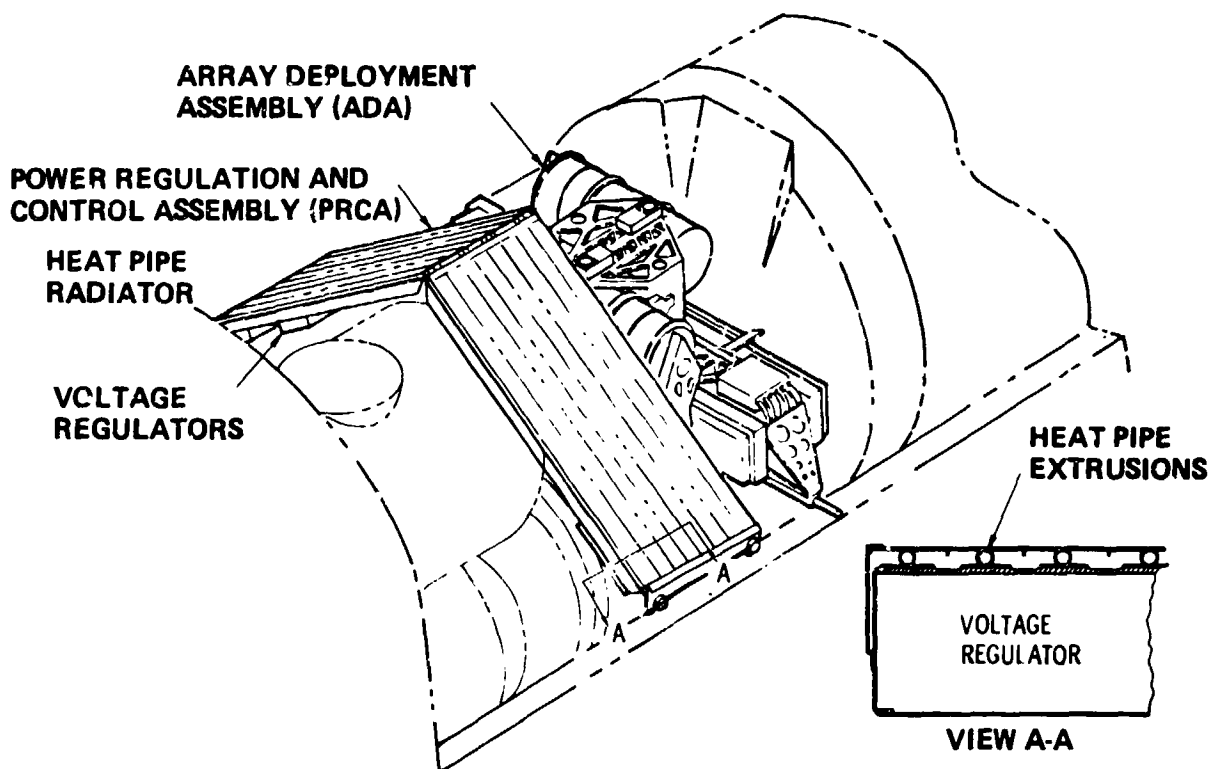


Figure 2.17-3. Passive Thermal

join at this point by a hinge connection. The panels are aft of the airlock hatch to preclude interference with hatch operation during EVA. Heat from the voltage regulators is distributed over the panel surfaces by heat pipes and subsequently rejected to space.

Extruded sections are welded together to form the panels. These extrusions contain the heat pipes, the radiating surface and flanges for mounting the regulators on the panel underside. Additional stiffening panels are added to obtain adequate rigidity to withstand vibration, acoustics and acceleration loads. Thermal characteristics of the radiating surface is provided by silver teflon material with a low ratio of solar absorptivity/thermal emissivity.

A previously developed ammonia heat pipe was selected for the design which minimizes program risk and cost. This is a NASA-GSFC aluminum heat pipe with an inside diameter of 0.344 inches (0.87 cm) and a standard 0.0425 inches (0.11 cm) deep axial groove geometry.

A weight statement for the candidate thermal control configurations is given in Table 2.17-1. Structural/mechanical weights are higher by 77 lbs (35 kg) for the passive configuration because of the heat pipe and extended surface requirement. This is only partly offset by elimination of thermal control cold plates, 47 lbs (21.4 kg). Power distribution cables are 6 lbs heavier for passive because low voltage cable runs are longer. The total weight of the passive configuration is 38 lbs (17.3 kg) greater. This weight is offset somewhat by SCAR weight to Orbiter for fluid lines which amounts to about 13 lbs (5.9 kg).

Regulator Temperature Limits—Performance capability in terms of regulator temperatures was performed at two levels of detail. A detailed computer analysis was performed using TRASYS and SINDA computer programs for key orbital conditions. The model consisted of 136 nodes for the Orbiter and 18 nodes for the passive thermal control panels. This model was also used to assess the thermal effect of the passive configuration on the Orbiter payload bay.

A less detailed analytical approach was used to determine performance for all orientations which the PEP/Orbiter is expected to fly. This analysis assumed an adiabatic surface on the panel undersides and the Orbiter radiator panel effect was included in a cursory manner. Results of this simplified analysis approach agreed well with the detailed methods discussed in the above paragraph.

Table 2.17-1. Thermal Configuration Weight Statement

	Configuration (values in pounds)	
	Active	Passive
Solar array	1031	1031
Blanket assembly	615	615
Solar array wing box assembly	160	160
Solar array mast assembly	256	256
Structure/mechanical	300	375
Solar array supt. struc. assembly	126	126
Pwr regulation equip. supt. struc. assembly	68	143
Solar array canister supt. mech.	33	33
2-axis solar array drive gimbal assembly	73	73
Power distribution and regulation	698	703
Power distribution equipment	97	97
Voltage regulation equipment	432	432
Distribution cables	169	174
RMS power cable assembly	101	101
Thermal control	44	0
Avionics	92	94
Total weight (lb)	2266	2304
Weight delta (lb)		+38

Results of the detailed analysis is given in Figure 2.17-4 in terms of 4 node temperatures of over several orbits. Node 8211 represents the regulator base temperature. The orientation is for Orbiter nose towards earth with vehicle hold to minimize solar energy on Orbiter radiators. This is a favorable orientation and is typical of a low G long duration mission such as life sciences or material processing.

Data from the figure shows a regulator temperature variation of 47 to 96°F (8.3 to 35.6°C) over the orbit which is well below the 150°F (65°C) maximum allowed.

Figures 2.17-5 and 2.17-6 show the results of less detailed analyses. Orbital temperature variation is given in Figure 2.17-5 for key orientations. The gravity gradient orientation agrees with the detailed analysis results. Tem-

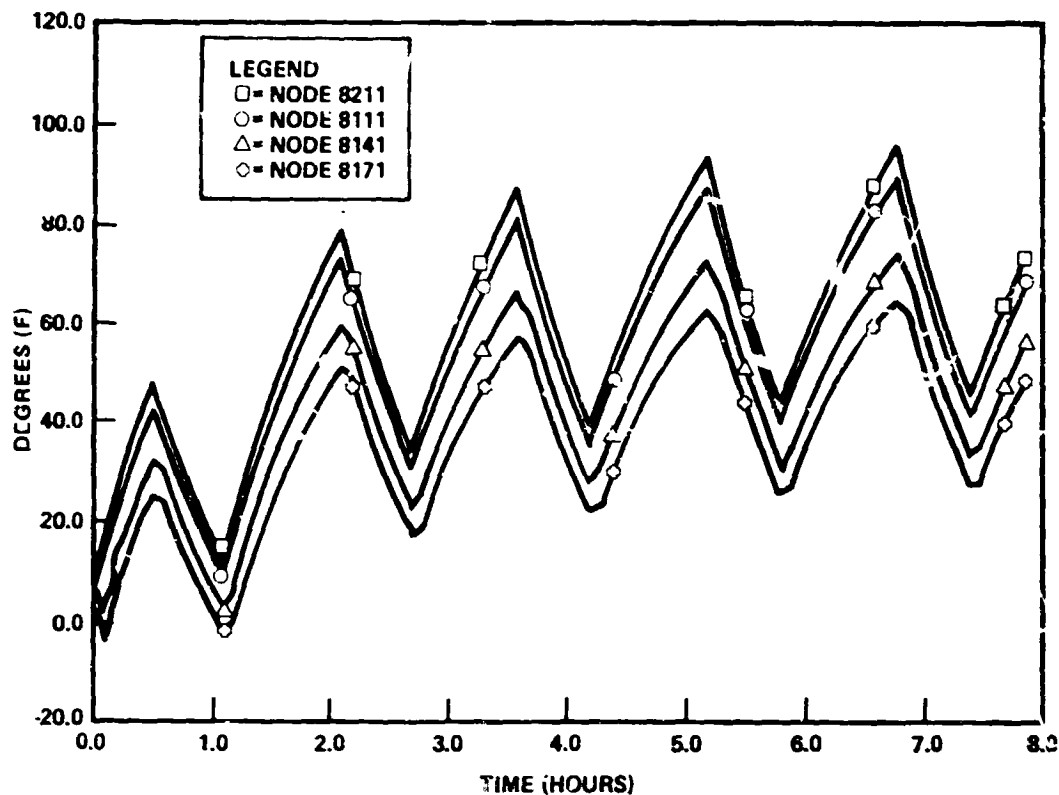


Figure 2.17-4. Power Extension Package Regulator and Radiator Temperatures — Beta = 0. STS Nose Toward Earth, One Roll Per Orbit.

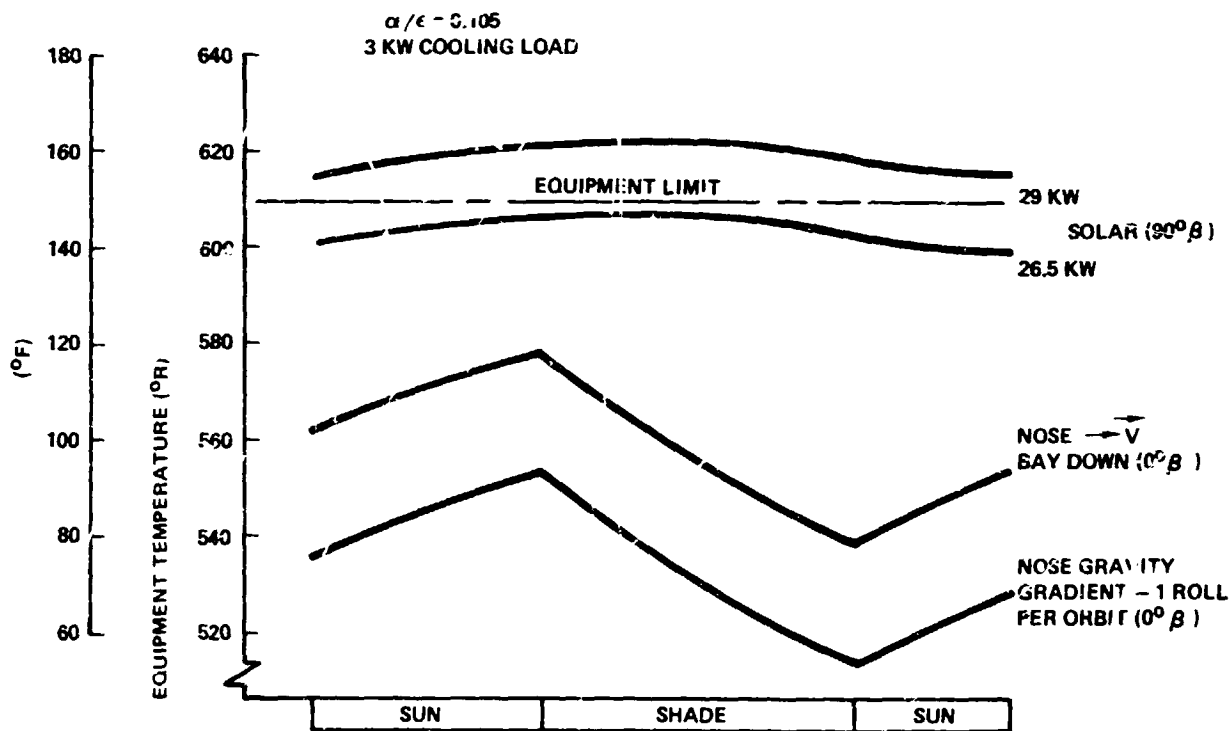


Figure 2.17-5. Passive Thermal Control Equipment Temperature Limit

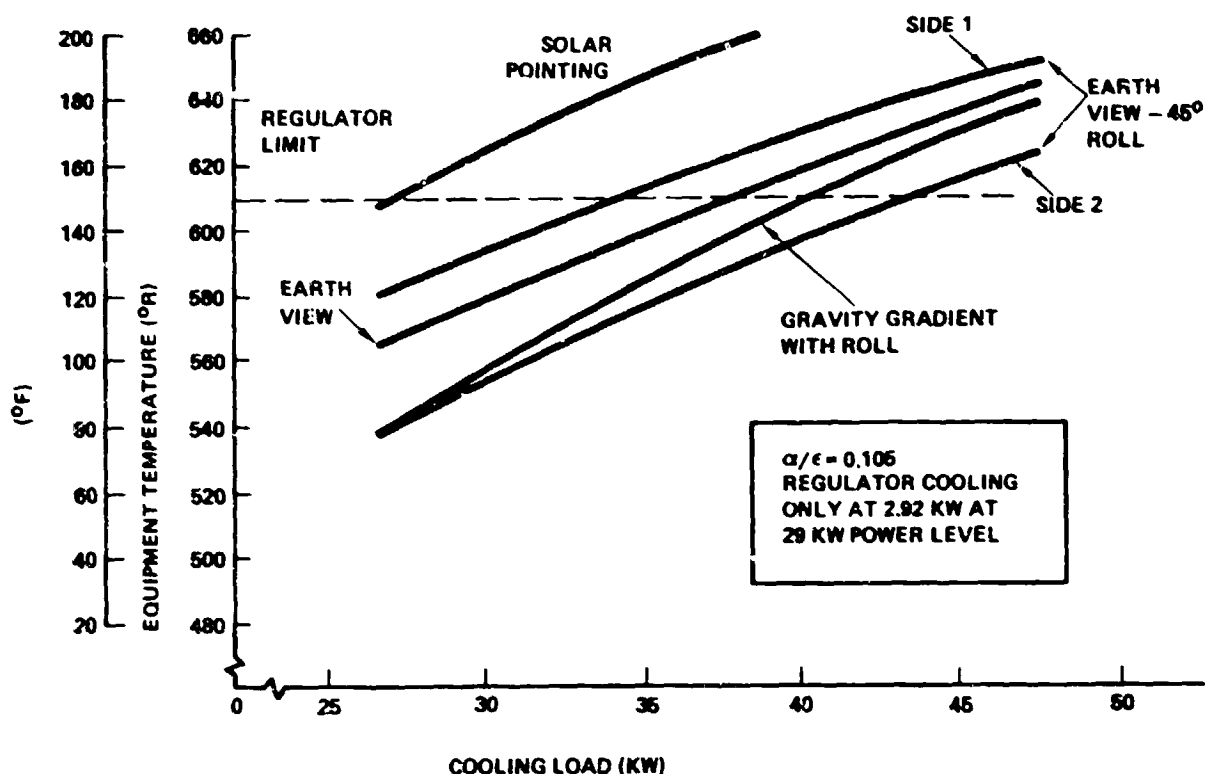


Figure 2.17-6. Passive Thermal Control — PEP Equipment Temperatures

peratures for bay down orientation are from 80 to 120°F (26.7 to 48.9°C) which also is well below the limit. Stellar pointing orientation is not shown in the figure, temperatures are between those for gravity gradient and bay down.

Results show that regulator temperature limits are exceeded for direct solar viewing at 90° beta angle and a power level of 29 kw. Regulator temperature limits can be maintained, however, at electrical power levels below about 27 kw. The main reason for the much higher regulator temperatures for the solar pointing case is due to the full sunlight orbit resulting in continuous regulator heat output and continuous hot environment. The slight deficiency in the passive design can be corrected by providing slightly larger panels. This may not be appropriate considering Orbiter performance at high inclinations with regard to payload launch capability and heat rejection capability. Orbiter heat rejection capability limits power output to about 17.4 kw for sustained operation and solar pointing operation. Power levels above 29 kw are possible but time limited due to water storage limits; i.e., more water is required for flash evaporation cooling than is being generated by the fuel cells. Since the fuel cells are at idle for 90° beta operation, considerable time is required

to store significant amounts of water. Therefore, sustained operation at near the 29 kw power level is unlikely and so the 27 kw power level limit imposed by the current passive configuration is not to not be the limiting factor for solar pointing operation.

Heat Rejection Limits--Heat rejection limits in terms of allowable power levels for Orbiter/PEP are given in Figures 2.17-7 to 2.17-10. The figures give maximum power levels for Orbiter without PEP, Orbiter with the reference design PEP with active cooling and Orbiter with the PEP passive configuration. Three levels of flash evaporator system operation are shown corresponding to no operation, sustained where just the amount of generated available water is used and maximum where the flash evaporator is operating at full capacity. Crew water use has been accounted for in determining sustained operation limits.

Figure 2.17-7 represents the most severe orientation and it can be seen that use of the passive configuration increases allowable power levels over Orbiter without PEP for inoperative or maximum flash evaporator operation. This is because fuel cell waste heat is lower with PEP. However, power levels for sus-

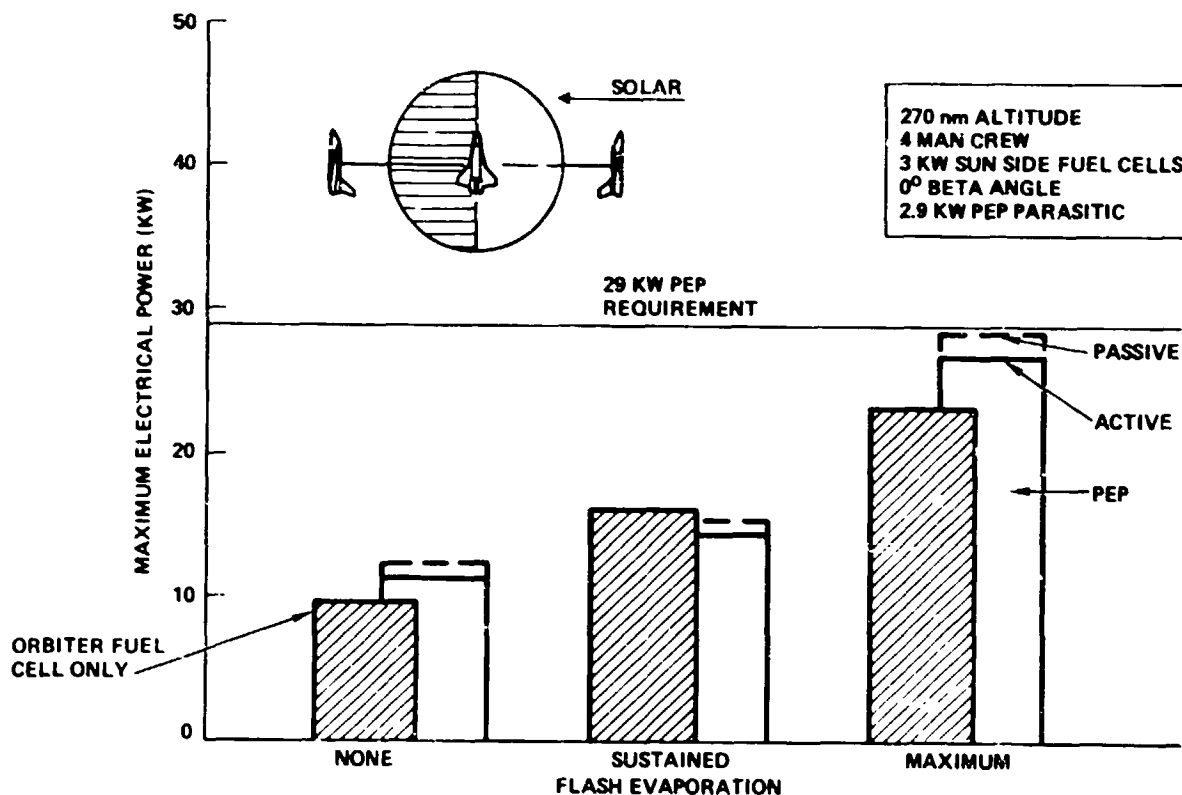


Figure 2.17-7. Heat Rejection Performance Comparison - Active versus Passive Earth Viewing

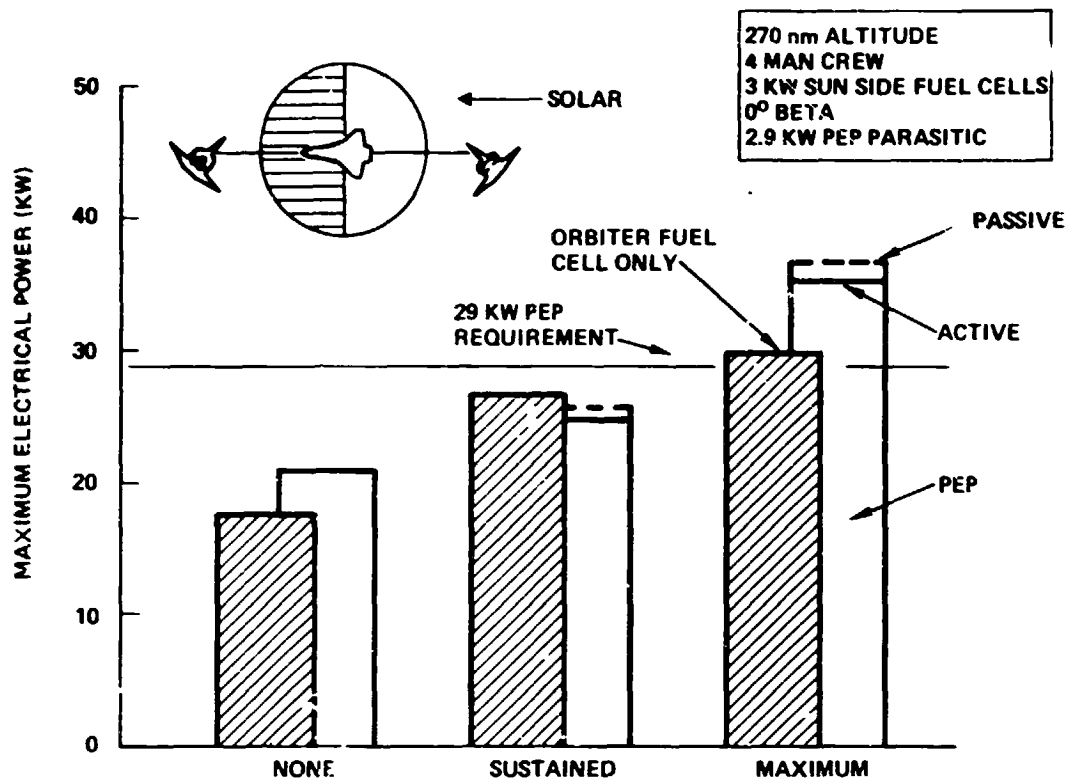


Figure 2.17-8. Heat Rejection Performance Comparison Active versus Passive Earth Viewing

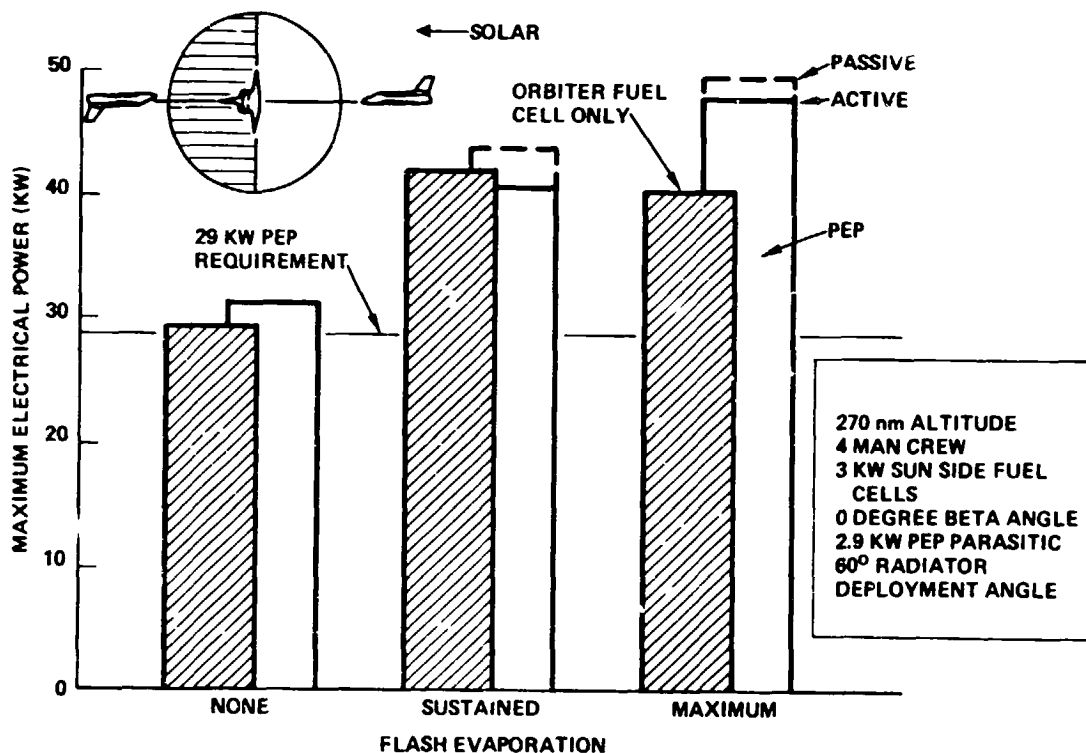


Figure 2.17-9. Heat Rejection Performance Comparison - Active versus Passive Low G Sustained Operation

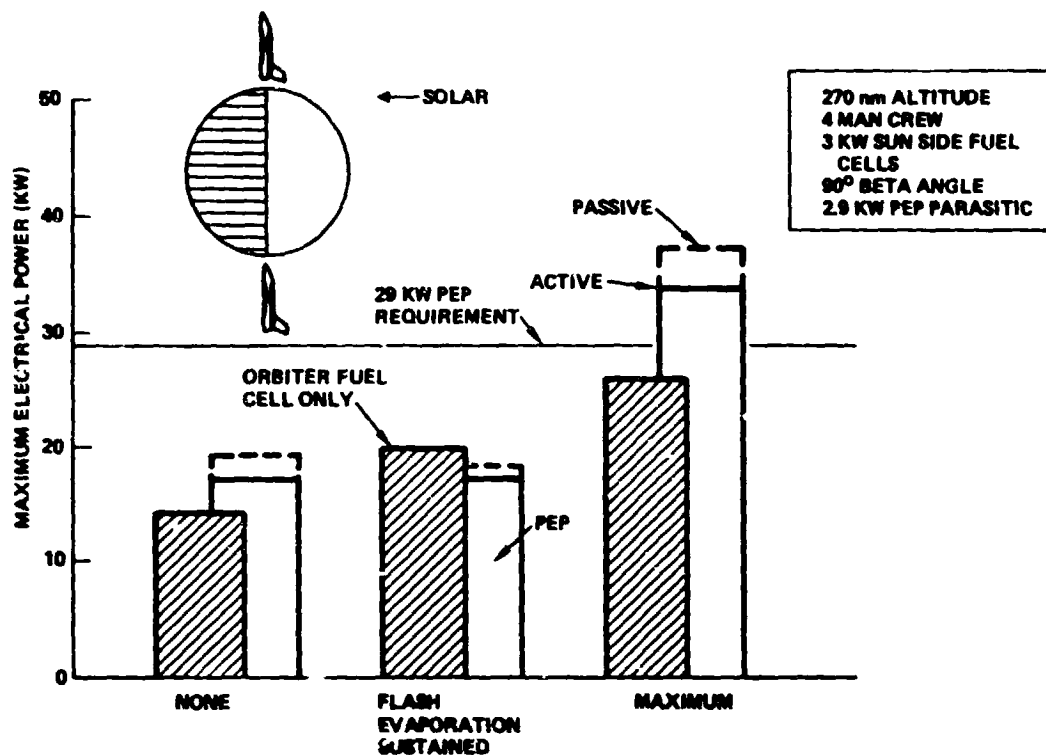


Figure 2.17-10. Heat Rejection Performance Comparison — Active versus Passive Solar Viewing

tained flash evaporation is less with passive PEP than Orbiter alone because the water generation rate is lower due to the idling fuel cells in sun when PEP produces most of the power. Therefore, less water is available for cooling.

The passive configuration offers a significant improvement over the active cooling configuration for earth viewing shown in Figure 2.17-7, amounting to 0.8 to 1.3 kw additional power level.

Heat rejection performance for a less severe earth viewing orientation is given in Figure 2.17-8. This orientation is nose along velocity vector with bay rolled 45° from local vertical. No difference in performance exists for operation with no flash evaporation cooling because shade side capability is controlling. This occurs because shade side required heat rejection is larger due to large fuel cell waste heat loads in the shade. Based on the data in the figure, the passive configuration allows up to 1.6 kw higher power levels for this orientation.

A favorable orientation of nose gravity gradient with roll is given in Figure 2.17-9. The passive concept allows up to 2.5 kw higher power levels. Since the maximum PEP power output of 29 kw can be accommodated with the active configuration, the increased capability can be considered a performance margin.

Figure 2.17-10 shows that for solar viewing the passive concept results in 1 to 3.4 kw higher allowable power levels. The improvement of 2.1 kw for no flash evaporation is particularly significant since little water is available for 90° beta operation. This results from the reduced fuel cell operation which produces only 1.5 lbs/hr (0.68 kg/hr) of water for cooling use.

Summarizing, the passive configuration offers significant performance gains in terms of higher allowable PEP/Orbiter power levels as limited by heat rejection. This improvement amounts to power levels up to 3.4 kw for solar pointing with maximum flash evaporator cooling. Values for inoperative flash evaporator are up to 2.1 kw higher. This is particularly significant for earth viewing, stellar and solar pointing orientations where an inoperative flash evaporator may be advantageous to avoid water vapor in sensor fields of view.

Ground Operations--The aspects of ground operations which are particularly impacted by thermal control configuration are; (1) serial impact time to Orbiter during initial PEP installation and (2) time required for operational installation and removal. Complexity and number of tasks required are also important because of effects on ground crew size and potential turnaround schedule holds.

Analysis of initial installation time lines shows that 48 hours are required for routing, installation, brazing and X-raying the interfacing freon fluid lines in the Orbiter. The passive configuration does not require these tasks thereby eliminating 34.5 hours of serial impact time to the Orbiter. Cost savings for this impact could amount to as high as 0.69 million dollars. This cost is based on a serial impact cost of 20K dollars per impact hour in 1980 dollars.

Tasks associated with operational installation amounts to 1.5 hours for fluid line connections. Operational removal requires 1.0 hours for disconnecting fluid lines. These tasks are not required for the passive concept and represent a savings in the timeline.

Some other ground operational tasks will be altered for the passive concept; however, complexity and time requirements are estimated to be similar to the reference active configuration.

Vibration/Acoustics--An acoustics/vibration analysis was performed to determine the adequacy of the passive design. Results showed the adequacy of the current design to withstand the induced Orbiter environment.

Bay Thermal Effects--The SINDA computer program was used to calculate payload bay temperatures near the passive thermal control panels. Results are shown in Figure 2.17-11 for 5 orbits and a vehicle orientation of nose gravity gradient with Orbiter roll for favorable radiator viewing. Adiabatic panel undersides were assumed. The temperatures of key bay liner nodes show an orbital range of from about  $-200$  to  $40^{\circ}\text{F}$  ( $-129$  to  $-40^{\circ}\text{C}$ ). This temperature range is within the  $-250$  to  $200^{\circ}\text{F}$  ( $-156.7$  to  $95.5^{\circ}\text{C}$ ) range expected for bay surfaces specified in JCD 2-19001, Shuttle Orbiter/Cargo Standard Interfaces.

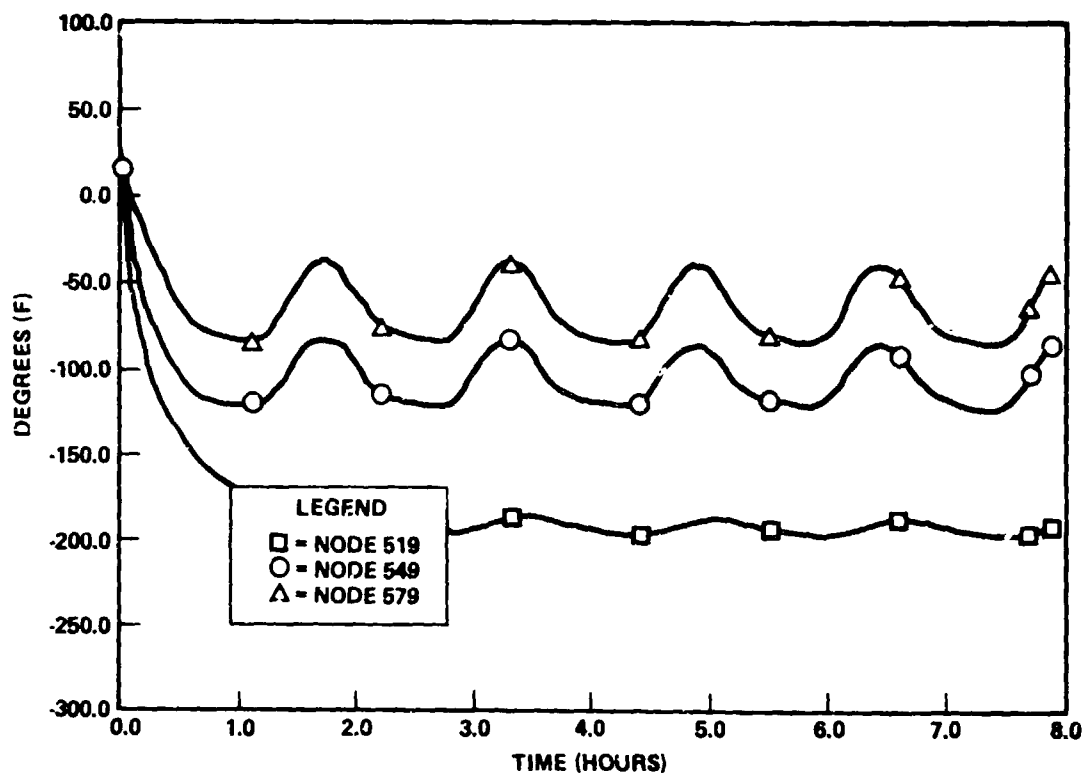


Figure 2.17-11. Power Extension Package Payload Bay Liner Temperatures -- Beta = 0.  
Nose Toward Earth, One Roll Per Orbit.

The low temperatures resulting from this analysis suggest the possibility of higher performance for the passive concept if heat loss from panel undersides is allowed.

Costs--Table 2.17-2 gives the costs of items impacted for a program change from the reference design to the passive configuration. Hardware costs for passive are about 270 thousand dollars higher. The higher costs for heat pipes is not quite offset by cost savings for eliminated active components. Additionally, system level costs are about 230 thousand dollars higher resulting in a total cost differential of 503 thousand dollars.

Cost estimates presented in the above paragraph do not include passive configuration cost savings for reduced GSE, simplified ground operations and elimination of Orbiter fluid interface modifications.

Table 2.17-2. Cost - Passive Versus Active Thermal Control  
(in thousands of 1978 \$)

Passive		Active	
Heat Pipe	\$ 780	Support Rack	\$ 290
		Cold Plates	228
		Plumbing	50
Trunions	50	Fittings	40
Cable	1,481	Cable	1,434
HARDWARE TOTAL	\$2,311	HARDWARE TOTAL	\$2,042
System Level	2,004	System Level	1,770
TOTAL	\$4,315	TOTAL	\$3,812
Delta	\$ 503		

Volume Intrusions--The passive configuration potentially intrudes into the payload volume to a greater extent than the active configuration. There is an intrusion above the sill, from x-axis Station 639.5 to 679.5. Referring to EVA requirements, Figure 2.17-2, the passive configuration does not intrude into area 1-A which consists of the first 48 inches (122 cm) in the cargo bay.

The passive concept reduces the EVA routes shown for airlock outside configuration, 1-B. This route is intended to provide access into the Orbiter bay. Since the passive panels restrict an EVA directly to the area above the airlock hatch, routes may have to be altered so the EVA crewmen get to top bay region from the front bulkhead area. The passive configuration is not believed to unduely restrict this type of operation.

Area 1-C, shown in Figure 2.17-2, is required only for those missions wherein experiments may be deployed outside the dynamic envelope or where other experiments require EVA. A proposed alternate route is over the top of the passive panel near the top hinge line of the panels. Hand rails will be required across the panel and perhaps along a portion of the edge as required for EVA translation from the airlock top door to the back of the airlock. Some means of protection should also be considered to prevent damage to the thermal coatings along the top of the panels. It is felt that an acceptable EVA path can be obtained with the passive concept.

The passive configuration potentially intrudes into payload volume for "Get Away Specials" type payloads located in the passive panels sill support area, Stations 639.5 and 679.5.

Loss of this area for payloads would not significantly reduce the total volume available to payloads. Therefore, intrusion of the passive configuration into payload volume is not believed to be a significant factor.

## 2.18 ORBITER DAP UTILIZATION/INTERFACE EVALUATION

### Objectives

The object of this analysis was to evaluate potential constraints on the Orbiter DAP when operating with PEP. Areas addressed were RCS thruster selection, limit-cycle operation and Orbiter maneuvers.

### Conclusions and Recommendations

The following preliminary conclusions are based on the discussion below. A 0.02 Hz solar array wing cantilever frequency and a 200 ft-lb array mast strength were assumed based on the structural design criteria work reported in Section 2.8.

- The PEP will impose constraints on the Orbiter DAP; these constraints will have to be defined on a mission specific basis.

- Nominal limit cycle operation should use the VRCS
- Preliminary results indicate that inhibiting certain Orbiter limit cycle frequencies will not be required if a relatively small amount of PEP compliance structure damping (one percent of critical) exists.
- The PRCS may be used for nominal limit cycle operations when insignificant plume impingement occurs.
- Maneuvers can be initiated with either the PRCS or VRCS. For maneuver rates greater than 0.03 to 0.04 deg/sec, the solar array must be oriented so that a thruster plume will not impinge directly on the surface of the array (i.e., thrust vector perpendicular to the array surface). Essentially any maneuver rate is possible with the VRCS from a dynamic load viewpoint when plume impingement does not occur. Maneuver rates with the PRCS will be limited to 0.15 deg/sec to near 1 deg/sec depending on RMS and array orientation when no impingement occurs.
- Inhibiting certain thrusters to minimize plume impingement appears feasible (rotational controllability maintained) with the PRCS from a thruster location and orientation standpoint. Actual DAP software jet select logic must be analyzed to verify this, however. The forward jets should be inhibited when the array is forward and the left side jets should be inhibited when the array is positioned to the left. Only PRCS thrusters with plumes above the Orbiter should be used when the array is below the Orbiter. Orbiter translational controllability cannot be maintained in general when these thrusters are inhibited.
- Inhibiting VRCS thrusters to minimize plume impingement is not required except for maneuvers where plume impingement is significant. The limited number of VRCS thrusters make inhibition of VRCS thrusters undesirable though geometrically feasible if only one VRCS thruster is inhibited.

#### Approach/Discussion

Orbiter-induced PEP dynamic loads result from Orbiter motions and RCS thruster plume impingement. Attitude motions can be divided into limit cycle motions and attitude maneuvers. The dynamic loads are treated in Paragraphs 2.8 and 2.14 and some additional limit cycle analysis and specific DAP-related discussions are presented here.

A first-cut approach to the loads due to Orbiter limit cycle analyzed the mast root moment sensitivity to idealized one- and two-sided limit cycles. A

Fourier series representation of the Orbiter ideal limit cycle rate histories was used with an Orbiter-rate-to-mast-root-moment transfer function to generate mast root moments per deg/sec as a function of limit cycle period. The solar array/compliance structure was modeled as a single axis rigid array connected to Orbiter rotation through the mast root compliance structure. The compliance structure frequency was 0.02 Hz and the compliance structure damping was varied.

Twenty-five high fidelity Orbiter on-orbit flight control simulation results were obtained from JSC/LEC (Space Shuttle Functional Simulation--SSFS). These simulations were for a rigid Orbiter and did not include a deployed PEP. Since PEP is relatively light, it was assumed that simulation results were valid. Each case simulated one orbit and was reviewed and the limit cycle rates, period between thruster firings (minimum, maximum, average), minimum impulse bit and type of limit cycle (one- or two-sided) determined. The cases included both the PRCS and VRCS and several orientations.

Plume impingement moments were evaluated by graphically integrating the thruster pressure distribution over the array. Plume force and moment impulse per Orbiter rate change was used so the effects on the PEP could be interpreted directly as a function of Orbiter rate change rather than thruster on-time. Two solar array positions were analyzed for plume impingement. One with the array parallel to the x-z plane and the RMS extended maximum to the left (RMS/PEP Position 2, Figure 2.8-1). The second is with the array below the Orbiter and directly below an aft thruster (Position 3, Figure 2.8-10). Restricting various thrusters from firing when the array would lie in the plume is a potential solution to plume loading.

Orbiter angular rate changes cause linear and angular rate changes of the PEP which result in dynamics structural loads. These loads were evaluated (Paragraph 2.8) with a simplified model and preliminary maximum allowable Orbiter angular rate changes were defined. DAP operation must preclude angular rate changes exceeding the PEP constraints. If high rates are required, the rate must be implemented gradually to reduce the array and RMS loads. These constraints will vary on a mission specific basis and can be minimized by judicious RMS/PEP placement.

## Results

Figures 2.18-1 and 2.18-2 define the peak mast root moment on each wing per Orbiter limit cycle rate as a function of limit cycle period for several compliance structure damping ratios. Both two- and one-sided limit cycles are included. Only the peaks are shown but the function is continuous as a function of limit cycle period. Between each peak, the function drops to the 200 to 300 ft-lb/deg/sec level for all cases. Note that the one-sided limit cycle peaks every 50 seconds of limit cycle period (both even and odd harmonics) while the two-sided limit cycle peaks only every 100 seconds (odd harmonics). Assuming that the mast root moment limit is 167 ft-lb (200 ft-lb minus 33 ft-lb due to blanket tension), a VRCS limit cycle rate of  $\pm 0.006$  deg/sec, and an 0.01 compliance damping ratio, there is no requirement on Orbiter limit cycle period. This correlates with the simulation results discussed in Paragraph 2.14. Reducing the damping ratio to 0.001 constrains the Orbiter limit cycle period to be larger than 150 seconds for the two-sided limit cycle case and greater than 50 (or possibly 100) seconds for the one-sided limit cycle case. Figure 2.18-3 defines the relationships between limit cycle period, rate and attitude for the two- and one-sided limit cycle trajectories.

The above discussion is worst case from the viewpoint of limit cycle period since it assumes an ideal limit cycle operating at exactly a frequency which is a harmonic of the 0.02 Hz compliance frequency. As discussed below, actual limit cycles are much more irregular. The mast root moments shown in Figures 2.18-1 and -2 are not conservative from a plume impingement viewpoint since plume impingement is not included.

Realistic Orbiter limit cycle characteristics were available from the 25 simulation cases obtained from JSC/LEC (SSFC). The attitude dead bands were 0.1 and 0.5 degrees for the VRCS and one and three degrees for the PRCS. The orientations included Z-axis local verticals, inertial holds and passive thermal control (PTC) attitudes with the X-axis in the orbit plane and canted 45 degrees from the orbit plane. The PRCS limit cycles were two-sided in all axes except for three Z-axis cases which exhibited a combination over a complete orbit. The VRCS limit cycles were both one-sided and two-sided depending on the external moments. Of primary interest were the limit cycle rates and the time periods between firings which defined the limit cycle frequency content.

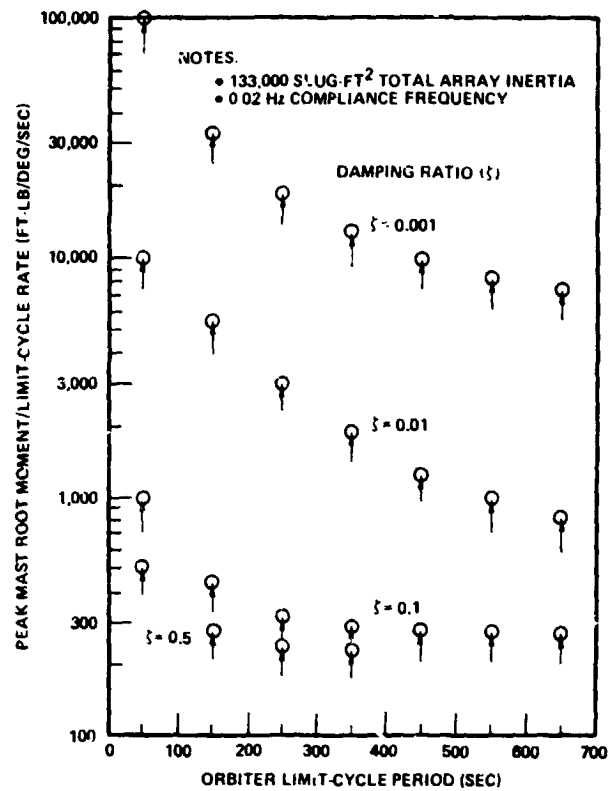


Figure 2.18-1. Peak Mast Root Moment Per Wing, Two-Sided Limit Cycle

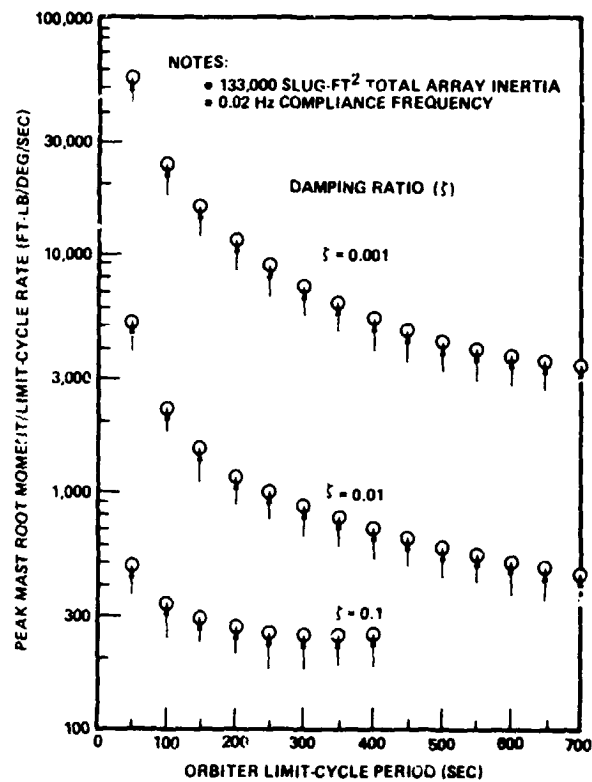


Figure 2.18-2. Peak Mast Root Moment Per Wing, One-Sided Limit Cycle

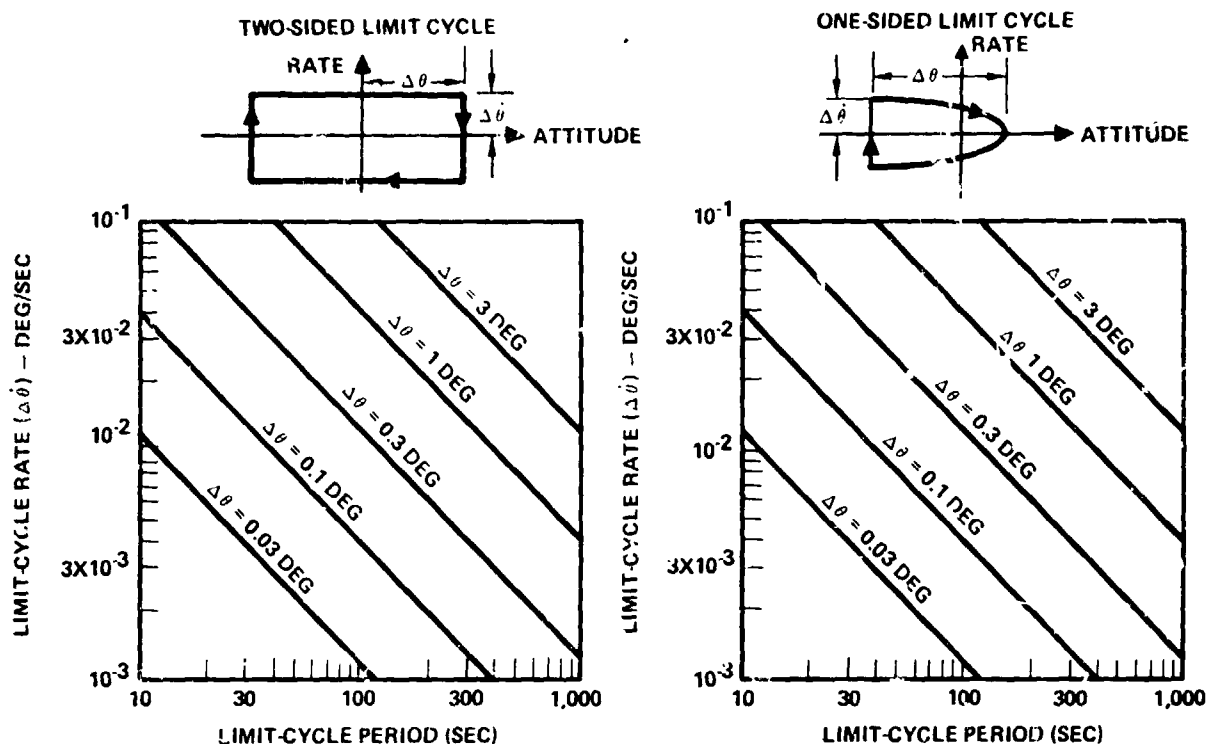


Figure 2.18-3. Orbit Limit-Cycle Period, Rate, and Attitude Relationships

The maximum PRCS limit cycle rate observed was  $\pm 0.06$  deg/sec. Similarly for the VRCS, the maximum limit cycle rate seen was  $\pm 0.01$  deg/sec (X-axis). The maximum seen about the Y- and Z-axes was  $\pm 0.006$  deg/sec with the VRCS.

The minimum angular rate changes due to minimum impulse bit firings observed in the 25 cases were about:

PRCS

Roll (X-axis)	0.06 deg/sec
Pitch (Y-axis)	0.05 deg/sec
Yaw (Z-axis)	0.045 deg/sec

VRCS

Roll (X-axis)	0.006 deg/sec
Pitch (Y-axis)	0.002 deg/sec
Yaw (Z-axis)	0.002 deg/sec

Some smaller changes were observed, but these are considered typical.

The limit cycle periods observed were very irregular. This is due primarily to the time varying external aerodynamic and gravity gradient moments and also,

due to the non-symmetric control accelerations and complex thruster on-off logic. Because of the extent of the limit cycle irregularities observed, it was not possible to accurately define the frequency content in the limit cycles. Consequently, the potential for limit cycle interaction with the PEP compliance structure resonances could not be significantly limited. Paragraph 2.14 discusses some effort at quantification of the interaction effects.

The plume impingement analysis showed that the PRCS and VRCS plume pressures varied approximately as the thrust level. Since the lever arms associated with the primary and vernier thrusters are about the same, the solar array plume impingement impulse for a given Orbiter angular rate change is approximately the same for the PRCS and the VRCS. The negative aspect of using the PRCS is that the limit cycle rates are higher than for the VRCS because of the relative minimum impulse bit magnitudes. Thus, the limit cycle plume loads are effectively greater for the PRCS. For maneuver rates larger than the PRCS minimum rate change, PRCS or VRCS thrusters may be used if the rate change constraints are met since the loads will be the same. Plume load calculations are discussed in Section 2.8. The maximum plume load condition is for RMS Position 3 (see Figure 2.8-10) with the solar array 38 feet below the aft thrusters. The allowable pitch rate change is 0.03 deg/sec when an 0.02 Hz compliance frequency is used (Figure 2.8-10). Similarly in Position 2, the maximum yaw rate change is 0.04 deg/sec when the solar array is in the thruster plume and perpendicular to it. These rate changes are smaller than possible with the PRCS as noted in the JSC/LEC (SSFC) simulation results.

Plume impingement for RMS/PEP Position 1 (Figure 2.8-1) is relatively small compared to Positions 2 and 3 if the forward thrusters are inhibited. Complete attitude control is possible using only aft thrusters if primary thrusters are used for pitch-up accelerations.

Orbiter maneuver limitations are defined by Figures 2.8-8 to 2.8-10 and discussed in Paragraph 2.8. For any large rate maneuvers, the array must not fall significantly in a jet plume since the loads are excessive. The inertial load constraints are less restrictive than the plume load constraints. An alternate plume load reduction approach for large maneuvers is to "feather" the array by manually commanding the Beta gimbal. Plume loads will be reduced by about 90 percent and the thermal constraints may become dominant. Either primary or

vernier thrusters may be used for the maneuvers as long as the rate change constraints are observed.

The following results are based on Figures 2.8-8, 2.8-9 and 2.8-10 (200 ft-lb mast strength), and a 0.02 Hz compliance frequency when the array is not in the thruster plume. The three cases analyzed are considered worse case for each RMS position. Position 1 limits the pitch maneuver rate to 0.15 deg/sec with the array along the Z-axis and 1 deg/sec with the array along the Y-axis. The 1 deg/sec is large because with the array along the Y-axis, the pitch array moment of inertia is very small and the compliance structure attenuates the plunge load effects. The rate change limit in Position 2 is 0.22 deg/sec (no plume effects) or more depending on the array orientation and maneuver axis. RMS/PEP Position 3 limits the pitch maneuver to 0.35 deg/sec when the array is out of the plume.

## 2.19 POINTING/CONTROL AVIONICS CONCEPT AND OPERATIONS ANALYSIS

### Objectives

To analyze requirements/criteria for array extension, retraction and Alpha/Beta gimbal control for various PEP operational phases and define system functions/specifications for integration into the Electronics Assembly, Control (CEA).

### Conclusions and Recommendations

The keyboard functions/commands necessary to effect array extension, retraction and gimbal control were defined. In addition, CEA requirements for initialization and self test were developed along with microprocessor functional flows and function timing.

It is concluded that software organization and microprocessor operation is similar to that employed in the Spinning Upper Stage Sequence Control Assembly (SCA) and that much of the work performed on the SCA is applicable to this program.

### Approach

This task is an extension of the results of Tasks 2.14, Solar Array Control Avionics Requirements/Criteria Definitions and 2.15, Control Systems Management - GPC and Array Control Processor Interface Definition. In some respects,

the analysis has been reoriented to provide data of interest to NASA personnel as defined by action items.

In general, operations to be performed after the application of power to the CEA were reviewed and means for implementing these operations were hypothesized.

#### Assumptions

- A microprocessor will be employed for CEA peripherals control.
- The connection between the CEA and the GPC will consist of data bus only.
- The input for commands to the CEA and display of CEA data will be via the MCDS only.

#### Results

The results of the analysis are contained in the following paragraphs.

Operational Controls--Since the PEP employs only one panel-mounted switch, which is for power turn on/off, no AFD-generated interrupts are generated. An external clock interrupt will be required for software sequencing. Keyboard commands will be entered via the MCDS keyboard and, when received by the hardware, placed in microprocessor Random Access Memory (RAM). An interrupt can then be generated to tell the software that a command is in the buffer.

Keyboard Commands--The CEA should be capable of receiving the following commands and executing them upon receipt.

1. Set Discrete Output--Commands the software to set a specific output which is specified by the second data byte.
2. Reset Discrete Output--Commands the software to reset a specific output which is specified by the second data byte.
3. Select CEA Unit No. 1 to Transmit--Enables CEA Unit No. 1 to transmit while inhibiting Unit No. 2.
4. Select CEA Unit No. 2 to Transmit--Enables CEA Unit No. 2 to transmit while inhibiting Unit No. 2.
5. Rotate Canisters and Extend Masts--Command will only execute if preceded by a command to set discretely enabling canister drive motors.
6. Retract Masts and Rotate Canisters--Command will only execute if preceded by a command to set discrete enabling canister drive motors.

7. Release Canister Restraints--Command will only execute if preceded by a command to set discretes enabling latch release solenoids.

8. Latch Canister Restraints--Command will only execute if preceded by a command to set discretes enabling latch solenoids.

9. Start Manual Mode--Slew to position sequence.

10. Start Manual Mode--Constant array rate.

11. Start Automatic Mode--Track sun.

12. Start Automatic Mode--Trail position.

13. Transfer Data Command--The software should maintain a transmit buffer containing status fields from both units (1 and 2) of the CEA. The buffer need be updated no more than once a second.

Initialization--Upon turn on of the CEA, the software should perform self-test routines verifying internal CEA operation. These tests would include (1) the CPU internal registers, (2) ROM check sums, (3) RAM tests, (4) digital and discrete input operation, and (5) power supply voltage levels (see Figure 2.19-1). Upon test completion of all CEA functions, internal registers could be initialized, the discrete and digital data checked against tables in data base, interrupts enabled and an idle loop entered.

Operation--Subsequent to initialization the software, as shown by the timing diagram in Figure 2.19-2, should:

- A. Poll all variables
- B. Enter variables in buffer
- C. Schedule work in activity queue
- D. Perform work in activity queue
- E. Return to idle loop

The receipt of commands and their implementation would follow the flows of Figure 2.19-3, i.e., upon receipt of Command No. 7, wing box restraints would be released and the event displayed upon the MCDS CRT. This would be followed by Command No. 5 and also verified by the crew.

Upon receipt of Commands 9, 10, 11 or 12, the gimbal drive sequence would be entered which provides outputs to the gimbal servo amplifiers. The process would be governed by the computation of the equations defined in Task 2.13, Solar Array Control Avionics Requirements/Criteria Definitions.

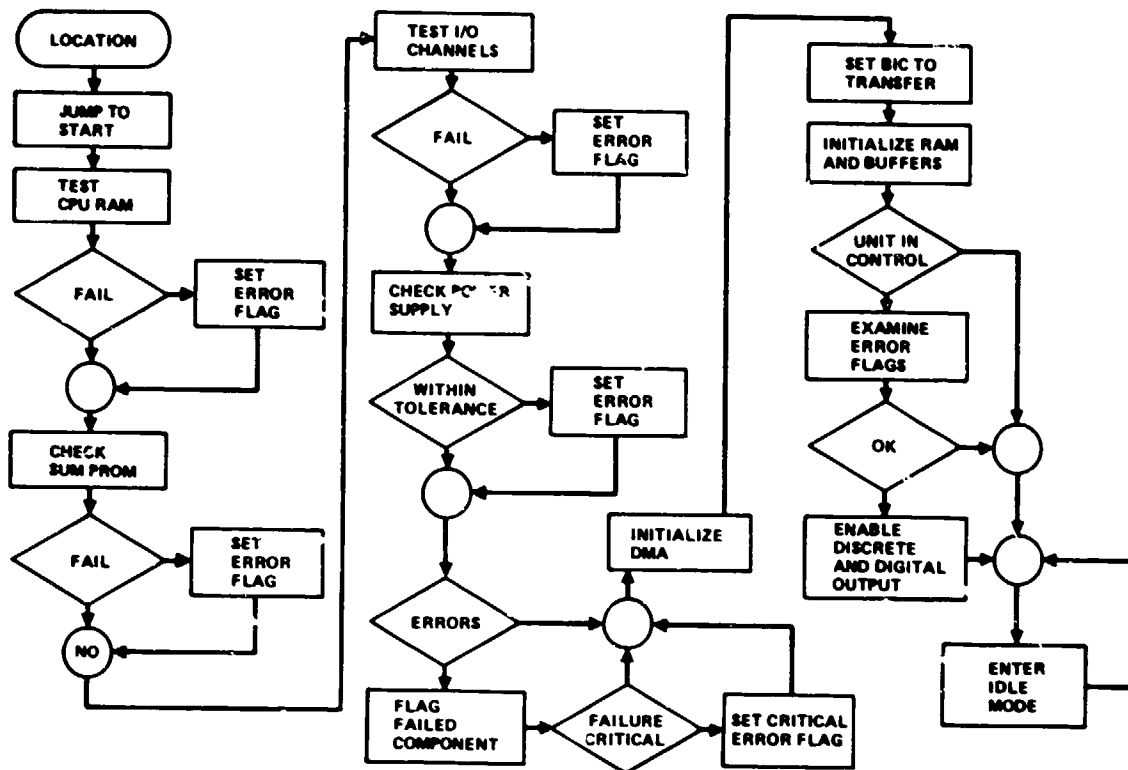


Figure 2.19-1. Initialization

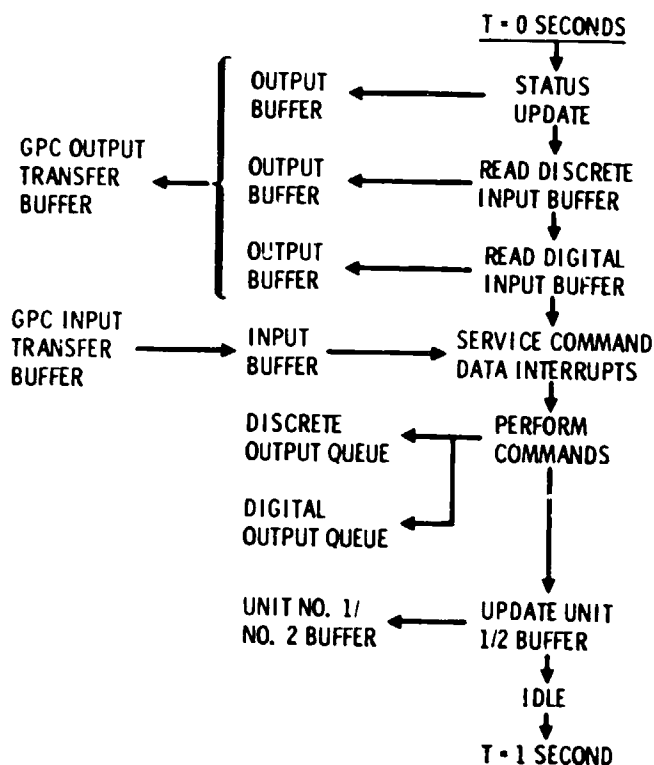


Figure 2.19-2. Timing

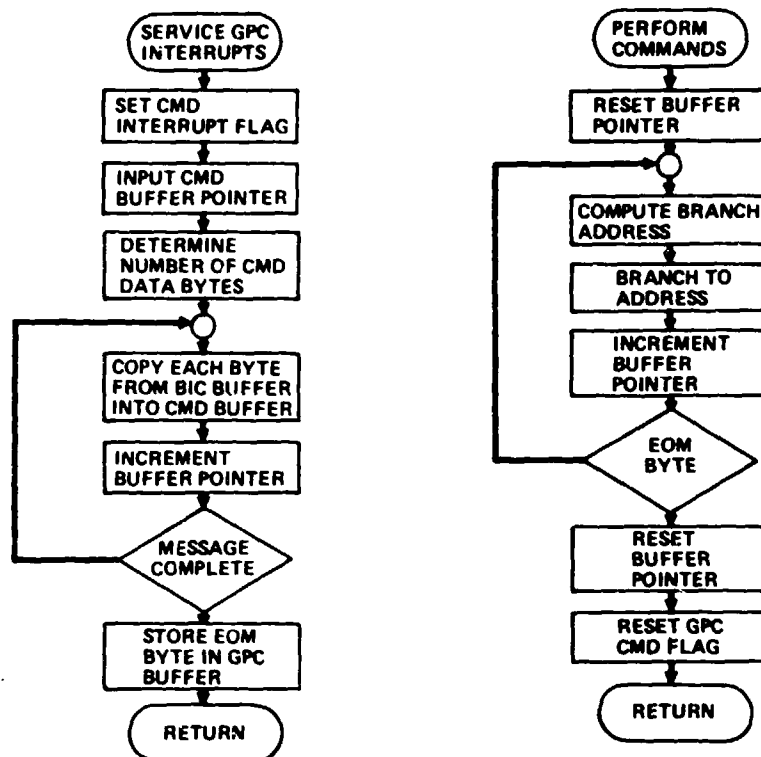


Figure 2.19-3. Operations Flows

## 2.20 EMC ANALYSIS

### Objective

To determine the radiated electric field intensity external to the Orbiter due to Orbiter transmitters and antennas.

### Conclusions

High field intensities impinging on PEP will be produced by the Ku band communications ( $\approx 149$  V/M) and the S-band high power (100W) quad antenna systems ( $\approx 9$  V/M). Since PEP does not operate at these frequencies shielding and filtering of circuits should be highly effective. It is recommended that R.F. signals and signal thresholds be as large as permissible (consistent with available transistorized logic elements) and that care be exercised in grounding/shielding PEP assemblies.

### Assumptions

- Antenna locations are as shown in Figure 2.20-1.
- Transmit power levels, transmit losses and transmit antenna gains as specified in Space Shuttle Communications and Tracking RF Link Circuit Margin Summary, EH2-M/79-039, dated April 1979.

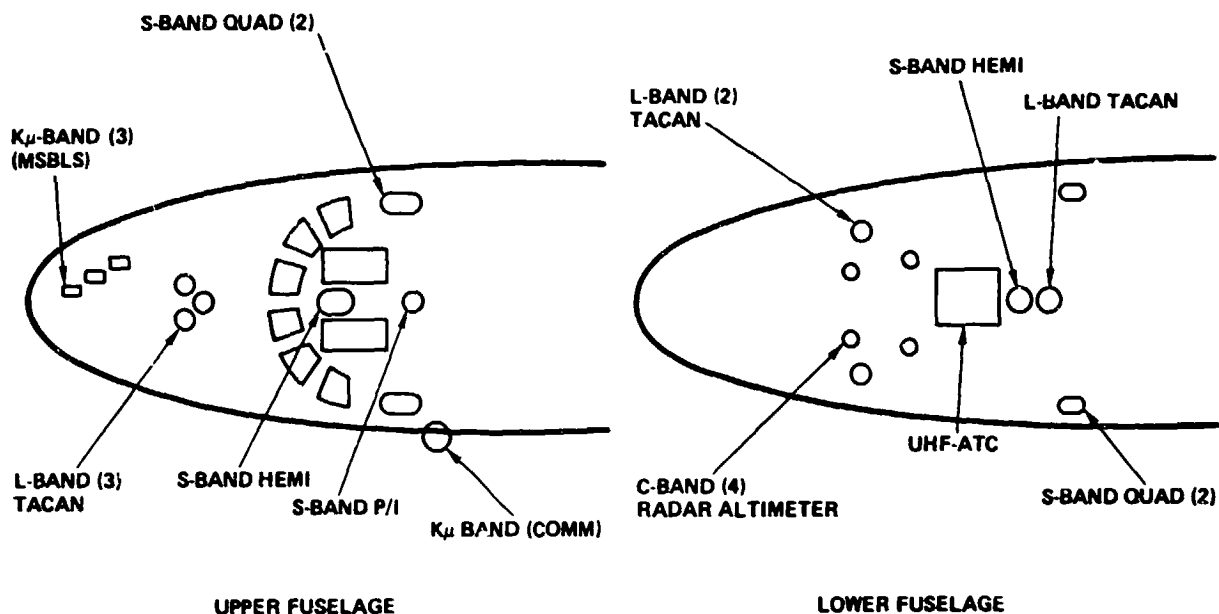


Figure 2.20-1. Antenna Element Locations on Vehicle

#### Approach

The initial step was to determine the distance at which a beam would be well formed. This occurs at a distance of:

$$1/4 D^2/\lambda$$

Where:

D is the diameter of the illuminator

$\lambda$  is the wavelength of the radiation

For the Ku band antenna a distance of 12.5M results.

Two methods of calculating the electric field strength were then considered.

Method 1—The Ku band transmitter power to the antenna was found to be 13 dB (20W) or transmitter power output of 17 dB—4 dB attributable to circuit losses. The power would radiate through an area defined by the distance to the object and the approximate antenna beamwidth.

Given a 1.6 degree beamwidth for the Ku band antenna a distance between the antenna and PEP of 14.6M, the diameter of the beam would be  $14.6 \times 1.6/57.3 = 0.41$  meters and its area would be 0.13 square meters. Since the beamwidth is specified as the radiation half power points, the power density ( $P_D$ ) was taken as total radiated power/2 X 1/0.13 = 76 W/m<sup>2</sup>. The electric field intensity was

then found to be 169 volts/meter using the equation  $= (P_D \times 377)^{1/2}$  where 377 is the free space impedance.

Since antenna gain is defined as the ratio of the power intensity of the subject antenna to the power intensity of an omnidirectional antenna with the same power input, it can also be looked upon as the ratio of the area of a sphere of radius R to the radiation area of the subject antenna's beam at radius R; i.e.,

$$\text{GAIN} = \frac{P_1}{P_2} = \frac{\frac{P_0}{A_1}}{\frac{P_0}{A_2}} = \frac{A_2}{A_1}$$

where

$P_1$  = subject antenna power intensity

$P_2$  = Reference antenna power intensity

$A_1$  = Area covered by subject antenna's radiation

$A_2$  = Area covered by reference antenna's radiation

Then multiplying the gain by the power input to the antenna and dividing by the area of the reference antenna yields the power density at the range of interest or

$$P_D = P_a / A_1 = P_a A_2 / A_1 A_2 = P_a G / A_2 = P_a G / 4\pi R^2$$

where

$P_D$  = Reference antenna power density

$P_a$  = Power to reference antenna terminals

G = Gain

R = Distance

But  $P_a G$  is simply the reference antenna isotropic radiated power (EIRP) and the electric field intensity can now be found as before; i.e.,

$$= (P_D \times 377)^{1/2} = (EIRP \times 377 / 4)^{1/2} \times 1/R$$

For an EIRP of 52 dB from the referenced document and a range of 14.6M the electric field intensity is found to be 149 volts/meter which is within 12% of the figure obtained by Method 1. Due to its simplicity Method 2 was selected

to calculate the field intensities for all Orbiter antennas in use when PEP is deployed.

### Results

The field strengths calculated as a function of distance between the Shuttle antennas and PEP are shown in Table 2.20-1.

Table 2.20-1. Electric Field Intensities Produced by Orbiter Antennas

Antenna	Transmitter power (W)	Spherical coverage (%)	Field strength (V/M)
Ku band (comm)	50	1.6	2181/R
Ku band (radar)	TBD	TBD	TBD
S band quad	100	72	42/R
S band quad	2	41	6.9/R
S band hemi	10	40-50	8.8/R
S band P/I	5	TBD	5.29/R
UHF (EVA)	0.25	85	0.27/R

For distances closer than 12.5M for Ku band and at S band and lower frequencies the validity of these values are questionable since the beams will not be well formed. However, they should be a worst case.

Figure 2.20-2, PEP Clearances - Deployed, can be used in conjunction with Figure 2.20-2, to estimate electric field intensities impinging upon PEP equipment. The 14.6M separation used in the "Approach" calculations was obtained from Figure 2.20-2a. A distance of 4.8 meters, obtained from Figures 2.20-2a and -c may be used to calculate a value 8.75 V/M from the S-band Quad on the lower fuselage.

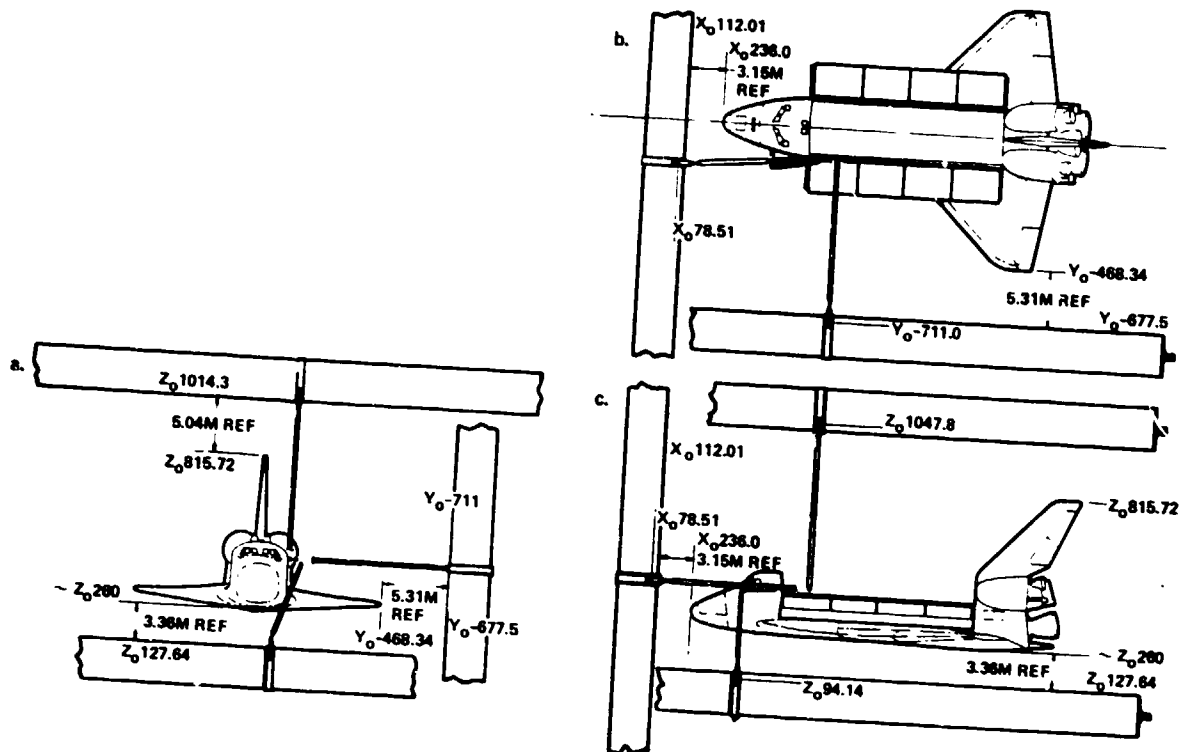


Figure 2.20-2. PEP Clearances — Deployed

## 2.21 ALTERNATE SOLUTIONS FOR PEP/RMS SIGNAL AND DRIVE POWER WIRING

### Objective

To determine the best method for transferring power, control signals and data between the array deployment assembly and equipment in the payload bay and/or aft flight deck.

### Conclusions and Recommendations

On the basis of qualitative and quantitative trades, it is concluded that the baseline, augmented by a switch box allowing both PEP and payloads access to SPEE wiring, is the superior method for power, signal and data transfer.

### Assumptions

Payloads may wish to use the SPEE wiring.

### Approach

Two solutions to the wiring problem were considered. Option 1 consists of the baseline, shown in Figure 2.21-1, modified to place a switch box in the jump er cable between J9575 where the SPEE wiring enters the on-orbit station and the added connector through which it leaves. Option 2 is to install a new

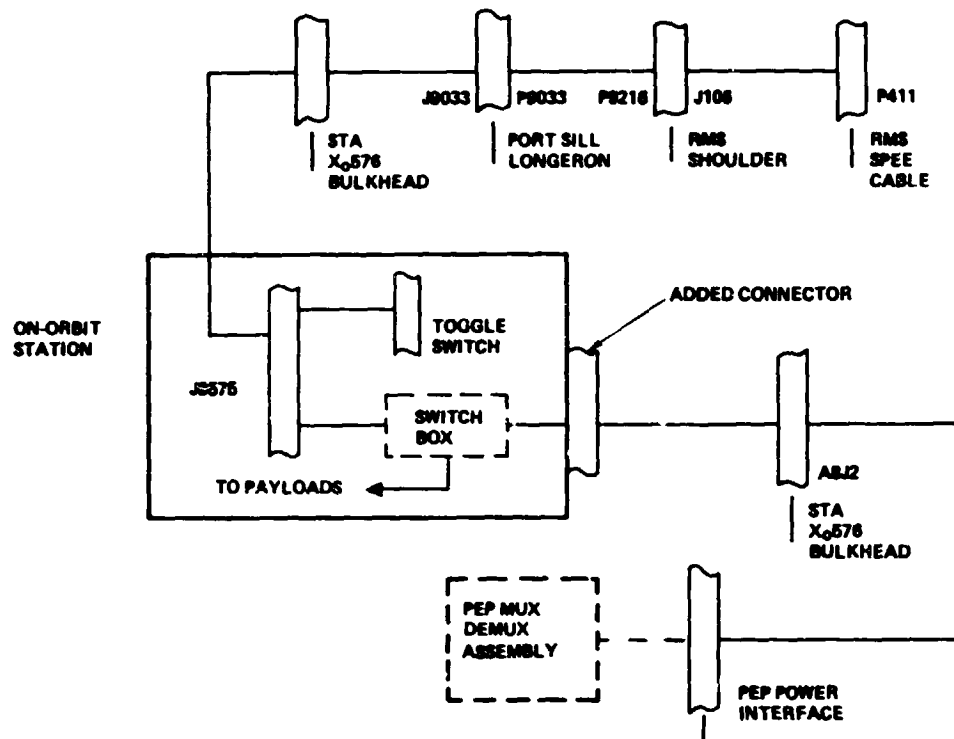


**Figure 2.21-1. RMS Wiring/PEP Interface**

cable to the RMS providing the requisite functions to the array deployment assembly, from the payload bay, reversing the position of the power connector actuator to the SPEE rather than the grapple fixture side, and providing a new switching capability in the on-orbit station for PEP component power on/off.

### Results

The options were first considered on a qualitative basis as shown in Table 2.21-1. The major arguments against Option 1 stem from the constraints which arise from using an existing design rather than any large impact resulting from joint PEP/payload use of the SPEE wiring. The major argument for Option 2 is that it removes these constraints. Overshadowing its positive aspects is the requirement to modify the RMS. Since the modification appears to be extensive, it does not appear to be an attractive solution.

In order to provide a more conclusive determination, the modifications for the options were listed. The results, shown in Table 2.21-2, indicate that the addition of a switch box on the AFD requires fewer modifications. Whether the component should be chargeable to PEP or, indeed, whether the assumption that payloads will require access to the SPEE wiring is correct is beyond the scope of this trade.

Table 2.21-1. Options for PEP/RMS Signal and Drive Power Wiring Trade

Option	Pro	Con
1	<ul style="list-style-type: none"> <li>● Makes maximum use of existing hardware.</li> <li>● Reconfiguration of payload bay wiring has precedent in the form of the payload station distribution panel.</li> <li>● Switch box may be charged to payload integration.</li> </ul>	<ul style="list-style-type: none"> <li>● Existing SPEE wiring does not provide complete redundancy.</li> <li>● Restricts available power to 224W for 24 VDC at shoulder.</li> <li>● Requires switch box in AFD to allow payload and PEP use.</li> </ul>
2	<ul style="list-style-type: none"> <li>● Removes constraints on power level and deployment assembly implementation.</li> <li>● Isolates PEP system from payload changes.</li> </ul>	<ul style="list-style-type: none"> <li>● Requires additional RMS modification.</li> <li>● Adds restraining torque to RMS movement.</li> <li>● Actuator location on SPEE could interfere with payloads.</li> </ul>

Table 2.21-2. Option Modification Listing

Modifications - Option 1

- Replace 21 wire cable approximately 10 feet long with two five-foot cables.
- Add switch box containing 21 segment motor-driven switch.
- Add switch to switch panel.
- Add five-foot, two-wire cable between switch box and switch.
- Add two-wire cable between switch and 28 VDC.

Modifications - Option 2

- Modify RMS end effector to accept power connector actuator.
- Add approximately 30 pins to power connectors.
- Add 60-foot, 30-wire cable between end effector and shoulder disconnect.
- Add connector to shoulder bracket.
- Add 20-foot, 30-wire cable between shoulder bracket and MDA on power control and regulator assembly.
- Add 20-foot, four-wire cable between power distribution box and A8J2 on bulkhead Xo 576.
- Add 10-foot, four-wire cable between A8J2 and switch panel on aft on-orbit station.
- Add two switches to standard switch panel.
- Delete (neg cost) 19-wire, 10-foot cable between J9575 and A8J2 on AFD.
- Delete (neg cost) 19-wire, 20-foot cable between A8J2 and power regulation and control assy.

## 2.22 COLLISION HAZARD ELIMINATION

### Objective

Identify potential PEP collision hazards and assess potential solutions.

### Conclusions

It is concluded that PEP operations safety can be assured with minimum additions to PEP hardware and without significant changes to currently defined Orbiter operations. Crew involvement and development of detailed procedures in advance are key elements of the approach outlined below.

### Approach

In all aspects, the PEP system intends to comply with the fail-safe design philosophies adopted by the Shuttle program at its inception. Where collision avoidance is concerned, fail-safe operation is achieved by a combination of design features and operational procedures. In this regard, capabilities of the astronaut/operator are depended upon to monitor and control automated functions and use of existing Orbiter/RMS equipment emphasized. Complex collision avoidance software has not only been found to be unnecessary, but, in PEP, it is undesirable as a means of avoiding such accidents.

Table 2.22-1 lists PEP operations leading to potential collision hazards in chronological order. It is important to note that five of the seven cases involve the normal RMS operations of moving an object from point to point. In these cases, it is intended that all protocol evolved for this subsystem can be applied in the operation of PEP. Hence, standardized procedures will be utilized to enhance safety whenever applicable.

The close proximity of the ADA to the PRCA and the Spacelab Module when stowed (short tunnel installation) represents a collision hazard peculiar to PEP (Figure 2.22-1). While penetration of the Spacelab pressure shell is a hazard, the external fiberglass insulation represents a form of armor against collision. This is particularly true of its forward pressure bulkhead, where considerable distance exists between the insulation and pressure wall. This protection, combined with careful rounding of all external ADA corners and use of low-RMS tip rates should eliminate the hazard. If a thorough analysis of this type of collision reveals that penetration is still possible, the Spacelab can be sealed off during the PEP removal/replacement operations, thus removing this hazard from the catastrophic category.

Table 2.22-1. PEP Operations Involving Possible Collision Hazards

	Function	Failure	Catastrophic hazard
1/6	Removing/replacing PEP from/in Orbiter payload bay	RMS or RMS operator	Puncture of Spacelab or PEP cold plates
2/7	Moving PEP to operating position/Orbiter payload bay	RMS or RMS operator	Damage to Orbiter structure and/or insulation
3	Establishing correct operating position	RMS or RMS operator	Damage to Orbiter insulation
4	Inadvertent RMS movement system operator	Orbiter control system RMS control insulation failure	Damage to Orbiter structure and/or insulation
5	Changing array (Orbiter maneuvers)	RMS or RMS operator Orbiter control system	Damage to Orbiter structure and/or insulation

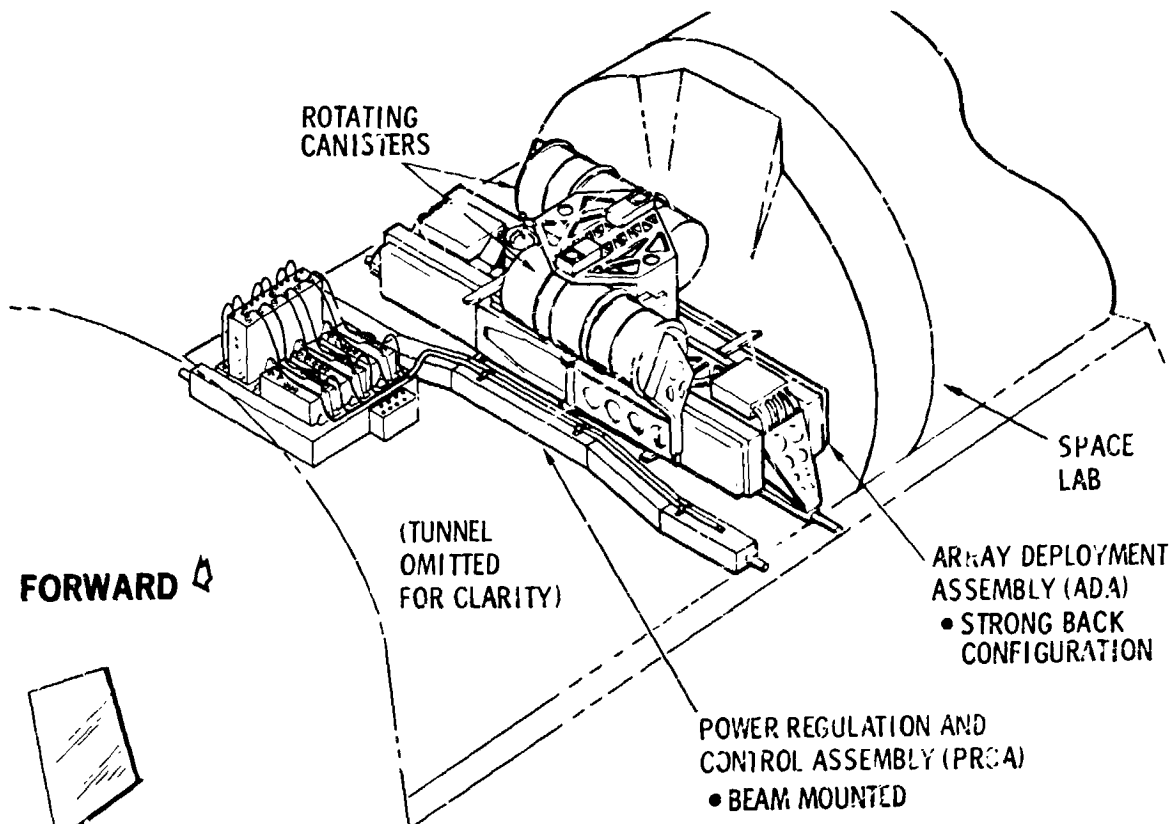


Figure 2.22-1. PEP Installed with Spacelab (Short Tunnel)

Collision with PRCA is not an electrical problem since the solar array is retracted and the Orbiter buses are not electrically connected to the PRCA during this period. However, the voltage regulators are mounted on standard Orbiter cold plates and each of these is connected to both Orbiter thermal systems. Thus, complete penetration of a cold plate can be a catastrophic hazard. In PEP, this hazard is eliminated by design. Cold plates and their fluid lines are protected on all sides from collision penetrations.

Procedural approaches to hazard reduction can also be used in the removal and replacement operations. Use of two operators as visual monitors would eliminate reliance upon human depth perception. A monitor employing direct vision in the most critical portion of Removal/Replacement essentially sees the Z-Y plane (Orbiter coordinates) but one viewing a video display of the RMS elbow or wrist camera would see the X-Y plane. Thus, a two-monitor system would be better able to avoid collision during Removal/Replacement. Use of the RMS automation capabilities will also reduce the probability of operator error. This will be practical in both Removal/Replacement and moving PEP to and from its operating position (2 / 7 in Table 2.22-1) since relatively few end positions are involved. For example, the ADA will generally occupy the same location within the Orbiter for all missions with a Spacelab Module. Similarly, the operating position of the RMS can be the same for all missions using a Y-POP Orbiter orientation (as in earth observation and solar observations in Spacelab 2). Programming of these multiple use RMS actions can be thoroughly verified prior to use. Hence, the only manual operation of the RMS in PEP will involve the actual grappling of the ADA during removal and final placement into the retention latches upon return. This should amount to no more than a few inches of correction to the end point of the automated trajectory.

In regular operations, it is planned to move the ADA from its stowed position to its operating position prior to deploying the array wings and to retract them before returning. This allows simple compliance with a groundrule that operators have visual reference to all portions of an RMS payload at all times. Again, this RMS trajectory will be automated and two operator/monitors employed with the two independent sources of visual information (video and direct).

As described above, the basic PEP/RMS operations (moving the ADA positions) are, as a minimum, fail-safe/fail safe from a collision standpoint. An independent monitor system applied to an automated RMS is safe under any combination of two operator/RMS failures and many RMS failures require multiple electrical point failures. Possible catastrophic hazards resulting from a collision within the Orbiter bay during Removal/Replacement have been eliminated by design features that limit damage due to impacts.

Safety in event of gimbal or array pointing system failure is a basic feature of PEP system design. Fundamentally, the solar array is stabilized with respect to the sun. Thus, if the Orbiter is stabilized to its local vertical (as in earth-viewing operations), the array rotates with respect to its carrier. This orbital rate gimbal ( $\alpha$ ) gimbal axis is typically positioned perpendicular to the orbital plane. On PEP, the second ( $\beta$ ) axis is perpendicular to the axis, parallel to the array's long dimension, and on the array side of the rotating ( $\alpha$ ) interface.

In practice, the RMS is always located so that the array rotation path about the alpha axis clears the Orbiter (Figure 2.22-1). In this geometry, the array cannot collide with the Orbiter with any combination of gimbal or gimbal control (pointing) system failures. Thus, the gimbal/pointing system is inherently fail-safe.

But safe operation is obviously dependent upon establishing this initial RMS position accurately. As previously described, this position will be reached by programming the RMS and its position can be verified by reading all RMS joint angles. This is not, however, a positive check because a joint encoder (position feedback) failure could conceivably result in verifying an erroneous position. To guard against this failure, the PEP system utilizes a completely independent means of verifying the safety of this initial position. On the RMS, the wrist camera is initially used to sight a grapple (docking) target immediately adjacent to the PEP gimbal system. Two 10-inch mirrors, canted 45 degrees to the camera's LOS, lie on each side of the small PEP target. These are oriented so that an operator sees, as background to the grapple target, a split video image with an optic axis along each array wing and parallel to the axis. After verifying the final RMS position by all indicated joint angles,

and prior to deploying the array wings, the operator rotates the ADA through 180 degrees RMS wrist roll. Since the wrist roll axis is fixed parallel to the gimbal axis, the two operators/monitors can view, by wrist camera video display, the total path swept out by the array during operations. Thus, a completely independent safety check of the operating position is accomplished.

This discussion indicates why dependence upon collision-avoidance software in PEP operations is undesirable. Such software must, in turn, depend upon the accuracy of each RMS joint angle feedback encoder. If this instrument provides erroneous information, collision avoidance software can approve a collision path. While it could be useful in extensive manual operations where each movement cannot be preplanned (as in retrieval of a free-flying object), it has little value when the RMS is primarily used in a preprogrammed mode. Here the only failures that could cause collision are either in the software or in the joint encoders (assuming one joint at a time programming where failure of any one joint to reach its goal interrupts the program). Here, software can be thoroughly checked on ground simulators and a joint encoder error cannot be detected by collision software. Thus, it is believed that programmed RMS motion, combined with dual operator/monitors following procedures that allow them to visually detect (by completely independent means) impending collisions due to any failure source, represents the safest mode of operation.

After the final operating position of the RMS has been verified, it is locked into its idle mode. In this mode, power is removed from joint servo amps and the brakes are applied to each RMS joint. RMS brakes are a "dead man" design (i.e., power off is brake on) and multiple electrical point failures are required to disengage (power on) the brake or to power a servo which, under some conditions, could over-power the brake.

The brake could also be overcome by external forces which may be caused by a failure in the Orbiter's attitude control system. To guard against any failure which inadvertently causes RMS motion during PEP operations, output of each joint shaft encoder are connected to the RMS audible warning system. In this regard, it is noted that (in some PEP operating positions) the angular clearance between the deployed array is small (on the order of five degrees). However, in an attitude-hold mode, the amplitude of typical limit cycles is generally small (usually less than one degree) and the period long (an analysis

of many different mission simulations yields an average limit cycle period of 2.5 minutes . But even in a case of complete RMS brake failure, joint angular motion should be less than limit cycle amplitude and it would also be oscillatory. While differences in friction may, in this situation, produce a drift of the joints center position, the time available before action is required to avoid collision will typically be several limit cycle periods even in the most critical array positions. While RMS failure during an Orbiter attitude maneuver may need more rapid corrective action, operational procedure will require the crew to place the array in a noncritical position (generally requires only RMS wrist rotation) prior to undertaking a maneuver. Additionally, the PEP/RMS will be continuously monitored during an attitude change.

As mentioned, operational procedures may require relocation of the array prior to a maneuver. This is done to remove the array from close proximity to the Orbiter, but to also remove it from direct plume impingement regions (particularly those of the primary RCS thrusters). If PRCS is to be used, plume avoidance additionally involves inhibiting all forward thrusters, and for this reason the PEP array will be retracted if PRCS translational maneuvers are required. Also, PEP and the RMS will be stowed in the payload bay during any firing of the OMS engines. For these reasons, array repositioning accompanying an Orbiter maneuver may be a two-step process: it will first be moved to a noncritical region and then (post maneuver) moved to its new operating position.

Current RMS operating rules prohibit PRCS firings when a loaded arm is being moved. In general, this does not impact PEP operations since most maneuvers are very low rates (Spacelab 2, which uses frequent pitch maneuvers, is limited to 0.25 deg/sec) through large amplitudes. Hence, time can be available during a coast period to allow arm movement to its new operating position. In some cases, notably Spacelab 2, which primarily maneuvers about a POP axis, changing the array position can be accomplished with the PEP gimbal system.

In changing the PEP array position in response to Orbiter maneuvers, procedures are generally identical to those previously discussed. Point-to-point movement of the RMS will be controlled by validated software and visually monitored by two operators using independent means (direct or video). RMS paths will be chosen to maximize their visibility and if constant visual reference

(array to Orbiter) by both operators cannot be maintained, the array will be retracted prior to movement. Similarly, if the motion involves a new RMS position that cannot be accurately checked by other visual means (in addition to joint position feedback display), the 180 degree wrist rotation visual sweep will be accomplished. In this regard, it will not be necessary to retract the array prior to this safety check because wrist camera field of view will be sufficient to allow collision avoidance if the array path is obstructed.

To summarize, the MDAC approach to collision hazard elimination involves maximum use of existing Orbiter/RMS equipments combined with crew capability to avoid expensive automated avoidance systems. It features:

- A. Strict adherence to RMS operations protocol.
- B. Use of existing RMS automation to reduce probability of operator error.
- C. Redundant crew monitoring by independent means of all critical RMS/PEP operations.
- D. A positive means of verifying safety of the PEP array/operating position independent of (and redundant to) RMS instrumentation.
- E. Use of existing RMS audible alarm to indicate any inadvertent movement of the RMS from the verified PEP operating position.
- F. An array gimbal pointing system that fundamentally fail safe, i.e., no combination of electromechanical failures (other than primary structure), can cause a collision.

## 2.23 EVA OPERATIONS

### Objective

Assess the need for EVA to support PEP operations and any EVA restrictions due to an installed PEP.

### Conclusions

No new routine EVA tasks are required in support of PEP; however, EVA may be utilized to correct PEP failures which would result in a safety hazard. The PEP installation does not violate EVA guidelines nor place any undue restriction on existing EVA keepout areas.

Two aspects of EVA were considered in the design of the PEP. First, design criteria were considered which were necessary to enable an EVA crewman to perform PEP manual tasks such as latching/unlatching deployment/retraction,

maintenance, and visual cueing for the RMS operator. These tasks can be considered for either planned or unscheduled classes of EVA. Contingency EVA includes tasks required to effect safe return of crew such as jettison assist.

The second aspect of EVA design criteria considered relates to designing the PEP to be compatible with EVA tasks which might be carried out for both PEP and other Orbiter systems or payloads. This criteria precludes damage to PEP by EVA crews and also ensures unimpaired crew performance and safety during EVA. Types of EVA compatibility criteria includes avoidance of exposed edges, corners and protrusions, inclusion of handholds and translation devices and design to withstand crew kickoff loads. A key document for EVA design considerations is, "Shuttle EVA Description and Design Criteria, JSC-10615."

The PEP design must also consider the EVA reserved areas which ensure a corridor for the EVA crewman to access critical areas in the cargo bay. These stay-out areas are given in "Space Shuttle System Payload Accommodation," JSC-07700, Volume IV. Installation of the PEP in the payload bay must not prevent crew translation in the reserved envelopes.

Table 2.23-1 presents a summary of the EVA tasks and design considerations for the three classes of EVA. Also noted are the items where a design criteria has been included in the PEP design. As can be seen from the table, EVA design provisions have been included for all EVA tasks and considerations except planned EVA on the PEP. No normal planned PEP EVA tasks are planned due to the ease with which automatic provisions could be provided and because the relatively long EVA time, about 12 hours of EVA-related time, would be required for each mission for manual deployment/retrieval of the PEP. Due to the relatively large number of planned missions (80), the accumulated crew EVA time would be large, thereby meriting an automated approach.

Design criteria are incorporated to allow unscheduled and contingency PEP operations by EVA. Also included are design criteria for non-PEP tasks. Criteria is included for EVA compatibility for all EVA classes.

EVA envelope considerations were addressed by comparing PEP stowed volumes with EVA-reserved envelopes. The results are shown in Figure 2.23-1 in the form of two view overlays. No EVA reserve envelope intrusion occurs for airlock inside and MMU requirements. The PRCA cross beam intrudes into the EVA

Table 2.23-1. EVA Design Considerations for PEP

EVA class	PEP task	EVA task/consideration	Incorporation of EVA design criteria
Planned	X	Latch/unlatch	None
	X	Deploy/retract	None
	X	Maintenance	None
		EVA compatibility	Yes
		EVA envelope intrusion	
Unscheduled	X	Latch/unlatch	Yes
	X	Deploy/retract	Yes
	X	Visual cue	Yes
	X	Maintenance/repair	Yes (limited)
		EVA compatibility	Yes
Contingency		EVA envelope intrusion	
	X	Jettison assist	Yes
		EVA compatibility	Yes
		EVA envelope intrusion	Yes

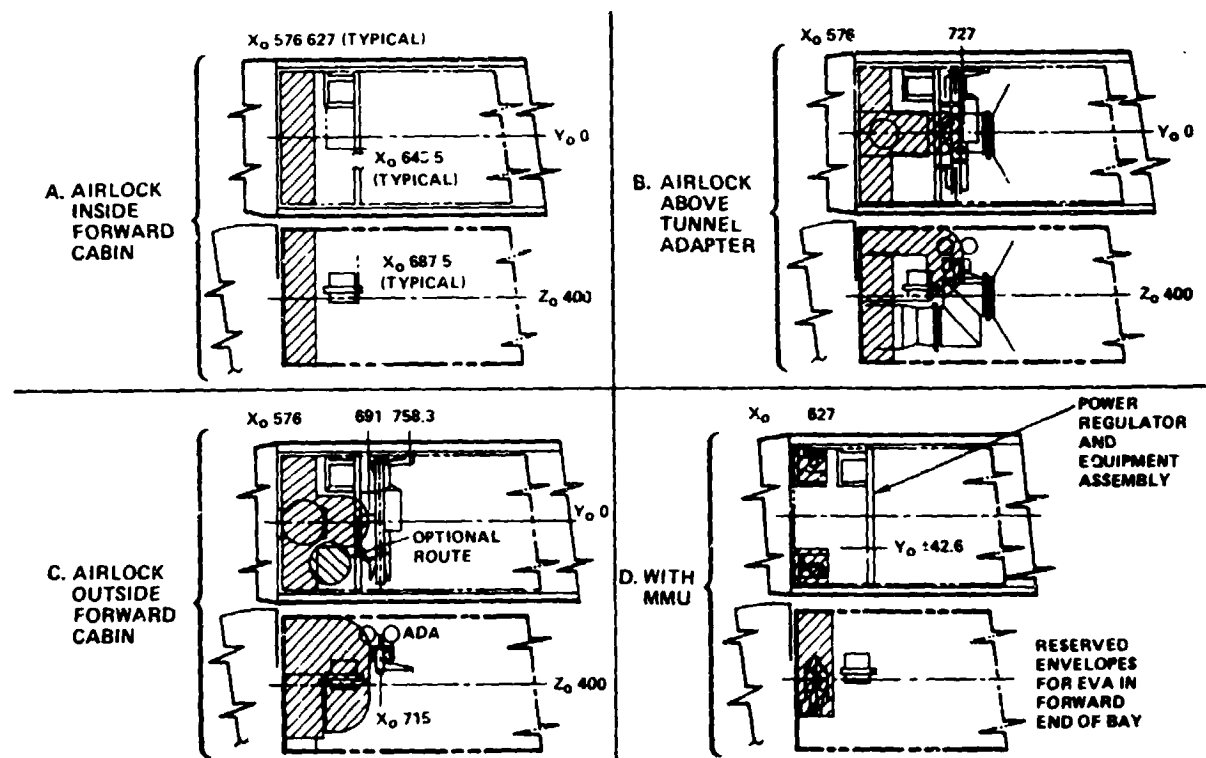


Figure 2.23-1. PEP Stowed Volumes and EVA Reserved Envelopes

envelope for the airlock above tunnel adapter, Figure 2.23-1. This is a slight intrusion and in a somewhat hidden area which should not affect crew EVA along the top of the tunnel. The ADA does obstruct the path across the tunnel when not deployed. Two options are possible to obviate this requirement. The first option is to deploy the ADA from the bay to allow crew translation to the Spacelab. The second option is to provide a translation route and aids over the top of the ADA. Either of these options appears feasible since this route is required only for bay doors open conditions wherein the Spacelab scientific airlock deploys or may deploy experiments outside the dynamic envelope, or deploys other experiments requiring EVA.

Airlock outside requirements, Figure 2.23-1C, results in the PRCA cross-beam intruding into the EVA envelope. A route 44 inches wide (112 cm) exists between the cross-beam and the airlock. This is four inches (10.1 cm) less than the 48-inch (122 cm) reserved envelope, but it is larger than the 40-inch (102 cm) hatch openings. A 40-inch (102 cm) minimum corridor for straight line translation is given in JSC-10615. Therefore, it appears feasible for the EVA crew to translate between the PRCA cross-beam and the airlock.

A second option for airlock outside configuration is to shift the EVA route in the -Y coordinate direction so the EVA crewmen pass the side of the airlock and between the sill area. This is a slightly more devious route, but the full 48 inches (122 cm) would be available for crew translation.

The ADA intrusion into the EVA reserved volume is slight and this intrusion is overridden by the PRCA considerations.

Conclusions to the study to compare PEP stowed volume intrusions into EVA envelopes are two-fold, (1) EVA envelopes are restricted by PEP equipment but general EVA guidelines are not violated, and (2) alternate routes are available for configurations where serious intrusions exist.

Appendix A

SPAR-R.940

ISSUE A

POWER EXTENSION PACKAGE

POWER BUS DESIGN

Prepared for:

McDonnell Douglas Astronautics Company  
Huntington Beach  
California

PRECEDING PAGE BLANK NOT FILLED

SPAR aerospace products ltd.  
825 Caledonia Rd.  
Toronto, Ontario. M6B 3X8  
Canada.

**SPAR**

TABLE OF CONTENTS

<u>Section</u>	<u>Title</u>	<u>Page</u>
1.0	INTRODUCTION	1-1
2.0	REQUIREMENTS	2-1
3.0	STATEMENT OF COMPLIANCE OR DEVIATIONS	3-1
4.0	PROPOSED CABLE HARNESS DESIGN CONFIGURATIONS	4-1
4.1	General Arrangement SRMS/PEP Power Bus	4-1
4.2	Shoulder Yaw Joint Cable Harness	4-1
4.3	Shoulder Pitch Joint Cable Harness	4-1
4.4	Elbow Joint Cable Harness	4-2
4.5	Wrist Pitch Joint Cable Harness	4-2
4.6	Wrist Yaw Joint Cable Harness	4-3
4.7	Wrist Roll Joint Cable Harness	4-3
4.8	End Effector Cable Harness	4-5
4.9	Arm Booms, Cable Harness	4-5
4.10	Electronic Compartment Cable Harnesses	4-6
4.11	SRMS/Orbiter Interface	4-6
4.12	SRMS/PEP Interface	4-7
4.12.1	Design Considerations	4-7
4.12.2	Design Description Connector Half Assembly (Driven)	4-7
4.12.3	Design Description Connector Half Assembly (Fixed)	4-8
5.0	THERMAL DESIGN CONSIDERATIONS	5-1
5.1	Thermal Analysis	5-1
5.2	Thermal Design	5-1
5.2.1	Summary	5-1
5.2.2	Design Considerations	5-2
5.2.3	Configuration	5-2
5.2.4	Design Cases	5-2
5.3	Conclusions	5-14

TABLE OF CONTENTS - (CONT'D)Page

6.0	ELECTRICAL DESIGN CONSIDERATION (INC. EMC)	6-1
	6.1 PEP Gimbal Power	6-1
	6.2 PEP Solar Array Power Transmission	6-3
	6.3 EMC Considerations	6-6
7.0	MATERIALS AND PROCESSES	7-1
	7.1 General Materials	7-1
	7.2 Power Cable Materials	7-1
8.0	STRUCTURAL DYNAMICS	8-1
	8.1 Dynamic Envelope	8-1
	8.2 Cable Attachment	8-1
	8.3 Structural Loads	8-1
	8.4 Stress Considerations	8-2
9.0	MASS PROPERTIES	9-1
	9.1 PEP Power Bus on SRMS	9-1
	9.2 SRMS/PEP Interface Connector Assembly (Driver.)	9-1
	9.3 Grapple Fixture and "Spec" Connections	9-1
	9.4 Orbiter/SRMS Interface Connectors	9-1
10.0	DEVELOPMENT AND TEST PROGRAM	10-1
11.0	DESIGN PROPOSAL LAYOUTS	11-1

LIST OF FIGURES

<u>Figure</u>	<u>Title</u>	<u>Page</u>
5.1-1	CABLE ARRANGEMENTS	5-3
5.2-1	TYPICAL MISSION PROFILE - COLD ORBIT	5-4
5.2-2	TYPICAL MISSION PROFILE - COLD ORBIT	5-5
5.2-3	STEADY STATE TEMPERATURES CONFIGURATION 1	5-8
5.2-4	STEADY STATE TEMPERATURES CONFIGURATION 2	5-9
5.2-5	STEADY STATE TEMPERATURES CONFIGURATION 3	5-10
5.2-6	TRANSIENT RESPONSE OF CONFIGURATION 1	5-11
5.2-7	TRANSIENT RESPONSE OF CONFIGURATION 2	5-12
5.2-8	TRANSIENT RESPONSE OF CONFIGURATION 3	5-13
6.1-1	PEP GIMBAL POWER DETAILS	6-2
6.2-1	PEP POWER TRANSMISSION DETAILS	6-5

## 1.0

INTRODUCTION

This report contains details of the proposed cable handling system designed to transmit power from the Power Extension Package (PEP) to the Orbiter by way of the Shuttle Remote Manipulator System (SRMS). The design has been based upon earlier design concept studies outlined in SPAR-R.928 (Power Extension Package Power Bus Study). Some changes to the basic design concept were found necessary during the design process, and are illustrated in the following report.

## 2.0 REQUIREMENTS

The following requirements were given by McDonnell Douglas.

- (a) PEP power bus will be six pairs of #6 Superflex cable.
- (b) RMS with power bus attached will be capable of performing other "Manipulator" tasks when not employed in conjunction with the PEP.
- (c) Reduction of RMS capability due to attachment of the power bus will be minimized.
- (d) RMS with attached power bus must be compatible with all configurations of Spacelab modules and pallets. Other intrusions into the payload volume may be considered.
- (e) A Spar Standard End Effector will be used to attach the PEP to the RMS and the Special Purpose End Effector wiring will be utilized to transmit PEP signals and gimbal power.
- (f) The RMS power bus will terminate at the voltage regulators mounted on the PEP equipment beam. This is at (approximately) Orbiter stations:  
  
X = 665  
Y = + 70  
Z = +420
- (g) An emergency SRMS/Orbiter disconnect will be provided.
- (h) Design will consider (a) means of crossing RMS/PEP interface (b) ways to cross all RMS joints (c) cable retention at RMS/Orbiter interface.

In addition, the following assumptions have been made.

- (i) The time between the deployment and retrieval of the PEP will be of the order of a few orbits. Each orbit is assumed to take approximately 90 minutes.

Consideration has been given to the case where the PEP is required to be active for a time considerably greater than that above.

- (j) The remote manipulator when deployed will have the power "off" and brakes "on". The temperature control system will normally be "off". This is to eliminate any power drain. The temperature measurement which requires the D&C panel to be switched on will be carried out at predetermined intervals of time.

The temperature control system will be switched to automatic under the following conditions (determined by operational profiles):

- i) Low arm temperature could produce damage
- ii) Prior to activation of the arm
- (k) The power bus design is such that minimum modifications to the present Remote Manipulator System baseline design are required.
- (l) The intention of the design of the power bus is to minimize its mass thereby ensuring that the induced loads on the arms are also minimized. The effect of the increased inertia of the arm due to the additional cable harness has been considered.

- (m) The power loss along the power bus must be minimized to maximize the power available to the orbiter from the PEP.
- (n) The operation of the remote manipulator wrist roll joint is to be considered as a back-up for a failure of the PEP array gimbals.

### 3.0 STATEMENT OF COMPLIANCE OR DEVIATIONS

3.1 Reference 2.0 (a). Complies to requirements. See also Section 7.2

3.2 Reference 2.0 (b) and (c). Reductions to SRMS capability due to attachment of PEP power bus is as follows:

3.2.1 Wrist Roll - restricted to  $\pm 180^\circ$  rotational travel, possibility of full  $\pm 447^\circ$  provided manual disconnect at wrist electrical comp/wrist roll joint is acceptable (requires EVA).

Layouts indicate that the major restriction preventing further rotational travel of the wrist roll joint is the location of the connector box situated on the upper surface of the electronics housing. However, future development models may prove an increase in the  $\pm 180^\circ$  rotational travel possible

At the present stage, no other joint articulation restrictions are indicated.

3.3 Reference 2.0 (d).

3.3.1 Shoulder joint. Additional envelope required to accommodate PEP Power Bus, reference layout 31221L2.

3.3.2 Wrist pitch/yaw joint - additional envelope required to accommodate PEP Power Bus, reference layout 31221L3. Another design configuration being considered would require additional envelope on the payload side of the wrist pitch joint. This is illustrated on layout 31221L4.

3.3.3 Wrist Roll Joint - stowed condition of arm requires additional envelope. See layout 31221L1. Operational envelope to accommodate  $\pm 180^\circ$  rotation of cable.

3.3.4 All other increased envelope requirements are illustrated on layout 31221L4 and 31221L5.

3.4 Reference 2.0 (e).

See Section 6.1 (PEP Gimble Power).

3.5 Reference 2.0 (f). (For information only).

3.6 Reference 2.0 (g).

The arrangement shown on layout 31221L2 illustrates a three connector interface between the SRMS and the orbiter. This arrangement considered emergency disconnect to be provided in a similar manner to the existing SRMS system (i.e. pyrotechnic guillotine). In future design work, consideration will be given to provide emergency release using in-flight electrically released connects as per very recent discussions with McDonnell Douglas.

3.7 Reference 2.0 (h). Complies. See layouts.

3.8 Reference 2.0 (i). (Used for Analysis).

3.9 Reference 2.0 (j). Complies.

3.10 Reference 2.0 (k). Complies. Reference design layouts 31221L1 through 5.

3.11 Reference 2.0 (l). Complies. Reference Sections 8.0 and 9.0.

3.12 Reference 2.0 (m). Complies. Reference Electrical Analysis. Section 6.2.

3.13 Reference 2.0 (n). Complies. Refer to 4.7.

#### 4.0 PROPOSED CABLE HARNESS DESIGN CONFIGURATIONS

##### 4.1 General Arrangement SRMS/PEP Power Bus

Design layout 31221L4 illustrates the basic proposed cable configuration throughout the total length of the SRMS. This has been used as a basis for all electrical and thermal analysis specified in this proposal.

Wherever practical, the powerbus has been routed on the payload side of the SRMS to provide access during installation and removal. All cable clamps and fittings will be configured to facilitate this requirement. Routing of cables under existing SRMS equipment which would prove inconvenient during installation or removal has been avoided.

##### 4.2 Shoulder Yaw Joint Cable Harness

The shoulder yaw joint cable harness configuration is illustrated on the design proposal layout number 311221L2. Cable handling to accommodate the  $\pm 180^\circ$  rotational travel of the shoulder yaw joint has been based upon the existing methods used for the SRMS shoulder joint cable system. From the orbiter/SRMS interface situated at the connector box forward end, the cables are routed across and clamped to the connector box cover in a flat configuration to a point where they are split into two discrete bundles. Each bundle of six cables is looped in a similar manner to the existing cable harness and is routed approximately parallel to it.

Each bundle is securely clamped at the pitch/yaw interface flange by a split clamp fitting. The split clamp fitting clamps against a bushing into which all the cables have been potted. The insulation on each cable is etched for a length necessary to ensure adequate keying in the potting compound. The six cables are controlled to maintain a bundle configuration by a beta cloth sleeving.

#### 4.3 Shoulder Pitch Joint Cable Harness

From the joint yaw/pitch interface flange, both bundles run parallel to the existing SRMS wiring harness over the pitch joint and are clamped to the connector bracket. The cable bundles are then configured as shown on layout 31221L4. Again, beta cloth sleeving will be used to maintain cable configuration for the pitch joint section of the harness.

#### 4.4 Elbow Joint Cable Harness

The elbow joint cable harness has been based upon the present SRMS Cable Handling design principles, but located on the opposite side of the arm. This will minimize EMC interference with the existing SRMS signal wires. Wherever possible, the wire arrangement will be such to maximize heat dissipation. This cable system is illustrated on design layout 31221L4.

#### 4.5 Wrist Pitch Joint Cable Harness

The wrist pitch joint cable harness general arrangement is illustrated on design layout 31221L3. The cables are arranged along the wrist electronic housing in an open configuration, and are clamped in the area between the wrist pitch joint forward flange and joint rotational axis on the outboard side. (An alternative arrangement to mount the cable harness on the inboard side is in process. This will eliminate tight envelope problems and facilitate installation and removal of power bus with SRMS installed in the orbiter). At the clamp exit, a cable transition converts the arrangements to a double radial layer, six cables wide, to accommodate joint articulation. A fibreglass guide, mounted to the joint, controls the required cable harness configuration ensuring clearance on other equipment during joint rotational travel. At the aft end of the wrist pitch joint, the harness is formed into an "S" arrangement which is maintained by a guide and clamps. This configuration provides sufficient cable length to accommodate full joint rotational

travel. The "stepped" cable arrangement on the upper bend is necessary to provide clearance at maximum wrist yaw.

#### 4.6 Wrist Yaw Joint Cable Harness

The wrist yaw joint cable harness general arrangement is shown on design layout 31221L3. From the wrist pitch joint aft cable clamp, the cables are routed under the arm to the wrist yaw joint, and are clamped forward of the yaw joint rotational axis. The cable harness arrangement is identical to the wrist pitch joint configuration, but terminates at the bushing provided for the wrist roll cable harness system (Reference Section 4.7).

#### 4.7 Wrist Roll Joint Cable Harness

Due to the nature and size of the power bus, it was found necessary to restrict the rotational travel of the wrist roll joint to  $\pm 180^\circ$  (Refer to 3.2.1) (from the stowed position). Any substantial increase in rotational travel requirements would necessitate major redesign of the arm in this area, and would require considerable increase in static and dynamic envelope constraints.

The rotational restriction resulted in many advantages in other aspects of the design. These are as follows:

- i) Minimal cable length reduces inefficiencies and weight.
- ii) Proposed configuration enables power cables to be clear of Electronics Compartment, thereby eliminating potential thermal problems.
- iii) Exposure of Existing Electronic Compartment radiation areas are maintained, again eliminating thermal problems.

- iv) Enables power cables to be separated from existing SRMS cabling, thus reducing electrical EMC problems.
- v) Minimal impact on existing thermal blankets.
- vi) Minimal impact on ICD envelope restrictions in critical areas (i.e. radiator, bay door and payload area). Note - envelope increase is required as shown on layout.
- vii) Enables previously proven and accepted cable handling systems concept to be employed (i.e., the proposed wrist roll cable system configuration is basically identical to that of the present SRMS shoulder yaw joint. This system has been subjected to both thermal vacuum and vibration testing, and has been accepted at the Critical Design Audits and Reviews (CDR and CDA's) attended by JSC, NRCC, Rockwell and Spar personnel).

The general configuration of the wrist roll cable harness is illustrated on layout no. 31221L1. The harness comprises a looped cable captured in two locations. At these locations, the insulation of each cable is etched and potted in a strain relief bush which in turn is clamped to fittings attached to the joint flanges. The cables are allowed relative freedom of movement during joint rotation, but are controlled from total freedom by a helical spring housing. Direct contact between the cables and spring housing is prevented by a loose beta cloth sleeve.

A similar sleeve covers the helical spring to provide a smoother outer surface. Control of the complete harness assembly during vehicle launch and re-entry is provided by a hood assembly attached to the forward cable fitting. During operation, the cable harness assembly rolls into, or "out of" the hood assembly depending upon its position and direction of rotation.

Not illustrated on the design layout is the provision to restrict the joint rotational travel to  $\pm 180^\circ$  when the power bus system is installed.

It is expected that this will be controlled by limit switches which would include back-up; but not to incorporate a mechanical limit stop system.

A variation on the proposed design has been considered which would provide a manual cable disconnect at the aft end of the electronic compartment. This would be used if SRMS operation is required without the PEP System, but would require extravehicular activity (EVA). The full rotational travel of  $+447^\circ$  would be available with this arrangement. Further evaluation of this proposal would be necessary if this becomes a desirable feature.

#### 4.8 End Effector Cable Harness

The End Effector portion of the power bus has been routed on the inboard side and clamped to the end effector as shown on layout 31221L4. From the wrist roll cable system beneath the SRMS, the cables are routed around the wrist roll joint to a position which enables a flat configuration to be utilized. The power bus then terminates at the connector assembly (shown on layout 31221L5). Additional envelope will be required in these areas and is shown on design layouts 31221L4 and 31221L5.

#### 4.9 Arm Boom Cable Harness

Cable routing across the arm booms has been configured in a flat, low profile arrangement wherever possible. This arrangement has been selected to maximize heat dissipation and to maintain a low profile to minimize envelope violations. Cable clamp arrangements are illustrated on layout 31221L4. It has been assumed that cable clamp mounting to the booms will be similar to existing SRMS cable clamp arrangement.

Beta cloth sleeving will be used throughout to protect the cables from external heat. Reference Section 5.0.

#### 4.10 Electronic Compartment Cable Harness

Cables spanning all electronic compartments have been configured to maintain a flat, low profile arrangement wherever possible. The main constraints in these areas are radiation panels running axially across the electronic compartments which if covered, would create considerable thermal upset of the SRMS electronics. For this reason, these areas have been avoided.

Beta cloth sleeving will be used throughout to protect the cables from external heat. Reference Section 5.0.

#### 4.11 Orbiter/SRMS Power Bus Interface

The interface connection from the Orbiter cable system to the power bus attached to the SRMS is illustrated on layout 311221L2. It comprises three individual 4 pin connectors mounted to a bracket which in turn is mounted directly to the forward face of the connector box. The cables will exit the mating connector sockets in a loop configuration to ensure that access to the SRMS wiring connector fuses is maintained (i.e. the loop will provide sufficient flexibility to enable the cables to be displaced sideways, thus providing clear access to the fuses. From the loop configuration, the cables are "fanned" into a flat arrangement across the top of the connector box cover to provide a low profile. This is necessary to ensure that no interference exists between them, and the moving section of the cable harness. The cables are thermally isolated from the connector box cover using fibreglass washers under the cable clamps.

The selection of the three individual connectors was based upon the following considerations:

- i) Availability - selection of a "standard" connector as opposed to a "special" arrangement increases reliability and reduces cost.

- ii) Handleability - considerably less effort required to connect a 4 pin arrangement than a 12 pin. This improves serviceability.
- iii) Smaller wire bundles provide greater flexibility for further cable routing.

Alternative to the above outlined configurations, a two connector arrangement which also provides emergency disconnect within the connector assembly will be considered. This arrangement would eliminate the necessity to upgrade the present pyrotechnic guillotine for emergency.

#### 4.12 SRMS/PEP INTERFACE CONNECTION

##### 4.12.1 Design Considerations

The design selected for the SRMS/PEP interface connection was based upon the following considerations:

- i) To provide automatic power bus connection after full grapple of the P.E.P. system thereby eliminating potential alignment and subsequent damage problems.
- ii) To eliminate "couples" during automatic connection thus preventing potential "jamming" problems.
- iii) To provide an alignment system that does not rely upon a high parallel accuracy, again to prevent "jamming".
- iv) To provide a system that minimizes thermal differential affects.
- v) To use existing or similar hardware to that used on the present SRMS system.

##### 4.12.2 Design Description (Connector Half Assembly - Driven)

The connector design configuration illustrated on design layout No. 31221L5 shows a one piece

aluminum housing machined to accept two inserts. The inserts are machined to suit the configuration of a size 4 connector contact. Each insert contains 6 contacts, suitable for a No. 6 AWG wire.

A master location pin is securely afixed into the housing, and is located on the geometric center of the connector half assembly. The primary function of the locator pin is to provide alignment of the connector halves, but is also used as a slide rail on which the connector is guided during mating. Secondary alignment between connector halves is made by a pin protruding from the outer edge. This pin locates a slot on the mating connector housing, and avoids the high degree of parallel accuracy required if the two straight location pin methods would be used.

Both location pins ensure full alignment before mating of the electrical connector contacts.

The connector half assembly is suspended by the master pin, and is supported by two linear bearing bushes mounted to the frame. The distance between the bearings is sufficient to provide full linear movement during connector mating.

Rotation of the connector about the master pin is prevented by a pin and groove system located on the outer edge of the housing. This was selected to minimize thermal differential effects and prevent potential "jamming".

Actuation (or mating) of the connector assembly is accomplished by a modified version of the lever brace linear actuator mechanism. To prevent any "coupling" effect, the axial load produced by the linear actuator is applied directly to the master pin.

#### 4.12.3 Design Description (Connector Half Assembly - Fixed)

The mating half of the connector is configured to provide a small amount of float in the plane

required for alignment during connector mating. The alignment accuracy between the grapple fixture attached to the PEP package, and the end effector, together with locational accuracies of the connector mounting will determine the alignment capacity necessary within the connector assembly.

For neatness of design, it is expected that the driven connector assembly will be mounted to the PEP system, and the mating half to the SRMS End Effector. This system would eliminate the necessity of additional wiring to the end effector, the connector drive and signals being supplied to the PEP system via the existing "SPEE" connector. The other advantage of this configuration is that necessary increases in SRMS dynamic envelopes will be minimized.

The design will provide a male pin connector on the End Effector, and female on the PEP system. It is assumed that the cable shown at the exit from the driven connector half assembly, and which is attached to the PEP, can be configured as illustrated on layout 31221L5. Note cable length allowance to accommodate the connector linear travel.

## 5.0 THERMAL DESIGN CONSIDERATIONS

### 5.1 Thermal Analysis

Detailed thermal math models of the various cable configurations have been made and analyzed for a number of cases. This section refers to the thermal design and also summarizes some of the analyses performed.

### 5.2 Thermal Design

#### 5.2.1 Summary

##### (a) Summary of Design

The PEP cable bundle shall employ passive thermal control to the greatest extent practicable. A low  $\alpha$ , high  $\epsilon$  finish shall be utilized to reduce the impact of solar energy and allow as cold a cable harness as possible.

If operational constraints and the mission profile are such that passive means cannot be utilized to ensure adequate cable temperatures then the design may be augmented by heaters and thermostats. It is considered unlikely that such devices will need to be employed.

##### (b) Summary of Design Requirements

1. To maintain the PEP cable at as low a temperature as possible during power transfer.
2. To maintain the PEP cable at a temperature to ensure sufficient flexibility of the cable harness during RMS deployment.

### 5.2.2 Design Considerations

The thermal design of the PEP RMS mounted equipment must be such that the cable harness temperature is maintained as low as possible under the worst environmental conditions and maximum power dissipation in the cable harness, in order to reduce the power losses and maintain the cable within its design temperature range. The thermal design must also ensure the cable harness does not become so cold that either the design range of the cables are exceeded or that the cable is so cold that the stiffness of the cable bundle is so high that the bundle flexibility prevents proper operation of the RMS joints.

### 5.2.3 Configuration

The configuration considered consists of the 12 cables #6AWG attached to the RMS via penetrations in the thermal blanket. Thus the cables are supported outside the RMS blankets and are exposed directly to the space environment.

The cables are spread as much as possible into a 12 x 1 arrangement, however, near the shoulder and wrist pitch and yaw joints a 2 x 6 arrangement is required, at the roll joint a 3 x 4 cable bundle is required. See Figure 5.1-1.

### 5.2.4 Design Cases

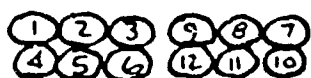
The following mission profile must be accommodated by the thermal design. The critical design driver cases are identified. See Figure 5.2-1 and 5.2-2.

#### (a) Pre Launch

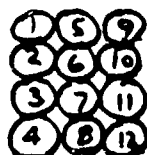
During pre launch the cargo bay is purged by conditioned dry gas and thus presents no problem thermally.



12x1 CABLE ARRANGEMENT (#1)

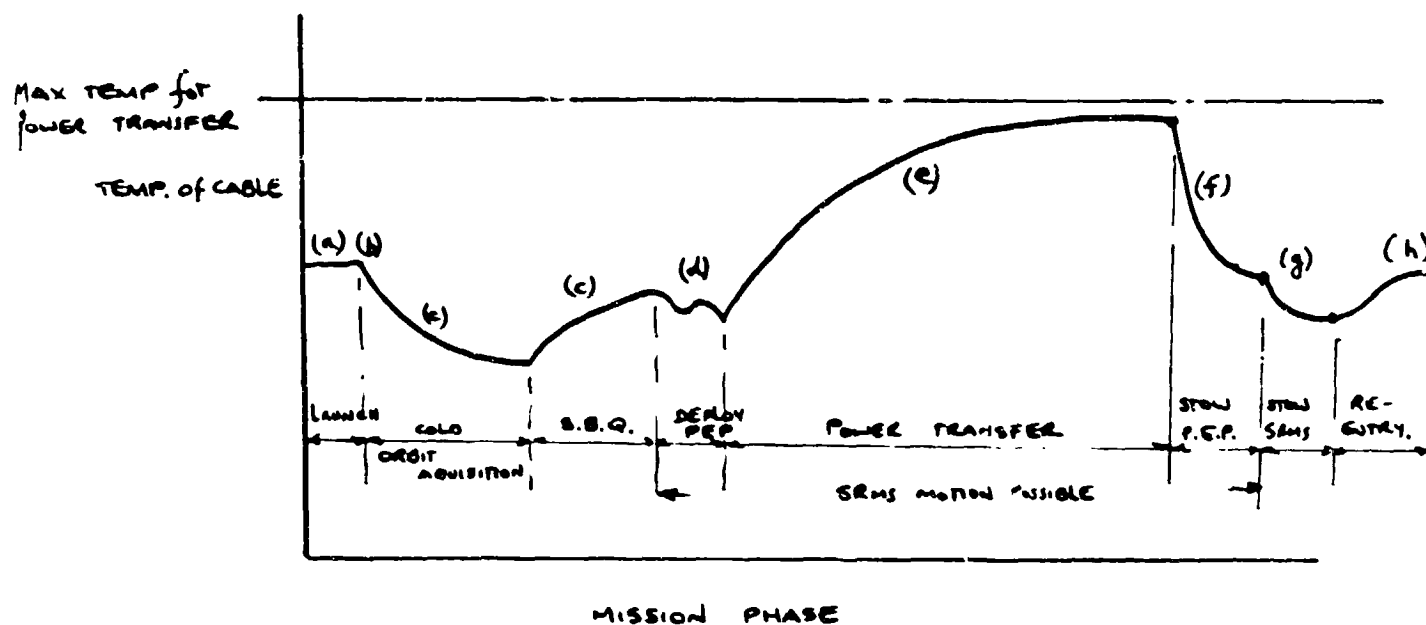


6x2 CABLE ARRANGEMENT (#2)



3x4 CABLE ARRANGEMENT (#3)

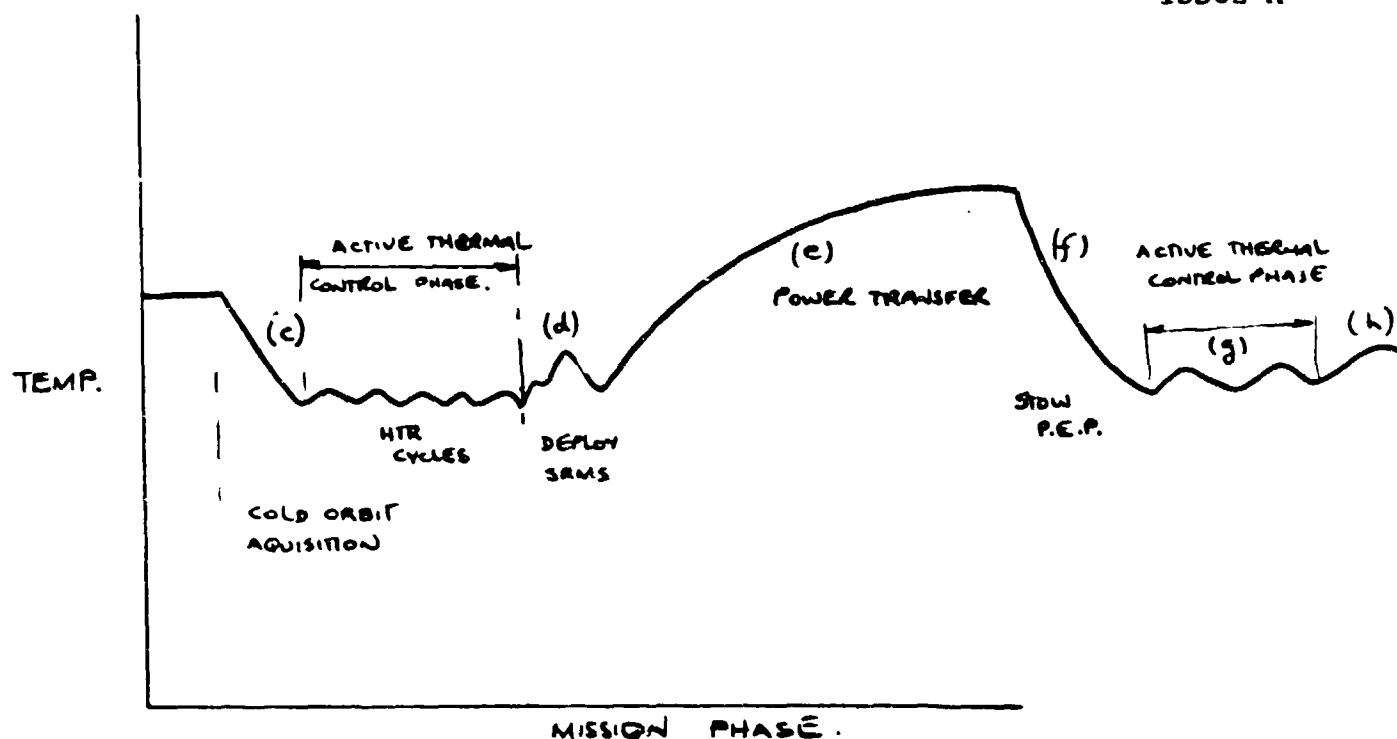
FIG. 5.1 - 1



TYPICAL MISSION PROFILE - COLD ORBIT

FIG 5.2-1.

DEMONSTRATES POSSIBLE USE OF THERMAL CONDITIONING PRIOR TO  
RMS DEPLOYMENT.



TYPICAL MISSION PROFILE ~ COLD ORBIT

FIG 5.2-2.

DEMONSTRATES POSSIBLE USE OF HEATERS TO MAINTAIN THE CABLE TEMPERATURES PRIOR TO AND DURING RMS DEPLOYMENT.

(b) Launch

During launch the cargo bay air expands and its temperature falls as the pressure falls. However, due to the large thermal inertia of the cable harness this is not considered a significant design case.

(c) On Orbit Cargo Bay Open - Stowed

After orbit acquisition, the cargo bay doors are opened and the RMS and PEP cables are exposed to the space environment. The temperature of the PEP cables depends on the orbit and attitude acquired, the view factors to space, to the orbiter and to the payload in the cargo bay.

The thermal design shall be such that by selection of a low  $\alpha$  and high  $\epsilon$  finish on the cable harness, the hot case attitude and orbit (top sun, side earth  $\beta = 90^\circ$ ) shall be accommodated by passive means.

The cold case orbit and attitude (bottom sun tail earth  $\beta = 90^\circ$ ) will result in low temperatures in the cable harness. If such low temperatures would result in an unacceptably stiff cable bundle then heater provisions would be made to prevent such low temperatures, if the thermal inertia of the cable bundle was inadequate. An alternative means of increasing the cable bundle temperature is to thermal condition before RMS deployment by a barbeque mode or move to a hotter attitude.

(d) On Orbit - RMS Deployed

When the RMS is deployed, the cable must be warm enough to flex adequately. If, prior to deployment, the means of achieving suitable temperatures is passive then the inertia of the cable bundle and attitude of the RMS

shall be such that the cable maintains its flexibility until the power transfer phase. This may be achieved by heating of the cable above its minimum temperature prior to deployment and allowing it to cool down during this period. See Figure 5.2.1.

If active thermal control was employed, then heaters would maintain suitable temperatures in the cable bundle. See Figure 5.2.2.

(e) Power Transfer

After the PDP has been activated, the power transfer via the cable harness is 32kW at 120V.

During this phase, the cables will obviously warm up due to their power dissipation, the operating time and thermal inertia of the cables is such that the steady state temperatures of the cables must be designed for.

In order to lower the temperature of the cables as much as possible a high emittance surface finish is proposed to the cable bundles, and to reduce the effect of incident solar finish a low absorbtivity surface is proposed.

Such a space qualified material, which also provides a suitable flexible finish to the cable bundle, is beta cloth.  $\alpha = 0.22$   
 $\epsilon = 0.9$

Initial calculations indicate cable temperatures as shown in Figures 5.2-3 to 5.2-8. Figures 5.2-3 to 5.2-5 show the variation of steady state temperature with cable current. Figures 5.2-6 to 5.2-8 show the transient response of the cables to both switch on and cool down conditions. From these curves, the temperature response to power profile can be estimated.

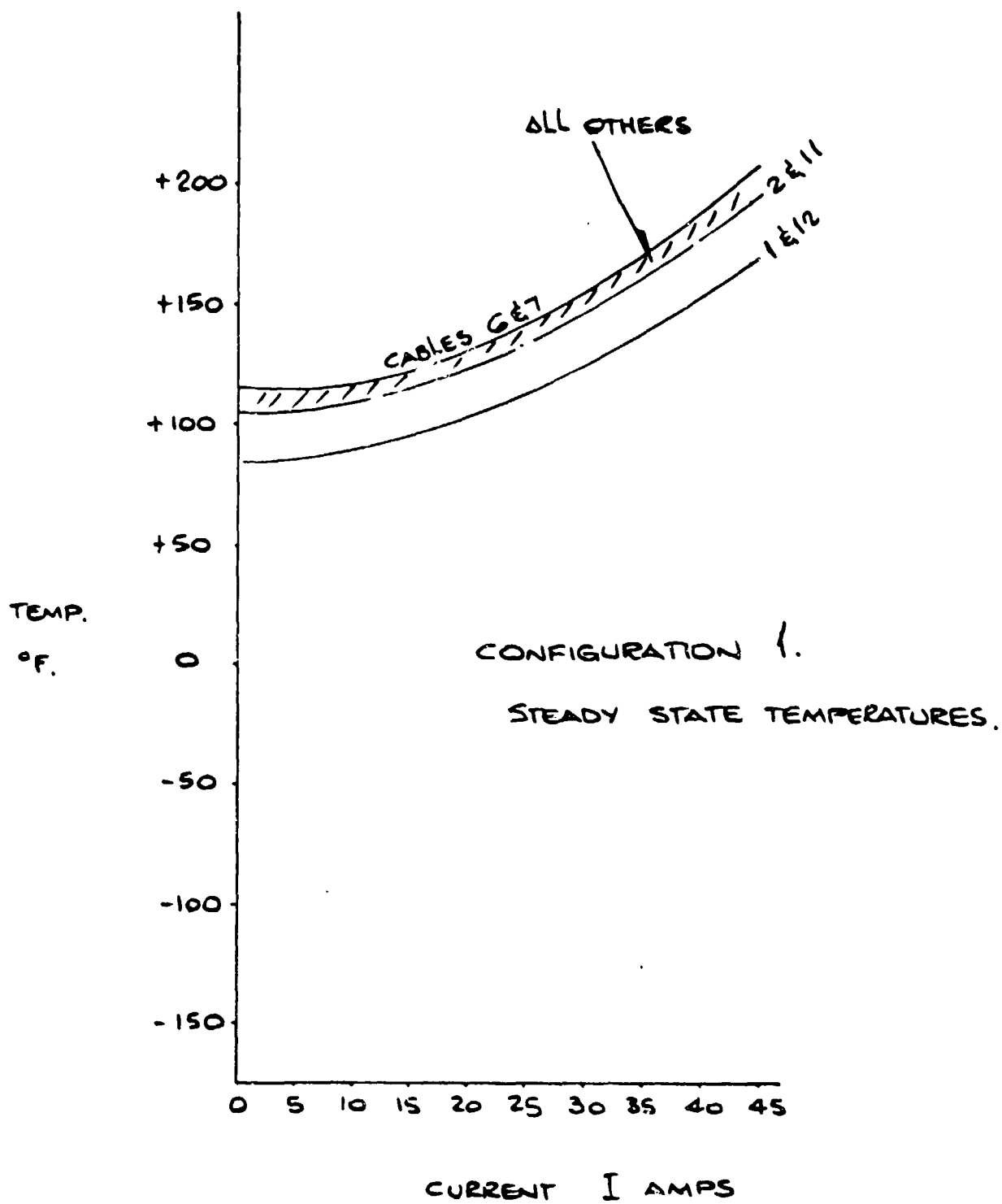


FIG. 5.2-3

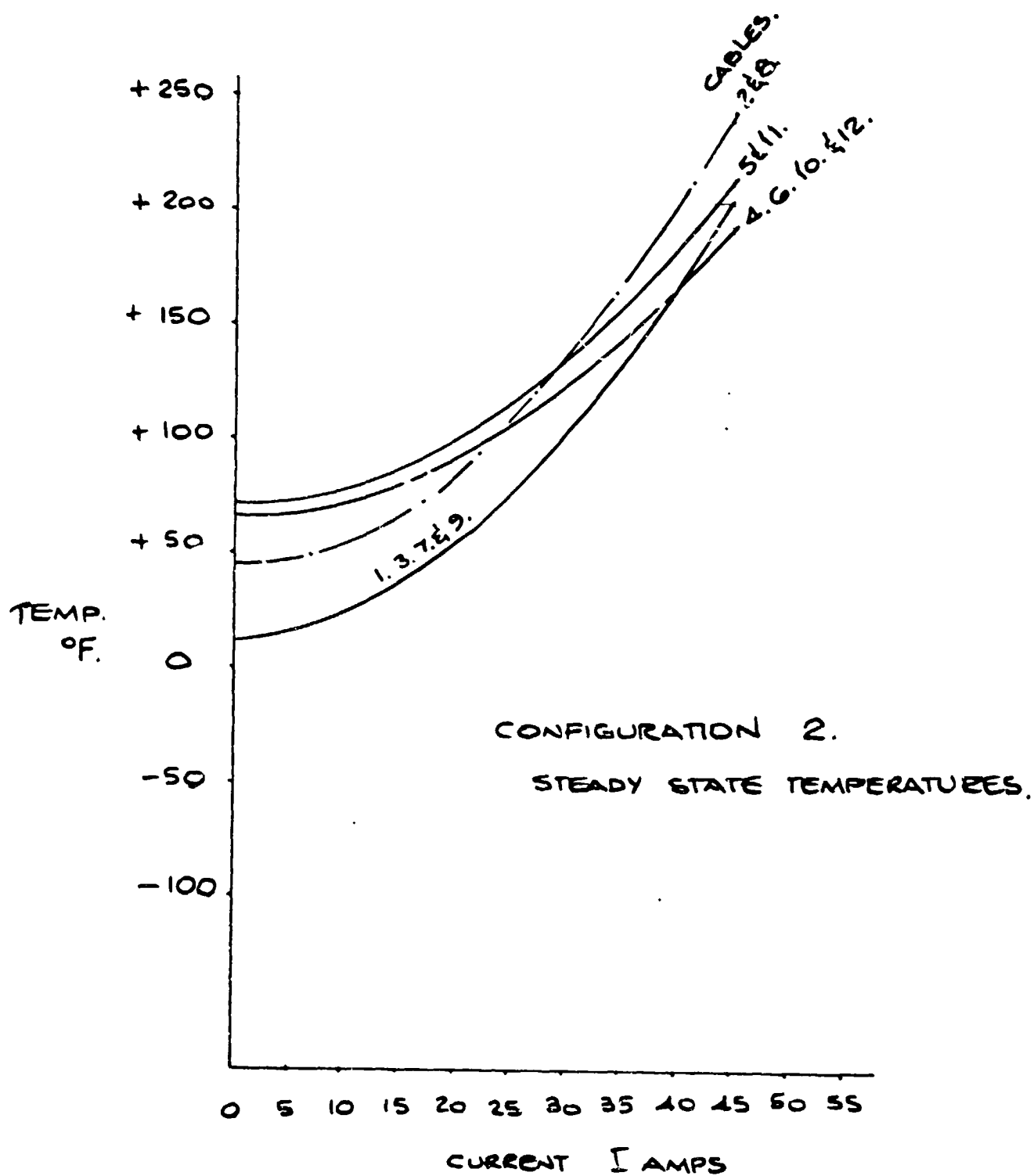


FIG. 5.2-4

CONFIGURATION 3.  
STEADY STATE TEMPERATURES

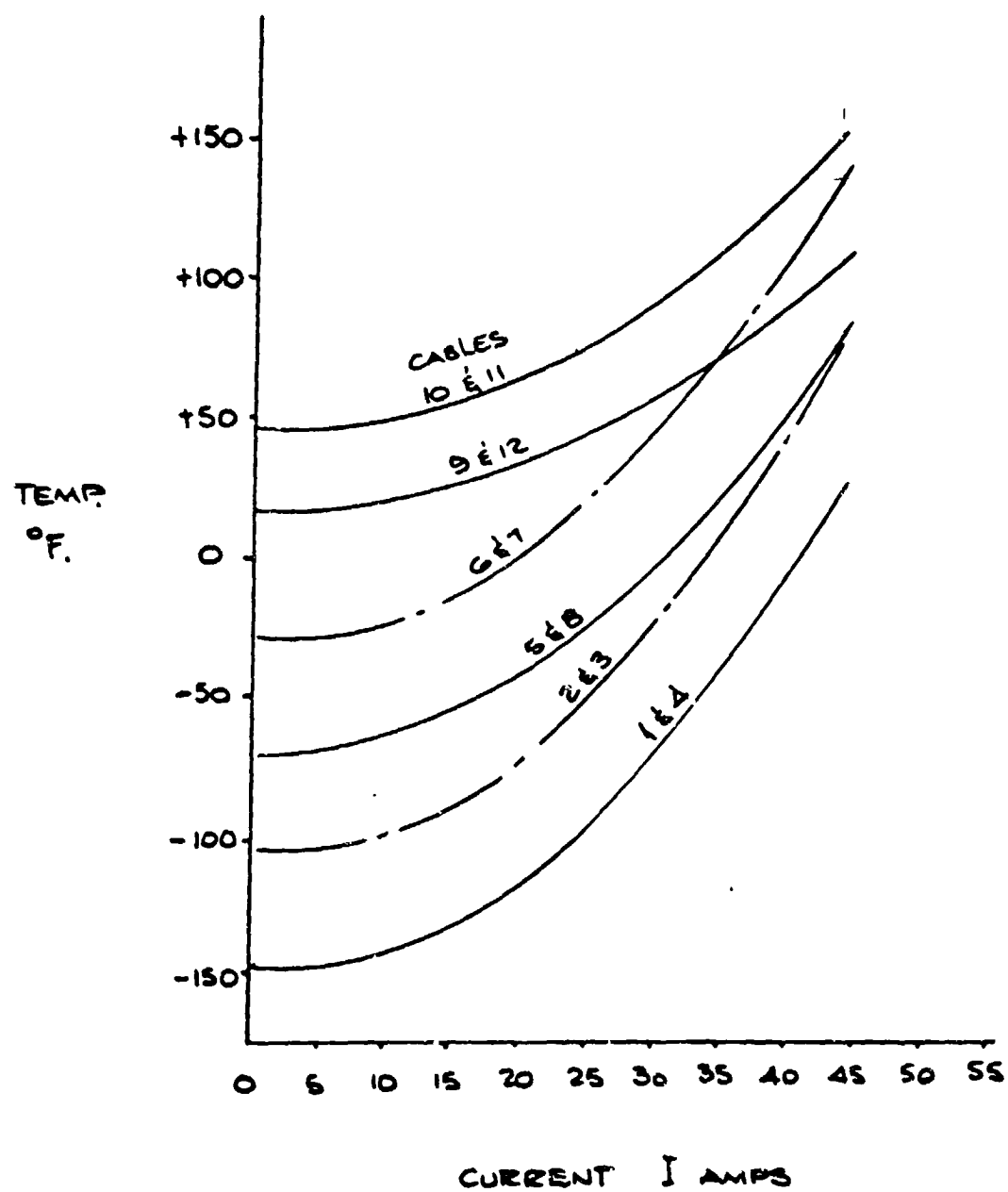


FIG 5.2 - 5

SPAR

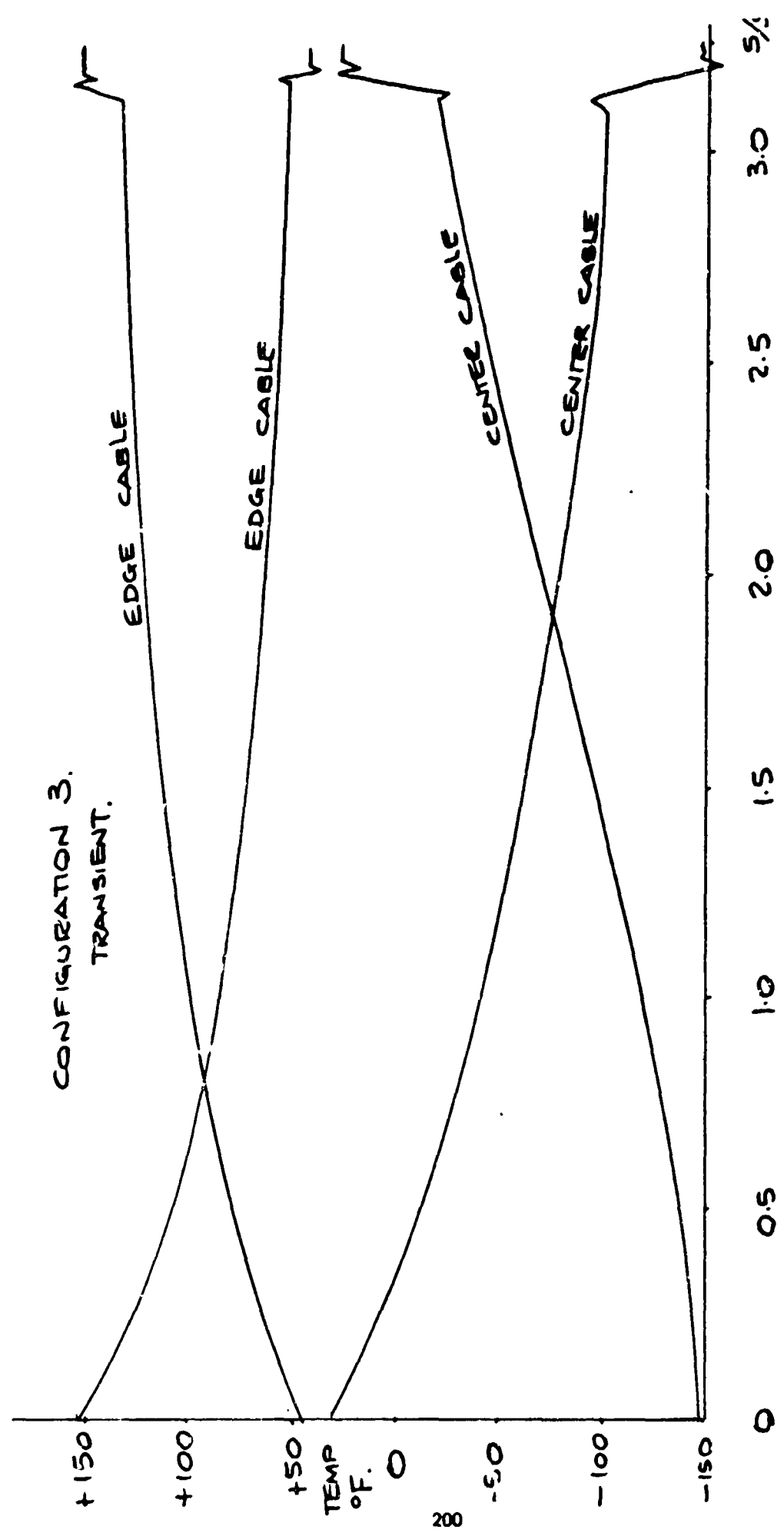


FIG. 5.2-8

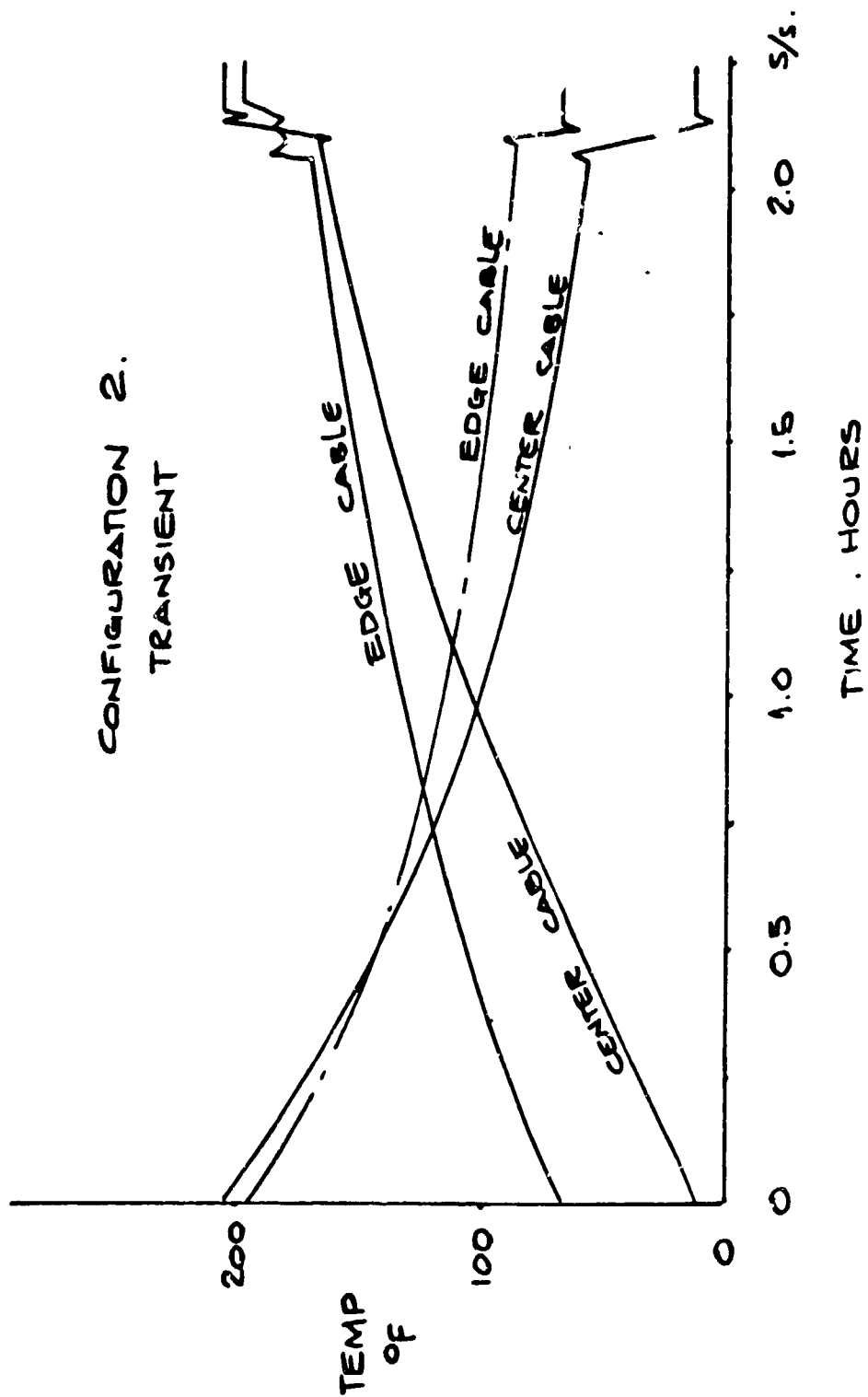


FIG. 5.2-7

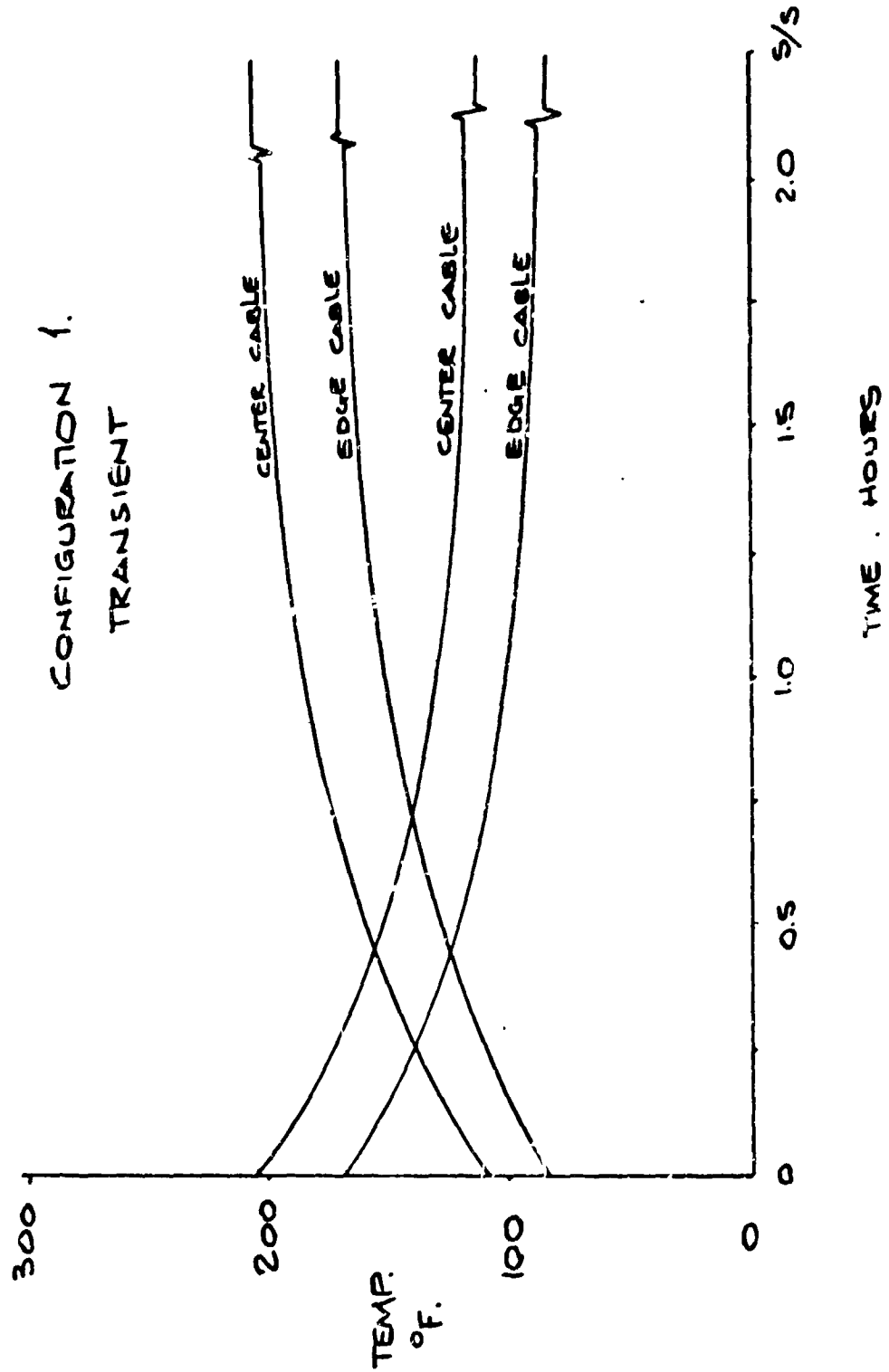


FIG. 5.2-6

From these figures, it can be seen that the effect of cable bundling significantly increases the inner cable temperatures and is therefore avoided as much as possible in the cable harness design.

(f) Stowage of RMS and PEP

During this phase the PEP cable harness transfers no power and merely cools down as the RMS is deployed to stow the PEP and the RMS itself is stowed. This is not considered a design critical phase.

(g) Stowed RMS as Phase (c).

(h) Re-Entry

During re-entry, the PEP cables will be exposed to a hot or cold cargo bay, however, the inertia of the cables should prevent excessive temperature excursions during this transient period and therefore this phase is not anticipated to be design critical.

5.3 Conclusion

It has been shown that the temperatures of enclosed cables under full sun conditions potentially can be high. In detailed design considerations, this will need to be carefully considered so as to ensure these conditions will be accommodated.

It has also been shown that the temperature gradients through the single cable bundle are rather high. This is partly due to the simplification in the analysis, i.e. no account of the stainless steel spring at the roll joint was included.

A more detailed analysis will be made at a later date.

## 6.0 ELECTRICAL DESIGN CONSIDERATIONS

The electrical details with respect to the PEP Gimbal Power, used for the Attitude and Orientation, will be discussed below in Section 6.1.

The main electrical factors of the actual Solar Array Power Transmission of the PEP, along the SRMS, will then be explained in Section 6.2, while a brief discussion relating to a possible slip ring concept is given in Section 6.3.

### 6.1 PEP Gimbal Power

The solar array assembly, carried by the SRMS, requires electrical power for the deployment and orientation.

The wiring available between the receptacle J101 of the SRMS, which is connected to the main 28Vd.c. orbiter power, and the receptacle J411 at the End Effector will be used. From Figure 6-1 we note that there are seven No. 22 A.W.G. leads in parallel along the SRMS, while the End Effector carries two No. 20 A.W.G. in parallel.

Since the seven leads are fused with 5A each, the total available current to the PEP Gimbal Power cannot exceed  $5 \times 7 = 35A$ . The orbiter voltage at J101 will be 28+4V. The lead resistance, forward and return, of the complete wiring, as shown in Figure 6-1, at the highest predicted temperature of 70°C, will then be:

$$\begin{aligned} \#22 \text{ A.W.G.: } & \frac{1}{7} 0.01614 [1 + 0.00397 (70-20)] \\ & = 0.00276 \text{ ohms/foot} \end{aligned}$$

$$\begin{aligned} \#20 \text{ A.W.G.: } & \frac{1}{2} 0.01015 [1 + 0.00397 (70-20)] \\ & = 0.00608 \text{ ohms/foot} \end{aligned}$$

The total resistance at 70°C for 62.5 feet within the SRMS, and 2 feet within the End Effector will be:

$$0.00276 (62.5+62.5) + 0.00608 (2+2) = 0.369 \text{ ohms}$$

The continuous maximum available current is  $2 \times 5.63 = 11.3\text{A}$  limited by the two #20 gauge wires in parallel.

Therefore we have:

$$24 - 11.3 \times 0.369 = 19.8\text{V minimum}$$

$$28 - 11.3 \times 0.369 = 23.8\text{V nominal}$$

$$32 - 11.3 \times 0.369 = 27.8\text{V maximum}$$

Any electrical equipment then, related to the Gimbal Power and its Attitude and Orientation must be designed to operate within the above stated voltage limits. Furthermore, the "in-rush" current drain must not exceed 35A at any voltage. From this it follows that the available power cannot be expected to exceed

$$19.8 \times 11.3 = 224 \text{ W}$$

under worst case conditions; hence the continuous Gimbal Power, etc. must stay within that budget.

The loss within the SRMS and End Effector wiring, again at worst case conditions, will be:

$$11.3^2 \times 0.369 = 47 \text{ W}$$

## 6.2

### PEP Solar Array Power Transmission

The Solar Array Assembly, to be carried by the SRMS, is rated at 32 kW at 120V. The transmission of its electrical power will be effected by means of six parallel leads, each having 207 strands of No. 29 A.W.C., therefore equivalent to No. 6 A.W.G.



Figure 6-2 illustrates the electrical concept, also identifying the receptacles at the orbiter end of the SRMS.

The worst case predicted temperatures of this power transmission wiring are higher, since it is placed outside the thermal blanket of the SRMS. For the first 8 feet in the shoulder and the last 10 feet in the wrist 98°C and for the remaining 47 feet 95°C temperature is predicted. (Configurations #1 and #2 respectively).

The resistances then

Shoulder  $\frac{1}{6} \times 0.0003951 [1 + 0.00397 (93-20)]$   
and  
Wrist : = 0.00008624 ohms/foot

Rest of  
SRMS:  $\frac{1}{6} \times 0.0003951 [1 + 0.00397 (95-20)]$   
= 0.00008545 ohms/foot

from which we can calculate the total power transmission resistance to be

$$0.00008624 (8+8+10+10) + 0.00008545 (47+47) = 0.01114 \text{ ohms}$$

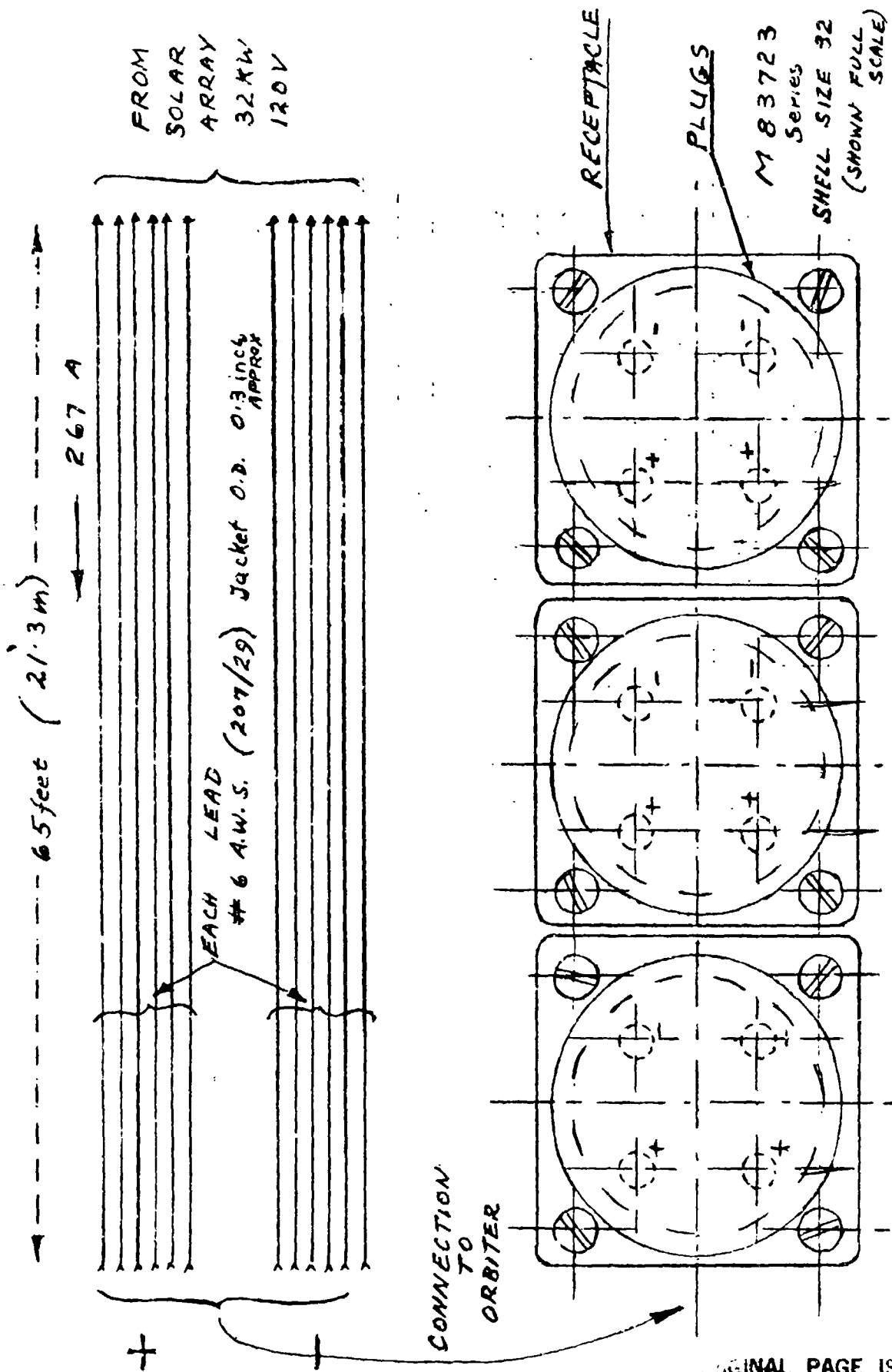
Returning now to the solar array itself. This is rated at 32kW and 120V, which relates to a current of

$$\frac{32000}{120} = 267A$$

The available voltage and power at the orbiter is then

$$120 - 267 \times 0.01114 = 117V$$

and



ORIGINAL PAGE IS  
OF POOR QUALITY

Fig 6-2-1 PEP POWER TRANSMISSION DETAILS

$$117 \times 267 = 31.2 \text{ KW}$$

respectively.

The power loss within the PEP Power Transmission wiring will then be

$$267^2 \times 0.01114 = 794 \text{ W}$$

The losses in the connectors will have to be added to this. Voltage drop is listed at 38mV at 110A test current which is assumed to reduce to

$$30\text{mV at } \frac{267}{6} \text{ A} = 44.5\text{A/contact}$$

The power loss at the three connectors with a total of twelve size 4 contacts at the orbiter end will be

$$0.030 \times 44.5 \times 12 = 16\text{W}$$

The total power loss of the PEP Transmission, not considering the actual solar array connections, would be

$$794 + 16 = 810\text{W}$$

or

$$\frac{810}{31200} = 2.6\%$$

### 6.3 EMC Considerations

The PEP power bus will be routed as far as practical from the Manipulator Arm (MA) cable harness and from the electronics units mounted within the arm. In order to minimize magnetic fields coupling the 12 power bus lines will be laid out in pairs, each consisting of a positive line and a return line. Twisting of wire pairs will not be employed as wire size (AWG #6) prohibits it.

The Elbow and Wrist-Y/P flexible sections of the PEP harness will be routed opposite to the arm harness while the Wrist-Roll harness will be routed external to the joint. Cable separation in the Shoulder-Y/P flexible section cannot be achieved due to mechanical constraints. At this section, the harnesses will be laid out side by side. Magnetic field coupling from the PEP harness to the MA harness at the shoulder, has been analyzed based on the following preliminary data received from McDonnell Douglas:

- (a) PEP bus current ripple - total amplitude of 5 Amps peak to peak
- (b) Low frequency ( $\sim 70$  Hz) ripple - 4 amps peak to peak
- (c) High frequency ( $\sim 20$  KHz) ripple - 1 amp peak to peak

It was concluded that the coupled noise will not affect the MA operation.

7.0 MATERIALS7.1 General Materials

Materials selection for the SRMS/PEP program shall be based essentially on the same requirements and guidelines as are currently being used for SRMS. Materials shall be selected by considering the operational requirements of a given application and the design engineering properties of a given material. Candidate materials shall be evaluated in accordance with SPAR-SG.368 "Materials and Processes Requirements for SRMS" and shall be selected from a list of rated material in SPAR-SG.369 "Materials and Processes Selection List for SRMS". SPAR-SG.369 contains lists of materials which have been assigned ratings by test or analysis in the anticipated service environments. The ratings which are based on NASA JSC 09604 "Materials Selection List" cover the following hazardous environments:

corrosion	}	Metals
stress corrosion cracking		
gaseous oxygen		
flammability	}	Non-Metals
thermal vacuum stability		
age life		
low pressure gaseous oxygen		

In addition, the materials used shall be compatible with the interfacing hardware of the SRMS and shall not jeopardize the functioning of other components.

7.2 Power Cable Materials

The available data related to the power cable materials at this time is insufficient to assess whether or not they are qualified for space applications. It has been assumed that the cables will be available as fully qualified items.

## 8.0 STRUCTURAL DYNAMICS CONSIDERATIONS

### 8.1 Dynamic Envelope

The increased weight of the stowed arm structure would result in increased sway of the arm under dynamic load conditions. The total weight of the cable system equals 103 lbs. The increase in dynamic sway (at the arm C/L) is estimated to be 0.060". The static envelope available for the stowed arm is expected to reduce by 0.060" on radius (i.e. 0.120" on diameter) at the arm centre/line. The decrease in static envelope in other areas is estimated to be about 13% (i.e. specific envelope allowances for cameras, etc).

The above increase in dynamic envelope requirements will necessitate close examination in all areas to ascertain if there are interference problems. Critical areas are primarily the cargo bay door radiators.

### 8.2 Cable Attachment

The cable attachment chips will be designed for 25g load on the cable for vibration environment. The areas along the boom where the cable harness bundle is split into two portions, this load condition would imply 24 lbs. load at each clip if they are 12 inches apart. The local loads in other areas would depend upon the cable configuration, location of attachments, etc. The design of cable clamps will be such that the local resonant frequencies are above 100 Hz to prevent interaction with arm dynamics.

### 8.3 Structural Loads

Addition of 103 lbs. of cable to the structure will also increase the loads in the primary structural elements of the arm. The increase in loads due to quasi-static conditions is estimated to be 13% while the random loads are expected to increase by 5%.

#### 8.4 Stress Considerations

The cable clamps and attachment bolts will be analyzed to the loads specified and will be designed to exceed the first resonant frequency minimum requirement. Intermediate straps will be required along the arm booms at a suitable pitch based on support strength and envelope requirements. The margins of safety will be calculated as follows:

$$\text{M.S. (Yield)} = \frac{\text{Material Yield Stress (Fty)}}{\text{Max. Working Stress} \times 1.0} - 1.0$$

$$\text{M.S. (Ultimate)} = \frac{\text{Material Ultimate Stress (Ftu) or Crippling Stress}}{\text{Max. Working Stress} \times 1.4} - 1.0$$

Fracture mechanics analysis of known critical components will be performed for the new load spectra which will include the total number of SRMS/PEP missions and modifications or structural stiffening will be added if possible to maintain 100 safe mission life capability. Where there is impractical, a waiver will be sought on total life requirement.

## 9.0 MASS PROPERTIES

### 9.1 PEP Power Bus on SRMS

The weight of the PEP Power Bus that interfaces with the orbiter at the SRMS shoulder joint and with the solar array system at the end effector total 108 lb as follows: -

12, #6 cables approximately 70 ft. long (93 lb.)

3 connectors (4 cables/connector) at the shoulder joint interface (3 lb.)

1 special connector (12 cables) at the end effector interface (3 lb.)

Cable provisions to support the cables at each joint and along the length of the arm per layouts 31221L1 through 3 (9 lb.)

### 9.2 SRMS/PEP Interface Connector Assembly (Driven)

A special connector (12 cable) at the end effector interface and mounted to the PEP system is estimated to weigh 3 lb. with additional weight for the lower actuator of 2 lb. for a total of 5 lb.

### 9.3 Grapple Fixture and Connectors

The weight of a grapple fixture that interfaces with the end effector based on an existing design is 10 lb.

### 9.4 Orbiter/SRMS Interface Connector (Ref. Only)

The weight of 3 mating connectors (4 cables/connector) at the orbiter interface (SRMS shoulder joint, required for the PEP Power Bus, is estimated to be 3 lb. This is not included as part of the PEP System Package, and should be used as reference only.

## 10.0 DEVELOPMENT AND TEST PROGRAM

The proposal presented in the preceding sections is based upon design layout studies only. To verify the feasibility of a design of this nature, an extensive development program will be necessary whereby representative cable configurations and materials will be used. Fully working joint mockups will be required to determine cable system handleability.

Until such a program has been undertaken, it can only be assumed that the proposed methods of cable handling will satisfy the requirements.

Further to the development program outlined above, a comprehensive environmental test program will be required. Thermal vacuum (including operational cycling on simulated SRMS joints) and vibration testing of critical areas will be necessary to reduce system failure risk.

Fully detailed thermal and structural dynamic analyses will be conducted to establish test parameters.

11.0 DESIGN PROPOSAL LAYOUTS

<u>Design Layout #</u>	<u>Title</u>
31221L1	SRMS/PEP Cable Handling System Proposal - Wrist Roll Joint
31221L2	SRMS/PEP Cable Handling System Proposal - Shoulder Joint
31221L3	SRMS/PEP Cable Handling System Proposal - Wrist Pitch and Yaw Joint
31221L4	SRMS/PEP Cable Handling System Proposal-General System
31221L5	SRMS/PEP Cable Handling System Proposal - SRMS/PEP Interface Connector Assembly

Appendix B

PRELIMINARY SPECIFICATION  
WEP GIMBAL ASSEMBLY,  
SOLAR ARRAY DRIVE,  
TWO-AXIS



McDonnell Douglas Astronautics Company  
Huntington Beach, California

New  
June 15, 1979

## 1.0 SCOPE

This specification defines the requirements for an electromechanical, two-axis gimbal assembly consisting of two direct current actuators, supports, bearings, electrical connectors and slip ring assembly or equivalent to transfer electrical power and signals across the continuously rotating interface.

### 1.1 Intended Use

The gimbal assembly is to be used as part of the Power Extension Package (PEP) to point a large solar array at the sun during Orbiter operations.

## 2.0 APPLICABLE DOCUMENTS

### 2.1 General

The following documents, of the exact issue shown, or if no issue is specified, the issue in effect at the date of invitation to bid, form a part of this drawing to the extent specified herein. In the event of conflict between documents referenced here and other detail contents of Sections 3, 4 and 5, the detail requirements of Section 3, 4 and 5 shall be considered the superseding requirements.

### Specifications

#### Federal

QQ-S-571 Solder, tin alloy, tin-lead alloy and lead alloy

#### Military

MIL-A-8625 Anodic coatings, for aluminum and aluminum alloys

MIL-B-5087 Bonding, electrical and lightning protection for Aerospace System.

MIL-B-7883 Brazing of steels, copper, copper alloys, nickel alloys, aluminum and aluminum alloys.

MIL-C-5541 Chemical conversion coatings on aluminum and aluminum alloys

MIL-C-6021 Casting, classification and inspection of

MIL-C-27500 Cable, electrical, shielded and unshielded, aerospace

MIL-M-8609B Motors, direct current, 28 volt system aircraft

MIL-S-5002 Surface treatments and metallic coatings for metal surfaces

MIL-T-1528	Treatment, moisture and fungus resistant, of communications, electronic, and associated electrical equipment
MIL-W-6858C	Welding, resistance, aluminum, magnesium, non-hardening steels or alloys, nickel alloys, heat-resisting alloys, titanium alloys, spot and seam
MIL-W-8939	Welding, resistance, electronic circuit modules
MIL-W-22759	Wire, electric, fluorocarbon insulated, copper or copper alloy
MIL-W-81381	Wire, polyimide insulated, copper or copper alloy
MIL-W-5088	Wiring, aerospace vehicle
MIL-STD-129F	Marking for shipment and storage
MIL-STD-130D	Identification marking of U. S. military property
MIL-STD-143	Specification and Standards, Order of Precedence for selection of
MIL-STD-454 (Requirement 5)	Standard, general requirements for electronic equipment (Soldering)
MIL-STD-461A	Electromagnetic interference characteristics req for equipment
MIL-STD-889	Dissimilar metals
MIL-STD-1523	Age-sensitive elastomeric material, age controls of
NBS Handbook H28	Screw thread standards for federal service
<u>NASA</u>	
SL-E-0002	Electromagnetic interference characteristics requirements for equipment for Space Shuttle
SN-C-0005	Contamination control requirements for the Space Shuttle Program
SP-R-0022A	Vacuum stability requirements of polymeric material for Spacecraft application, general specification for
MSFC-SPEC-222A	Resin systems, electrical and environmental insulation
MSFC-SPEC-522A	Design criteria for controlling stress corrosion cracking

### 3.0 REQUIREMENTS

#### 3.1 Item Definition

The gimbal assembly shall be an electromechanical device which provides 2 axis positioning of a large solar array. One axis, referred to as the Alpha axis

will have continuous rotation capability. The other axis, referred to as the Beta axis will have a total of  $90^{\circ}$  rotation. Electrical power circuits and signal circuits must be transferred across both axes. One side of the gimbal assembly will be structurally attached to the solar array structure, the other side will be attached to a grapple fixture. During operation the grapple fixture will be attached to the end effector of the RMS. The control of the gimbal assembly will utilize a closed-loop position control servo system.

### 3.1.1 Interface Definition

#### 3.1.1.1 Mechanical

The gimbal assembly mounting, axes location and envelope shall be in accordance with figure 1.

#### 3.1.1.2 Electrical

The gimbal assembly electrical interface shall be in accordance with figure 2.

### 3.1.2 Gimbal Assy Power Requirements

The actuators for the Alpha and Beta axis drive shall utilize D.C. power from the orbiter buss. The voltage range is 18 to 32 VDC. The actuators power drain shall not exceed 50 watts steady state for both actuators operating simultaneously and including position feedback transducers excitation. With both actuators at stall the power drain shall not exceed 100 watts.

## 3.2 Design

### 3.2.1 Alpha Axis Drive Performance

#### 3.2.1.1 Stall Torque

The stall torque of the Alpha axis drive shall be 100 ft pounds minimum, 150 ft pounds maximum, in both rotational directions at 32 volts.

#### 3.2.1.2 Rate

The rate of the Alpha axis drive shall be  $0.5^{\circ}$  per second minimum at 32 volts with no externally applied torque load. The speed-torque relationship shall be linear within  $\pm 10\%$  between stall and full rate.

#### 3.2.1.3 Feedback Position Transducer

The feedback position transducer may be either analog or digital. The accuracy, or resolution, of the transducer shall resolve the true position of the gimbal within  $1.0^{\circ}$ .

#### 3.2.1.4 Travel

The Alpha axis shall have continuous rotation capability in either direction.

#### 3.2.2 Beta Axis Drive Performance

##### 3.2.2.1 Stall Torque

The stall torque of the Beta axis drive shall be 100 ft. pounds minimum, 150 ft pounds maximum, in both rotational directions at 32 volts.

##### 3.2.2.2 Rate

The rate of the Beta axis drive shall be  $0.5^{\circ}$  per second minimum at 32 volts with no externally applied torque load. The speed-torque relationship shall be linear within  $\pm 10\%$  between stall and full rate.

##### 3.2.2.3 Feedback Position Transducer

The feedback position transducer may be either analog or digital. The accuracy or resolution of the transducer shall resolve the true position of the gimbal within  $1.0^{\circ}$ .

##### 3.2.2.4 Travel

The travel of the Beta axis drive shall be  $90^{\circ}$  minimum  $92^{\circ}$  maximum the travel shall be limited by mechanical stops. No limit switches shall be used to interrupt power to the actuator motor.

#### 3.2.3 Life Requirements

The gimbal assembly shall be designed to provide the most cost effective life capability, considering minimum maintenance and refurbishment as well as state-of-the-art design. Upon completion of trade studies by the seller to establish the relationship between these evaluation items, the following life objectives will be changed to requirements.

##### 3.2.3.1 Operating Life

As a design objective the gimbal assembly shall be capable of meeting the performance specified herein after operating for a period of 33,600 hours. This time is equivalent to 100 orbital missions in a 10 year period. The average orbital mission will be 14 days. Preventive maintenance, servicing repair, and replacement of parts shall be consistent with the sellers trade study results.

##### 3.2.3.2 Shelf Life

As a design objective, the gimbal assembly shall be capable of operating in

accordance with the requirements specified herein any time within a period of 10 years from date of delivery when exposed to the applicable environmental conditions of paragraph 3.3.

#### 3.2.4 Weight

The gimbal assembly weight shall be less than 40 pounds.

#### 3.2.5 Gearing

The gearing required to produce the gimbal torque and motion requirements must be internal, permanently lubricated and sealed to prevent lubricant leakage externally. Relubrication will not be accomplished during the service life of the actuator.

#### 3.2.6 Bearings

The gimbal assembly bearings shall be selected on the basis of operation at the maximum load and temperature conditions during vacuum operation. The bearings shall be permanently lubricated. Relubrication will not be accomplished during the service life of the actuator.

#### 3.2.7 Attachments

All mechanical attachments shall be secured by suitable means to prevent loosening in the vibration environment of Paragraph 3.4.3. Standard parts shall be used whenever they are suitable for the purpose. The materials shall be corrosion resistant or suitably processed to resist corrosion. Because of the susceptibility to hydrogen embrittlement, the use of the cadmium plated steel attach hardware shall be avoided where possible.

#### 3.2.8 Attitude

The gimbal assembly shall be capable of operation in any attitude on the ground or in a zero g environment.

#### 3.2.9 Selection of Specifications and Standards

Specifications and standards for the identification and control of materials, parts, and processes of this equipment shall be selected in accordance with MIL-STD-143.

#### 3.2.10 Materials and Processes

All materials and processes shall be compatible with the performance and environmental criteria for this component. Materials and parts that conform to Government specifications shall be used as much as practicable.

#### 3.2.10.1 Non-magnetic

Non-magnetic material shall be used for all metallic parts except where magnetic parts are essential.

#### 3.2.10.2 Non-Metallic Materials

Insofar as practicable, a non-metallic item shall be resistant to lubrication materials, environmental temperatures and conditions, and combinations thereof.

Non-metallic parts shall not have a corrosion stimulating effect on other materials when exposed to the specific useful life. Fungus nutrient materials as defined in paragraph 3.3.3.2.2 of MIL-T-152B shall not be used. A list of all non-metallic materials and their individual weights shall be provided to the buyer.

#### 3.2.10.3 Limited Life Items

The buyer must be notified in writing whenever age critical or time/cycle significant item/material (limited life items) are contained in the gimbal assembly. These item/materials must meet the minimum service life in Para. 3.2.3 and the requirements of MIL-STD-1523. The date of installation and manufacture of age critical material must be noted on the shipping paper.

#### 3.2.10.4 Lubricants

The use of lubricants and sealants shall require written buyer approval prior to use.

#### 3.2.10.5 Threads

All threads shall be in accordance with NBS Handbook H28.

#### 3.2.10.6 Finish Requirements

Selection of proper surface treatments, finish materials, and application methods shall be governed by the type of material used, environmental and functional design requirements, and handling and storage requirements. The materials and the processes used for their application shall not deleteriously affect the parts and shall produce satisfactory corrosion resistant surfaces.

#### 3.2.10.7 Fabrication Operations

Maximum protection shall be afforded all surfaces of the item by performing all fabrication operations practicable prior to the application of protective finishes.

#### 3.2.10.8 Corrosion Resistant Steel

Corrosion resistant steels shall be passivated in accordance with MIL-S-5002.

#### 3.2.10.9 Stress Corrosion

All metallic parts within the actuator shall conform to the requirements of MSFC-SPEC-522A.

#### 3.2.10.10 Outgassing

The gimbal materials shall be selected for low outgassing characteristics to insure that any effluents do not jeopardize performance of other Orbiter/Payload systems. Selection criteria shall be 1% total mass loss and 0.1% volatile condensable material (VCM) as defined in specification SP-R-0022.

#### 3.2.10.11 Dissimilar Metals

Unless suitably protected against electrolytic corrosion, dissimilar metals, as defined in MIL-STD-8889, shall not be used in intimate contact.

#### 3.2.10.12 Potting or Encapsulation

For general use, potting or encapsulation materials shall conform to MSFC-SPEC-222, or any other suitable material which is compatible with the specified environments may be used.

#### 3.2.10.13 Chemical Surface Treatment

Apply chemical surface treatment per MIL-A-8625, Type I, Class 1, or MIL-C-5541, Class I, for all aluminum alloys which are to be painted or where maximum corrosion protection is required on surfaces not to be painted.

Apply chemical surface treatment per MIL-C-5541, Class 3, for corrosion resistance on all aluminum alloy surfaces where low electrical resistance is required.

Standard attachment parts such as rivets, bolts, nuts and washers which are component parts of assemblies which will be primed or painted upon completion do not require primer prior to assembly provided they meet the dissimilar metal requirements of MIL-STD-889.

Painting is not to be used unless thermal analysis indicates the external surfaces of the assembly require paint to obtain a specific solar absorption/surface emissivity ratio in order to regulate temperature.

### 3.2.11 Maintainability

The gimbal design objective is to operate and meet all performance requirements throughout its life without maintenance. The supplier shall consider all constraining items which would require special attention after each mission or group of missions (i.e., lubricant degradation/depletion, material deterioration, etc.) and recommend field tests and inspections, the results of which would indicate whether or not this design objective were being met. Should the field tests and inspections indicate refurbishment of the gimbal is necessary, it will be done according to a maintenance procedure submitted by the supplier and approved by the buyer.

The gimbal design shall incorporate features to accommodate maintenance.

### 3.2.12 Interchangeability

The gimbal assembly and all replaceable detail parts which are identified with the same part number, shall be physically and functionally interchangeable.

### 3.2.13 Casting

Castings shall be in compliance with the requirements of MIL-C-6021, Class 1, Grade B.

### 3.2.14 Brazing

Brazing shall be conducted in compliance with the requirements of MIL-B-7883.

### 3.2.15 Motors

The motor designs shall be compatible with the gimbal assembly requirements specified herein and the requirements of MIL-M-8609 paragraphs 3.3, 3.3.1, 3.3.2, 3.3.3, 3.4.3, 3.4.3, 3.4.7, 3.4.9.2, 3.4.9.3, 3.5, 3.6, 3.7, 3.8, 3.9, 3.10.2, 3.12, except as otherwise specified herein.

#### 3.2.15.1 Motor Types

Permanent magnet motors shall be utilized.

#### 3.2.15.2 Wire Routing and Protection

The motor designs shall provide for clear unobstructed wire routing. All leads shall be suitably supported to prevent insulation chafing by adjacent structure during a vibration environment. All insulated leads shall be suitably protected to prevent damage during motor assembly. Sharp edges on attachments or structural parts in close proximity to wires are not allowed.

#### 3.2.15.3 Armature Balance

The armature of the motors shall be dynamically balanced to prevent vibration and armature bearing loading when operating at the no-load speed with  $32 \begin{smallmatrix} +0 \\ -.5 \end{smallmatrix}$  volts.

#### 3.2.15.4 Armature Assembly Preload

Axial motion of the armature assembly shall be controlled through the use of an axial preload.

#### 3.2.15.5 Thermal Protection

No thermal switches shall be incorporated in the design of the gimbal assy. The assembly shall be designed to sustain locked rotor current continuously without causing a fire hazard.

#### 3.2.15.6 Electromagnetic Interference Filter

The motors with EMI filters shall comply with the CE01 and CE03 conducted interference limits of MIL-STD-461A and RE02 radiated interference limits and the TT01 requirements defined in SL-E-0002. All bonding necessary to meet this requirement shall be accomplished per MIL-B-5087, Class R. The components used in the filter and tests conducted on the filter shall be approved by the buyer.

#### 3.2.15.7 Insulation Resistance

With the individual motor windings shorted at the connector, the insulation resistance between the insulated points and the motor case with the motor stabilized at  $+70^{\circ} \pm 20^{\circ}\text{F}$  shall not be less than 50 megohms when tested with  $75 \pm 5$  volts DC.

#### 3.2.15.8 Dielectric Strength

With the individual motor windings shorted at the connector and the filter isolated, the dielectric strength between the insulated points and insulated points and the motor case shall be  $600 \pm 60$  volts RMS 60 Hz for a minimum of 60 seconds. Leakage current shall not exceed 1.3 milliamps.

#### 3.2.15.9 Bonding

All mechanical interfaces in the gimbal assy, including electrical connectors, shall be bonded per MIL-B-5087, Class R (2.5 milliohms maximum per interface).

#### 3.2.15.10 Electrical Connections

All electrical connections within the motor shall be brazed, welded or mechanically attached. Soft solder shall not be used unless otherwise approved by the buyer.

#### 3.2.16 Slip Ring Assembly (SRA)

The gimbal assembly shall include a slip ring assembly or equivalent to transfer solar array power and command and instrumentations across the continuously rotating alpha axis.

##### 3.2.16.1 Electrical Requirements

Electrical and electronic parts and materials selected shall be used within their electrical ratings and environmental capabilities. Derating shall be accomplished, as necessary, to assure the required equipment reliability within the specified operating conditions. Unless otherwise specified, the SRA shall meet the following electrical requirements under any combination of operational environments specified herein.

##### 3.2.16.2 Circuits

The SRA shall consist of 36 total circuits or rings. The types, capacities and quantities of the circuits are as follows.

<u>Ring No.</u>	<u>Type</u>	<u>Current</u>	<u>Function</u>	<u>Voltage</u>
1-12	I	60 amps, max	Solar array power	90 to 240
13-32	II	1 ma to 100 ma	Signal and instrumentation	0 to 32
33-36	III	10 amps max	Actuator power	18 to 32

All circuits shall be designed for continuous operation with the maximum current specified.

##### 3.2.16.3 Rotational Speed

The SRA will be designed for rotation in both directions and shall meet the performance specified herein with rotational speeds from 0 to the maximum rate of the alpha gimbal actuator.

##### 3.2.16.4 Dielectric Strength

The SRA shall be designed to withstand at least 500 volts RMS, 60 Hz, applied for a minimum of one minute between each contact and every other contact of other noncommon rings, and between each contact and the SRA shaft, housing and connector case excluding grounded contacts. There shall be no evidence

of arcing, flashover, breakdown, nor any leakage current in excess of 50 microamperes.

#### 3.2.16.5 Insulation Resistance

The insulation resistance between any contact and every other noncommon contact, and between any contact and the SRA shaft, housing, and connector case excluding grounded contacts shall be 50 megohms minimum at 500  $\pm 10$  VDC. Insulation resistance shall be one megohm minimum at 100  $\pm 10$  VDC during and immediately after exposure to relative humidity equal to or greater than 98%. Voltage shall be applied uninterrupted for up to one minute.

#### 3.2.16.6 Crosstalk

During any combination of voltage, current, rotational speeds and environments specified herein, the crosstalk induced into any Type II circuit from any other SRA circuit shall be attenuated at least 30 dB with a termination load of 5000 ohms at 20 Hz to 20 KHz.

#### 3.2.16.7 Impedance Noise

Equivalent electrical peak to peak impedance noise of any SRA circuits shall not exceed 10 milliohms per circuit pair during any combination of voltage, current, rotational speeds and environments specified herein.

#### 3.2.16.8 Voltage Drop

At zero to .5°/sec rotational speed the end to end (connector contact to connector contact) circuit voltage drop shall be as follows.

<u>Type</u>	<u>Current</u>	<u>Max Voltage Drop</u>
I	10 to 60 amps	200 MV
II	1 ma to 100 ma	1.0 MV
III	10 amps	100 MV

#### 3.2.16.9 Derating

The SRA wiring shall be selected according to MIL-W-5088 for the electrical and environmental requirements of this specification such that the rated maximum conductor temperature is not exceeded for any combination of electrical loading, ambient temperature, and heating effects of bundles, conduit and other enclosures. Factors to be considered in the selection are voltage, current, ambient temperature, mechanical strength, abrasion,

flexure and pressure-altitude requirements. The SRA electrical components, less wiring, shall be designed with a minimum derating factor of 50%.

#### 3.2.16.10 Continuity

At speeds ranging from 0 to .5°/sec cumulative electrical discontinuity of any circuit shall not exceed one microsecond within any 100 millisecond period.

#### 3.2.16.11 Wiring

The SRA wiring shall be selected according to the electrical and environmental requirements of this specification, and shall conform to either MIL-W-22759/9/10/11 or MIL-W-81381/7/8/9/10. Cable design shall conform to MIL-C-27500.

#### 3.2.16.12 Soldering

Soldering shall be in accordance with MIL-STD-454, Requirement 5. Solder shall be in accordance with QQ-S-571. Solvents used for cleaning and flux removal shall be of high purity grade, non-conductive, non-corrosive, and shall not degrade the reliability of the soldered connection of adjacent parts or materials. Each soldered connection shall exhibit a bright shiny appearance, no porosity, good adherence, and no excess flux or solder when visually examined under direct light at five power magnification.

#### 3.2.16.13 Welding

Resistance welding shall be conducted in compliance with the requirements of MIL-W-8939 for electrical welds, and MIL-W-6858, Class A, for mechanical welds.

#### 3.2.17 Gimbal Assy Dynamic Performance

With either the Alpha or Beta axes attached to an inertia load of 1650 slug-ft<sup>2</sup> (about the gimbal axis), the open-loop gimbal rate shall reach 0.5 deg/sec within the period 5 to 10 seconds following an input voltage of 18 volts. The open loop gimbal design shall not preclude the capability to operate smoothly at low rates (0.01 to 0.1 deg/sec) when used in a closed loop manner with an angular position sensor resolution of 1 degree.

#### 3.3 Operating Environments

The gimbal assy shall be capable of meeting the requirements of Paragraph 3.0 of this specification during and after exposure to the following environments.

### 3.3.1 Temperature

The ambient temperature range for gimbal assy ground operation is 0°F to 110°F. The in-orbit operational temperatures will be dependent on the design of the gimbal assembly. When determining these extremes analytically, the supplier shall use the following data:

<u>Environmental Parameter</u>	<u>Design Value</u>
Solar radiation	443.7 btu/ft <sup>2</sup> /hr
Earth albedo	30%
Earth radiation	77 btu/ft <sup>2</sup> /hr
Space sink temperature	0° Rankin

### 3.3.2 Vacuum

The gimbal assy shall be capable of meeting the requirements of this specification during and following exposure to a vacuum of  $1 \times 10^{-7}$  Torr.

### 3.3.3 Humidity

During ground testing, the gimbal assy shall be capable of performing continuously in a relative humidity of 30 to 90%.

### 3.4 Non-operating Environments

The gimbal assy shall be capable of meeting the requirements of this specification after exposure to any combination of the following non-operating environments.

#### 3.4.1 Acceleration

The gimbal assy shall withstand  $\pm 6 \pm .25$  g's in both directions in the axis perpendicular to the mounting plane and in each of the two mutually perpendicular axes.

#### 3.4.2 Shock

The gimbal assy shall be subjected to two transient excitations with shock response spectrums as shown in Figure 3 in each of the three mutually perpendicular axes.

#### 3.4.3 Vibration

##### a. Random Vibration - Qualification

The unit shall be subjected to the following levels in each of the three mutually perpendicular axes for 400 seconds per axis.

<u>Frequency (Hz)</u>	<u>Level</u>
10-100	0.014 G <sup>2</sup> /Hz
100-440	+4 db/octave
440-2000	0.1 G <sup>2</sup> /Hz

Grms - 13.2

##### b. Random Vibration - Acceptance

The unit shall be subjected to the following levels in each of the three mutually perpendicular axes for 120 seconds per axis.

<u>Frequency (Hz)</u>	<u>Level</u>
10-100	0.0035 G <sup>2</sup> /Hz
100-440	+4 db/octave
440-2000	0.025 G <sup>2</sup> /Hz

Grms - 6.6

#### 3.4.4 Transportation Shock

Equipment packed in the manner intended for shipment shall be qualified to the following shock tests: one drop on each flat face, edge and corner (26 drops) from a height of 30 inches. The tests shall be non-operational.

#### 3.4.5 Bench Handling Shock

This test is conducted to determine the ability of unpackaged equipment to withstand the shock encountered during servicing. Using one edge as a pivot, tilt the opposite edge of the assembly until the horizontal axis forms an angle of 45° with the table, or the opposite edge is four inches above the table, whichever occurs first, and permit the assembly to drop freely to the horizontal. Repeat, using other practicable edges of the same horizontal face as pivots, for a total of four drops. This process shall be repeated for each face on which the equipment could be placed practicably during servicing. The tests shall be non-operational.

#### 3.4.6 Storage

The assembly shall be designed for storage life, not to exceed the useful life period, in non-environmentally controlled buildings having the following characteristics:

Temperature - -65°F to +180°F

Relative humidity - 10% to 100%

Salt -  $5 \times 10^{-7}$  g/cm<sup>2</sup>/day fallout

100 micron coat/day

Fungus - rapid growth when temperature is greater than 68°F and relative humidity is greater than 75%

#### 3.5 Cleaning

All parts shall be processed in accordance with Specification SN-C-0005, Table 1, Level VC (visibly clean).

#### 3.6 Protective Treatment

Materials that are subject to deterioration when exposed to climatic and environmental conditions likely to occur in service shall be protected against such deterioration in a manner that will in no way prevent compliance with the performance requirements of this specification. Protective coatings that will chip, crack, or scale with age or in the extreme of climatic and environmental conditions specified herein shall not be used.

#### 3.7 Interchangeability

The item and all replaceable detail parts, identified with the same part number, shall be physically and functionally interchangeable by the use of dimensions and tolerances.

### 3.8 Workmanship

Those aspects of a product which may not be specifically controlled by requirements such as cleanliness, attachment, wire routing, torque, alignment, finish, etc., and which directly affect the product's appearance, orderliness, and neatness of assembly, or production uniformity are defined as characteristics of workmanship. The supplier shall establish documented standards of acceptance for such characteristics and shall apply those standards as criteria in determining the acceptability of the product. Workmanship standards shall not be in conflict with requirements set forth in the engineering drawings or the purchase document and shall not be used as an instrument to alter the design of the product or to circumvent the need to upgrade or revise engineering requirements.

### 3.9 Identification

#### 3.9.1 Identification Plate - Nomenclature

Identify the gimbal assy permanently per MIL-STD-130 using electro-etch methods. The identification shall depict, but not be limited to, the following information:

Nomenclature:	gimbal assy (Flt Crt Item)
Mfr:	(supplier code identification no.)
Part No.:	TBD
Supplier Part No.:	TBD
Serial No.:	
Date of Mfr:	
Contract:	

#### 3.9.2 Serialization

Each gimbal assy shall have a different serial number. Serialization shall be accomplished without reference to configurations. (There shall be no two parts with the same basic part number with the same serial number.) Gaps in serial number sequence are permissible, but the serial number must conform to the order of production. The serial number shall not be revised after once being assigned to a particular item.

### 3.10 Reliability

The gimbal assy is designated as a Flight Critical Item (FCI) and as such shall conform to the government and industry accepted design practices of

analysis plus control and derating for achieving a high reliability product. The gimbal assembly shall provide for reliable operation in any mode or combination of modes and under any natural combination of loads and environmental conditions specified herein. Successful completion of the testing herein shall not relieve the supplier of the responsibility for compliance of production units with specified reliability and performance requirements during any subsequent testing or service usage within the limitations specified herein.

#### 4.0 QUALITY ASSURANCE PROVISIONS

##### 4.1 Requirements/Verification Matrix

The ability of the gimbal to meet the requirements of Section 3.0 of this specification shall be verified according to the Requirements/Verification Matrix. The Requirements Verification Matrix is to be completed by the bidder as part of the proposed test plan.

##### 4.2 Buyer Tests

The buyer reserves the right to repeat any or all tests on the gimbal assembly.

##### 4.3 Design Changes

No changes of any kind shall be made to any portion of the gimbal assy. by the manufacturer after receipt of buyer engineering approval of manufacturer's detail design drawings unless formal authorization has been granted by buyer engineering. All requests for changes shall be submitted by the manufacturer in writing and accompanied by adequate evidence that the change will not adversely affect the performance of the unit. At the option of buyer engineering, additional tests may be required prior to approval of such changes. If the design change is approved, a new part number or modification designation number shall be assigned to the assembly incorporating the revision if interchangeability is affected.

#### 5.0 PREPARATION FOR DELIVERY

##### 5.1 General

Unless otherwise specified, the supplier shall be responsible for the preservation and packaging of the gimbal assembly in a manner that will prevent contamination, corrosion, deterioration, and physical damage and

ensure safe delivery in good condition. The minimum requirements for protection from physical damage shall be as defined in 3.4.

### 5.2 Cleaning and Packaging

Cleaning and packaging shall be in accordance with requirements for maintaining cleanliness specified in Paragraph 2.9 and 2.14 and Table 1, Level VC, of Specification SN-C-0005.

### 5.3 Marking

Individual cleaned gimbal assemblies shall be identified by a suitable tag or label. The tag or label shall be readable without degradation of the preservation means. The tag or label shall contain the following information.

- a. Part number
- b. Date of final cleaning
- c. Manufacturer's serial number
- d. "Flight Critical Item"

#### 5.3.1 Marking for Delivery

Each individual container shall be durably and legibly marked or labeled per MIL-STD-129 with the following minimum information; the label shall be so placed that it is not destroyed by opening the container:

Supplier part number  
Supplier name  
Part serial number  
MDAC-HB purchase order number  
MDAC-HB part number  
"Flight Critical Item"

Crated parts shall be labeled to indicate which side would be opened for inspection and shall note the location of the packing slip.

## 6.0 NOTES

### 6.1 Approved Source

<u>MDAC-Huntington Beach Specification Control No.</u>	<u>Supplier Part Number</u>	<u>Supplier Name &amp; Address</u>	<u>Supplier Code</u>
1BXXXXX	TBD	TBD	TBD

## 6.2 Definitions

G	Acceleration due to gravity
db	Decibel
°F	Degrees Fahrenheit
Hz	Hertz, cycles per second
MDAC-HB	McDonnell Douglas Astronautics Co.-Huntington Beach
ms	Millisecond
rms	Root mean square
Temperature	The stage at which temperature change is at a rate no greater than 1°F/min.
Stabilization (TBD)	Rate no greater than 1°F/min. To be determined.
Ambient	Atmosphere pressure of 30 $\pm$ 2 inches of mercury.
Condition	Temperature of 70 $\pm$ 25°F and relative humidity of 90% or less.

### 6.2.1 Standard Verification/Test Types

The standard verification/test types and their basic objectives are.

- a. Development - Conducted to formulate a design to meet performance requirements, define design requirements, to determine feasibility of a design or concept, or to evaluate hardware performance.  
(Normally conducted only on the minimum number of units necessary to obtain the desired development information.)
- b. Qualification - Conducted on an item representative of a production unit to verify that the released design and production methods result in a product that meet performance and design requirements established by contract, specification and/or engineering drawing.  
(Normally conducted on only one unit.)
- c. Acceptance - Conducted to measure the product performance characteristics and to verify conformance to selected design requirements as a basis for acceptance. (Normally conducted on each item to confirm acceptability, except where minimum lot sampling is specified.)

- d. Operational Test - Functionally operating the item to verify that performance requirements have been met, or performing an operation on the item (e.g., corrosion, fatigue, or strength tests) to verify design requirements.
- e. Similarity - Verification by evaluation of analytical or test data from an analysis or test program for an item which is sufficiently similar to the required item for the data to be valid. The data must show that the item used on a basis for verification has satisfied equivalent or more stringent requirements. Similarity is not shown as a drawing requirement, but is negotiated separately to satisfy specific requirements.

### 6.3 Recording of Serial Numbers

This is a "Flight Critical" item. A record of the serial number shall be maintained.

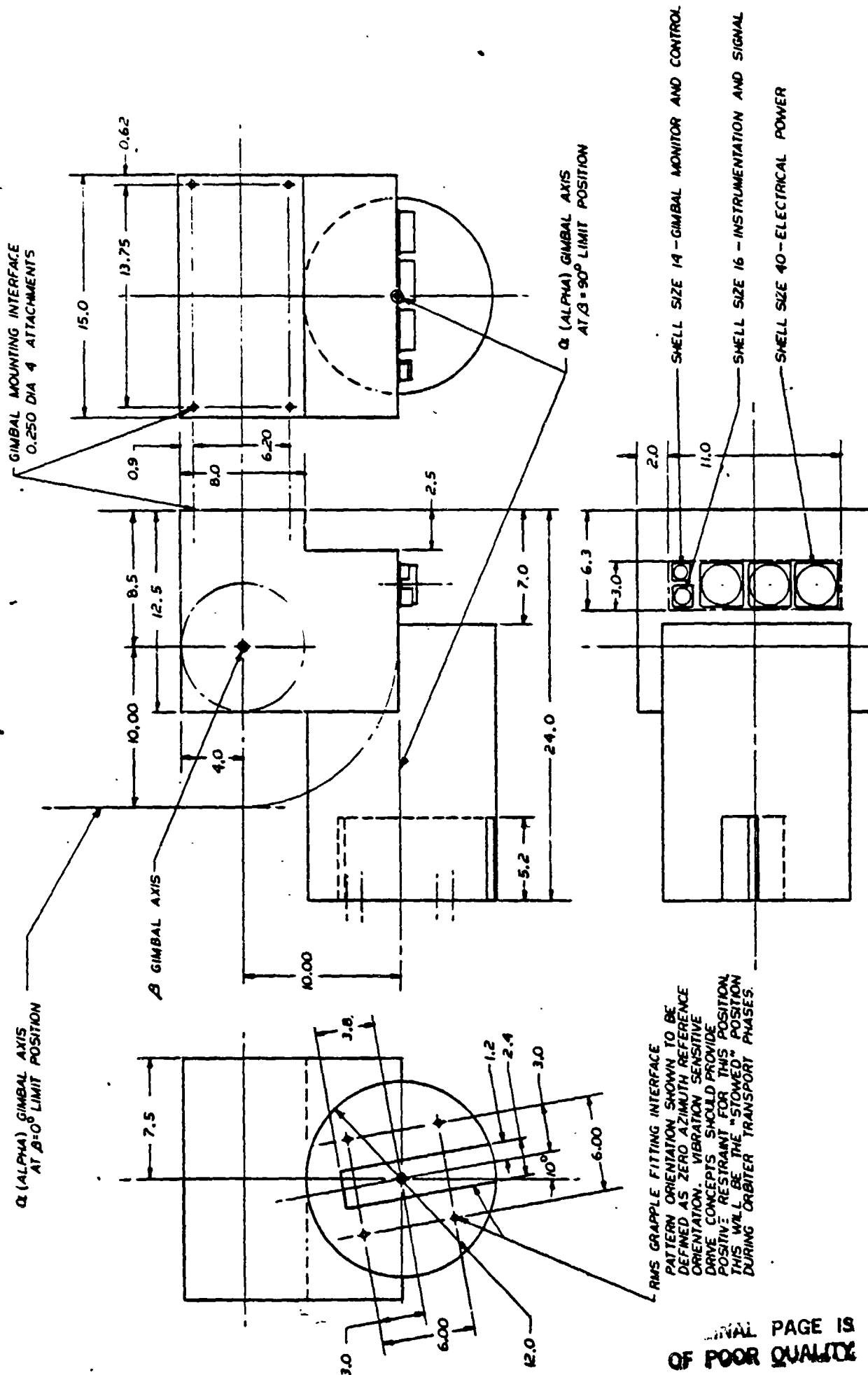


Figure 1 PEP GIMBAL ASSEMBLY ENVELOPE

ORIGINAL PAGE IS  
OF POOR QUALITY

### VERIFICATION BY SIMILARITY

ANL - ANALYSIS  
INS - INSPECTION  
DEM - DEMONSTRATION  
O/T - OPERATIONAL TEST  
TBR - TO BE RECOMMENDED BY  
SUPPLIER AS PART OF BID  
ANALYSIS. (TBR MAY BE  
USED ONLY ON BID  
ANALYSIS RELEASE)

**NA - NO ADDITIONAL VERIFICATION  
DETAILS REQUIRED**

To be completed by supplier as part of DT&E plan.

**McDONNELL DOUGLAS**

**DRAWING NO.**

**18355**

**SHEET**

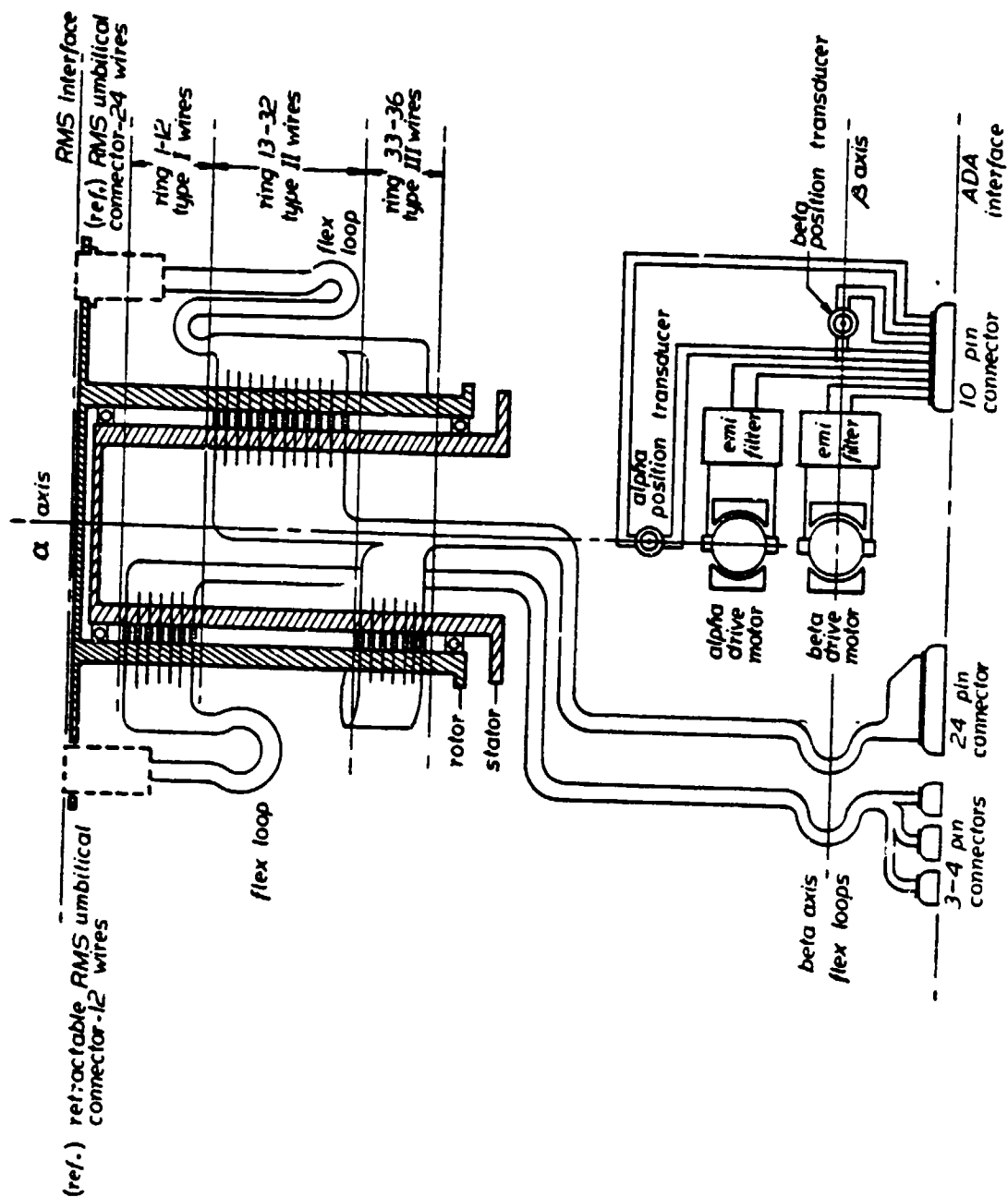


FIGURE 2. GIMBAL ASSEMBLY ELECTRICAL SCHEMATIC

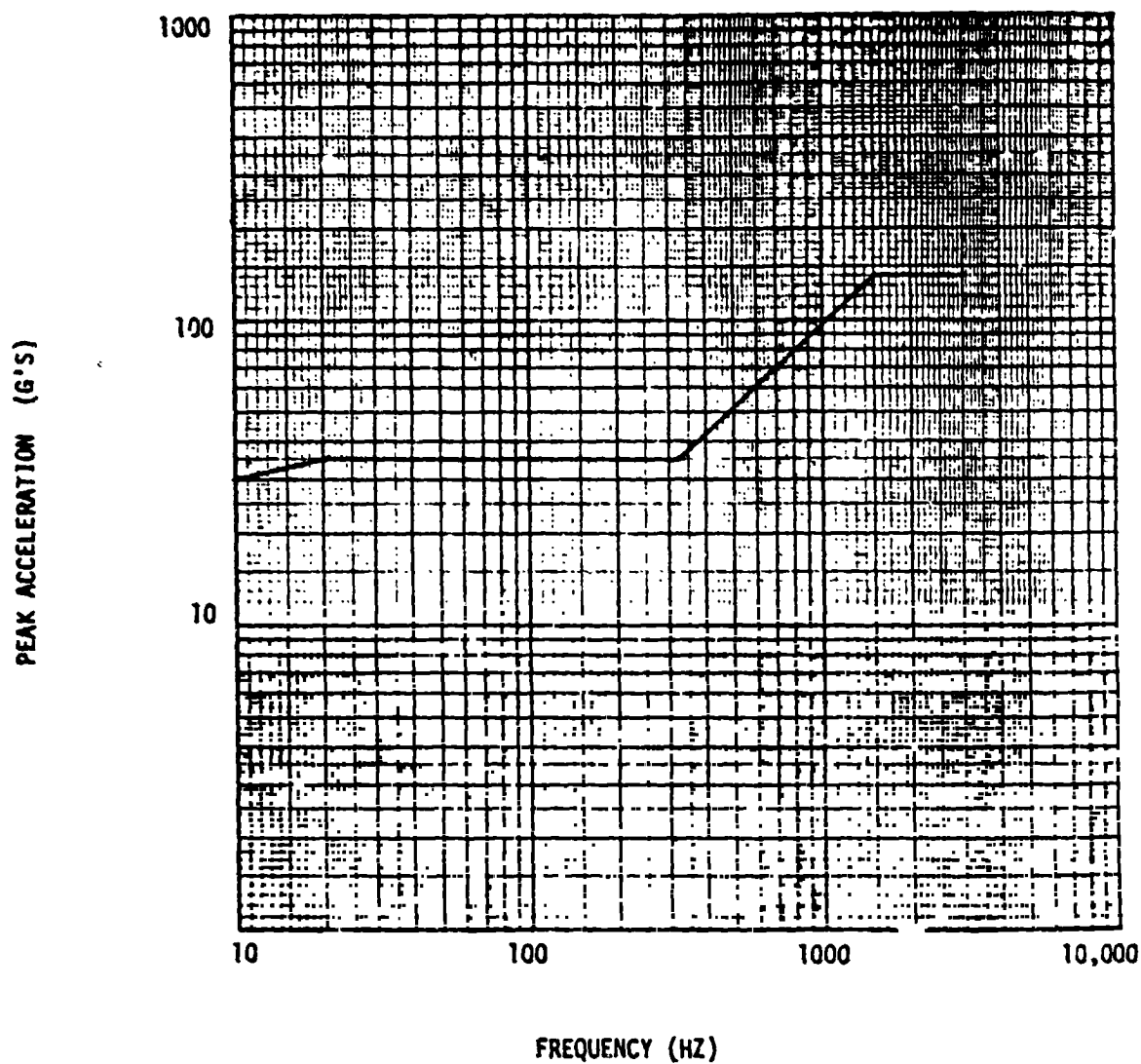


FIGURE 3

ORIGINAL PAGE IS  
OF POOR QUALITY